Pore water transport and microbial activity in intertidal Wadden Sea sediments

Dissertation zur Erlangung des Doktorgrades der Naturwissenschaften

dem Fachbereich Biologie/Chemie der Universität Bremen vorgelegt von

Markus Billerbeck

Bremen

November 2005

Die vorliegende Arbeit wurde in der Zeit von Mai 2001 bis November 2005 am Max-Planck-Institut für marine Mikrobiologie in Bremen angefertigt.

Gutachter

Prof. Dr. Bo Barker Jørgensen (Erstgutachter)
Prof. Dr. Gunter Kirst (Zweitgutachter)

Prüfer

Prof. Dr. Wilhelm Hagen
Prof. Dr. Markus Hüttel

Weitere Mitglieder des Prüfungsausschusses

Dr. Perran Cook
Angela Scharfbillig

Datum des Promotionskolloquiums: 21. Dezember 2005

Herzlichen Dank!

Ganz herzlich möchte ich mich bei Herrn Prof. Dr. Bo Barker Jørgensen für die Vergabe, Unterstützung und Begutachtung dieser Arbeit bedanken. Herrn Prof. Dr. Gunter Kirst danke ich für die Übernahme des Zweitgutachtens.
Mein ganz besonderer Dank gilt meinem Betreuer Markus Hüttel für seine tatkräftige Unterstützung, inspirierende Diskussionen und seine vielen Ideen während der gesamten Zeit. Eine bessere Betreuung kann ich mir nicht vorstellen.
Hans Røy und Dirk de Beer möchte ich für die tolle Hilfe insbesondere während der Endphase meiner Arbeit danken. Vielen Dank auch an Antje Boetius für die unermüdliche Unterstützung des „Flux-Überbleibsels".
Diese Arbeit wurde von der Deutschen Forschungsgemeinschaft (DFG) innerhalb des Projektes FG 432-5 „Biogeochemistry of the Wadden Sea" unter Leitung von Herrn Prof. Dr. Jürgen Rullkötter gefördert. Das MPI Teilprojekt wurde von Michael Böttcher geleitet, wofür ich mich herzlich bedanken möchte.
Vielen tausend Dank an Dich, Uschi Werner und an die glücklichen Umstände, die zu unserer Zusammenarbeit geführt haben. Deine Unterstützung im Feld und im Labor und die vielen Diskussionen und Aufmunterungen in schwierigen Zeiten waren von unschätzbarem Wert.
Die vielen Feldreisen wurden mir durch wunderbare Mitarbeiter versüßt: Uschi Werner, Eva Walpersdorf, Katja Bosselmann, Martina Alisch, Uli Franke, Lubos Polerecky, Christiane Hüerkamp, Kyriakos Vamvakopoulos und Ingrid Dohrmann. Den Crews der Plattboden-Schiffe, sowie den Mitarbeitern auf der Wattenmeerstation auf Sylt möchte ich für ihre Unterstützung und Gastfreundlichkeit danken.
Herzlichen Dank an die TA´s Martina Alisch, Gaby Schüßler, Susanne Menger, Cäcilia Wiegand, Daniela Franzke und Sindy Pabel für ihre Hilfe bei der Laborarbeit. Ohne die technische Unterstützung durch Jens Langreder, Axel Nordhausen, Georg Herz, Alfred Kutsche, Paul Färber, Volker Meyer und Harald Osmers wäre diese Arbeit nicht möglich gewesen. Danke an Bernd Stickfort für das Besorgen von manchmal seltsamer Literatur.
Ich möchte mich ganz herzlich bei Uschi Werner, Uli Franke, Christian Wild, Perran Cook, Hans Røy, Felix Janssen und Stefan Jansen für die vielen fruchtbaren Diskussionen bedanken. Christian Wild sei für die vielen netten Stunden gedankt, die wir mit einem Gläschen Wein vor dem Computer mit unserer „Arbeit" verbracht haben.
Meinen Bürokollegen Antje, Mohammed, Katja, Sybille und Arne danke ich für die angenehme Arbeitsatmosphäre und nette Diskussionen.
Meiner größter Dank gilt meiner Familie und Dir, Uschi, weil Ihr immer für mich da seid. Ohne Euch hätte ich das alles nicht geschafft.

TABLE OF CONTENTS

SUMMARY

This thesis demonstrates the importance of advective pore water transport processes for organic matter mineralization and interfacial solute fluxes in coastal, marine sediments. Results from four *in situ* studies conducted in the intertidal of the German Wadden Sea are presented. The core part of the thesis focused on the investigation of pore water transport during inundation and exposure of sandy tidal flats and its implications for aerobic and anaerobic mineralization and nutrient release from the sediment.

In the first study, the mechanism of drainage and pore water discharge during exposure was investigated in an intertidal sand flat (Spiekeroog, Germany). This drainage was driven by a hydraulic gradient developing at ebb tide between the pore water level and the faster dropping sea water level. The relatively slow drainage transport (0.5 to 0.9 cm h^{-1}) was associated with a substantial release of pore water from a seepage face near the low water line. Between 84,000 L and 147,000 L of pore water were discharged each tidal cycle from a 3.5 km long section of the investigated tidal flat. Nutrient fluxes associated with the seepage exceeded 5 to 8-fold those fluxes caused by the combined effects of diffusion, advection and bioirrigation during inundation and may enhance primary production in the Wadden Sea. Microalgal production, tidal flat filtration of this organic matter, mineralization within the intertidal sands and the subsequent release of nutrients, thus close a recycling loop in which the seepage plays an important role.

The second study assessed the influence of pore water advection on surface mineralization rates. The temporal and spatial scales of mineralization were measured near the low water line and on the upper flat on a tidal and seasonal basis. Oxygen consumption rates were high and sulfate reduction contributed 3 % to 25 % to total mineralization. During inundation of the tidal flat, oxygen penetrated deeper into the sediment than during exposure, which could be attributed to hydrodynamic forcing during submersion. This led to higher areal oxygen consumption and lower depth integrated sulfate reduction rates in the submerged flat than during exposure. The advectively flushed surface layer of the sediment is characterized by short flow paths and low pore water residence time. An immediate feedback of benthic mineralization to the ecosystem can be provided by this “skin filtration” during inundation. Pore water concentrations of nutrients, dissolved inorganic carbon (DIC) and dissolved organic carbon (DOC) reflected seasonal changes at the upper portion of the tidal flat. Although local mineralization rates were not different between both study sites, pore water

nutrient and DIC concentrations were independent of the season and up to 15-times higher near the low water line. This could be attributed to the drainage mechanism described in the first study. The drainage affects sediment layers extending deep below the advectively flushed surface layer and is characterized by long flow paths and pore water residence times. Nutrient concentrations in these deep layers and the seepage area may reflect distant mineralization processes. This “body filtration” is only active during low tide and can act as buffered nutrient source to the ecosystem.

In the third study, advective oxygen penetration into intertidal sand flat sediment at Sylt island, Germany was investigated. Deeper oxygen penetration during inundation was directly linked to bottom water current velocities. Benthic oxygen consumption rates were high and 70 % to 90 % of oxygen consumption occurred during inundation due to the deep oxygen penetration and relatively long submersion periods of this tidal flat. Aerobic mineralization was the dominant degradation process because of the efficient supply of oxygen by advective flushing of the sediment. Oxygen consumption and sulfate reduction rates decreased from the low water line towards the upper flat and were closely linked to the inundation time of the investigated stations, indicating the importance of pore water advection for this tidal flat.

The fourth study compares benthic photosynthesis in coarse sand, fine sand and muddy sediment during inundation. Intertidal sands were shown to support relatively high benthic primary production while submersed. Gross photosynthesis was on average 4 and 11 times higher in the net autotrophic fine and coarse sand than in the net heterotrophic mud, despite higher chlorophyll content in the mud. The phototrophic community was light limited at all study sites, which was less severe at the sandy sites, and two to three times more light was available to the microalgae in the sands than in the mud. Low phaeophytin contents in the sands indicated enhanced advective flushing of decomposition products or increased turnover of algal biomass, whereas chlorophyll degradation products accumulated in the mud where transport was limited to diffusion and bioirrigation. The advective flushing of the permeable sediments may have enhanced benthic photosynthesis in the sands by counteracting a possible CO_2 limitation of the microalgae.

The studies presented in this thesis underline the important contribution of intertidal sands to organic matter mineralization, interfacial solute fluxes and primary production in coastal, marine environments. This has major implications for the Wadden Sea area, where approximately 50 % of the area is covered by intertidal sands.

ZUSAMMENFASSUNG

In der vorliegenden Arbeit wird die Bedeutung von advektiven Porenwasser-Transportprozessen für die Mineralisierung von organischem Material und Grenschicht-Flüssen gelöster Substanzen in küstennahen, marinen Sedimenten demonstriert. Es werden Ergebnisse aus vier *in situ* Studien vorgestellt, die im Gezeitenbereich des Deutschen Wattenmeeres durchgeführt wurden. Hauptsächlich befassten sich diese Arbeiten mit der Untersuchung von Porenwasser-Transport auf freigefallenen und überfluteten Sandplaten und dessen Auswirkung auf aerobe und anaerobe Mineralisierung sowie Nährstoff-Freisetzung aus dem Sediment.

In der ersten Studie wurde der Mechanismus von Drainage und Porenwasser-Freisetzung während Freifall im Gezeitenbereich einer Sandplate (Spiekeroog, Deutschland) untersucht. Die Drainage wurde durch einen hydraulischen Gradienten angetrieben, der sich während Ebbe zwischen dem Porenwasserspiegel und dem schneller abfallenden Meeresspiegel ausbildete. Der relativ langsame Drainage-Transport (0.5 bis 0.9 cm h^{-1}) war mit einer bedeutenden Freisetzung von Porenwasser aus einer Austrittszone nahe der Niedrigwasser-Linie verbunden. Zwischen 84,000 und 147,000 L Porenwasser traten pro Tidenzyklus von einem 3.5 km langen Abschnitt der untersuchten Wattfläche aus dem Sediment aus. Die damit verbundenen Nährstoff-Flüsse übertrafen die während der Wasserbedeckung zusammengenommenen Flüsse aus Diffusion, Advektion und Bioirrigation 5- bis 8-fach und könnten einen wichtigen Beitrag zur Föderung der die Primärproduktion im Wattenmeer liefern. Zwischen der Produktion von Mikroalgen, Filtration dieses organischen Materials in die Wattfläche, Mineralisierung innerhalb des Sandes und der anschliessenden Freisetzung von Nährstoffen wird ein Recycling-Kreislauf geschlossen, in dem der Porenwasser-Austritt eine wichtige Rolle spielt.

In der zweiten Studie wurde der Einfluss von Porenwasser-Advektion auf Mineralisierungsraten im oberen Sedimenthorizont untersucht. Die zeitlichen und räumlichen Skalen der Mineralisierung wurden nahe der Niedrigwasserlinie und auf der oberen Sandplate im Tidenverlauf und in verschiedenen Jahreszeiten gemessen. Die Sauerstoffzehrungsraten waren hoch und Sulfatreduktion trug zwischen 3 % und 25 % zur Gesamtmineralisierung bei. Aufgrund des Einflusses der Hydrodynamik drang Sauerstoff während der Wasserbedeckung tiefer in das Sediment ein als während des Freifallens der Wattfläche. Dies führte zu erhöhten Flächenraten der Sauerstoffzehrung und geringeren tiefenintegrierten Sulfatreduktionsraten während Wasserbedeckung im

Vergleich zur freigefallenen Wattfläche. Die advektiv durchspülte Oberflächenschicht des Sandes ist durch kurze Transportwege und geringer Aufenthaltsdauer des Porenwassers im Sediment charakterisiert. Diese „Oberflächen-Filtration“ kann zu einer schnellen Kopplung zwischen benthischer Mineralisierung und dem Ökosystem führen. Auf der oberen Sandplate zeigten die Porenwasser-Konzentrationen von Nährstoffen, gelöstem anorganischem Kohlenstoff (DIC) und gelöstem organischen Kohlenstoff (DOC) saisonal bedingte Veränderungen. Obwohl es keine Unterschiede in den lokalen Mineralisierungsraten zwischen den beiden Standorten der Sandplate gab, waren die Nährstoff- und DIC-Konzentrationen nahe der Niedrigwasserlinie unabhängig von der Jahreszeit und bis zu 15-fach höher als auf der oberen Sandplate. Dies lies sich durch den Drainage-Mechanismus erklären, der in der ersten Studie beschrieben wurde. Die Drainage wirkt sich auf tiefliegende Sedimentschichten aus, die sich weit unterhalb der advektiv durchspülten Oberflächenschicht befinden. Diese tiefen Schichten sind durch weite Transportwege und eine lange Aufenthaltsdauer des Porenwassers charakterisiert. Die Nährstoff-Konzentrationen in diesen Schichten und in der Austrittszone können weit entfernte Mineralisierungsprozesse widerspiegeln. Diese „Tiefen-Filtration“ findet nur während Ebbe statt und kann eine zeitlich gepufferte Nährstoffquelle für das Ökosystem darstellen.

In der dritten Studie wurde der advektive Sauerstoff-Eintrag in sandiges Sediment einer Wattfläche im Gezeitenbereich der Insel Sylt (Deutschland) untersucht. Das tiefere Eindringen von Sauerstoff während Wasserbedeckung war direkt von den bodennahen Strömungsgeschwindigkeiten abhängig. Die benthischen Sauerstoff-zehrungsraten waren hoch und 70 % bis 90 % der Sauerstoffzehrung fanden, aufgrund des tiefen Eindringens von Sauerstoff und der relativ langen Überflutungsdauer dieser Wattfläche, während Wasserbedeckung statt. Die aerobe Mineralisierung war der dominante Abbauprozess, da die advektive Durchspülung des Sandes zu einer effizienten Sauerstoffversorgung des Sedimentes führte. Die Sauerstoffzehrungs- und Sulfatreduktionsraten nahmen von der Niedrigwasserlinie in Richtung des oberen Gezeitenbereichs ab. Diese Abnahme war eng mit der Überflutungsdauer verknüpft, was auf die Wichtigkeit der Porenwasseradvektion für diese Sandplate hindeutet.

In der vierten Studie wurde benthische Photosynthese während Wasserbedeckung in grobem Sand, feinem Sand und schlickigem Sediment untersucht und miteinander verglichen. Es konnte gezeigt werden, dass überflutete Sande im Gezeitenbereich relativ hohe Primärproduktionsraten aufweisen können. Die Brutto-Photosynthese war im Mittel 4- und 11-fach höher im netto-autotrophen Fein- und

Grobsand als im netto-heterotrophen Schlick, trotz höherem Chlorophyll-Gehalts im schlickigen Sediment. Die phototrophe Gemeinschaft war in allen Untersuchungsgebieten Licht-limitiert, jedoch weniger stark an den sandigen Standorten. Die Mikroalgen im sandigen Sediment profitierten von einer zwei- bis dreifach höheren Licht-Verfügbarkeit im Vergleich zum Schlick. Geringe Phaeophytin-Gehalte in den Sanden deuteten auf eine erhöhte advektive Ausspülung von Abbauprodukten oder erhöhtem Umsatz von Algenbiomasse hin, wohingegen es zu einer Anreicherung von Chlorophyll-Abbauprodukten im schlickigen Sediment kam, in denen der Transport auf Diffusion und Bioirrigation beschränkt ist. Die advektive Durchspülung der permeablen Sedimente könnte zudem die benthische Photosynthese in den Sanden durch das Entgegenwirken einer möglichen CO_2-Limitierung gefördert haben.

Die Studien in der vorliegenden Arbeit unterstreichen den wichtigen Beitrag, den Sande im Gezeitenbereich zur Mineralisierung von organischem Material, zu Grenzschicht-Flüssen von gelösten Substanzen und zur Primärproduktion in küstennahen, marinen Habitaten liefern. Dies ist von besonderer Bedeutung für das Wattenmeer, wo Sande im Gezeitenbereich etwa 50 % der Gesamtfläche bedecken.

CHAPTER 1: INTRODUCTION

Marine coastal sandy sediments with low organic matter content have traditionally been considered as biogeochemical deserts and were neglected for a long time in marine research (Boudreau et al. 2001). However, some studies show that organic matter mineralization rates in sands can reach those measured in organic rich, muddy sediment (Andersen & Helder 1987, Cammen 1991, D'Andrea et al. 2002). This thesis aims to contribute to the understanding of organic matter cycling and transport processes in permeable, sandy sediments. The thesis comprises four *in situ* studies that were conducted on intertidal flats in the German Wadden Sea, located on the North European shelf. The studies focus on the investigation of pore water transport during inundation and exposure of tidal flats and its implications for aerobic and anaerobic mineralization and nutrient release from the sediment. Furthermore, a comparative study of benthic photosynthesis during inundation was conducted in sandy and muddy sediment.

1.1 THE CONTINENTAL SHELF

The continental shelf represents the transition zone between the continents and the open ocean and comprises the gentle sloping (0.1°) area between the coast and the shelf break. On a global average, the water depth of the continental shelf is 130 m but can be up to 350 meter deep in Polar Regions. The width of the continental shelf varies broadly between 1 and 1500 km with a global average of 85 km (Wollast 2002). Shelf areas comprise about 7.5 % of the world ocean surface and only about 0.5 % of the global oceans water volume. Nevertheless, the continental shelf is important for the biogeochemical cycling of organic matter and comprises highly productive ecosystems such as intertidal flats, estuaries, coral reefs and mangrove forests.

1.1.1 Shelf sediments and hydrodynamics

During glacial periods like the last one 21,000 years ago, the sea water level was approximately 125 m lower than today and large parts of today's continental shelf were terrestrial (Fleming et al. 1998). The removal of the fine fraction of the terrestrial deposits after the last sea level rise left relatively coarse and well sorted relict sediment behind (Milliman et al. 1972). Since only 7000 years have elapsed since the sea level reached almost its present height (Lambeck & Chapell 2001), the time was not sufficient for the relict sediments to come to equilibrium with the present hydrodynamic

conditions. Therefore, about 50 to 68 % of today's continental shelf is still covered by these coarse grained relict sediments (Emery 1968, Johnson & Baldwin 1986). Most of the sediment that is deposited on the shelf today is of terrestrial origin generated by erosion on land and transported via rivers. While coarse grained present sediments are deposited preferably at shallow water depths with intense hydrodynamics, the deposition of fine grained particles is restricted to areas close to river mouths, deep water with reduced hydrodynamics like the Skagerrak or Norwegian Channel in the North Sea, and mudflats in areas of large tidal range (McCave 1972, de Haas & van Weering 1997, de Haas et al. 2002).

The hydrodynamics in the outer shelf are mainly determined by wind- and density driven currents (McCave 2002). Wind stress transfers kinetic energy across the air-sea interface and creates currents and surface gravity waves. Density currents are driven by vertical and horizontal temperature and/or salinity gradients that may be generated, for example, by freshwater discharge from rivers. However, these currents are rarely strong enough to result in sediment transport.

Towards the inner shelf, hydrodynamic forcing generally increases and is largely determined by wave action and tidal currents. Due to the shallow water depth, surface gravity waves generate oscillating currents at the sea floor that are often strong enough to induce sediment transport (Denny 1988). Hydrodynamic forcing from tidal currents is particularly strong near the coast in shallow water and can also result in significant sediment transport (Nittrouer & Wright 1994, McCave 2002).

1.1.2 Production and mineralization in shelf areas

In comparison to their relatively small area, continental shelves are disproportionately productive with pelagic primary production amounting to 6 to 8 billion tons of carbon per year or 25 % of the total oceanic production (Wollast 2002). This high productivity is caused by upwelling of nutrient rich water from the deep sea near the shelf break, a considerable input of nutrients from rivers and groundwater discharge, the close coupling of the pelagic and benthic systems and Aeolian input of trace elements from the continent (Wollast 1991, Gattuso et al. 1998, Herbert 1999). Due to the shallow water column of many shelf areas, sufficient light may penetrate to the sea floor supporting benthic primary production (MacIntyre et al. 1996, Jahnke et al. 2000). Global benthic microalgal production amounts to an estimated 0.5 billion tons of carbon per year (Cahoon 1999). Twenty to 60 % of the produced organic matter is

deposited on the shelf sediments due to the shallow water column (Wollast 1991, Gattuso et al. 1998). Furthermore, large amounts of terrestrial organic matter are transported to the continental shelf by river input. These factors make the continental shelf an important site for organic matter mineralization. More than 95 % of the organic matter introduced to the continental shelf is mineralized mostly within the sediments and, to a lesser extent, in the water column (de Haas et al. 2002). Only a rather small fraction of the organic matter is exported from the shelf and significant burial of organic matter is restricted to regions where the hydrological and sedimentological conditions are favourable (e.g. continental slopes, canyons and river deltas). Since the organic matter particles undergo several cycles of deposition – mineralization – resuspension – redeposition in shelf sediments, only the most refractory organic matter is exported from the continental shelves (Bacon et al. 1994).

1.2 THE WADDEN SEA

The North Sea is a semi-enclosed shelf sea in northern Europe that covers an area of about 580,000 km² at an average water depth of 70 m. One of the largest coherent tidal flat systems of the world, the Wadden Sea, is located at the southern and eastern coasts of the North Sea.

After a period of rapid sea level rise ensuing the end of the last glaciation period 16,000 years ago, the rise decelerated and short phases of stasis or even falling sea level followed ca. 8000 years ago. This resulted in the formation of barrier spits with sand dunes in the coastal North Sea. After these spits were breached ca. 7500 to 6000 years ago by the continued sea level rise and increased tidal range, the coastal configuration of the Wadden Sea with its barrier islands developed (Flemming 2002, Reise 2005). Thus, the Wadden Sea is still very young in geological timescales.

Today, the Wadden Sea comprises about 500 km of coastline from Den Helder in the Netherlands to Blåvands Huk in Denmark and covers approximately 13,000 km² (van Beusekom & de Jonge 2002); (Fig.1). Tidal flats (littoral) contribute ca. 50 % to the total area (30 % in Sylt-Rømø and Den Helder-Texel Bight, 70 % in North Frisian and Danish Wadden Sea and 80 % in East-Frisian Wadden Sea) (Reise & Riethmüller 1998). Salt marshes, sandbanks and the barrier islands are other characteristic landscape elements. The Wadden Sea is characterized by its semi-diurnal tides and high dynamics in salinity, temperature, light and oxygen. The tidal range is 1.2 to 2 m in the Dutch and Danish Wadden Sea and reaches 3 to 3.5 m in the central Wadden Sea near the Elbe and Weser estuaries (van Beusekom 2005). While current velocities can exceed 1 m s^{-1} in the tidal channels, only 0.3 m s^{-1} is usually reached above the tidal flats (Bartholomae 1993, Bartholomae & Flemming 1993). Since tidal currents and waves can reach down to the sea floor, the Wadden Sea is subjected to considerable amounts of physical stress.

1.2.1 Biological and economic value of the Wadden Sea

Intertidal areas provide an important habitat for feeding and breeding animals at least since the Upper Cretaceous (López-Martínez et al. 2000). Today, the Wadden Sea harbours a diverse fish fauna and serves as a nursery area for several North Sea fish species (van Beek et al. 1989). The abundant brown shrimp (*Crangon crangon*) is an important prey species for fish and birds in the Wadden Sea (Lozán 1994). About 10 to 12 million breeding and migrating birds of more than 50 species use the Wadden Sea as a resting, feeding and moulting area every year (Meltofte et al. 1994). Additionally, the

Wadden Sea and its tidal flats are home of the indigenous common seal (*Phoca vitulina*), grey seal (*Halichoerus grypus*) and harbour porpoise (*Phocoena phocoena*).

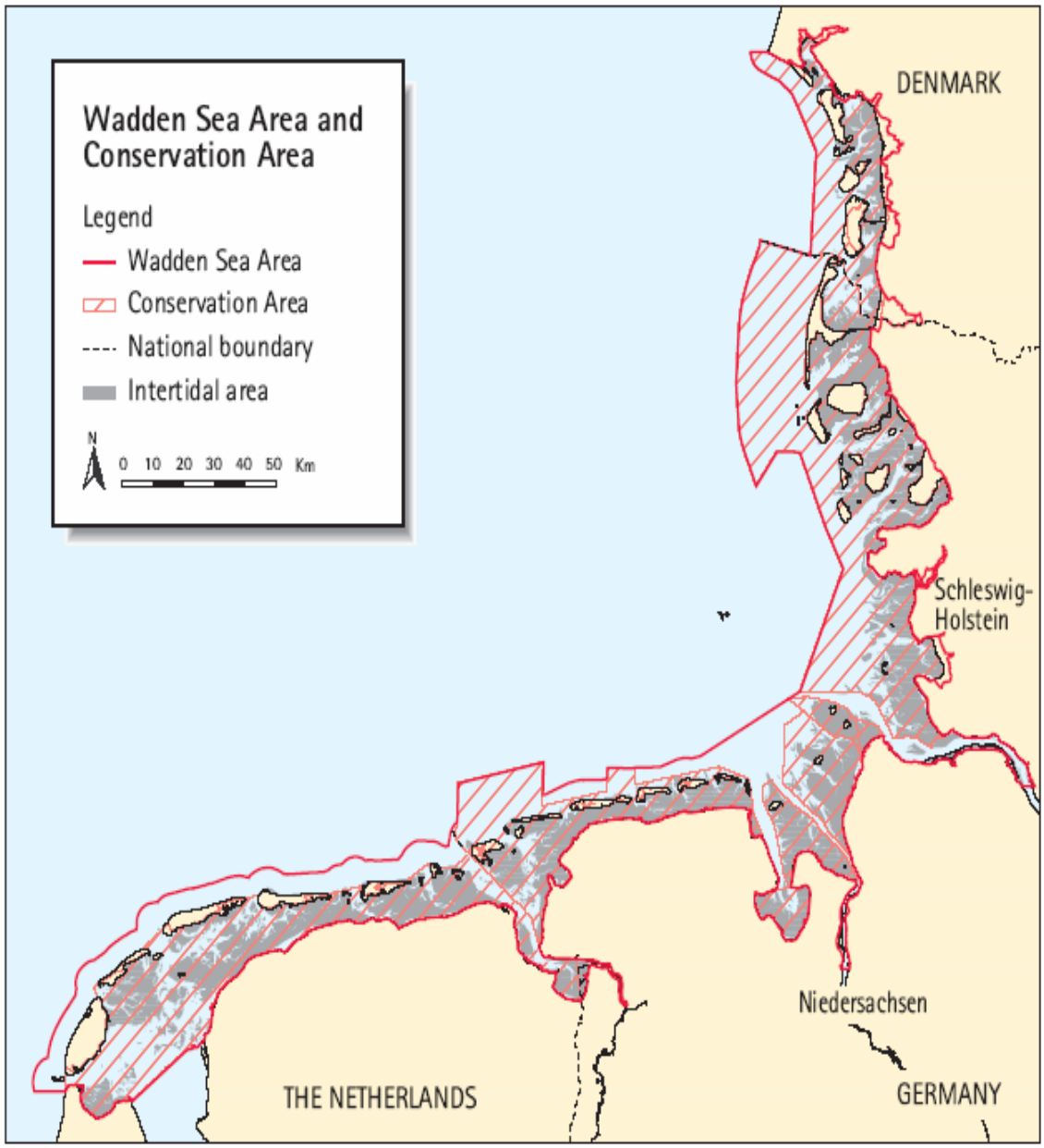

Figure 1: Wadden Sea area. Picture derived from Marencic et al. (2005).

The Wadden Sea is also of great economic and recreational value. About 3.7 million people live along its coast and 75,000 people live within the Wadden Sea area (Marencic et al. 2005). Furthermore, approximately 10 million tourists and 30 to 40 million day trippers visit the Wadden Sea area every year, creating an estimated annual turnover of 1.5 billion Euro (Gätje et al. 2005). Several gas and oil exploitation sites and a number of major ports situated within or at the border of the Wadden Sea area

(185 million tons shipping volume in 2002 (Reineking 2005)) underline the economic importance. Fishing activities within the Wadden Sea concentrate mainly on blue mussels (*Mytilus edulis*), cockle (*Cerastoderma edule*) and brown shrimp (*Crangon crangon*).

1.2.2 Consequences of human interaction with the Wadden Sea

As a consequence of human utilization of the Wadden Sea resources, increased population density and industrialization, the ecosystem changed dramatically at least since the last 1000 years (Lotze & Reise 2005 and references therein). This involves an overall simplification and homogenization of the species pool, food web and ecosystem and their goods for society (Lotze 2005). Nutrient concentrations in the Wadden Sea increased significantly since the 1950´s (Postma 1954, de Jonge & Postma 1974, van Beusekom et al. 2001, van Beusekom 2005). Adverse effects of the resulting eutrophication include a decline in seagrass communities (de Jonge & de Jong 1992), increased turbidity (de Jonge & de Jong 1992, 2002), toxic and nuisance blooms of phytoplankton and macroalgae (Lancelot et al. 1987, Reise & Siebert 1994) and the development of anoxic sediment surfaces (black spots) (Neira & Rackemann 1996, Rusch et al. 1998). The high nutrient input led to a 2 to 3-fold increase in primary production in the Wadden Sea and adjacent coastal waters during the last 50 years (Cadee 1984, de Jonge et al. 1993, Asmus et al. 1998). Consequentially, mineralization rates in the Wadden Sea increased due to the higher productivity and import of organic matter from the coastal zone to the Wadden Sea (van Beusekom et al. 1999). Van Beusekom (2005) estimated that pre-industrial primary production and mineralization in the Wadden Sea was 5 times lower than at present. During the last decade, however, the riverine nutrient input to the Wadden Sea gradually decreased. The result was a reduced phytoplankton biomass in the southern Wadden Sea suggesting a recent decrease in eutrophication (Cadee & Hegeman 2002, van Beusekom et al. 2005).

The most profound changes of the Wadden Sea ecosystem were, however, caused by the building of dikes and embankments for coastal defence and reclamation of arable land that commenced ca. 1000 years ago. The diking eventually resulted in a reduction of the Wadden Sea area to nearly half of its pristine size, straightening of the coastline and a strict separation between land and sea (Reise 2005). Large areas of mud flats, salt marshes, brackish lagoons, bogs and lakes, which characterized the pristine Wadden Sea, were cut off from the North Sea and transformed to arable land (Fig. 2).

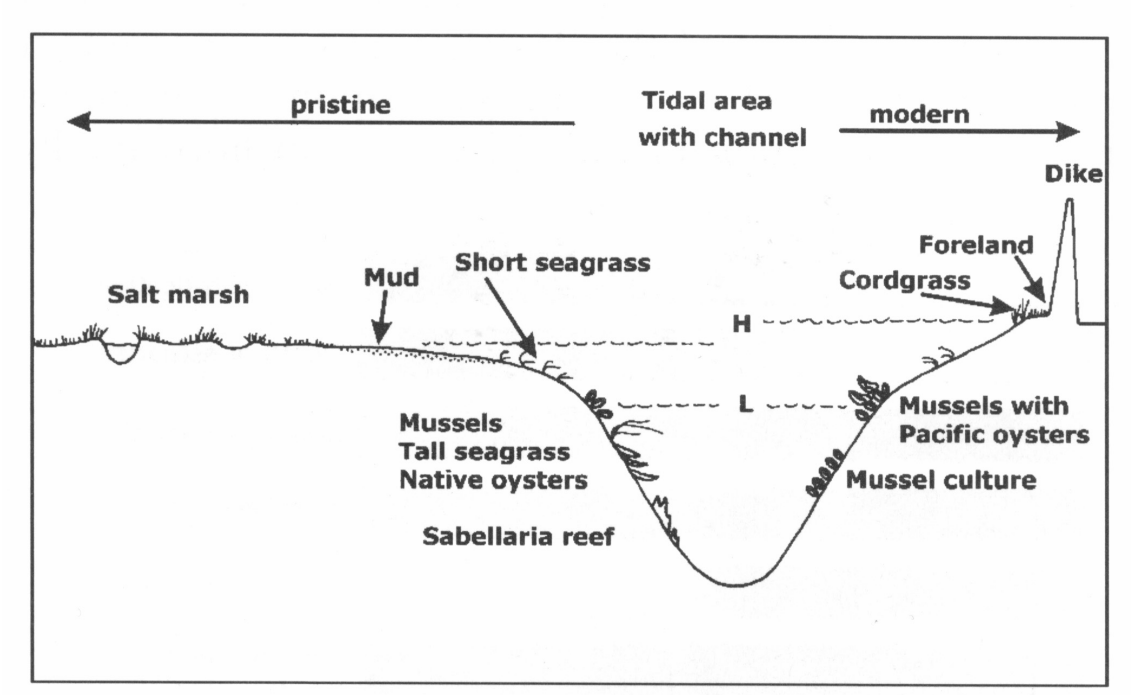

Figure 2: Schematic cross section through a tidal channel with adjacent tidal area in pristine (left) and modern time (right). H and L denote high and low tide level, respectively. Note that H but not L has risen over time. Figure reproduced from Reise (2005).

While production of organic matter in the early Wadden Sea was mainly autochthonous on the extensive mudflats and salt marshes (Reise 2005), the present Wadden Sea has to rely on an allochthonous supply of organic matter from the adjacent coastal zone (van Beusekom et al. 1999).

The narrowing of the Wadden Sea area, steeper slope in bottom topography and larger tidal range (Fig. 2) enhanced hydrodynamics. Therefore, the deposition of fine particles decreased and muddy sediments were lost from the Wadden Sea (Flemming & Nyandwi 1994). Riverine sediment loads are flushed right through the channels dredged for ship-traffic into the North Sea (Reise 2005). Today, fine to medium sands prevail in the intertidal regions of the Wadden Sea while muddy sediments are restricted to relatively narrow low energy zones close to the coastline (Flemming & Ziegler 1995). Considering the current sea level rise of approximately 1.8 mm per year and human efforts to "hold the line" against the sea, hydrodynamic forcing can be expected to increase in the future Wadden Sea. This will lead to a progressive loss of fine sediments and further dominance of sands in the Wadden Sea.

1.3 TRANSPORT AND INTERFACIAL EXCHANGE IN COASTAL MARINE SEDIMENTS

Transport processes and the interfacial exchange of solutes and particles between the sediment and water column play an important role for the biogeochemistry of marine sediments. Transport and interfacial exchange includes molecular diffusion, which transports solutes along a concentration gradient. Transport processes like faunal bioirrigation/bioturbation and pore water advection are mass transport processes with a net transport of water and/or sediment. These mechanisms involve transport of both, solutes and particles. In intertidal sediments, the dominant transport mechanism varies depending on the permeability of the sediment, sediment depth, faunal activity and tidal state (Fig. 3). All transport processes that are described in more detail below are potentially significant in the sediments of the Wadden Sea.

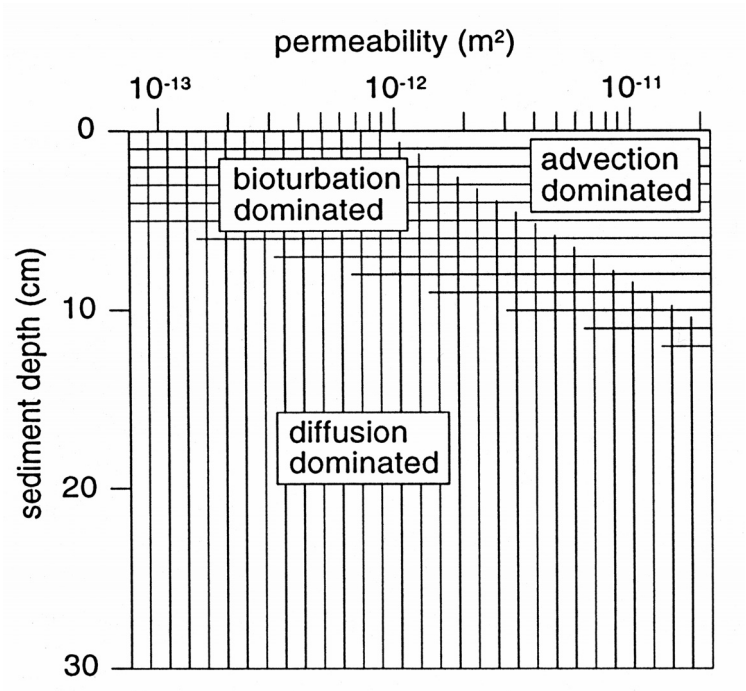

Figure 3: The permeability and depth ranges of the main transport mechanisms in aquatic environments. The zone where bioturbation is dominant is depicted for marine coastal environments. Graph derived from Huettel et al. (2003).

1.3.1 Molecular diffusion

Molecular diffusion is particularly important in fine grained, cohesive sediments, since the mass transport of water is restricted by the low permeability of these sediments. Diffusion is the random movement of soluble particles or molecules which causes a net transport from high to low concentration in the presence of a concentration gradient. Diffusion is faster for small molecules and depends on the temperature and

salinity of the seawater. The total diffusive flux J (mol m^{-2} s^{-1}) of a given solute is proportional to the concentration gradient and can be described by Fick´s first law:

$$J = -D_0 \frac{\delta C}{\delta x} \quad (1)$$

with D_0 denoting the temperature-, salinity- and substance-specific diffusion coefficient in seawater (m^{-2} s^{-1}) and $\delta C / \delta x$ the concentration gradient of the solute (mol m^{-3} m^{-1}). The ratio of the distance that a molecule travels around sediment particles and the direct path toward lower concentration is defined as the tortuosity of the sediment (Maerki et al. 2004). In order to calculate diffusive flux in sediments, D_0 must be reduced by the square of the sediment tortuosity to derive the diffusion coefficient in the sediment D_s (Boudreau 1996). Diffusive transport is only effective over small distances (µm to mm scale) since the travel time of a molecule to a certain point increases with the square of the distance. Thus, solute distribution is relatively stable in diffusion-dominated systems like cohesive sediments.

Fine grained deposits are relatively rare in the Wadden Sea (Flemming & Ziegler 1995) and mass transport processes dominate in the sands. Nevertheless, diffusive transport is important transporting solutes from deeper into the upper sediment layers where benthic animals or advective pore water flows enhance the transport. Diffusion also gains importance during low tide exposure of intertidal sand flats when most bioturbation/bioirrigation and advective pore water transport reach a minimum (Fig. 3).

1.3.2 Bioirrigation and bioturbation by benthic fauna

The activity of benthic fauna can have a profound impact on sediment biogeochemistry (Davis 1974, Aller & Aller 1998, Wenzhöfer & Glud 2004), solute and particle exchange across the sediment-water interface (Huettel 1990, Aller 1994, Graf & Rosenberg 1997) and microbial ecology (Reichardt 1988, Marinelli et al. 2002) in both sandy and muddy sediments.

Through the process of bioirrigation, animals actively ventilate their burrows with overlying seawater (Rhoads 1974, Aller 2001). The ventilation provides oxygen as well as suspended food particles to the animal and removes potentially toxic metabolites from the burrows. Natural populations (1000 to 3000 ind. m^{-2}) of an abundant polychaete in the Wadden Sea, *Nereis diversicolor*, flush impressive volumes of 2300 to 9500 L m^{-2} through their burrows every day (Vedel & Riisgård 1993). The

3-dimensional burrow mosaic in the sediment increases the exchange area between the sediment and overlying water with an oxic volume of the burrows that can be several times the volume of the oxic sediment surface (Aller 1988, Kristensen 2000).

Bioturbation, the reworking and mixing of the sediment by faunal activity, also results in enhanced solute exchange (Aller 1982) and significantly increased particle flux across the sediment-water interface, either directly through faunal activity or indirectly by the changed sediment structure and hydrodynamic conditions (Graf & Rosenberg 1997 and references therein). Populations of *Arenicola marina* (40 to 80 ind. m^{-2}), another characteristic polychaete in the Wadden Sea, can displace and mix sediment volumes of up to 400 L m^{-2} $year^{-1}$ by its feeding activity (Kristensen 2001). Thus, significant amounts of reactive organic matter may be redistributed within the sediment by bioturbation (Christensen et al. 2000, D'Andrea et al. 2004).

Bioturbation and bioirrigation of benthic fauna can substantially affect the mineralization of organic matter in marine sediments (see Section 1.5.1).

1.3.3 Pore water advection

Advective pore water transport is particularly important in permeable, sandy sediments (Huettel et al. 2003) and describes the mass transport of pore water through the sediment and exchange with the overlying water column. The pore water flow rate v in sandy, isotropic sediment is proportional to the permeability k and a pressure gradient Δp as described by a modified version of Darcy´s law:

$$v = k \frac{\rho g}{\eta \varphi} \Delta p \qquad (2)$$

with ρ denoting fluid density, g gravitational acceleration, η dynamic viscosity, and φ sediment porosity.

Permeability is a measure for the ease with which fluids can pass through a porous medium. Permeability (k) is often used equivalent to hydraulic conductivity. Permeability, however, is a function of the sediment properties only (units of squared length), whereas hydraulic conductivity (K) is a function of both sediment and fluid properties (units of length per time). Permeability depends on grain size, sorting, grain shape and sediment porosity. Permeability can be altered by biological activity. Tube-building or burrowing macrofauna can increase as well as decrease permeability (Meadows & Tait 1989, D'Andrea et al. 2002). Particles, algae and bacteria that are filtered from the water column into the permeable sediment (Huettel & Rusch 2000,

Rusch et al. 2001, Ehrenhauss et al. 2004a) can clog the interstices between sediment grains, impeding pore water flow. Permeability may also be reduced by diatoms producing adhesive extracellular polymeric substances (EPS) (Smith & Underwood 1998, Decho 2000) or by bacterial growth within the sediment (Thullner et al. 2002).

Pressure gradients of less than 1 Pa cm^{-1} are sufficient to cause advective pore water flow through sediment with permeability exceeding 10^{-12} m^2 (Huettel & Gust 1992a). These pressure gradients can be generated by density differences, bottom flow-topography interactions, undulating pressure differences between wave crests and troughs and hydrostatic pressure differences along a groundwater aquifer or between pore water and seawater level. The different advective pore water transport mechanisms are described in more detail in the following sections (see also Fig. 4).

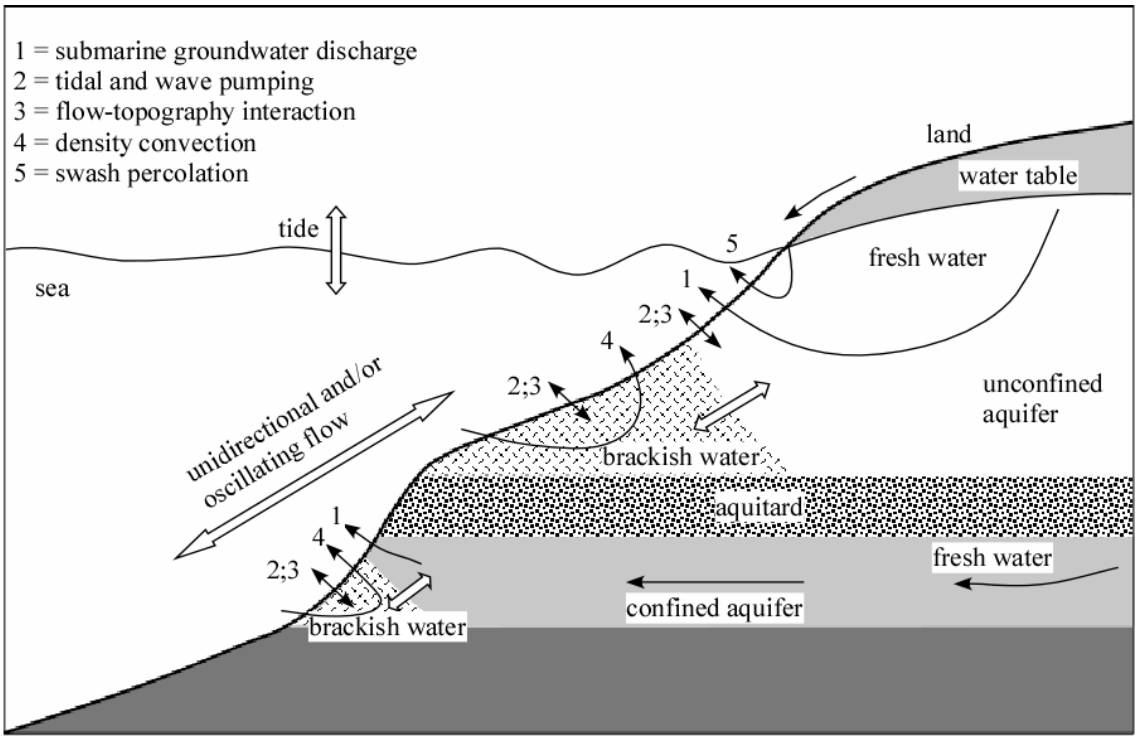

Figure 4: Mechanisms of advective pore water exchange in coastal marine systems. For details see text. Figure modified after Burnett et al. (2003).

1.3.4 Submarine groundwater discharge

Submarine groundwater discharge (SGD) has been known for many centuries. According to Kohout (1966), the Roman geographer Strabo mentioned a submarine freshwater spring about 4 km offshore near Syria in the Mediterranean 2000 years ago that was used as a source of potable water. However, SGD was studied scientifically only since Johannes (1980) showed that SGD delivered several times as much nitrate to

coastal waters in Western Australia as did river runoff. Since then, the definition of SGD was ambiguous in the literature (Younger 1996, Taniguchi et al. 2002). While only discharge of freshwater was considered by Zektser et al. (1983), other authors included also recirculated seawater to their definition of SGD (Simmons 1992, Church 1996, Moore 1997). In many studies, the driving force of the flow is considered to be the hydraulic head between an elevated terrestrial groundwater table on land and the seawater level (e.g. Reay et al. 1992, Cable et al. 1997a, Charette et al. 2003). This view will be adopted in the context of this thesis acknowledging that the discharge may also consist of recirculated seawater (No. 1 in Fig. 4). In a recent study, Burnett et al. (2003) defined SGD as "any and all flow of water on continental margins from the seabed to the coastal ocean, regardless of fluid composition or driving force". Their definition included also swash percolation, wave pumping and density convection. Groundwater (synonymous to pore water in saturated sediment) can flow through permeable sediment layers (aquifers) toward the sea (No. 1 in Fig. 4). The aquifers can be unconfined with the water table as the upper boundary and recharge mainly via the sediment surface. Alternatively, groundwater is discharged through confined aquifers that have an aquitard (low permeability) or aquiclude (completely impermeable) as an upper boundary (Fig. 4). The water table that is hydraulically connected to the confined aquifer lies above its upper boundary.

SGD has been studied extensively since the 1990´s for many regions in the world (Taniguchi et al. 2002), and can lead to discharge rates ranging between 0.5 and 90 L m^{-2} d^{-1} (Bokuniewicz & Pavlik 1990, Cable et al. 1997b, Charette et al. 2003, Schlueter et al. 2004, Taniguchi & Iwakawa 2004). Based on ^{226}Ra measurements, Moore (1996) estimated that SGD volume amounted 40 % of the river flow in the South Atlantic Bight. Large amounts of nutrients can be supplied to the coastal sea by SGD (Giblin & Gaines 1990, Reay et al. 1992, Simmons 1992, Corbett et al. 1999). In the coastal Wadden Sea, SGD is likely an important process with the discharged pore water nutrients fueling primary production.

1.3.5 Tidally driven pore water exchange

The seepage flux of SGD was found to be directly related to tidal state, in semi-diurnal to diurnal time scales as well as semi-monthly reflecting the neap-spring tidal cycle (Kim & Hwang 2002, Taniguchi 2002, Chanton et al. 2003). The tide dependent

discharge of pore water and recharge with sea water is referred to as tidal pumping (No. 2 in Fig. 4).

Tidal dynamics of the pore water table in beaches has been described by Nielsen (1990). Due to the sediment's hydraulic impedance, the pore water level drops slower than the sea water level during low tide, generating hydraulic head and pore water drainage. Since the resulting pore water discharge is slower than recharge during high tide, the water table in beaches is, on average, elevated above the mean sea level (Nielsen 1990). In addition to submarine pore water discharge (as described for SGD above) pore water may be released also above the sea level under certain conditions (Fig. 5): In relatively fine sediment (fine to medium sand) and large tidal range, the pore water table can decouple from the quickly dropping sea level and intersect with the sediment surface, creating a seepage face where pore water is discharged across the sediment-air interface (Nielsen 1990, Horn 2002).

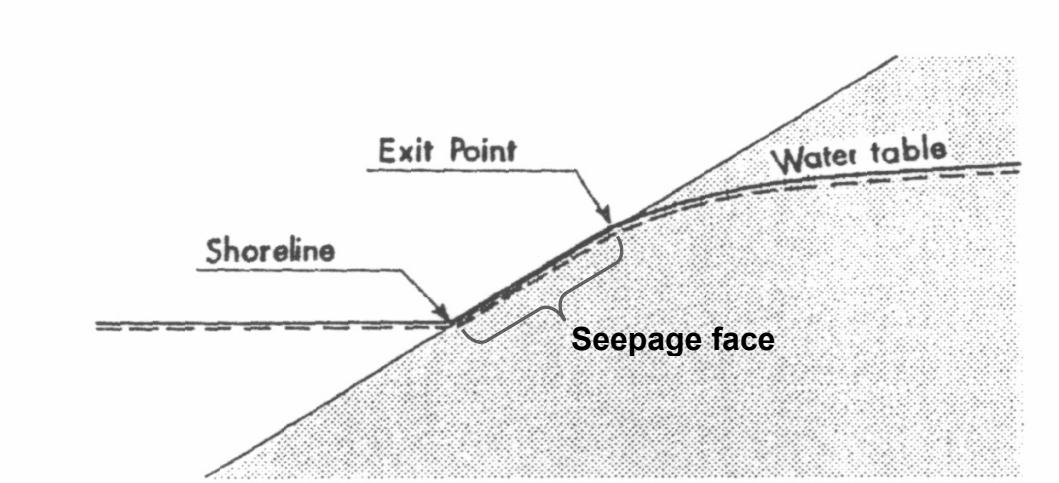

Figure 5: Decoupling of the pore water table from the sea level at large tidal range and/or relatively fine sediment. Pore water is released via the sediment/air interface from a seepage face. Figure modified after Nielsen (1990).

The same drainage and discharge mechanism described here for beaches can also be applied to other intertidal environments such as salt marshes and tidal flats. Tidally driven discharge of pore water and the associated nutrient export to the coastal sea has been well studied for beaches (Campbell & Bate 1998, Uchiyama et al. 2000, Ullman et al. 2003) and salt marshes (Agosta 1985, Jordan & Correll 1985, Harvey et al. 1987, Howes & Goehringer 1994). Pore water discharge rates ranging between 0.1 and 168 L m^{-2} d^{-1} have been determined for salt marshes (Agosta 1985, Yelverton & Hackney 1986, Whiting & Childers 1989) and large volumes of 150 to 4500 L d^{-1} are

released from beaches per meter shoreline (McLachlan & Illenberger 1986, McLachlan 1989, Campbell & Bate 1998). In a recent study conducted in the Westerschelde estuary in the Wadden Sea, Gribsholt & Kristensen (2003) suggested that substantial pore water seepage occurred at a salt marsh cliff. They observed that sulfate reduction rates accounted for more than the total carbon dioxide (TCO_2) release above the cliff, but only for 40 % of the massive TCO_2 release just below the cliff. The drainage flow can extend over horizontal distances between tens and hundreds of meters (Whiting & Childers 1989, Jahnke et al. 2003), suggesting that a local drainage-discharge of nutrients and TCO_2 may reflect distant mineralization processes.

Although drainage processes are a commonly observed feature of exposed tidal flats, very few studies have investigated and none has quantified drainage-induced discharge for this environment (Le Hir et al. 2000). In a tidal flat in Tokyo bay, drainage has been suggested a possible mechanism causing a drop in sedimentary water content during exposure (Usui et al. 1998). In contrast, Kuwae et al. (1998) concluded that pore water discharge in another tidal flat in Tokyo Bay was small, because the sediment stayed nearly water saturated during exposure. Similarly, Drabsch et al. (1999) estimated tidal pumping to be small in a New Zealand tidal flat from the observation of low pore water flow velocities. From the observation of runnel-runoff velocity in intertidal flats at the French and British coast, Le Hir et al. (2000) estimated a discharge volume of approximately 10 L m^{-2} $tide^{-1}$.

In chapter 2 of this study, a study of drainage flow, pore water discharge rates and associated nutrient release from an intertidal sand flat in the Wadden Sea is presented.

1.3.6 Interaction of boundary flow with sediment topography

Near bottom flow can be unidirectional or oscillating in shallow coastal areas. While unidirectional currents are caused by wind and tides, oscillating currents are generated at the sea floor from surface gravity waves at water depths less than half of the wavelength (Denny 1988). The interaction of these currents with sediment topography can induce advective pore water exchange (No. 3 in Fig. 4).

The flow of a unidirectional current over uneven topography, such as a mound, results in an upward deflection and deceleration of the flow upstream of the obstacle and development of a recirculation zone (Fig. 6). This causes an increase of pressure at the sediment surface upstream of the mound. Directly downstream and close to the

obstacle, flow velocity increases and the streamlines detach from the sediment surface, creating a low pressure zone.

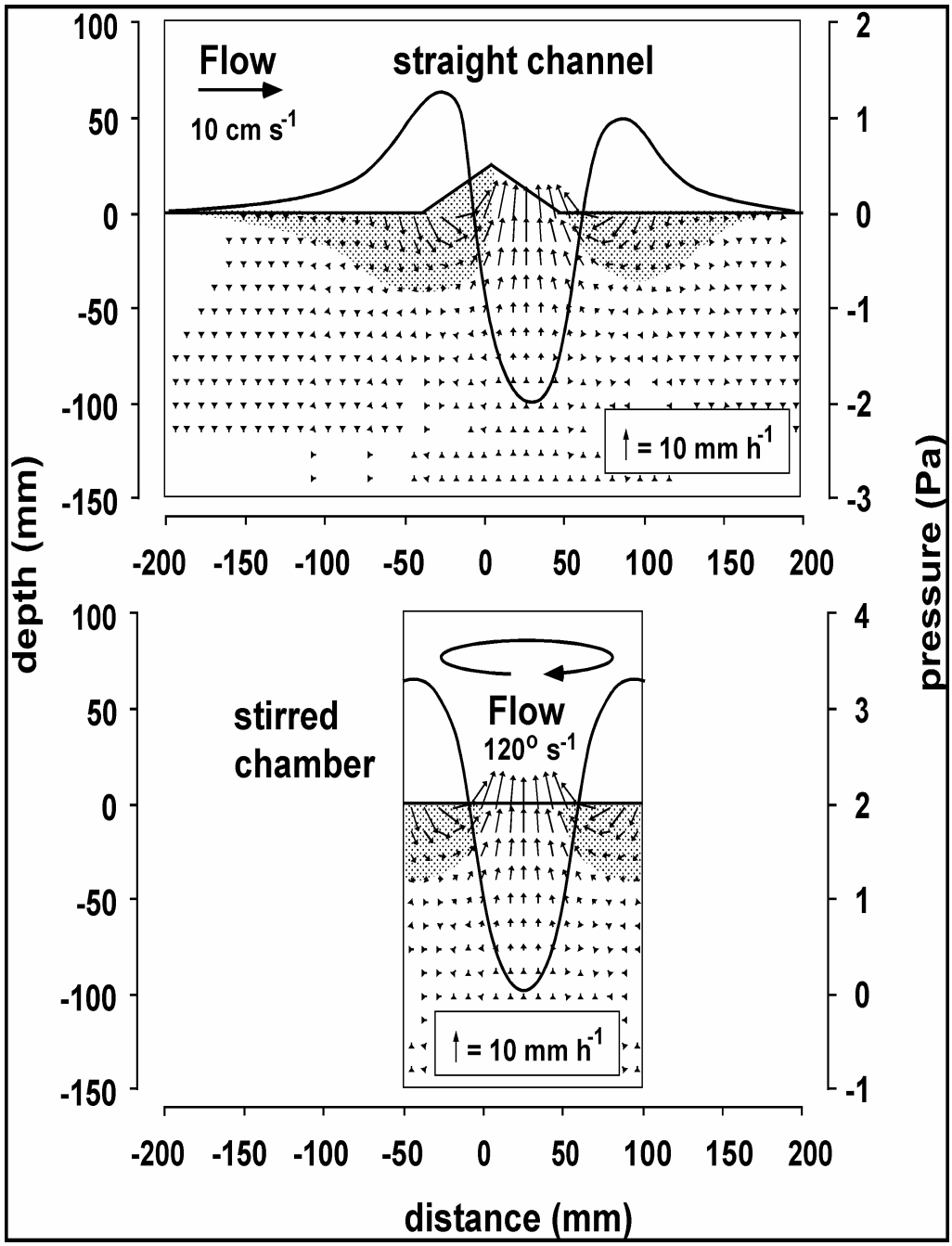

Figure 6: Advective pore water flow fields under sediment topography exposed to unidirectional flow in a straight open channel (upper part) and in sediment exposed to a rotating water column in a stirred chamber (lower part). Solid lines show the pressure distribution at the sediment–water interface. Shaded areas indicate the intrusion zones of water, and the arrows in the sediments show direction and magnitude of the advective pore water flows. Figure reproduced from Huettel & Rusch (2000).

A second high pressure zone develops downstream the obstacle, where the flow reattaches to the sediment surface. These pressure gradients can develop for numerous roughness elements at the sediment surface (e.g. wave ripples, mussel shells, burrows,

animals on the sediment surface) and were found to be positively correlated to flow velocity and obstacle height. (Huettel & Gust 1992a, Huettel et al. 1996, Hutchinson & Webster 1998).

Flow-topography interaction in permeable sediment generates pore water intrusion into the sediment in the high pressure zones upstream and downstream of the obstacle, whereas pore water is released from the sediment in the low pressure zone (Thibodeaux & Boyle 1987, Glud et al. 1996); (Fig. 6). The generated pore water flow velocities generally range between several mm to cm per hour (Huettel & Gust 1992a, Huettel et al. 1996). Pore water flow velocities in the range of several m per hour were measured for gravel sediment at high flow velocities (Thibodeaux & Boyle 1987). Since the areas of the intrusion zones are larger than the release zone (Fig. 6) and for reasons of mass balance, pore water flow velocities associated with inflow are slower than those related to outflow. Filtration rates ranging between 5 and 68 L m^{-2} d^{-1} were determined for unidirectional flow-topography interaction (Huettel & Gust 1992a, Huettel et al. 1996, Hutchinson & Webster 1998). The corresponding solute fluxes can be up to three orders of magnitude higher than molecular diffusion (Huettel & Gust 1992a).

The same physical principle generating pore water flow at unidirectional flow is also active for oscillating flow caused by wave action. In contrast to unidirectional flow, however, the pore water circulation pattern in the sediment is symmetrical, because the oscillating flow is similarly strong in both directions above an obstacle (Fig. 7).

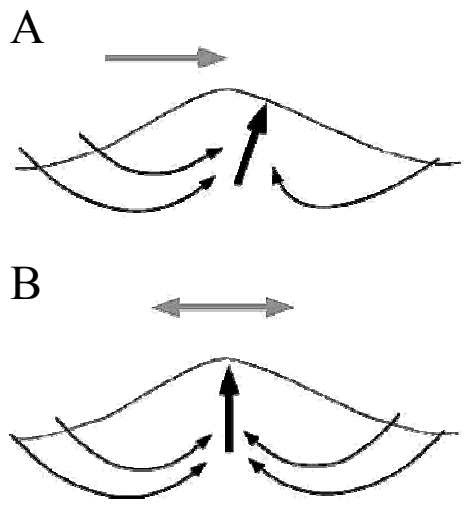

Figure 7: Schematic pore water flow fields in rippled, permeable sediment under (A) unidirectional and (B) oscillating bottom flow. Pore water is released close to the ripple crest at the ripple flanks under unidirectional flow (A) and directly from the ripple crest under oscillating flow (B). Figure modified after Precht & Huettel (2004).

Similar pore water circulation patterns have been observed in an early study with dye tracers by Webb & Theodor (1968) for oscillating flow interacting with a rippled, permeable sediment bed. The pore water flow rate was found to be dependent on the permeability of the sediment and surface gravity wave height (Webb & Theodor 1972). In later modeling studies, Shum (1992, 1993) demonstrated that the advection zone extends down to a few ripple heights into the sediment. Oxygen concentration can be many times higher below a ripple trough than at the same depth below a crest and the concentration gradient in the horizontal direction can be of the same order of magnitude as that in the vertical (Shum 1993). These modeling results were recently confirmed in laboratory wave tank experiments (Precht & Huettel 2003, Precht et al. 2004). Pore water flow velocities ranging between 2 and 50 cm h^{-1} and decreasing with sediment depth were observed Precht et al. (2004). The ensuing topography-related filtration rates ranged from 60 to 590 L m^{-2} d^{-1}, clearly exceeding the solute exchange rates caused by wave pumping (see also Section 1.3.9) or molecular diffusion (Precht & Huettel 2003). The results of these laboratory studies are consistent with *in situ* observations of wave-induced pore water flow. Wave-driven pore water flow velocities of 23 cm h^{-1} on average were determined by following the passage of a fluorescent dye tracer with optical sensors through rippled, coarse grained sediment in the Mediterranean Sea (Precht & Huettel 2004). High flow velocities up to 40 cm h^{-1} were measured directly below the ripple crest and an overall filtration rate of 140 L m^{-2} d^{-1} was calculated by the authors. Measurements of iodide tracer released above the sediment surface on the USA Middle Atlantic Bight shelf revealed pore water flow velocities of 6 to 53 cm h^{-1} at combined oscillating wave and unidirectional tidal currents (Reimers et al. 2004).

The interaction of bottom flow with sediment topography can be simulated with benthic chambers stirred with a rotating disc (Huettel & Gust 1992b, Glud et al. 1996). The stirring creates a low pressure zone in the center of the chamber and a high pressure zone near the rim (Fig. 6).

The influence of flow-topography interaction on interfacial fluxes of oxygen, dissolved inorganic carbon (DIC) and nutrients in Wadden Sea sediments was studied with benthic chambers in Chapters 2 and 5. Studies of the in situ dynamics of oxygen penetration depth in response to a natural current and wave regime and its influence on benthic mineralization rates are presented in Chapters 3 and 4.

1.3.7 Density driven pore water transport

Density driven pore water transport may be driven by differences in salinity (haline convection) and/or temperature (thermal convection) between the pore water and overlying water (Huettel & Webster 2001), (No. 4 in Fig. 4).

Haline convection occurs when bottom water with high salinity overlies pore water with a lower salinity, which leads to gravitational instability and transport of pore water out of the sediment. In the Wadden Sea, this situation may arise after a rainfall on an exposed intertidal flat that is subsequently inundated by the denser seawater during high tide. Pore water can also be less saline than the overlying seawater due to fresh water aquifers near the coast (Fig. 4). Transport by haline convection can be much more efficient than molecular diffusion as studied by Webster et al. (1996) in a laboratory flume.

Thermal convection comes into effect when relatively warm pore water is in contact with cooler, overlying seawater, e.g. due to geothermal heating (Burnett et al. 2003). Thermal convection can be effective in the Wadden Sea on a daily basis especially during the warmer seasons, when the pore water of tidal flats heats up during low tide exposure. Thermal convection led to a release of warm pore water and 75% of the accumulated ammonium pool after flooding of an intertidal flat in Portugal with cooler seawater (Rocha 1998). This mechanism can extend to sediment depths of 6 to 10 cm and may have 3 order of magnitude higher impact on sediment-water fluxes than diffusion (Rocha 2000).

1.3.8 Wave swash percolation

In coarse or pebbly sediment that is water unsaturated, wave swashes breaking on a beach can potentially percolate deep into the coarse sediment (Riedl 1971, Longuet-Higgins 1983, Li et al. 1999), (No. 5 in Fig. 4). For each meter of a beach, filtration rates of up to 85 $m^3\ d^{-1}$ were recorded (McLachlan 1989). These large volumes circulate quickly through the sediment back into the sea (McLachlan & Turner 1994) and can cause sediment oxygenation down to depths of several meters (Riedl & Machan 1972). However, in fine to medium sands, the sediment remains saturated with water due to capillarity (Gillham 1984, Drabsch et al. 1999, Atherton et al. 2001), and net swash infiltration is negligible (Turner & Nielsen 1997, Turner & Masselink 1998). Therefore, swash percolation is possibly only of minor importance in the relatively fine sands that are characteristic for the tidal flats in the Wadden Sea.

1.3.9 Wave pumping or subtidal pump

Wave pumping is caused by passage of wave crests and troughs over a permeable bed which creates undulating hydrostatic pressure gradients and interfacial pore water exchange at the sea floor (No. 2 in Fig. 4). This mechanism was described as "subtidal pump" by Riedl et al. (1972). These authors estimated that the entire ocean volume could be filtered through the shelf sands within 14,000 years by wave pumping. In later studies, the concept of the subtidal pump was extended (van der Loeff 1981, Harrison et al. 1983, Webster & Taylor 1992) and reviewed (Shum & Sundby 1996).

Wave pumping may be especially important in deeper shelf areas, where the water depth is larger than half of the maximum wavelength (Precht & Huettel 2003). In the shallow Wadden Sea, however, where the water depth is usually less than half of the wavelength, waves create oscillating flow at the sea floor (Denny 1988). The interaction of this oscillating flow with sediment topography (see Section 1.3.6) is potentially much more important for interfacial solute exchange in shallow coastal areas than wave pumping (Precht & Huettel 2003).

1.3.10 Advective particle transport

All described mechanisms of advective pore water exchange potentially result in a filtration of suspended particles from the water column into the sediment. Jenness & Duineveld (1985) suggested that tidal currents and concurrent sediment ripple movement caused burial of algae into sandy sediment of the North Sea. In flume experiments, Huettel et al. (1996) demonstrated that neutrally buoyant particles were transported into permeable sediment by bedform-induced flow. Intertidal sands of the Wadden Sea were shown to be efficient traps for detritus, bacteria, and algae from the overlying water column (Huettel & Rusch 2000, Rusch & Huettel 2000, Rusch et al. 2000, Rusch et al. 2001). Transport of diatoms into North Sea sands was recently confirmed in stirred benthic chamber experiments in the field and laboratory (Ehrenhauss & Huettel 2004, Ehrenhauss et al. 2004a). It was generally found that the permeability of the sediment, particle size (e.g. chain size in diatoms) and structure determines the particle penetration depth.

1.4 BENTHIC PHOTOSYNTHESIS IN COASTAL MARINE SEDIMENTS

The most important source of organic matter in marine systems is photosynthesis, which occurs in plants, algae and some bacteria. Aside from photosynthesis, chemoautotrophic bacteria can be important primary producers at the oxic-anoxic interface in some coastal areas (Howarth 1984); (see Section 1.5).

By the process of photosynthesis, light energy is used to drive the synthesis of organic compounds. In the light reactions of oxygenic photosynthesis, electrons are withdrawn from water and protons are transferred to nicotinamide-adenine-dinucleotide-phosphate (NADP) leading to the formation of $NADPH_2$ and oxygen:

$$H_2O + NADP \xrightarrow[2ADP + 2Pi \rightarrow 2ATP]{light} \frac{1}{2}O_2 + NADPH_2 \qquad (3)$$

Associated with this electron transport, adenosine-di-phosphate (ADP) is converted with inorganic phosphate to adenosine-tri-phosphate (ATP) (1-2 ATP for every reduced molecule of NADP). In the dark reactions (Calvin cycle), the electrons from $NADPH_2$ are used to reduce CO_2 to carbohydrate (CH_2O):

$$CO_2 + 2NADPH_2 \xrightarrow[3ATP \rightarrow 3ADP + 3Pi]{} (CH_2O) + H_2O + 2NADP \qquad (4)$$

The energy that is necessary to support the increase in free energy of the carbohydrate is provided by the concurrent breakdown of ATP in the dark reactions.

The overall photosynthesis reaction can be given in simplified form as:

$$H_2O + CO_2 \xrightarrow{light} (CH_2O) + O_2 \qquad (5)$$

Gross primary production is the amount of organic carbon produced by photosynthesis during a specific time period and corresponds to the gross evolution of oxygen, assuming no respiratory losses. Net primary production denotes gross primary production minus the oxygen or carbon losses due to autotrophic respiration over time. The primary production that is measured in natural systems often includes autotrophic as well as heterotrophic respiratory losses and is, therefore, more accurately described as net community production.

On the highly productive continental shelves, the microphytobenthos (MPB) contributes significantly to the total primary production, because enough light can reach the seafloor due to the shallow water column (MacIntyre et al. 1996, Underwood & Kromkamp 1999). In a Mississippi salt marsh, MPB provided about one third of the total primary production (Sullivan & Moncreiff 1988). The global production by MPB amounts to an estimated 0.5 billion tons of carbon per year (Cahoon 1999).

The most important MPB taxa are pennate diatoms and, to a lesser extent, centric diatoms. Other important members of MPB community include cyanobacteria, chlorophytes, dinoflagellates and euglenoids (Barranguet et al. 1997, Cahoon 1999). The abundance of MPB varies between 10^5 and 10^7 cells cm^{-3} in the upper 5 to 10 mm of the sediment, depending on location, season and sediment properties (MacIntyre et al. 1996). While the MPB is often concentrated within the uppermost few mm of the sediment in low energy, organic rich environments, functional microalgae may be uniformly distributed to sediment depths of tens of centimetres in high energy, sandy environments (Steele & Baird 1968, Fenchel & Straarup 1971).

Aside from being distributed by physical mixing, many benthic diatoms can migrate vertically in synchrony with the solar and tidal cycle (Janssen et al. 1999, Mitbavkar & Anil 2004). Typically, these diatoms move to the surface during daylight exposure and descend during inundation (Round & Palmer 1966, Paterson 1989) with a movement velocity of 1 to 25 $\mu m\ s^{-1}$ (Round 1971). Soft substrate associated diatoms capable of fast movement are traditionally assigned to the free-living epipelon, while the other, relatively immobile diatoms, contribute to the particle-attached epipsammon. The proportion of each fraction in the sediment varies with the degree of hydrodynamic exposure (de Jonge 1985), and more epipsammic than epipelic diatoms were found in sandy intertidal sediment in the Wadden Sea (Barranguet et al. 1997).

The benthic microalgae serve important functions in marine sediments. They can generate high oxygen concentrations in the surface layer of the sediment (Revsbech et al. 1980, Berninger & Huettel 1997) and influence oxygen and nutrient fluxes across the sediment water interface (Bartoli et al. 2003, Tyler et al. 2003). The MPB constitutes an important organic carbon source for heterotrophic macrofauna, meiofauna and bacteria in the sediment (Middelburg et al. 2000). Furthermore, the exudation of extracellular polymeric substances (EPS) by MPB (Smith & Underwood 1998, Decho 2000) can stabilize the sediment by increasing the erosion threshold (Widdows et al. 2000, Yallop et al. 2000).

1.4.1 Factors controlling the primary production of microphytobenthos

The primary production of MPB is controlled by a number of factors including light, biomass, temperature, salinity, nutrients and CO_2 availability.

The most obvious factor influencing primary production is light availability that varies from hourly (clouds) over daily (day/night) to seasonal (day length) time scales.

In intact sediments, benthic primary production was found to be saturated at light intensities ranging between 100 and 1260 µmol photons m^{-2} s^{-1} (MacIntyre et al. 1996 and references therein). Nevertheless, benthic microalgae appear able to sustain growth at very low light intensities of ca. 5 to 10 µmol photons m^{-2} s^{-1}, which is often well below 1 % of surface incident radiation that is generally considered to be the threshold for phytoplankton growth (Cahoon 1999). In most studies, the proportion of variability in primary production that can be explained by changes in irradiance ranges between 30 and 60 % (MacIntyre et al. 1996). However, Miles & Sundbäck (2000) found a significant relationship between production and *in situ* irradiance only at 2 subtidal sites, while no such relationship existed for an intertidal MPB community. Also in other studies of exposed intertidal flats, primary production correlated only weakly with irradiance (Colijn & de Jonge 1984, Grant 1986), even during shading of the sampling sites (Perkins et al. 2001). Possibly, light intensities were always at saturating levels during exposure of the tidal flats. Nevertheless, a significant relationship between irradiance and production exists over the full tidal cycle, as MPB productivity was shown to be dependent on tidal stage and sun angle (Pinckney & Zingmark 1991).

In intertidal environments, photoinhibition is potentially important. In principal, growth of MPB can be inhibited by strong irradiance, as was demonstrated in laboratory experiments for suspended microalgae (Blanchard et al. 2004). These authors showed that MPB productivity was initially enhanced during the first 90 minutes of exposure to strong light before being strongly inhibited. In field measurements, however, photoinhibition was generally absent (Rasmussen et al. 1983, Blanchard & Cariou-Le Gall 1994, Barranguet et al. 1998, Migne et al. 2004). This was mainly attributed to a vertical migration of the MPB into the sediment in response to strong light.

The biomass of MPB often has a patchy distribution at various temporal and spatial scales (Shaffer & Onuf 1985, Saburova et al. 1995). Short time variations in biomass at a certain sediment depth can occur due to vertical migration of the microalgae in tidal and daily rhythm (Barranguet et al. 1998, Janssen et al. 1999). Seasonal variation is particularly pronounced in temperate regions with typically high biomass during spring or summer. Spatial variation is dependent on a complex combination of factors such as sediment properties, tidal height, resuspension/deposition and grazing (Davis & David McIntire 1983, Santos et al. 1997, Blanchard et al. 2001). The biomass of MPB is often closely related to benthic primary production and typically 30 to 40% of variability in production can be explained by

changes in sedimentary chlorophyll (MacIntyre et al. 1996). Accordingly, benthic primary production was significantly correlated with MPB biomass on intertidal flats in the Dutch Wadden Sea (Cadee & Hegeman 1977, van Es 1982, Colijn & de Jonge 1984) and on the French coast (Migne et al. 2004). Muddy sediments tend to have a higher microphytobenthic biomass than sandy sediments due to the depositional nature of this low energy environment (Colijn & Dijkema 1981, de Jong & de Jonge 1995) and intertidal mudflats have long been known for high rates of benthic primary production (Pomeroy 1959, Leach 1970). Despite higher microalgal abundance in mud than in sand on an exposed intertidal flat in the Dutch Wadden Sea, however, the MPB was equally productive in both sediments on an annual basis (Barranguet et al. 1998).

Temperature can be expected to influence the chlorophyll-specific photosynthesis rate of MPB (MacIntyre et al. 1996). This has been demonstrated in laboratory experiments by Colijn & van Buurt (1975) and Rasmussen et al. (1983), who showed that the light saturated photosynthetic rate increased about 10 % per °C within a temperature range of 4° to 30°C. Light saturated photosynthesis could potentially increase by 40% during the observed temperature increase from 16°C to 25°C in the surface layer of an exposed mud flat on the French Atlantic coast (Blanchard et al. 1996). Field measurements also suggest that temperature can exert a tight control on primary production under conditions of saturating light (Grant 1986, Barranguet et al. 1998). Therefore, temperature regulation of benthic photosynthesis can be significant on exposed intertidal flats subjected to high irradiance and relatively large temperature fluctuations.

Nutrient limitation is a potentially important regulating factor for MPB growth in coastal marine systems (Granéli & Sundbäck 1985). However, studies showing enhanced growth of MPB in response to nutrient additions were conducted in mesocosms either with sieved sediment to exclude macrofauna (Nilsson et al. 1991) or by placing microbial mats on sterile sand (Pinckney et al. 1995). In natural coastal or estuarine systems, the MPB is unlikely to be limited by nutrients, because of relatively high nutrient concentrations in the water column and high mineralization rates in the sediment (Admiraal et al. 1982, MacIntyre et al. 1996). Accordingly, growth of MPB in natural, undisturbed sediment of intertidal flats is often not nutrient limited (Barranguet et al. 1998, Serôdio & Catarino 2000, Migne et al. 2004). Nevertheless, nutrient limitation might be a factor during times of low nutrient concentrations in the water

column and in coarse grained sediment where nutrients are rapidly flushed out of the photic zone.

The production of MPB can be limited by the availability of inorganic carbon, as was demonstrated in laboratory experiments by Admiraal et al. (1982) and Cook & Røy (in press). Intense CO_2 assimilation of MPB can result in pH values above 9 within the photic zone of the sediment (Revsbech & Jørgensen 1986), which reduces the concentrations of free CO_2 in the pore water. This mechanism may have limited primary production on an exposed intertidal sand flat in the Danish Wadden Sea (Rasmussen et al. 1983). Possible CO_2 limitation of MPB on intertidal flats has also been argued by Miles & Sundbäck (2000) and Perkins et al. (2001). However, benthic microalgae may counteract the lack of CO_2 by vertical migration (Kromkamp et al. 1998).

Benthic diatom populations in coastal and estuarine systems are largely insensitive to intermediate salinity fluctuations (Admiraal 1977, van Es 1982). However, in the range of low salinities (0 to 9), a salinity increase was associated with a higher MPB biomass (Santos et al. 1997). Markedly increased salinities of about 50 caused a drop in photosynthetic rate by more than 60 % in the Danish Wadden Sea (Rasmussen et al. 1983).

1.4.2 Microphytobenthos in the dynamic Wadden Sea environment

Annual benthic primary production in the intertidal of the Wadden Sea ranges between 0.1 and 367 g C m^{-2} a^{-1} (Table 1). Most of the reported values correspond well to the average benthic primary production of ca. 100 g C m^{-2} a^{-1} reported for intertidal environments (Barranguet et al. 1998 and references therein).

Table 1: Benthic primary production rates measured on intertidal flats in the Wadden Sea. Annual rates in parentheses were calculated by multiplying the reported daily rates by 270 for temperate regions according to Cahoon (1999).

Reference	mg C m^{-2} d^{-1}	g C m^{-2} a^{-1}	
Cadee & Hegeman 1974	50-1100	58-170	in situ full tidal cycle
Cadee & Hegeman 1977		29-188	in situ full tidal cycle
Asmus 1982	100-535	68	in situ high tide
van Es 1982		132	in situ low tide
Colijn & de Jonge 1984		50-250	in situ low tide
Kromkamp et al. 1995	9-103	(2-28)	laboratory
Kristensen et al. 1997		241-367	laboratory
Asmus et al. 1998		300	laboratory
Barranguet et al. 1998	350-410	(95-111)	laboratory
Wolfstein et al. 2000	0.3-449	(0.1-121)	laboratory

Most measurements of benthic primary production in the Wadden Sea were either conducted in the laboratory or during low tide in case of *in situ* studies (Table 1). The frequently turbid water near the coast limits primary production in the water column of the Wadden Sea (Veldhuis et al. 1988, Tillmann et al. 2000, Colijn & Cadee 2003) and may also restrict benthic photosynthesis during inundation. Therefore, benthic photosynthesis has been assumed to be restricted to the exposure period in several studies of intertidal environments (Serôdio & Catarino 2000, Guarini et al. 2002, Migne et al. 2004).

Nevertheless, the early studies of Cadee & Hegeman (1974) and Cadee & Hegeman (1977) suggested that benthic primary production takes place also during inundation, but their measurements integrated over the full tidal cycle. In an *in situ* study using benthic chambers with flexible tops, Asmus (1982) showed that the MPB contributed 68 % to total primary production during inundation of a sand flat in Sylt, Germany. The water is relatively clear in this area (Asmus et al. 1998) and light limitation during flooding is possibly more severe over mud flats than sand flats, as fine sediments are more easily resuspended by waves and currents. Benthic microalgae also depend on the light availability within the sediment. Since light is typically more effectively absorbed in muddy sediment than in sand (Haardt & Nielsen 1980, Kühl et al. 1994), the MPB in sandy sediment may profit from a better light availability.

Hydrodynamic forcing is strongest in high energy environments like sand flats, which can lead to recurrent mixing of the MPB from the photic sediment surface to aphotic layers and vice versa. The microalgae remain viable in the aphotic layers and show similar photosynthetic characteristics as algae from the photic layer (Blanchard & Cariou-Le Gall 1994), provided that they do not stay many days to weeks in the dark. The mixing into deeper sediment layers can be advantageous for the MPB as shown by Saburova & Polikarpov (2003), who found that 80 to 90 % of the diatom cells in depths of several cm in a sand flat consisted of dividing cells taking advantage of the more stable conditions and high nutrient concentrations at depth.

Hydrodynamic forcing can also lead to resuspension of benthic algae, leading to high turnover of algal biomass especially in sandy sediment (Middelburg et al. 2000). Steady removal of MPB by resuspension or grazing can keep the algal standing stock below the maximum carrying capacity of the system, which may be a prerequisite for high microphytobenthic productivity (Kristensen 1993, Blanchard et al. 2001).

However, high productivity can only be sustained as long as the MPB biomass is not reduced below a critical level.

In intertidal sand flats, advective flushing of the sediment or drainage discharge can transport nutrient rich pore water into the photic sediment layer (see Section 1.3), supporting MPB growth. Furthermore, recent laboratory and field studies suggest that a possible CO_2 limitation of the MPB (see Section 1.4.1) can be relieved by increased flushing of the photic sediment layer (Wenzhöfer et al. in preparation, Cook & Røy in press).

Intertidal sand flats can possibly sustain relatively high benthic primary production during inundation due to comparatively high light availability, enhanced turnover of algal biomass and advective flushing of sandy sediment. This is in contrast to mud flats that possibly receive less light during inundation. Senescent or inactive algal cells may accumulate and advective flushing is less important in the muddy sediment.

A comparative study on benthic photosynthesis during inundation was conducted in two intertidal sand flats and one mud flat in the German Wadden Sea with stirred benthic chambers in dark and light incubations (Chapter 5). The study focuses on the differences in light availability, advective flushing and metabolic state of the MPB in the three sediments.

1.5 MINERALIZATION OF ORGANIC MATTER IN COASTAL MARINE SEDIMENTS

The organic matter that is provided by benthic photosynthesis or deposited and advectively filtered from the water column constitutes an important food source for benthic fauna and microbes in the sediment. The chemical composition of organic matter can be generalized by: $(CH_2O)_x(NH_3)_y(H_3PO_4)_z$, where x, y and z depend on the origin and age of the material. The typical stoichiometry for fresh marine phytoplankton is the Redfield ratio with x = 106, y = 16, z = 1 (Redfield 1958). The C:N:P stoichiometry ratios of riverine organic matter (119:8.9:1) and marine macroalgae or seagrass (550:30:1) can be significantly different (Meybeck 1982, Atkinson & Smith 1983). Most of the organic matter is mineralized by an array of aerobic and anaerobic mineralization processes (Fig. 8) with concurrent incorporation of organic matter into microbial or faunal biomass and release of inorganic nutrients and CO_2. Prokaryotes are of particular importance in this context because of their versatile metabolism, covering both aerobic and anaerobic pathways. Prokaryotes can reach high abundances of up to 4×10^9 bacteria cm^{-3} in the sediments of the German Wadden Sea (Llobet-Brossa et al. 1998).

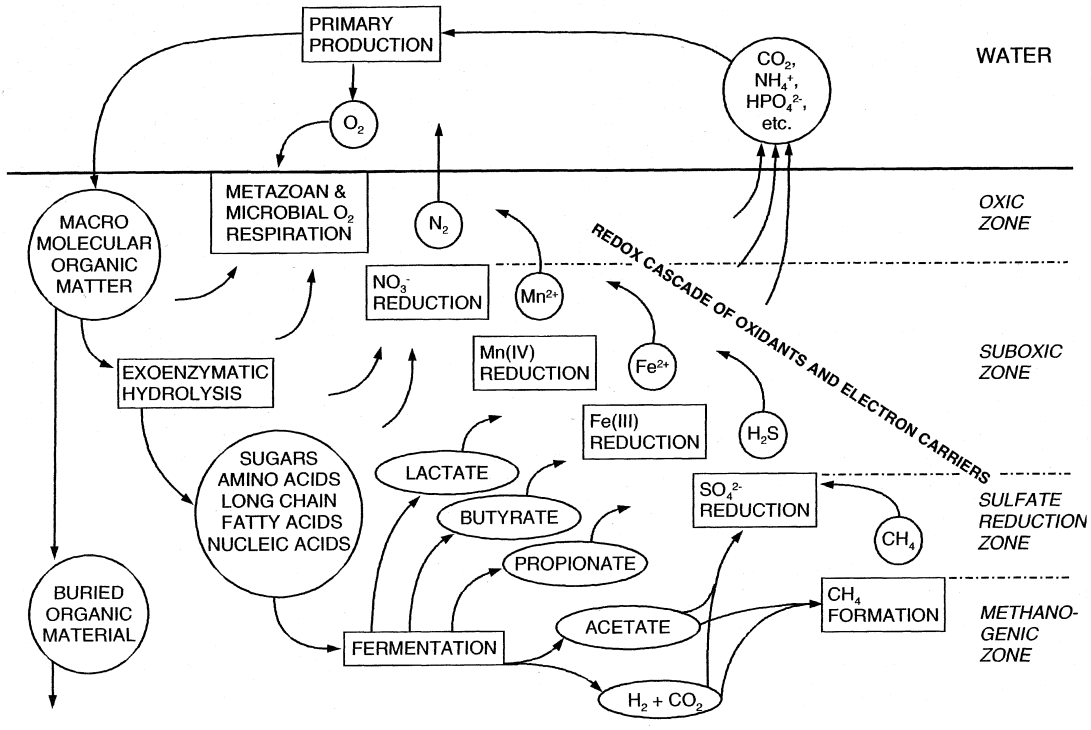

Figure 8: Pathways of organic carbon degradation in marine sediments and their relation to the geochemical zonations and consumption of oxidants. Figure reproduced from Jørgensen (2000).

A large variety of metazoans and prokaryotes can mineralize organic matter completely to inorganic nutrients, CO_2 and H_2O by using oxygen as the terminal electron acceptor according to:

$$(CH_2O)_x(NH_3)_y(H_3PO_4)_z + xO_2 \rightarrow xCO_2 + yNH_3 + zH_3PO_4 + xH_2O \quad (6)$$

The free energy yield of aerobic mineralization is highest compared to all other pathways of organic matter degradation and takes place in the uppermost, oxic sediment horizon (Fig. 8). However, oxygen penetrates only down to a few mm to cm into coastal marine sediments (Jørgensen & Revsbech 1985, Andersen & Helder 1987, Brotas et al. 1990). Therefore, anaerobic mineralization processes dominate in the bulk of the sediments.

A large fraction of more or less degraded organic matter is mineralized within suboxic and anoxic sediment layers in a stepwise process by prokaryotes. Since prokaryotes can only take up organic molecules of small molecular size (Weiss et al. 1991), large and complex polymers have to be split into soluble monomers (e.g. propionate and acetate) via hydrolysis with exoenzymes and fermentation. This initial hydrolytic and fermentative enzymatic attack of structural organic components is often the rate limiting step for anaerobic decay (Kristensen et al. 1995). In the Wadden Sea, approximately 15 to 20 % of bacteria belong to the mainly aerobic microbes that specialize on the degradation of complex organic matter (Cytophaga-Flavobacterium group); (Llobet-Brossa et al. 1998).

The small organic compounds may then be completely oxidized to H_2O and CO_2 by a number of anaerobic respiration pathways using nitrate, manganese- and iron-oxides, sulfate and CO_2 as terminal electron acceptors. In the sediment, these anaerobic respiration processes generally occur in a sequence according to the decreasing free energy yield of the individual metabolic pathways as determined by the redox potentials of the respective electron acceptors (Froelich et al. 1979) (Fig. 8). The general sequence of electron acceptors used with increasing sediment depth is: $O_2 \rightarrow NO_3^- \rightarrow Mn(IV) \rightarrow Fe(III) \rightarrow SO_4^{2-} \rightarrow CO_2$. When a favorable electron acceptor is depleted, the next favorable will be used, although there may be some vertical overlap. The gradual decrease in energy yield with sediment depth is accompanied by a smaller spectrum of substrates that the prokaryotes can use (Jørgensen 2000). The strict vertical zonation of mineralization processes shown in (Fig. 8) is, however, only valid in diffusion dominated systems (see also Section 1.5.1).

Anaerobic respiration can proceed via denitrification (eqn. 7), manganese- (eqn. 8) and iron-reduction (eqn. 9), sulfate reduction (eqn. 10) and methane production (eqn. 11). Examples of reactions are given below:

$$5CH_2O + 4NO_3^- \rightarrow 2N_2 + 4HCO_3^- + CO_2 + 3H_2O \quad (7)$$

$$CH_2O + 3CO_2 + H_2O + 2MnO_2 \rightarrow Mn^{2+} + 4HCO_3^- \quad (8)$$

$$CH_2O + 7CO_2 + 4Fe(OH)_3 \rightarrow 4Fe^{2+} + 8HCO_3^- + 3H_2O \quad (9)$$

$$CH_3COO^- + SO_4^{2-} + 2H^+ \rightarrow 2CO_2 + HS^- + 2H_2O \quad (10)$$

$$4H_2 + HCO_3^- + H^+ \rightarrow CH_4 + 3H_2O \quad (11)$$

Under anoxic conditions, the facultative anaerobic dentrifying bacteria progressively reduce nitrate via nitrite, nitrous oxide and dinitrogen oxide to nitrogen that can leave the sediment (Herbert 1999). Dentrifying bacteria perform aerobic mineralization when oxygen is present. The rate of dentrification is dependent on the nitrate concentration in the water column, but also on the rate of nitrification in the sediment and, thus, on the oxygen penetration depth (Rysgaard et al. 1995). The mineralization of organic matter by manganese- and iron reduction plays a significant role in many continental shelf areas (Sørensen & Jørgensen 1987, Hines et al. 1991, Lovley 1991). Iron reduction typically takes place only in sediment zones where oxygen, nitrate and manganese are depleted, since Fe(III) reducing bacteria preferentially perform nitrate reduction (Lovley 1991). Iron reducers contributed up to 6 % of detectable cells in muddy sediments of the Wadden Sea (Mußmann et al. 2005).

Sulfate reduction takes place below the zone of iron reduction, because iron reducers outcompete sulfate reducers for electron donors (Lovley & Phillips 1987, Chapelle & Lovley 1992). The diverse group of sulfate reducers can use a variety of electron acceptors and electron donors (Coleman et al. 1993). However, several sulfate reducers can only perform an incomplete oxidation of substrates such as lactate and propionate and their products, e.g. acetate, are subsequently decomposed by other sulfate reducing species (Widdel & Pfennig 1982, Jørgensen 2000). Sulfate reducers are among the most abundant bacteria in Wadden Sea sediment, reaching up to 6.5 to 11 % of all detectable cells (Llobet-Brossa et al. 1998, Mußmann et al. 2005). The methanogenic archaea use a narrow spectrum of substrates (H_2, formiate, acetate, CO_2). Methane forming is only active below the zone of sulfate reduction, when CO_2 is left as the only electron acceptor. Methanogens are outcompeted by sulfate reducers for

available substrates as long as sulfate is not depleted (Lovley et al. 1982, Jørgensen 2000).

The rates of the mineralization processes decrease strongly with sediment depth as caused by the less efficient electron acceptors and more refractory organic matter with depth (Kristensen 2001). Despite the relatively low rates of sulfate reduction and methanogenesis, these processes extend down to many meters into the sediment and are important on an areal basis (Jørgensen 2000). Sulfate reduction alone can contribute 25 to 50 % of organic matter mineralization in marine sediments (Jørgensen 1982). Quantitatively, aerobic respiration (especially in permeable sediment) and sulfate reduction are the most important degradation processes in shelf sediments. Often of minor importance for organic matter mineralization are the rates of denitrification (Marinelli et al. 1998, Trimmer et al. 2000) and metal reduction (Jørgensen 2000). In sandy sediments of Sylt, German Wadden Sea, contents of Fe(III) and Mn(IV) were not high enough to support a significant heterotrophic metal reduction by bacteria (de Beer et al. 2005). However, denitrification and metal reduction can be enhanced by pore water advection and faunal activity (see Section 1.5.1).

The reduced products of mineralization (NH^{4+}, NO^{2-}, H_2S, Fe^{2+}, Mn^{2+}) can be used by chemolithotrophic bacteria as electron donors. Via the pathways of nitrification, sulfide oxidation, iron- and manganese oxidation, reduced electron acceptors from anaerobic respiration are regenerated. Together with the previously described respiration pathways, these processes constitute the redox cascade depicted in (Fig. 8).

Aerobic mineralization is often difficult to assess accurately in marine sediments (Canfield et al. 1993), because a significant portion of the oxygen is used for the reoxidation of reduced inorganic metabolites from anaerobic decay (Jørgensen 1982). Therefore, the total oxygen uptake (TOU) of sediments represents an integrated signal of aerobic and anaerobic mineralization processes. Aerobic mineralization can be estimated by subtracting the amount of O_2 used in oxidizing reduced species (e.g. H_2S, Fe^{2+}, Mn^{2}+, NH_4^+) from the measured TOU (Canfield et al. 1993).

Total oxygen uptake, sulfate reduction and estimated aerobic mineralization and were studied in permeable sediment of intertidal flats in the Wadden Sea (see Chapter 3 and 4).

1.5.1 The importance of advective and faunal transport for benthic mineralization

As described in Section 1.3., pore water advection and faunal activity leads to an efficient and dynamic interfacial exchange of solutes and particles. Therefore, the distribution of electron acceptors and mineralization processes becomes much more complex and dynamic in the sediment than described for a diffusion-dominated system in the previous section.

The mixing and filtration of fresh organic matter into the sediment can enhance the overall sedimentary mineralization with labile organic matter being degraded at similar rates under oxic or anoxic conditions (Andersen 1996, Hulthe et al. 1998, Kristensen & Holmer 2001). The degradation rate of filtered organic matter (e.g. algae) may be enhanced by increased mechanical stress, direct contact with sand grain associated bacteria and high exoenzyme concentrations in the sediment (Clement et al. 1997, Huettel & Rusch 2000). Accordingly, Forster et al. (1996) recorded a stimulation of total oxygen uptake after the addition of fresh algal material to incubated sand cores. A faster disintegration of fresh algal cells filtered into permeable sediment than in the water column was shown by Huettel & Rusch (2000). A quick degradation of filtered diatom cells was also evident from a fast release of nutrients and dissolved organic carbon (DOC) from permeable North Sea sediment (Ehrenhauss et al. 2004a, Ehrenhauss et al. 2004b).

The deeper penetration and mixing of electron acceptors into the sediment by fauna or advection, either in soluble (O_2, NO_3^-, SO_4^{2-}) or particulate form (Mn(IV), Fe(III)) is another important reason for the enhancement of mineralization. The distribution of oxygen is here of particular importance due to the highly efficient and complete aerobic mineralization. At low mineralization rates, organic matter degradation was faster in the presence of oxygen than under anaerobic conditions in sandy North Sea sediment (Dauwe et al. 2001). More specifically, aerobic mineralization was found to be much faster for partly degraded and refractory organic matter (Sun et al. 1993, Kristensen et al. 1995, Hulthe et al. 1998). The available area for aerobic mineralization can be largely increased by advective pore water flow (Lohse et al. 1996, Ziebis et al. 1996) and faunal burrows (Aller 1988, Kristensen 2000).

Anaerobic mineralization activity may also be increased by advective and faunal transport. Nitrification rates are enhanced within oxic sediment layers or macrofaunal burrow walls, which in turn can stimulate denitrification activity and nitrogen release from the sediment (Kristensen et al. 1985, Huettel 1990, Lohse et al. 1993).

Furthermore, the percolation of overlying water rich in nitrate and sulfate may fuel denitrification and sulfate reduction. In strongly bioturbated sediment, metal oxides can be mixed deep into anoxic sediment layers. Under these conditions, anaerobic manganese and iron-respiration was found to be particularly important (Aller 1990, Canfield et al. 1993). The biological or physical reworking of manganese oxides from the surface sediment into underlying anoxic zones can lead to a coupled anoxic nitrification/manganese reduction in marine sediments, thereby increasing coupled sedimentary nitrification/denitrification (Hulth et al. 1999).

The TOU (total oxygen uptake = aerobic mineralization + oxidation of reduced substances from anaerobic decay) of permeable sediments has been found to scale with flow velocity and oxic sediment volume in flume experiments (Forster et al. 1996). In sandy sediment of the North Sea, *in situ* chamber incubations showed that TOU was significantly enhanced in the presence of advection (Janssen et al. 2005). In a comparative study using benthic chambers with flexible (allows wave-induced interstitial water flow) and solid tops, Malan & McLachlan (1991) demonstrated that benthic oxygen consumption was significantly increased under the influence of wave action.

Potentially inhibitory products of mineralization like CO_2, ammonium and sulfide ions can accumulate in the pore water (Joye & Hollibaugh 1995). These substances can be efficiently removed by bioirrigation and advective pore water exchange (Huettel 1990, Huettel et al. 1998), which may be a prerequisite for the further degradation of organic matter. Field observations of low pore water concentrations and the shape of nutrient profiles suggested an advective removal of mineralization products under natural conditions (Marinelli et al. 1998, D'Andrea et al. 2002). Oldham & Lavery (1999) observed that increased mean flow velocities and turbulence at the sediment-water interface in an estuary coincided with a doubling of water column ammonium concentrations.

1.5.2 Dynamic transport and implications for mineralization in the Wadden Sea

The distribution of electron acceptors and mineralization processes in the sediment is prone to constant change in the dynamic Wadden Sea environment. During inundation of intertidal flats, short term differences in bottom flow velocity may result from the turbulent water column and wave-driven oscillating currents. Tidal current velocity and direction changes during the tidal cycle and local wind conditions driving

currents and waves may change on a daily and seasonal basis. Short term variations in faunal activity and day/night changes in benthic photosynthesis may produce extremely variable and patchy sedimentary oxygen distribution (Wenzhöfer & Glud 2004). Furthermore, bioturbation can alter the sediment topography in periods of hours to days (Wheatcroft 1994) and sediment ripples may migrate in time scales of minutes. The possible implications of dynamic topography and flow velocity on sedimentary oxygen distribution are presented in Fig. 9.

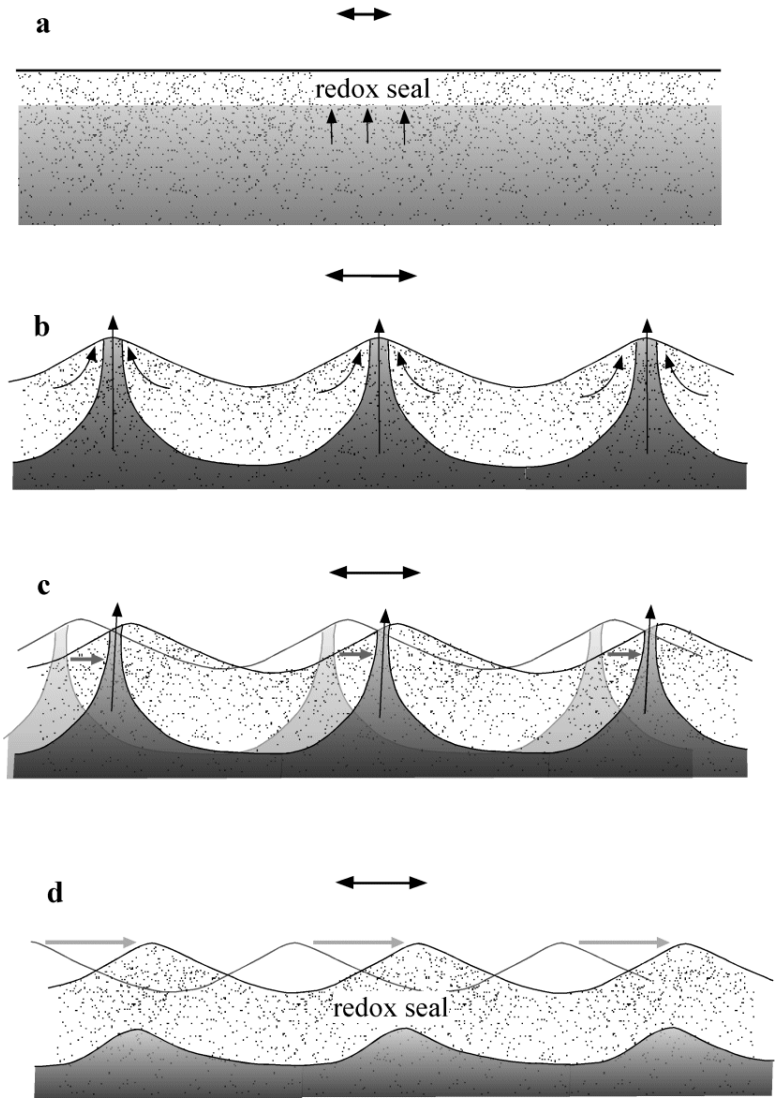

Figure 9: Effect of oscillating current velocity (black arrows) and ripple migration (grey arrows) on sediment redox conditions. a) no topography and low current velocity leads to establishment of a redox seal; b) stationary ripples, anoxic pore water is released from the ripple crests; c) ripples moving slower than the pore water, vertically alternating oxic and anoxic zones relocate corresponding to the velocity of ripple migration; d) ripples move faster than the pore water, a redox seal is established. Figure reproduced from Precht et al. (2004).

While low flow velocity over a flat bed or quickly migrating ripples may seal the anoxic sediment layer off from the sediment surface, flow over a rippled topography may lead to release of reduced substances from the sediment to the water column. The vertically alternating oxic and anoxic zones developing within a rippled bed may relocate corresponding to the speed of moderate ripple migration (c in Fig 9). Such alternating exposure to anoxic and oxic conditions leads to increased degradation of organic matter within the sediment (Andersen 1996, Hulthe et al. 1998, Kristensen & Holmer 2001). Faunal activity and advective transport during inundation affect mostly the uppermost 10 to 15 cm of the sediment. Organic matter is quickly remineralized within this surface layer and immediate feedback may be provided to the Wadden Sea ecosystem in a matter of hours to days by the removal of the metabolic products from the sediment. The supply of organic matter and electron acceptors to the sediment by advective filtration should depend on the inundation time. Thus, tidal flat areas close to the low water line may profit from a better availability of oxygen and fresh organic matter.

During exposure of intertidal flats, topography-flow interaction stops. Although some benthic bioturbators are still active during exposure (Orvain & Sauriau 2002), bioirrigation activity largely ceases. During daylight exposure, benthic microalgae may profit from a higher light availability resulting in high oxygen concentrations in the photic layer (see Section 1.4). Nevertheless, a recent *in situ* study showed that oxygen penetrated deeper during inundation than during exposure of a sandy intertidal flat (de Beer et al. 2005), stressing the importance of topography-flow interaction in permeable sediments. Since the fine to medium sands in intertidal flats of the Wadden Sea remain water saturated during low tide exposure (Drabsch et al. 1999, Atherton et al. 2001), diffusion largely governs the vertical transport of oxygen into the sediment. However, the elevated pore water level in an exposed tidal flat facilitates drainage of pore water through permeable sediment layers (see Section 1.3.5). Sediment layers extending deep below the regularly flushed upper layer can be affected by the drainage over large horizontal distances (Whiting & Childers 1989, Jahnke et al. 2003). Since the residence time of the pore water is long within these deeper layers, the feedback of mineralization products to the ecosystem is delayed. Therefore, the bulk of intertidal sand flats may act as a source of nutrients that can support primary production in the system during times of low nutrient concentrations in the sea water.

Tidal and seasonal dynamics of oxygen penetration depth, anaerobic and aerobic mineralization and pore water nutrients were investigated on two intertidal sand flats in the German Wadden Sea (Chapters 3 and 4). The studies focus on the importance of surficial and deep pore water circulation patterns as well as inundation time for benthic mineralization and interfacial nutrient exchange.

1.6 OBJECTIVES OF THE THESIS

The main focus of this thesis was the investigation of advective pore water transport in permeable sediment of intertidal flats during inundation and exposure and its implications for sedimentary aerobic and anaerobic mineralization and interfacial nutrient fluxes. A further aim was to compare the effect of advective transport and light availability on benthic photosynthesis during inundation between three intertidal sediments of different permeability. Three main study areas were chosen: A medium sand flat and a mixed sand/mud flat within the Spiekeroog backbarrier system in the East Frisian Wadden Sea and a coarse sand flat on the island of Sylt in the North Frisian Wadden Sea.

In the first study (Chapter 2), pore water seepage and the associated nutrient release from a sloping, intertidal sand flat (Janssand, Spiekeroog) during low tide exposure was investigated. The tidal dynamics of pore water drainage were measured with optical sensors in the sediment. The release of pore water and nutrients across the sediment/water and sediment/air interfaces was quantified with benthic chamber incubations and pore water collection devices.

Chapter 3 presents results of an *in situ* investigation of the tidal and seasonal dynamics of oxygen penetration depth, surface mineralization rates (oxygen consumption, sulfate reduction) and pore water nutrients in the Janssand sand flat. Concordant to the results presented in Chapter 2, two main pore water circulation patterns are hypothesized: 1) a rapid circulation through the uppermost sediment layer during inundation, characterized by short flow paths. 2) a slow pore water circulation during low tide in deeper sediment layers characterized by long flow paths and residence times.

A seasonal study of in situ transport, oxygen distribution and mineralization on a sand flat in Sylt, Germany is presented in Chapter 4. Three stations along a transect stretching from the high- towards the low water line were chosen. It was hypothesized that the tidal oxygen dynamics are closely linked to pore water advection and that the magnitude and relative importance of oxygen consumption, aerobic mineralization and sulfate reduction rates depended on the inundation time. The tidal dynamics of pore water solutes and drainage transport was investigated in this context.

Chapter 5 presents comparative measurements of benthic photosynthesis during inundation in a coarse sand (Sylt), medium sand, and mixed sand/mud flat (Spiekeroog). The specific question addressed whether benthic photosynthesis may decrease less

during inundation in sands compared to muds due to a higher light availability, enhanced solute transport and more active metabolic state of the microalgal community in sandy sediment. Interfacial fluxes of oxygen, DIC and nutrients were measured in dark and light incubations with stirred benthic chambers. Furthermore, measurements of sedimentary chlorophyll, *in situ* incident light intensity and scalar irradiance within the sediment were conducted to support the flux measurements.

LITERATURE CITED

Admiraal W. (1977) Salinity tolerance of benthic estuarine diatoms as tested with a rapid polarographic measurement of photosynthesis. Mar. Biol. 39:11-18

Admiraal W., Peletier H., Zomer H. (1982) Observations and experiments on the population dynamics of epipelic diatoms from an estuarine mudflat. Est. Coast. Shelf Sci. 14:471-487

Agosta K. (1985) The effect of tidally induced changes in the creekbank water table on pore water chemistry. Estuar. Coast. Shelf Sci. 21:389-400

Aller R. C. (1982) The effects of macrobenthos on chemical properties of marine sediment and overlying water. In: McCall D. L., Tevesz M. J. (eds) Animal-sediment relations. Plenum, New York, p 53-102

Aller R. C. (1988) Benthic fauna and biogeochemical processes in marine sediments: the role of burrow structures. In: Blackburn, T. H., Sørensen, J. (eds) Nitrogen cycling in coastal marine environments. Vol. John Wiley

Aller R. C. (1990) Bioturbation and manganese cycling in hemipelagic sediments. Philos. Trans. R. Soc. London, Ser. A 331:51-68

Aller R. C. (1994) Bioturbation and Remineralization of Sedimentary Organic-Matter - Effects of Redox Oscillation. Chem. Geol. 114:331-345

Aller R. C. (2001) Transport and reactions in the bioirrigated zone. In: Boudreau B. P., Jørgensen B. B. (eds) The Benthic Boundary Layer. Oxford University Press, Oxford, p 269-301

Aller R. C., Aller J. Y. (1998) The effect of biogenic irrigation intensity and solute exchange on diagenetic reaction rates in marine sediments. J. Mar. Res. 56:905-936

Andersen F. (1996) Fate of organic carbon added as diatom cells to oxic and anoxic marine sediment microcosms. Mar. Ecol. Prog. Ser. 134:225-233

Andersen F. O., Helder W. (1987) Comparison of Oxygen Microgradients, Oxygen Flux Rates and Electron-Transport System Activity in Coastal Marine-Sediments. Mar. Ecol.-Prog. Ser. 37:259-264

Asmus R. (1982) Field measurements on seasonal variation of the activity of primary producers on a sandy tidal flat in the northern Wadden Sea. Neth. J. Sea Res. 16:389-402

Asmus R., Jensen M. H., Murphy D., Doerffer R. (1998) Primary production of microphytobenthos, phytoplankton and the annual yield of macrophytic biomass in the Sylt-Rømø Wadden Sea. In: Gätje C., Reise K. (eds) The Wadden Sea ecosystem - Exchange, transport and transformation processes. Springer, Berlin, Heidelberg, New York, p 367-391

Atherton R. J., Baird A. J., Wiggs G. F. S. (2001) Inter-tidal dynamics of surface moisture content on a meso-tidal beach. J. Coast. Res. 17:482-489

Atkinson M. J., Smith S. V. (1983) C:N:P ratios of benthic marine plants. Limnol. Oceanogr. 28:568-574

Bacon M. P., Belastock R. A., Bothner M. H. (1994) Pb-210 balance and implications for particle-transport on the continental-shelf, US Middle Atlantic Bight. Deep-Sea Res. Part II-Top. Stud. Oceanogr. 41:511-535

Barranguet C., Herman P. M. J., Sinke J. J. (1997) Microphytobenthos biomass and community composition studied by pigment biomarkers: importance and fate in the carbon cycle of a tidal flat. J. Sea Res. 38:59-70

Barranguet C., Kromkamp J., Peene J. (1998) Factors controlling primary production and photosynthetic characteristics of intertidal microphytobenthos. Mar. Ecol. Prog. Ser. 173:117-126

Bartholomae A. (1993) Zeitliche Variabilität und räumliche Inhomogenität in den Substrateigenschaften und der Zoobenthosbesiedlung im Umfeld von Miesmuschelbänken. D. Hydrodynamik. Senckenberg am Meer Bericht 93:117-123

Bartholomae A., Flemming B. W. (1993) Zeitliche und räumliche Variabilität in den Sedimentparametern und der Morphologie auf der Gröninger Plate (Spiekerooger Watt). Senckenberg am Meer Bericht 93:5-48

Bartoli M., Nizzoli D., Viaroli P. (2003) Microphytobenthos activity and fluxes at the sediment-water interface: interactions and spatial variability. Aquat. Ecol. 37:341-349

Berninger U. G., Huettel M. (1997) Impact of flow on oxygen dynamics in photosynthetically active sediments. Aquat. Microb. Ecol. 12:291-302

Blanchard G. F., Cariou-Le Gall V. (1994) Photosynthetic characteristics of microphytobenthos in Marennes-Oleron Bay, France: preliminary results. J. Exp. Mar. Biol. Ecol. 182:1-14

Blanchard G. F., Guarini J.-M., Dang C., Richard P. (2004) Characterizing and quantifying photoinhibition in intertidal microphytobenthos. J. Phycol. 40:692-696

Blanchard G. F., Guarini J. M., Orvain F., Sauriau P. G. (2001) Dynamic behaviour of benthic microalgal biomass in intertidal mudflats. J. Exp. Mar. Biol. Ecol. 264:85-100

Blanchard G. F., Guarini J. M., Richard P., Gros P., Mornet F. (1996) Quantifying the short-term temperature effect on light-saturated photosynthesis of intertidal microphytobenthos. Mar. Ecol. Prog. Ser. 134:309-313

Bokuniewicz H., Pavlik B. (1990) Groundwater seepage along a barrier-island. Biogeochemistry 10:257-276

Boudreau B., Huettel M., Forster R., Jahnke A., McLachlan J., Middelburg J., Nielsen P., Sansone F., Taghon G., Van Raaphorst W., Webster I., Weslawski J., Wiberg P., Sundby B. (2001) Permeable Marine Sediments: Overturning an Old Paradigm. EOS Trans. Am. Geophys. Union 82:133-136

Boudreau B. P. (1996) The diffusive tortuosity of fine-grained unlithified sediments. Geochim. Cosmochim. Acta 60:3139-3142

Brotas V., Amorim-Ferreira A., Vale C., Catarino F. (1990) Oxygen profiles in intertidal sediments of Ria Formosa (S. Portugal). Hydrobiologia 207:123-129

Burnett W. C., Bokuniewicz H., Huettel M., Moore W. S., Taniguchi M. (2003) Groundwater and pore water inputs to the coastal zone. Biogeochemistry 66:3-33

Cable J. E., Burnett W. C., Chanton J. P. (1997a) Magnitude and variations of groundwater seepage along a Florida marine shoreline. Biogeochemistry 38:189-205

Cable J. E., Burnett W. C., Chanton J. P., Corbett D. R., Cable P. H. (1997b) Field evaluation of seepage meters in the coastal marine environment. Est. Coast. Shelf Sci. 45:367-375

Cadee G. C. (1984) Has input of organic matter into the western part of the Dutch Wadden Sea increased during the last decades? Neth. Inst. Sea Res. Publ. Ser 10:71-82

Cadee G. C., Hegeman J. (1974) Primary production of the benthic microflora living on tidal flats in the Dutch Wadden Sea. Neth. J. Sea Res. 8:260-291

Cadee G. C., Hegeman J. (1977) Distribution of primary production of the benthic microflora and accumulation of organic matter on a tidal flat area, Balgzand, Dutch Wadden Sea. Neth. J. Sea Res. 11:24-41

Cadee G. C., Hegeman J. (2002) Phytoplankton in the Marsdiep at the end of the 20th century; 30 years monitoring biomass, primary production and *Phaeocystis* blooms. J. Sea Res. 48:97-110

Cahoon L. B. (1999) The role of benthic microalgae in neritic ecosystems. Oceanogr. Mar. Biol., Annu. Rev. 37:47-86

Cammen L. M. (1991) Annual Bacterial Production in Relation to Benthic Microalgal Production and Sediment Oxygen-Uptake in an Intertidal Sandflat and an Intertidal Mudflat. Mar. Ecol.-Prog. Ser. 71:13-25

Campbell E. E., Bate G. C. (1998) Tide-induced pulsing of nutrient discharge from an unconfined aquifer into an Anaulus australis-dominated surf-zone. Water SA 24:365-370

Canfield D. E., Jørgensen B. B., Fossing H., Glud R. N., Gundersen J. K., Ramsing N. B., Thamdrup B., Hansen J. W., Nielsen L. P., Hall P. O. J. (1993) Pathways of organic carbon oxidation in three continental margin sediments. Mar. Geol. 113:27-40

Chanton J. P., Burnett W. C., Dulaiova H., Corbett D. R., Taniguchi M. (2003) Seepage rate variability in Florida Bay driven by Atlantic tidal height. Biogeochemistry 66:187-202

Chapelle F. H., Lovley D. R. (1992) Competitive exclusion of sulfate reduction by Fe(III)-reducing bacteria: a mechanism for producing discrete zones of high-iron ground water. Ground Water 30:29-36

Charette M. A., Splivallo R., Herbold C., Bollinger M. S., Moore W. S. (2003) Salt marsh submarine groundwater discharge as traced by radium isotopes. Mar. Chem. 84:113-121

Christensen B., Vedel A., Kristensen E. (2000) Carbon and nitrogen fluxes in sediment inhabited by suspension-feeding (*Nereis diversicolor*) and non-suspension-feeding (*Nereis virens*) polychaetes. Mar. Ecol. Prog. Ser. 192:203-217

Church T. M. (1996) An underground route for the water cycle. Nature 380:579-580

Clement T. P., Peyton B. M., Skeen R. S., Jennings D. A., Petersen J. N. (1997) Microbial growth and transport in porous media under denitrification conditions: Experiments and simulations. J. Contaminant Hydrol. 24:269-285

Coleman M. L., Hedrick D. B., Lovley D. R., White D. C., Pye K. (1993) Reduction of Fe(III) in sediments by sulfate-reducing bacteria. Nature 361:436-438

Colijn F., Cadee G. C. (2003) Is phytoplankton growth in the Wadden Sea light or nitrogen limited? J. Sea Res. 49:83-93

Colijn F., de Jonge V. N. (1984) Primary production of microphytobenthos in the Ems-Dollard estuary. Mar. Ecol. Prog. Ser. 14:185-196

Colijn F., Dijkema K. S. (1981) Species composition of benthic diatoms and distribution of Chl *a* on an intertidal flat in the Dutch Wadden Sea. Mar. Ecol. Prog. Ser. 4:9-21

Colijn F., van Buurt G. (1975) Influence of light and temperature on the photosynthetic rate of marine benthic diatoms. Mar. Biol. 31:209-214

Cook P. L. M., Roy H. (in press) Advective relief of inorganic carbon limitation in microphytobenthos in highly productive sandy sediments. Limnol. Oceanogr.

Corbett D. R., Chanton J., Burnett W., Dillon K., Rutkowski C., Fourqurean J. W. (1999) Patterns of groundwater discharge into Florida Bay. Limnol. Oceanogr. 44:1045-1055

D'Andrea A. F., Aller R. C., Lopez G. R. (2002) Organic matter flux and reactivity on a South Carolina sandflat: The impacts of porewater advection and macrobiological structures. Limnol. Oceanogr. 47:1056-1070

D'Andrea A. F., Lopez G. R., Aller R. C. (2004) Rapid physical and biological particle mixing on an intertidal sandflat. J. Mar. Res. 62:67-92

Dauwe B., Middelburg J. J., Herman P. M. J. (2001) Effect of oxygen on the degradability of organic matter in subtidal and intertidal sediments of the North Sea area. Mar. Ecol.-Prog. Ser. 215:13-22

Davis M. W., David McIntire C. (1983) Effects of physical gradients on the production dynamics of sediment-associated algae. Mar. Ecol. Prog. Ser. 13:103-114

Davis R. B. (1974) Tubificids alter profiles of redox potential and pH in profundal lake sediments. Limnol. Oceanogr. 19:342-346

de Beer D., Wenzhoefer F., Ferdelman T. G., Boehme S. E., Huettel M., van Beusekom J. E. E., Boettcher M. E., Musat N., Dubillier N. (2005) Transport and mineralization rates in North Sea sandy intertidal sediments, Sylt-Rømø Basin, Wadden Sea. Limnol. Oceanogr. 50:113-127

de Haas H., van Weering T. C. E. (1997) Recent sediment accumulation, organic carbon burial and transport in the northeastern North Sea. Mar. Geol. 136:173-187

de Haas H., van Weering T. C. E., de Stieger H. (2002) Organic carbon in shelf seas: sinks or sources, processes and products. Cont. Shelf Res. 22:691-717

de Jong D. J., de Jonge V. N. (1995) Dynamics and distribution of microphytobenthic chlorophyll-*a* in the Western Scheldt estuary (SW Netherlands). Hydrobiologia 311:21-30

de Jonge V. N. (1985) The occurrence of 'epipsammic' diatom populations: A result of interaction between physical sorting of sediment and certain properties of diatom species. Estuar. Coast. Shelf. Sci. 21:607-622

de Jonge V. N., de Jong D. J. (1992) Role of tide, light and fisheries in the decline of *Zostera marina* L. in the Dutch Wadden Sea. Neth. Inst. Sea Res. Publ. Ser. 20:161-176

de Jonge V. N., de Jong D. J. (2002) 2002) 'Global Change' impact of interannual variation in water discharge as a driving factor to dredging and spoil disposal in the river Rhine system and of turbidity in the Wadden Sea. Estuar. Coast. Shelf Sci. 55:969-991

de Jonge V. N., Essink K., Boddeke R. (1993) The Dutch Wadden Sea: a changed ecosystem. Hydrobiologia 265:45-71

de Jonge V. N., Postma H. (1974) Phosphorus compounds in the Dutch Wadden Sea. Neth. J. Sea Res. 8:139-153

Decho A. W. (2000) Microbial biofilms in intertidal systems: an overview. Cont. Shelf Res. 20:1257-1273

Denny M. W. (1988) Biology and the Mechanics of the Wave-Swept Environment, Vol. Princeton University Press

Drabsch J. M., Parnell K. E., Hume T. M., Dolphin T. J. (1999) The capillary fringe and the water table in an intertidal estuarine sand flat. Estuar. Coast. Shelf Sci 48:215-222

Ehrenhauss S., Huettel M. (2004) Advective transport and decomposition of chain-forming planktonic diatoms in permeable sediments. J. Sea. Res. 52:179-197

Ehrenhauss S., Witte U., Buhring S. L., Huettel M. (2004a) Effect of advective pore water transport on distribution and degradation of diatoms in permeable North Sea sediments. Mar. Ecol. Prog. Ser. 271:99-111

Ehrenhauss S., Witte U., Janssen F., Huettel M. (2004b) Decomposition of diatoms and nutrient dynamics in permeable North Sea sediments. Cont. Shelf Res. 24:721-737

Emery K. O. (1968) Relict sediments on continental shelves of the world. Am. Assoc. Pet. Geol. Bull. 52:445-464

Fenchel T., Straarup B. J. (1971) Vertical distribution of photosynthetic pigments and the penetration of light in marine sediments. Oikos 22:172-182

Fleming K., Johnston P., Zwartz D., Yokoyama Y., Lambeck K., Chappell J. (1998) Refining the eustatic sea-level curve since the last glacial maximum using far- and intermediate-field sites. Earth Planet. Sci. Lett. 163:327-342

Flemming B. W. (2002) Effects of climate and human interventions on the evolution of the Wadden Sea depositional system (southern North Sea). In: Wefer G., Berger W., Behre K. E., Jansen E. (eds) Climate development and history of the North Atlantic realm. Springer, Berlin, Heidelberg, New York, p 399-413

Flemming B. W., Nyandwi N. (1994) Land reclamation as a cause of fine-grained sediment depletion in backbarrier tidal flats (southern North Sea). Neth. J. Aquat. Ecol. 28:299-307

Flemming B. W., Ziegler K. (1995) High-resolution grain size distribution patterns and textural trends in the backbarrier environment of Spiekeroog Island (southern North Sea). Senckenb. Marit. 26:1-24

Forster S., Huettel M., Ziebis W. (1996) Impact of boundary layer flow velocity on oxygen utilisation in coastal sediments. Mar. Ecol.-Prog. Ser. 143:173-185

Froelich P. N., Klinkhammer G. P., Bender M. L., Luedtke N. A., Heath G. R., Cullen D., Dauphin P., Hammond D., Hartman B., Maynard V. (1979) Early Oxidation of Organic-Matter in Pelagic Sediments of the Eastern Equatorial Atlantic - Suboxic Diagenesis. Geochim. Cosmochim. Acta 43:1075-1090

Gätje C., Laursen K., Eekhof H., Borchardt T. (2005) Tourism and recreation. In: Essink K., Dettmann C., Farke H., Laursen K., Lüerßen G., Marencic H., Wiersinga W. (eds) Wadden Sea quality status report 2004. Wadden Sea ecosystem No. 19. Trilateral monitoring and assessment group. Common Wadden Sea Secretariat (CWSS), Wilhelmshaven, Germany, p 39-48

Gattuso J.-P., Frankignoulle M., Wollast R. (1998) Carbon and carbonate metabolism in coastal aquatic ecosystems. Annu. Rev. Ecol. Syst. 29:405-434

Giblin A. E., Gaines A. G. (1990) Nitrogen inputs to a marine embayment - the importance of groundwater. Biogeochemistry 10:309-328

Gillham R. W. (1984) The capillary-fringe and its effect on water-table response. J. Hydrol. 67:307-324

Glud R. N., Forster S., Huettel M. (1996) Influence of radial pressure gradients on solute exchange in stirred benthic chambers. Mar. Ecol. Prog. Ser. 141:303-311

Graf G., Rosenberg R. (1997) Bioresuspension and biodeposition: A review. J. Mar. Syst. 11:269-278

Granéli E., Sundbäck K. (1985) The response of planktonic and microbenthic algal assemblages to nutrient enrichment in shallow coastal waters, southwest Sweden. J. Exp. Mar. Biol. Ecol. 85:253-268

Grant J. (1986) Sensitivity of benthic community respiration and primary production to changes in temperature and light. Mar. Biol. 90:299-306

Gribsholt B., Kristensen E. (2003) Benthic metabolism and sulfur cycling along an inundation gradient in a tidal Spartina anglica salt marsh. Limnol. Oceanogr. 48:2151-2162

Guarini J. M., Cloern J. E., Edmunds J., Gros P. (2002) Microphytobenthic potential productivity estimated in three tidal embayments of the San Francisco Bay: a comparative study. Estuaries 25:409-417

Haardt H., Nielsen G. A. E. (1980) Attenuation measurements of monochromatic light in marine sediments. Oceanol. Acta 3:333-338

Harrison W. D., Musgrave D., Reeburgh W. S. (1983) A Wave-Induced Transport Process in Marine-Sediments. J. Geophys. Res. -Oceans and Atmospheres 88:7617-7622

Harvey J. W., Germann P. F., Odum W. E. (1987) Geomorphological control of subsurface hydrology in the creekbank zone of tidal marshes. Estuar. Coast. Shelf Sci. 25:677-691

Herbert R. A. (1999) Nitrogen cycling in coastal marine ecosystems. Fems Microbiol. Rev. 23:563-590

Hines M. E., Bazylinski D. A., Tugel J. B., Lyons W. B. (1991) Anaerobic microbial biogeochemistry in sediments from two basins in the Gulf of Maine: Evidence for iron and manganese reduction. Est. Coast. Shelf Sci. 32:313-324

Horn D. P. (2002) Beach groundwater dynamics. Geomorphology 48:121-146

Howarth R. W. (1984) The ecological significance of sulfur in the energy dynamics of salt marsh and coastal marine sediments. Biogeochemistry 1:5-27

Howes B. L., Goehringer D. D. (1994) Porewater drainage and dissolved organic carbon and nutrient losses through the intertidal creekbanks of a New England salt marsh. Mar. Ecol. Prog. Ser. 114:289-301

Huettel M. (1990) Influence of the lugworm Arenicola marina on porewater nutrient profiles of sand flat sediments. Mar. Ecol. Prog. Ser. 62:241-248

Huettel M., Gust G. (1992a) Impact of bioroughness on interfacial solute exchange in permeable sediments. Mar. Ecol. Prog. Ser. 89:253-267

Huettel M., Gust G. (1992b) Solute release mechanisms from confined sediment cores in stirred benthic chambers and flume flows. Mar. Ecol. Prog. Ser. 82:187-197

Huettel M., Røy H., Precht E., Ehrenhauss S. (2003) Hydrodynamical impact on biogeochemical processes in aquatic sediments. Hydrobiologia 494:231-236

Huettel M., Rusch A. (2000) Transport and degradation of phytoplankton in permeable sediment. Limnol. Oceanogr. 45:534-549

Huettel M., Webster I. T. (2001) Porewater flow in permeable sediments. In: Boudreau B. P., Jørgensen B. B. (eds) The Benthic Boundary Layer. Oxford University Press, Oxford, p 144-179

Huettel M., Ziebis W., Forster S. (1996) Flow-induced uptake of particulate matter in permeable sediments. Limnol. Oceanogr. 41:309-322

Huettel M., Ziebis W., Forster S., Luther G. W. (1998) Advective transport affecting metal and nutrient distributions and interfacial fluxes in permeable sediments. Geochim. Cosmochim. Acta 62:613-631

Hulth S., Aller R. C., Gilbert F. (1999) Coupled anoxic nitrification manganese reduction in marine sediments. Geochim. Cosmochim. Acta 63:49-66

Hulthe G., Hulth S., Hall P. O. J. (1998) Effect of oxygen on degradation rate of refractory and labile organic matter in continental margin sediments. Geochim. Cosmochim. Acta 62:1319-1328

Hutchinson P. A., Webster I. T. (1998) Solute uptake in aquatic sediments due to current-obstacle interactions. J. Environ. Eng. -ASCE 124:419-426

Jahnke R. A., Alexander C. R., Kostka J. E. (2003) Advective pore water input of nutrients to the Satilla River Estuary, Georgia, USA. Estuar. Coast. Shelf Sci. 56:641-653

Jahnke R. A., Nelson J. R., Marinelli R. L., Eckman J. E. (2000) Benthic flux of biogenic elements on the Southeastern US continental shelf: influence of pore water advective transport and benthic microalgae. Cont. Shelf Res. 20:109-127

Janssen F., Huettel M., Witte U. (2005) Pore-water advection and solute fluxes in permeable marine sediments (II): Benthic respiration at three sandy sites with different permeabilities (German Bight, North Sea). Limnol. Oceanogr. 50:779-792

Janssen M., Hust M., Rhiel E., Krumbein W. E. (1999) Vertical migration behaviour of diatom assemblages of Wadden Sea sediments (Dangast, Germany): a study using cryo-scanning electron microscopy. Internatl. Microbiol. 2:103-110

Jenness M. I., Duineveld G. C. A. (1985) Effects of Tidal Currents on Chlorophyll a Content of Sandy Sediments in the Southern North-Sea. Mar. Ecol.-Prog. Ser. 21:283-287

Johannes R. E. (1980) The Ecological Significance of the Submarine Discharge of Groundwater. Mar. Ecol.-Prog. Ser. 3:365-373

Johnson H. D., Baldwin C. T. (1986) Shallow Siliclastic Seas. In: Reading H. G. (ed) Sedimentary environments and facies. Blackwell Scientific Publications, p 229-282

Jordan T. E., Correll D. L. (1985) Nutrient chemistry and hydrology of interstitial water in brackish tidal marshes of Chesapeake Bay. Estuar. Coast. Shelf Sci. 21:45-55

Jørgensen B. B. (1982) Mineralization of Organic-Matter in the Sea Bed - the Role of Sulfate Reduction. Nature 296:643-645

Jørgensen B. B. (2000) Bacteria and marine biogeochemistry. In: Schulz H. D., Zabel M. (eds) Marine Geochemistry. Springer Verlag, Berlin, p 173-207

Jørgensen B. B., Revsbech N. P. (1985) Diffusive Boundary-Layers and the Oxygen-Uptake of Sediments and Detritus. Limnol. Oceanogr. 30:111-122

Joye S. B., Hollibaugh J. T. (1995) Influence of sulfide inhibition of nitrification on nitrogen regeneration in sediments. Science 270:623-625

Kim G., Hwang D.-W. (2002) Tidal pumping of groundwater into the coastal ocean revealed from submarine ^{222}Rn and CH_4 monitoring. Geophys. Res. Lett. 29:1678, doi:1610.1029/2002GL015093

Kohout F. A. (1966) Submarine springs: a neglected phenomenon of coastal hydrology. Hydrology 26:391-413

Kristensen E. (1993) Seasonal variations in benthic community metabolism and nitrogen dynamics in a shallow, organic-poor Danish lagoon. Estuar. Coast. Shelf. Sci. 36:565-586

Kristensen E. (2000) Organic matter diagenesis at the oxic/anoxic interface in coastal marine sediments, with emphasis on the role of burrowing animals. Hydrobiologia 426:1-24

Kristensen E. (2001) Impact of polychaetes (Nereis spp. and Arenicola marina) on carbon biogeochemistry in coastal marine sediments. Geochem. Trans. 2:92-103

Kristensen E., Ahmed S. I., Devol A. H. (1995) Aerobic and anaerobic decomposition of organic matter in marine sediment: Which is fastest? Limnol. Oceanogr. 40:1430-1437

Kristensen E., Holmer M. (2001) Decomposition of plant materials in marine sediment exposed to different electron acceptors (O_2, NO_3^-, and SO_4^{2-}), with emphasis on substrate origin, degradation kinetics, and the role of bioturbation. Geochim. Cosmochim. Acta 65:419-433

Kristensen E., Jensen M. H., Andersen T. K. (1985) The impact of polychaete (Nereis virens Sars) burrows on nitrification and nitrate reduction in estuarine sediments. J. Exp. Mar. Biol. Ecol. 85:75-91

Kristensen E., Jensen M. H., Jensen K. M. (1997) Temporal variations in microbenthic metabolism and inorganic nitrogen fluxes in sandy and muddy sediments of a tidally dominated bay in the northern Wadden Sea. Helgol. Mar. Res. 51:295-320

Kromkamp J., Barranguet C., Peene J. (1998) Determination of microphytobenthos PSII quantum efficiency and photosynthetic activity by means of variable chlorophyll fluorescence. Mar. Ecol. Prog. Ser. 162:45-55

Kromkamp J., Peene J., van Rijswijk P., Sandee A., Goosen N. (1995) Nutrients, light and primary production by phytoplankton and microphytobenthos in the eutrophic, turbid Westerschelde estuary (The Netherlands). Hydrobiologia 311:9-19

Kühl M., Lassen C., Jørgensen B. B. (1994) Light penetration and light intensity in sandy sediments measured with irradiance and scalar irradiance fiber-optic microprobes. Mar. Ecol. Prog. Ser. 105:139-148

Kuwae T., Hosokawa Y., Eguchi N. (1998) Dissolved inorganic nitrogen cycling in Banzu intertidal sand-flat, Japan. Mangroves Salt Marshes 2:167-175

Lambeck K., Chapell J. (2001) Sea level change through the last glacial cycle. Science 292:679-686

Lancelot C., Billen G., Sournia A., Weisse T., Colijn F., Veldhuis M. J. W., Davies A. (1987) *Phaeocystis* blooms and nutrient enrichment in the continental coastal zones of the North Sea. Ambio 16:38-46

Le Hir P., Roberts W., Cazaillet O., Christie M., Bassoullet P., Bacher C. (2000) Characterization of intertidal flat hydrodynamics. Cont. Shelf Res. 20:1433-1459

Leach J. H. (1970) Epibenthic algal production in an intertidal mudflat. Limnol. Oceanogr. 15:514-521

Li L., Barry D. A., Stagnitti F., Parlange J. Y. (1999) Submarine groundwater discharge and associated chemical input to a coastal sea. Water Resour. Res. 35:3253-3259

Llobet-Brossa E., Rossello-Mora R., Amann R. (1998) Microbial community composition of wadden sea sediments as revealed by flourescence in situ hybridization. Appl. Environ. Microbiol. 64:2691-2696

Lohse L., Epping E. H. G., Helder W., vanRaaphorst W. (1996) Oxygen pore water profiles in continental shelf sediments of the North Sea: Turbulent versus molecular diffusion. Mar. Ecol.-Prog. Ser. 145:63-75

Lohse L., Malschaert J. F. P., Slomp C. P., Helder W., Van Raaphorst W. (1993) Nitrogen cycling in North-Sea sediments - Interaction of denitrification and nitrification in offshore and coastal areas. Mar. Ecol. Prog. Ser. 101:283-296

Longuet-Higgins M. S. (1983) Wave Set-up, Percolation and Undertow in the Surf Zone. Proc. R. Soc. London Ser. A-Math. Phys. Eng. Sci. 390:283-&

López-Martínez N., Moratalla J. J., Sanz J. L. (2000) Dinosaurs nesting on tidal flats. Palaeogeogr. Palaeoclimatol. Palaeoecol. 160:153-163

Lotze H. K. (2005) Radical changes in the Wadden Sea fauna and flora over the last 2,000 years. Helgol. Mar. Res. 59:71-83

Lotze H. K., Reise K. (2005) Ecological history of the Wadden Sea. Helgol. Mar. Res. 59:1

Lovley D. R. (1991) Dissimilatory Fe(III) and Mn(IV) Reduction. Microbiol. Rev. 55:259-287

Lovley D. R., Dwyer D. F., Klug M. J. (1982) Kinetic-analysis of competition between sulfate reducers and methanogens for hydrogen in sediments. Appl. Environ. Microbiol. 43:1373-1379

Lovley D. R., Phillips E. J. P. (1987) Competitive mechanisms for inhibition of sulfate reduction and methane production in the zone of ferric iron reduction in sediments. Appl. Environ. Microbiol. 53:2636-2641

Lozán J. L. (1994) Über die ökologische und wirtschaftliche Bedeutung der Nordseegarnele im Wattenmeer mit Bemerkungen über andere Krebsarten. In: Lozán J. L., Rachor E., Reise K., Westernhagen H. V., Lenz W. (eds) Warnsignale aus dem Wattenmeer. Blackwell, Berlin, p 117-122

MacIntyre H. L., Geider R. J., Miller D. C. (1996) Microphytobenthos: The ecological role of the 'Secret Garden' of unvegetated, shallow-water marine habitats. I. Distribution, abundance and primary production. Estuaries 19:186-201

Maerki M., Wehrli B., Dinkel C., Müller B. (2004) The influence of tortuosity on molecular diffusion in freshwater sediments of high porosity. Geochim. Cosmochim. Acta 68:1519-1528

Malan D. E., McLachlan A. (1991) In situ benthic oxygen fluxes in a nearshore coastal marine system - a new approach to quantify the effect of wave action. Mar. Ecol.-Prog. Ser. 73:69-81

Marencic H., Essink K., Kellermann A., Eskildsen K. (2005) Introduction. In: Essink K., Dettmann C., Farke H., Laursen K., Lüerßen G., Marencic H., Wiersinga W. (eds) Wadden Sea quality status report 2004. Wadden Sea ecosystem No. 19. Trilateral monitoring and assessment group. Common Wadden Sea Secretariat (CWSS), Wilhelmshaven, Germany, p 11-25

Marinelli R. L., Jahnke R. A., Craven D. B., Nelson J. R., Eckman J. E. (1998) Sediment nutrient dynamics on the South Atlantic Bight continental shelf. Limnol. Oceanogr. 43:1305-1320

Marinelli R. L., Lovell C. R., Wakeham S. G., Ringelberg D. B., White D. C. (2002) Experimental investigation of the control of bacterial community composition in macrofaunal burrows. Mar. Ecol. Prog. Ser. 235:1-13

McCave I. N. (1972) Transport and escape of fine-grained sediment from shelf areas. In: Swift D. J. P., Duane D. B., Pilkey O. H. (eds) Shelf sediment transport: process and pattern. Hutchinson & Ross, Dowden, p 225-248

McCave I. N. (2002) Sedimentary settings on continental margins - an overview. In: Wefer G., Billet D., Hebbeln D., Jørgensen B. B., Schlüter M., van Weering T. C. E. (eds) Ocean margin systems. Springer, p 1-14

McLachlan A. (1989) Water filtration by dissipative beaches. Limnol. Oceanogr. 34:774-780

McLachlan A., Illenberger W. (1986) Significance of groundwater nitrogen input to a beach surf zone ecosystem. Stygologia 2:291-296

McLachlan A., Turner I. (1994) The Interstitial Environment of Sandy Beaches. Mar. Ecol.-Pubbl. Stn. Zool. Napoli 15:177-211

Meadows P. S., Tait J. (1989) Modification of sediment permeability and shear-strength by 2 burrowing invertebrates. Mar. Biol. 101:75-82

Meltofte H., Blew J., Frikke J., Rösner H.-U., Smit C. J. (1994) Numbers and distribution of waterbirds in the Wadden Sea. Results and evaluation of 36 simultaneous counts in the Dutch-German-Danish Wadden Sea 1980-1991. IWRB Publ. 34. Water Study Group Bull. 74, Special Issue:1-92

Meybeck M. (1982) Carbon, nitrogen, and phosphorus transport by world rivers. Am. J. Sci. 282:401-450

Middelburg J. J., Barranguet C., Boschker H. T. S., Herman P. M. J. (2000) The fate of intertidal microphytobenthos carbon: An in situ ^{13}C-labeling study. Limnol. Oceanogr. 45:1224-1234

Migne A., Spilmont N., Davoult D. (2004) In situ measurements of benthic primary production during emersion: seasonal variations andannual production in the Bay of Somme (eastern English Channel, France). Cont. Shelf Res. 24:1437-1449

Miles A., Sundbäck K. (2000) Diel variation of microphytobenthic productivity in areas with different tidal amplitude. Mar. Ecol. Prog. Ser. 205:11-22

Milliman J. D., Ross D. A., Pilkey O. H. (1972) Sediments of the continental margin off the eastern United States. Geol. Soc. Am. Bull. 83:1315-1334

Mitbavkar S., Anil A. C. (2004) Vertical migratory rhythms of benthic diatoms in a tropical intertidal sand flat: influence of irradiance and tides. Mar. Biol. 145:9-20

Moore W. S. (1996) Large groundwater inputs to coastal waters revealed by Ra-226 enrichments. Nature 380:612-614

Moore W. S. (1997) High fluxes of radium and barium from the mouth of the Ganges-Brahmaputra River during low river discharge suggest a large groundwater source. Earth Planet. Sci. Lett 150:141-150

Mußmann M., Ishii K., Rabus R., Amann R. (2005) Diversity and vertical distribution of cultured and uncultured Deltaproteobacteria in an intertidal mud flat of the Wadden Sea. Environ. Microbiol. 7:405-418

Neira C., Rackemann M. (1996) Black spots produced by buried macroalgae in intertidal sandy sediments of the Wadden Sea: Effects on the meiobenthos. J. Sea Res. 36:153-170

Nielsen P. (1990) Tidal dynamics of the water table in beaches. Water Resour. Res. 26:2127-2134

Nilsson P., Jönsson B., Lindström Swanberg I., Sundbäck K. (1991) Response of a marine shallow-water sediment system to an increased load of inorganic nutrients. Mar. Ecol. Prog. Ser. 71:275-290

Nittrouer C. A., Wright L. D. (1994) Transport of Particles across Continental Shelves. Rev. Geophys. 32:85-113

Oldham C. E., Lavery P. S. (1999) Porewater nutrient fluxes in a shallow fetch-limited estuary. Mar. Ecol.-Prog. Ser. 183:39-47

Orvain F., Sauriau P. G. (2002) Environmental and behavioural factors affecting activity in the intertidal gastropod *Hydrobia ulvae*. J. Exp. Mar. Biol. Ecol. 272:191-216

Paterson D. M. (1989) Short-term changes in the erodibility of intertidal cohesive sediments related to the migratory behavior of epipelic diatoms. Limnol. Oceanogr. 34:223-234

Perkins R. G., Underwood G. J. C., Brotas V., Snow G. C., Jesus B., Ribeiro L. (2001) Responses of microphytobenthos to light: primary production and carbohydrate allocation over an emersion period. Mar. Ecol. Prog. Ser. 223:101-112

Pinckney J., Paerl H. W., Fitzpatrick M. (1995) Impacts of seasonality and nutrients on microbial mat community structure and function. Mar. Ecol. Prog. Ser. 123:207-216

Pinckney J., Zingmark R. G. (1991) Effects of tidal stage and sun angles on intertidal benthic microalgal productivity. Mar. Ecol. Prog. Ser. 76:81-89

Pomeroy L. R. (1959) Algal productivity in salt marshes of Georgia. Limnol. Oceanogr. 4:386-397

Postma H. (1954) Hydrography of the Dutch Wadden Sea. Arch. néerl. Zool. 10:405-511

Precht E., Franke U., Polerecky L., Huettel M. (2004) Oxygen dynamics in permeable sediments with wave-driven pore water exchange. Limnol. Oceanogr. 49:693-705

Precht E., Huettel M. (2003) Advective pore-water exchange driven by surface gravity waves and its ecological implications. Limnol. Oceanogr. 48:1674-1684

Precht E., Huettel M. (2004) Rapid wave-driven advective pore water exchange in a permeable coastal sediment. J. Sea Res. 51:93-107

Rasmussen M. B., Henriksen K., Jensen A. (1983) Possible causes of temporal fluctuations in primary production of the microphytobenthos in the Danish Wadden Sea. Mar. Biol. 73:109-114

Reay W. G., Gallagher D. L., Simmons G. M. (1992) Groundwater discharge and its impact on surface-water quality in a Chesapeake Bay inlet. Water Resour. Bull. 28:1121-1134

Redfield A. C. (1958) The biological control of chemical factors in the environment. Am. Scientist 46:206-222

Reichardt W. (1988) Impact of bioturbation by *Arenicola marina* on microbiological parameters in intertidal sediments. Mar. Ecol. Prog. Ser. 44:149-158

Reimers C. E., Stecher H. A., Taghon G. L., Fuller C. M., Huettel M., Rusch A., Ryckelynck N., Wild C. (2004) In situ measurements of advective solute transport in permeable shelf sands. Cont. Shelf Res. 24:183-201

Reineking B. (2005) Harbors and shipping. In: Essink K., Dettmann C., Farke H., Laursen K., Lüerßen G., Marencic H., Wiersinga W. (eds) Wadden Sea quality status report 2004. Wadden Sea ecosystem No. 19. Trilateral monitoring and assessment group. Common Wadden Sea Secretariat (CWSS), Wilhelmshaven, Germany, p 35-38

Reise K. (2005) Coast of change: habitat loss and transformations in the Wadden Sea. Helgol. Mar. Res. 59:9-21

Reise K., Riethmüller R. (1998) The Sylt-Rømø Bight in the Wadden Sea: an overview. In: Gätje C., Reise K. (eds) The Wadden Sea ecosystem - Exchange, transport and transformation processes. Springer, p 21-23

Reise K., Siebert I. (1994) Mass occurrence of green algae in the German Wadden Sea. Dtsch. Hydrogr. Z. Suppl. 1:171-180

Revsbech N. P., Jørgensen B. B. (1986) Microelectrodes: Their use in microbial ecology. In: Marshall K. C. (ed) Advances in microbial ecology, Vol 9. Plenum Press, New York and London, p 293-352

Revsbech N. P., Sørensen J., Blackburn T. H., Lomholt J. P. (1980) Distribution of oxygen in marine sediments measured with microelectrodes. Limnol. Oceanogr. 25:403-411

Rhoads D. C. (1974) Organism-sediment relations on the muddy sea floor. Oceanogr. Mar. Biol., Annu. Rev. 12:263-300

Riedl R. J. (1971) How much seawater passes through sandy beaches? Int. Revue ges. Hydrobiol. 56:923-946

Riedl R. J., Huang N., Machan R. (1972) The subtidal pump: Mechanism of interstitial water exchange by wave action. Mar. Biol. 13:210-221

Riedl R. J., Machan R. (1972) Hydrodynamic patterns in lotic intertidal sands and their bioclimatological implications. 13:179-209

Rocha C. (1998) Rhythmic ammonium regeneration and flushing in intertidal sediments of the Sado estuary. Limnol. Oceanogr. 43:823-831

Rocha C. (2000) Density-driven convection during flooding of warm, permeable intertidal sediments: the ecological importance of the convective turnover pump. J. Sea Res. 43:1-14

Round F. E. (1971) Benthic marine diatoms. Oceanogr. Mar. Biol. Rev. 9:83-139

Round F. E., Palmer J. D. (1966) Persistent, vertical-migration rhythms in benthic microflora: II. Field and laboratatory studies of diatoms from the banks of the River Avon. J. Mar. Biol. Assoc. UK 46:191-214

Rusch A., Forster S., Huettel M. (2001) Bacteria, diatoms and detritus in an intertidal sandflat subject to advective transport across the water-sediment interface. Biogeochemistry 55:1-27

Rusch A., Huettel M. (2000) Advective particle transport into permeable sediments - evidence from experiments in an intertidal sandflat. Limnol. Oceanogr. 45:525-533

Rusch A., Huettel M., Forster S. (2000) Particulate organic matter in permeable marine sands - Dynamics in time and depth. Estuar. Coast. Shelf Sci. 51:399-414

Rusch A., Topken H., Böttcher M. E., Hopner T. (1998) Recovery from black spots: results of a loading experiment in the Wadden Sea. J. Sea Res. 40:205-219

Rysgaard S., Christensen P. B., Nielsen L. P. (1995) Seasonal variation in nitrification and denitrification in estuarine sediment colonized by benthic microalgae and bioturbating fauna. Mar. Ecol. Prog. Ser. 126:111-121

Saburova M. A., Polikarpov I. G. (2003) Diatom activity within soft sediments: behavioural and physiological processes. Mar. Ecol. Prog. Ser. 251:115-126

Saburova M. A., Polikarpov I. G., Burkovsky I. V. (1995) Spatial structure of an intertidal sandflat microphytobenthic community as related to different spatial scales. Mar. Ecol. Prog. Ser. 129:229-239

Santos P. J. P., Castel J., Souza-Santos L. P. (1997) Spatial distribution and dynamics of microphytobenthos biomass in the Gironde estuary (France). Oceanol. Acta 20:549-556

Schlueter M., Sauter E. J., Andersen C. E., Dahlgaard H., Dando P. R. (2004) Spatial distribution and budget for submarine groundwater discharge in Eckernfoerde Bay (Western Baltic Sea). Limnol. Oceanogr. 49:157-167

Serôdio J., Catarino F. (2000) Modelling the primary production of intertidal microphytobenthos: time scales of variability and effects of migratory rhythms. Mar. Ecol. Prog. Ser. 192:13-30

Shaffer G. P., Onuf C. P. (1985) Reducing the error in estimating annual production of benthic microflora: hourly to monthly rates, patchiness in space and time. Mar. Ecol. Prog. Ser. 26:221-231

Shum K. T. (1992) Wave-Induced Advective Transport Below a Rippled Water-Sediment Interface. J. Geophys. Res.-Oceans 97:789-808

Shum K. T. (1993) The Effects of Wave-Induced Pore-Water Circulation on the Transport of Reactive Solutes Below a Rippled Sediment Bed. J. Geophys. Res.-Oceans 98:10289-10301

Shum K. T., Sundby B. (1996) Organic matter processing in continental shelf sediments - the subtidal pump revisited. Mar. Chem. 53:81-87

Simmons G. M., Jr. (1992) Importance of submarine groundwater discharge (SGWD) and seawater cycling to material flux across sediment/water interfaces in marine environments. Mar. Ecol. Prog. Ser. 84:173-184

Smith D. J., Underwood G. J. C. (1998) Exopolymer production by intertidal epipelic diatoms. Limnol. Oceanogr. 43:1578-1591

Sørensen J., Jørgensen B. B. (1987) Early diagenesis in sediments from Danish coastal waters: Microbial activity and Mn-Fe-S geochemistry. Geochim. Cosmochim. Acta 51:1583-1590

Steele J. H., Baird I. E. (1968) Production ecology of a sandy beach. Limnol. Oceanogr. 13:14-25

Sullivan M., Moncreiff C. (1988) Primary production of edaphic algal communities in a Mississippi salt marsh. J. Phycol. 24:49-58

Sun M.-Y., Lee C., Aller R. C. (1993) Laboratory studies of oxic and anoxic degradation of chlorophyll-a in Long Island Sound sediments. Geochim. Cosmochim. Acta 57:147-157

Taniguchi M. (2002) Tidal effects on submarine groundwater discharge into the ocean. Geophys. Res. Lett. 29:1561, doi:1510.1029/2002GL014987

Taniguchi M., Burnett W. C., Cable J. E., Turner J. V. (2002) Investigation of submarine groundwater discharge. Hydrol. Process. 16:2115-2129

Taniguchi M., Iwakawa H. (2004) Submarine groundwater discharge in Osaka Bay, Japan. Limnology 5:25-32

Thibodeaux L. J., Boyle J. D. (1987) Bedform-generated convective transport in bottom sediment. Nature 325:341-343

Thullner M., Zeyer J., Kinzelbach W. (2002) Influence of microbial growth on hydraulic properties of pore networks. Transp. Porous Media 49:99-122

Tillmann U., Hesse K. J., Colijn F. (2000) Planktonic primary production in the German Wadden Sea. J. Plankton Res. 22:1253-1276

Trimmer M., Nedwell D. B., Sivyer D. B., Malcolm S. J. (2000) Seasonal organic mineralisation and denitrification in intertidal sediments and their relationship to the abundance of *Enteromorpha* sp. and *Ulva* sp. Mar. Ecol. Prog. Ser. 203:67-80

Turner I. L., Masselink G. (1998) Swash infiltration-exfiltration and sediment transport. J. Geophys. Res. C 103:30813-30824

Turner I. L., Nielsen P. (1997) Rapid water table fluctuations within the beach face - implications for swash zone sediment mobility. Coast. Eng. 32:45-59

Tyler A. C., McGlathery K. J., Anderson I. C. (2003) Benthic algae control sediment-water column fluxes of organic and inorganic nitrogen compounds in a temperate lagoon. Limnol. Oceanogr. 48:2125-2137

Uchiyama Y., Nadaoka K., Rolke P., Adachi K., Yagi H. (2000) Submarine groundwater discharge into the sea and associated nutrient transport in a sandy beach. Water Resour. Res. 36:1467-1479

Ullman W. J., Chang B., Miller D. C., Madsen J. A. (2003) Groundwater mixing, nutrient diagenesis, and discharges across a sandy beachface, Cape Henlopen, Delaware (USA). Estuar. Coast. Shelf Sci. 57:539-552

Underwood G. J. C., Kromkamp J. (1999) Primary production by phytoplankton and microphytobenthos in estuaries. In: Nedwell D. B., Raffaelli D. G. (eds) Advances in Ecological Research - Estuaries, Vol 29. Academic Press, p 93-153

Usui T., Koike I., Ogura N. (1998) Tidal effect on dynamics of pore water nitrate in intertidal sediment of a eutrophic estuary. J. Oceanogr. 54:205-216

van Beek F. A., Rijnsdorp A. D., de Clerck R. (1989) Monitoring juvenilestocks of flatfish in the Wadden Sea and the coastal areas of the southeastern North Sea. Helgol. Mar. Res. 43:461-477

van Beusekom J. E. E. (2005) A historic perspective on Wadden Sea eutrophication. Helgol. Mar. Res. 59:45-54

van Beusekom J. E. E., Bot P., Göbel J., Hanslik M., Lenhart H.-J., Pätsch J., Peperzak L., Petenati T., Reise K. (2005) Eutrophication. In: Essink K., Dettmann C., Farke H., Laursen K., Lüerßen G., Marencic H., Wiersinga W. (eds) Wadden Sea quality status report 2004. Wadden Sea ecosystem No. 19. Trilateral monitoring and assessment group. Common Wadden Sea Secretariat (CWSS), Wilhelmshaven, Germany, p 141-154

van Beusekom J. E. E., Brockmann U. H., Hesse K. J., Hickel W., Poremba K., Tillmann U. (1999) The importance of sediments in the transformation and turnover of nutrients and organic matter in the Wadden Sea and German Bight. 51:245-266

van Beusekom J. E. E., de Jonge V. N. (2002) Long-term changes in Wadden Sea nutrient cycles: importance of organic matter import from the North Sea. Hydrobiologia 475:185-194

van Beusekom J. E. E., Fock H., de Jong F., Diel-Christiansen S., Christiansen B. (2001) Wadden Sea specific eutrophication criteria. Wadden Sea ecosystem No. 14, Vol. 14. Common Wadden Sea Secretariat (CWSS), Wilhelmshaven, Germany

van der Loeff M. M. R. (1981) Wave effects on sediment water exchange in a submerged sand bed. Neth. J. Sea Res. 15:100-112

van Es B. (1982) Community metabolism of intertidal flats in the Ems-Dollard estuary. Mar. Biol. 66:95-108

Vedel A., Riisgård H. U. (1993) Filter-feeding in the polychaete *Nereis diversicolor*: growth and bioenergetics. Mar. Ecol. Prog. Ser. 100:145-152

Veldhuis M. J. W., Colijn F., Venekamp L. A. H., Villerius L. (1988) Phytoplankton primary production and biomass in the western Wadden Sea (The Netherlands); a comparison with an ecosystem model. Neth. J. Sea Res. 22:37-49

Webb J. E., Theodor J. (1968) Irrigation of Submerged Marine Sands through Wave Action. Nature 220:682-683

Webb J. E., Theodor J. L. (1972) Wave-Induced Circulation in Submerged Sands. J. Mar. Biol. Assoc. U.K. 52:903-&

Webster I. T., Norquay S. J., Ross F. C., Wooding R. A. (1996) Solute exchange by convection within estuarine sediments. Estuar. Coast. Shelf Sci. 42:171-183

Webster I. T., Taylor A. C. (1992) Rotational dispersion in porous-media due to fluctuating flows. Water Resour. Res. 28:109-119

Weiss M. S., Abele U., Weckesser J., Welte W., Schulz G. E. (1991) Molecular architecture and electrostatic properties of a bacterial porin. Science 254:1627-1630

Wenzhöfer F., Glud R. N. (2004) Small-scale spatial and temporal variability in coastal benthic O-2 dynamics: Effects of fauna activity. Limnol. Oceanogr. 49:1471-1481

Wenzhöfer F., Glud R. N., Cook P. L. M., Huettel M. (in preparation) Benthic primary production of two sandy subtidal sediments.

Wheatcroft R. A. (1994) Temporal variation in bed configuration and one-dimensional bottom roughness at the mid shelf STRESS site. Cont. Shelf Res. 14:1167-1190

Whiting G. J., Childers D. L. (1989) Subtidal advective water flux as a potentially important nutrient input to southeastern U.S.A. saltmarsh estuaries. Estuar. Coast. Shelf Sci. 28:417-431

Widdel F., Pfennig N. (1982) Studies on dissimilatory sulfate-reducing bacteria that decompose fatty-acids. 2. Incomplete oxidation of propionate by Desulfobulbus-Propionicus Gen-Nov, Sp-Nov. Arch. Microbiol. 131:360-365

Widdows J., Brinsley M. D., Salked P. N., Lucas C. H. (2000) Influence of biota on spatial and temporal variation in sediment erodability and material flux on a tidal flat (Westerschelde, The Netherlands). Mar. Ecol. Prog. Ser. 194:23-37

Wolfstein K., Colijn F., Doerffer R. (2000) Seasonal dynamics of microphytobenthos biomass and photosynthetic characteristics in the northern German Wadden Sea, obtained by the photosynthetic light dispensation system. Est. Coast. Shelf Sci. 51:651-662

Wollast R. (1991) The coastal organic carbon cycle: fluxes, sources, and sinks. In: Mantoura R. F. C., Martin J.-M., Wollast R. (eds) Ocean Margin Processes in Global Change. John Wiley & Sons, p 365-381

Wollast R. (2002) Continental margins - review of geochemical settings. In: Wefer G., Billet D., Hebbeln D., Jørgensen B. B., Schlüter M., van Weering T. C. E. (eds) Ocean margin systems. Springer

Yallop M. L., Paterson D. M., Wellsbury P. (2000) Interrelationships between rates of microbial production, exopolymer production, microbial biomass, and sediment stability in biofilms of intertidal sediments. Microb. Ecol. 39:116-127

Yelverton G. F., Hackney C. T. (1986) Flux of dissolved organic carbon and pore water through the substrate of a Spartina alterniflora marsh in North Carolina. Estuar. Coast. Shelf Sci. 22:255-267

Younger P. L. (1996) Submarine groundwater discharge. Nature 382:121-122

Zektser I. S., Dzhamalov R. G., Safronova T. I. (1983) Role of submarine groundwater discharge in the water balance of Australia. IAHS-AISH Publication, No 142 "Groundwater in resources planning":209-219

Ziebis W., Huettel M., Forster S. (1996) Impact of biogenic sediment topography on oxygen fluxes in permeable seabeds. Mar. Ecol. Prog. Ser. 140:227-237

PUBLICATIONS OUTLINE

The thesis comprises four manuscripts, presented as chapters.

Chapter 2: Nutrient release from an exposed intertidal sand flat

by Markus Billerbeck, Ursula Werner, Katja Bosselmann, Eva Walpersdorf and Markus Huettel

The concept of the study was developed by M.B. and M.H. M.B. and U.W. conducted the experiments with contribution of K.B. and E.W.. M.B. evaluated the data and wrote the manuscript with editorial help from all co-authors.

The manuscript has been submitted to Marine Ecology Progress Series.

Chapter 3: Surficial and deep pore water circulation governs spatial and temporal scales of nutrient recycling in intertidal sand flat sediment

by Markus Billerbeck, Ursula Werner, Lubos Polerecky, Eva Walpersdorf, Dirk de Beer and Markus Huettel

M.B., U.W., M.H. and D.deB. developed the concept of this study. Experiments were conducted by M.B., U.W., E.W. and L.P.. M.B. evaluated all data. U.W. and L.P. measured the microbial rates in the surface layer. The oxygen penetration depths were measured by E.W.. M.B. wrote the manuscript with editorial help of all co-authors.

The manuscript has been submitted to Marine Ecology Progress Series.

Chapter 4: Spatial and temporal patterns of mineralization rates and oxygen distribution in a permeable intertidal sand flat (Sylt, Germany)

by Ursula Werner, Markus Billerbeck, Lubos Polerecky, Ulrich Franke, Markus Huettel, Justus van Beusekom and Dirk de Beer

The study was initiated by U.W., M.B., M.H. and D.deB.. The experiments were carried out by U.W., M.B., L.P. and U.F.. U.W. measured and evaluated all data except the following: M.B. and M.H. initiated the study on pore water nutrients, pore- and bottom water flow velocity, M.B. conducted the measurements and evaluated the data. L.P. and U.F. measured the oxygen consumption rates with planar optodes. J.v.B. provided the water column chl-*a* values. U.W. wrote the manuscript with editorial help from all co-authors.

The manuscript has been submitted to Limnology and Oceanography.

Chapter 5: Benthic photosynthesis in submerged Wadden Sea intertidal flats

by Markus Billerbeck, Hans Røy, Katja Bosselmann and Markus Huettel

M.B., H.R. and M.H. developed the concept of the study. Field experiments were carried out by M.B. and K.B.. H.R. measured and evaluated the scalar irradiance profiles. M.B. evaluated the data and wrote the manuscript with editorial help from H.R and M.H..

The manuscript is in preparation for submission.

Nutrient release from an exposed intertidal sand flat

Markus Billerbeck, Ursula Werner, Katja Bosselmann, Eva Walpersdorf
and Markus Huettel

submitted to Marine Ecology Progress Series

ABSTRACT

We studied pore water seepage and associated nutrient release in the intertidal sand flat "Janssand" (North Sea) during exposure at low tide. The hydraulic gradient developing at ebb tide between the pore water level in the elevated sand flat and the water level in the tidal gully generated interstitial water flows towards the seepage zone with velocities ranging from 0.54 (March) to 0.86 cm h^{-1} (July). Pore water was discharged from a ca. 20 m wide release zone near the seaward margin of the flat at rates of 2.4 (March) and 4.2 L m^{-2} d^{-1} (July). Nutrient and DIC concentrations of the seepage water exceeded those measured in the pore water of the upper section of the flat by 10- and 5-fold, respectively. Nutrient effluxes through seepage reached 1074 and 5078 µmol m^{-2} d^{-1} for NH_4, 280 and 1668 µmol m^{-2} d^{-1} for PO_4 and 141 and 1142 µmol m^{-2} d^{-1} for $Si(OH)_4$ in March and July, respectively. Benthic flux chambers revealed that nutrients and DIC were released from the still submerged sediment as soon as the ebb tide exposed the upper section of the elevated flat. A conservative estimate based on our measurements suggests that 84,000 L (March) to 147,000 L (July) pore water are discharged each tidal cycle from the sandy northeast margin of the Janssand (3.5 km length). Nutrients contained in this water corresponded to 6 – 25 kg d^{-1} carbon mineralized during March and 42 – 223 kg d^{-1} during July. Our study indicates that the Janssand intertidal flat does not accumulate organic matter but releases mineralization products that can account for all the organic matter that is potentially filtered through the permeable beds during a tidal cycle. Nutrient fluxes associated with seepage exceeded 5 to 8-fold those fluxes caused by the combined effects of diffusion, advection and bioirrigation during inundation, emphasizing the importance of sand flat drainage for the nutrient cycles in the Wadden Sea.

INTRODUCTION

Fine to medium sands prevail in the intertidal regions of the Wadden Sea that cover a total area of ca. 13,000 km^2 along the Dutch, German and Danish coast (Flemming & Ziegler 1995, van Beusekom & de Jonge 2002). The relatively high permeability of these sands (10^{-12} to 10^{-11} m^2) allows inflow of water through the interstices as soon as pressure gradients caused by currents or water level changes are present. During inundation, the pore water exchange transports solutes (Huettel et al. 1998) and particles (Huettel et al. 1996, Pilditch et al. 1997) into and out of the upper layers of permeable sediment. Through the associated enhanced exchange of organic matter, electron acceptors and metabolic products (Ziebis et al. 1996, Huettel et al. 1998), such permeable sands become sites of high organic matter turnover (Huettel & Rusch 2000, D'Andrea et al. 2002). During ebb tide, pressure gradients develop between the pore water level within elevated sand flats that gradually become exposed and the decreasing water level of the Wadden Sea. In these sands, the pore water table drops slower than the sea water level (Nielsen 1990) because of the sediments' hydraulic impedance and capillary forces, and the ensuing pressure gradient leads to water release that fills the numerous drainage channels typical for intertidal flats (Nielsen 1990, Horn 2002). Such discharge of pore water has been recognized as an ecologically important process in studies covering coastal submarine groundwater discharge (Simmons 1992, Moore 1996, Taniguchi & Iwakawa 2004), wave dominated beaches (McLachlan & Illenberger 1986, Uchiyama et al. 2000, Ullman et al. 2003) and salt marshes (Howes & Goehringer 1994, Osgood 2000, Jahnke et al. 2003). For tide dominated intertidal flats, however, studies on drainage and associated solute releases are scarce. Le Hir et al. (2000) estimated that intertidal mud flats at the French and British coast discharged roughly 10 L m^{-2} $tide^{-1}$. In a tidal flat in Tokyo Bay, drainage has been suggested as a possible mechanism causing a drop in sedimentary water content during exposure (Usui et al. 1998). In contrast, Kuwae et al. (1998) concluded that pore water release in another intertidal flat in Tokyo Bay was small because the sediment remained nearly saturated during exposure. Likewise, Drabsch et al. (1999) suggested that tidal pumping and total water flux in a tidal flat (Manukao Harbour, New Zealand) was small because pore water flow velocities ranged only between 0.2 and 4.0 cm d^{-1}. However, we observed considerable pore water seepage from a sandy intertidal flat in the North Sea, indicating that drainage may produce significant pore water release in more steeply

sloping sand flats. Therefore, we initiated this study that investigates the implications of this drainage process for sedimentary nutrient release in permeable intertidal sand flats. The specific objectives of this study were to

1. Assess the magnitude and tidal dynamics of pore water release in the Janssand tidal flat
2. Quantify the nutrient and dissolved inorganic carbon (DIC) release associated with pore water seepage

To this end, we measured pore water levels and velocities, seepage, and interfacial solute fluxes. The results suggest an important contribution of the intertidal sand drainage to the nutrient cycles in the Wadden Sea.

METHODS

Study site

The study was conducted during two field campaigns (July 2003 and March 2004) on the northeastern margin of the intertidal Janssand sandflat situated landward of the barrier island of Spiekeroog, North Sea (53°44'07'' N, 007°41'57'' E) (Fig. 1).

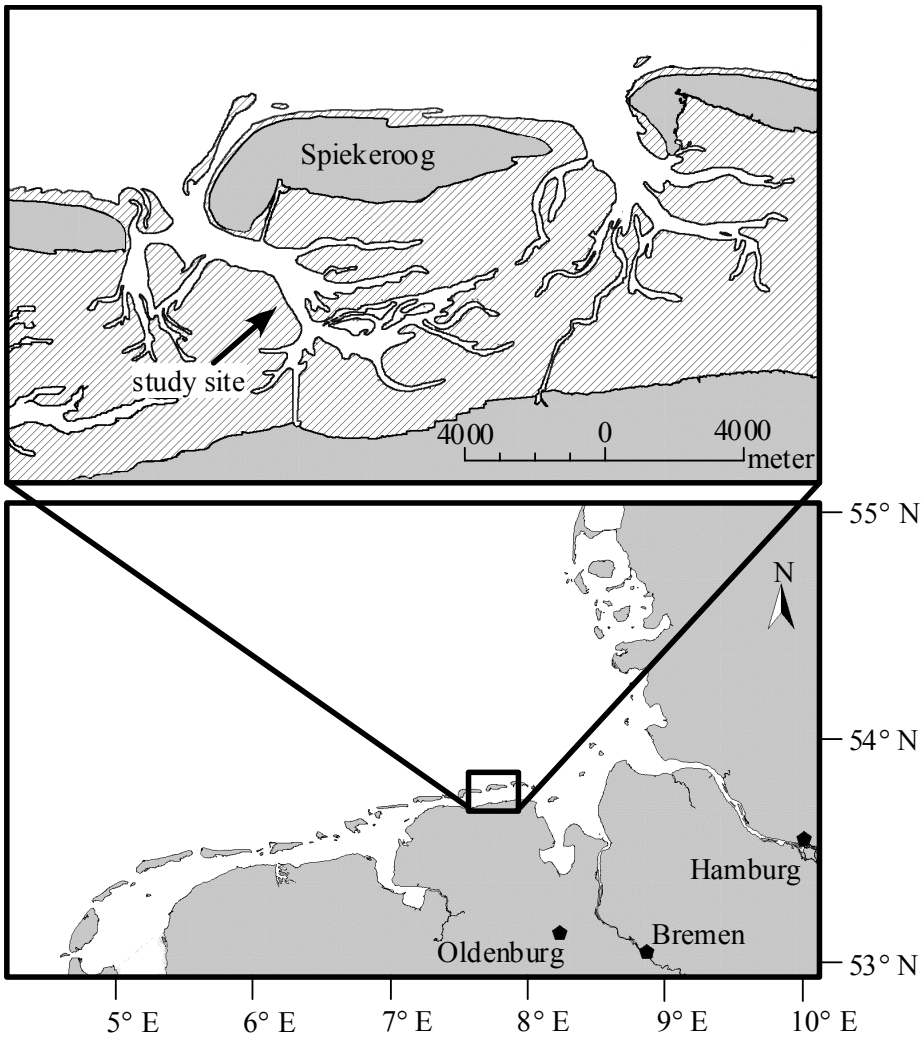

Figure 1: Location of the study site near the island of Spiekeroog, Wadden Sea, Germany.

Tides in this area are semi-diurnal, and the Janssand (11 km² area) is covered by approximately 1.5-2 m of water during high tide and becomes exposed to air for about 6 to 7.5 hours during low tide. The Janssand tidal flat is almost level except the ca. 80 m wide margin, where the sediment surface is sloping (1.6 cm m^{-1}, Fig. 2). Four study sites were chosen for our measurements (A-D in Fig. 2), with a "lower sand flat"-site (D) near the edge of the Janssand and an "upper sand flat"-site (A) about 45 m upslope from the mean low water line as the two main study sites.

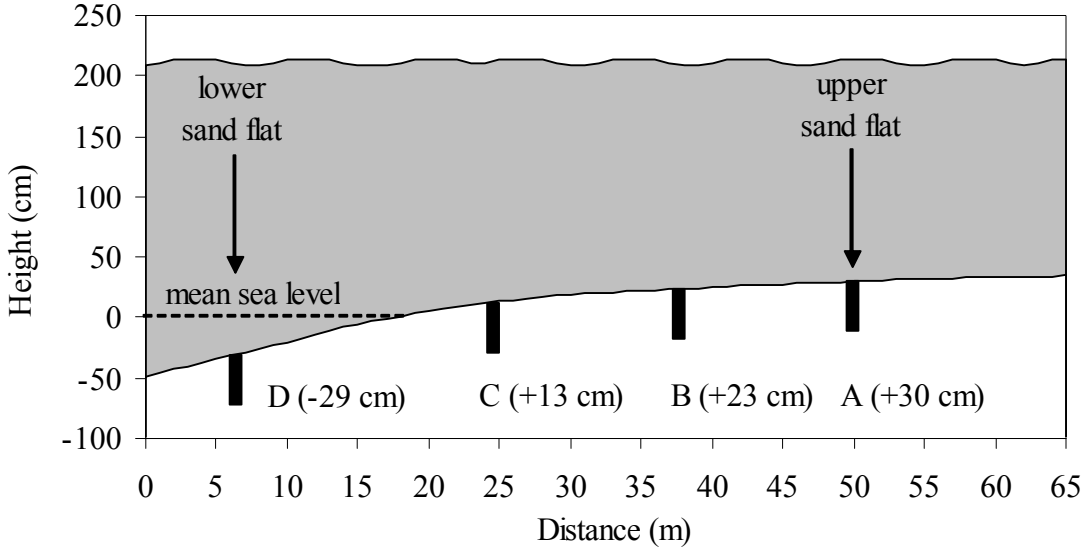

Figure 2: Janssand tidal flat topography as surveyed during July 2003 with the positions of the study sites A-D relative to mean sea level. Grey shading indicates the mean high water line and zero water height marks the position of the mean low water line during July 2003. Additional 10-15 m of the tidal flat was exposed during the March 2004 campaign due to wind conditions.

The Janssand is characterized by well sorted (σ<0.38 phi) fine quartz sands with a mean grain size of 176 µm (assessed through dry-sieving). At the upper sand flat, permeability of the sediment surface layer (upper 15 cm) as determined by constant head permeametry was 7.2 x 10^{-12} m² (standard deviation SD ± 0.6 x 10^{-12} m², July 2003), which permits advective pore water flows (Huettel et al. 2003). At the lower sand flat site, the same layer was less permeable (5.2 x 10^{-13} m² (SD ± 0.3 x 10^{-13} m²)), because of imbedded mud lenses. Macrofaunal abundances are relatively low, probably because of the strong tidal currents and associated mechanical stress (Hertweck 1995). All measurements and samplings are listed in Table 1 with their respective locations on the tidal flat and associated tidal range. The Spiekeroog tide gauge within 2 km of the study site provided the data on water level changes.

Table 1: Sampling and in situ measurements during the July 2003 and March 2004 field campaigns with tidal range and respective positions on the tidal flat. Positions (cm) relative to mean sea level according to Fig.2: A: 30, B: 23, C: 13, D: -29.

		Site characteristics				In situ measurements		
	Tidal range [m]	Sediment	Seawater	Pore water	Pore water level	Pore water flow velocity	Chambers	Seepage
7/21/2003	2.7					A; 2 cm depth		
7/22/2003	2.6			A				
7/23/2003	2.3	Topography, A-D		D				
7/25/2003	2.2					A; 10 cm depth		
7/26/2003	2.5	Grain size, A			A,B,C,D	A; 5 cm depth		
7/27/2003	2.7	Permeability, A,D						
7/29/2003	3.0	Chl *a* , A	High tide				A	
7/30/2003	3.2	Chl *a* , D	High tide				D-12 cm	
3/26/2004	3.0					A; 2 cm depth		D-21 cm
3/27/2004	2.8					A; 5 cm depth		D-21 cm
3/28/2004	2.5		High tide			A; 20 cm depth		D-21 cm, D-32 cm
3/29/2004	2.3					A; 30,40 cm depths		A,C,D-21 cm
3/30/2004	1.9			A,D		A; 50 cm depth		D-21 cm (rhombic)
3/31/2004	1.8					A+6cm; 5 cm depth		

Pore water level

To assess fluctuations of the pore water level in the sediment with change of the tidal water level, four acrylic pipes (20 cm long, 36 mm diameter) were vertically inserted into the sediment on a transect from the upper sand flat site towards the lower sand flat site (A,B,C, and D in Fig. 2). The open lower ends of the pipes were covered with nylon mesh (63 µm) and their open upper ends were level with the sediment surface. The water table in the pipes was measured to the nearest mm with a ruler throughout the exposure of the respective sites.

Pore water flow velocity

The horizontal flow velocity of pore water was measured at the upper sand flat site by following the passage of a fluorescent dye tracer through the sediment with a buried linear array of 6 optical sensors as described in Precht & Huettel (2004) (Fig. 3). The tracer solution was prepared by adding Fluorescein dye to filtered seawater to an end concentration of 100 mg L^{-1} and adjusting it to the local pore water density. Prior to the first measurement, fluorescein dye solution was injected with a syringe into the sand and dug out later to visually determine the main flow direction of the pore water. Then a small incision was cut into the sediment at low tide to the desired depth, and the setup was carefully inserted and pushed horizontally several cm into the undisturbed part of the sediment. The sensor array orientation was horizontal to the sediment surface and roughly perpendicular to the low water line; other orientations did not show any measurable pore water flow. During the July 2003 campaign, pore water flow velocities were measured at 2, 5, and 10 cm sediment depth throughout exposure. These measurements were extended by four 10 cm intervals to a sediment depth of 50 cm

during the March 2004 campaign. An additional measurement was conducted at 5 cm sediment depth about 30 m upslope the upper sand flat site (+ 6cm height) during the March campaign. Some measurements were continued during inundation of the tidal flat. All pore water flow velocity measurements were conducted during the transition from mean tide to neap tide for both campaigns. The average pore water flow velocity was calculated for all measurements from the time interval between the geometric centroids of the signal curves at consecutive sensors (Fig. 3).

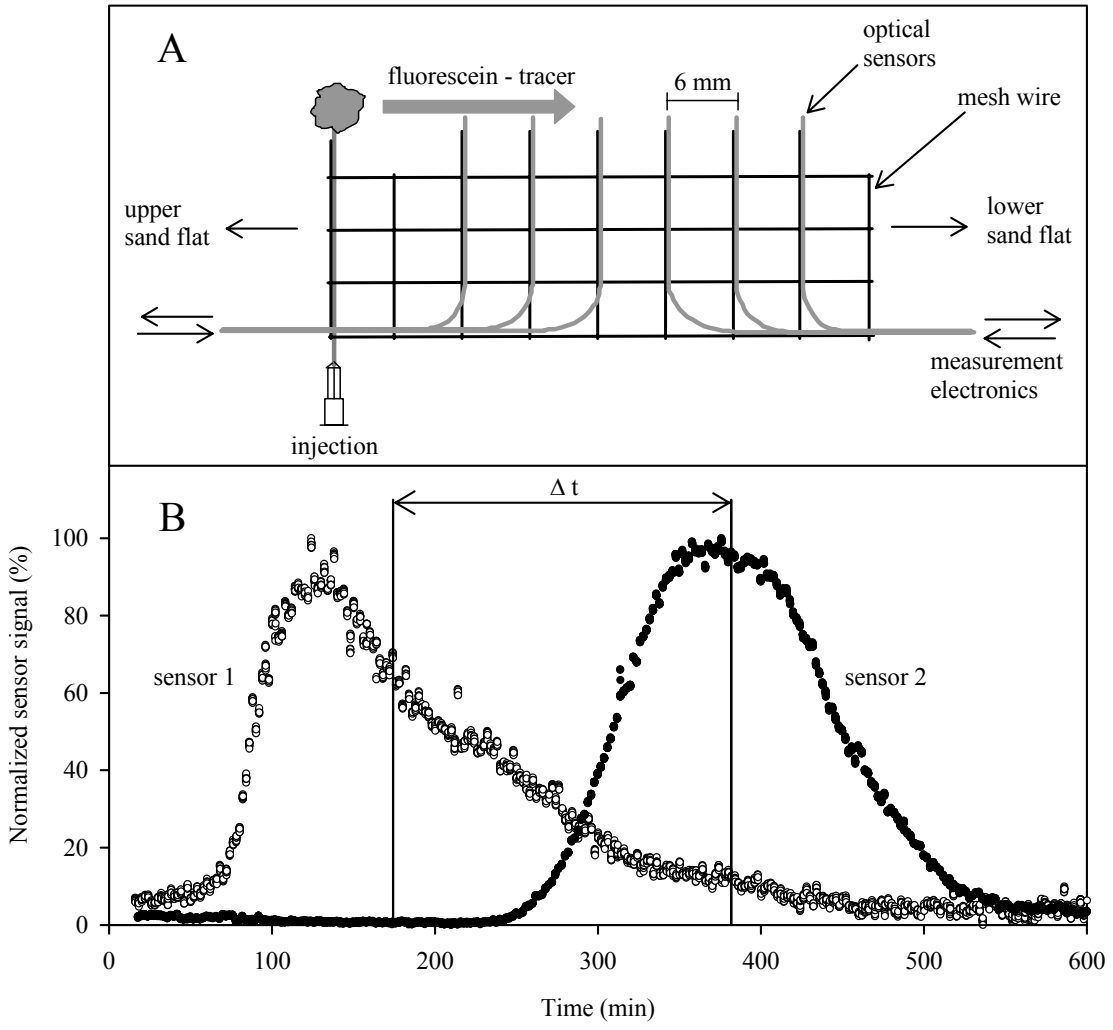

Figure 3: (A) Setup of the six optical sensors used for the measurement of pore water flow velocity. (B) Fluorescence signals of two optical fibres and the location of the geometric centroids (vertical lines) used for the calculation of the time span Δ t between dye passage at the respective sensor tips. Geometric centroids are located at the cumulative 50% of the respective signal curve area.

Pore water seepage

Pore water discharge from the sloping margin of the tidal flat was quantified in March during exposure by measuring the volume of fluid collected at the end of two flow barriers that guided draining pore water into a container (Fig. 4).

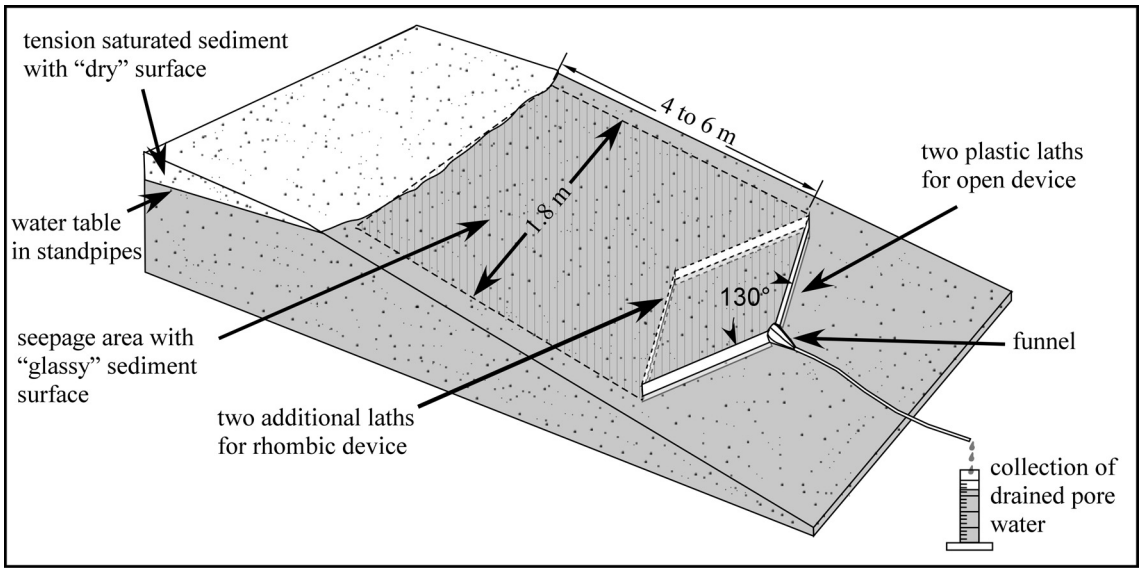

Figure 4: Setup of the open and rhombic discharge metering devices on the sloping sand flat. The discharge area was identified from the "glassy" sediment surface upslope the metering device (hatched area) and spanned an area of 6 to 13 m² for the open and 0.78 m² for the rhombic device.

The flow barriers consisted of two 5 cm wide plastic laths (100 cm length), inserted at an angle of 130° to a depth of 2 cm vertically into the sediment, thus collecting seepage water from a 1.8 m wide upslope section of the flat. At the meeting point of the two plastic laths, a plastic funnel with tubing was attached to collect the seeped pore water into a graduated cylinder. The amount of collected pore water was quantified to the nearest ml, and filtered samples were transferred to plastic vials and kept frozen for later nutrient analysis. Up to 3 of these collection devices were established along a transect (Sites A, C, D) and were ready for measurement within 20 minutes after exposure. The zones of pore water discharge upslope the collection devices could be identified from the "glassy" surface of the water saturated sediment and their areal dimensions were recorded throughout the measurements. In order to verify the seepage measurements with the open device, an additional measurement was conducted from a clearly defined rhombic area (0.78 m²) by inserting two additional plastic laths opposite of the open measuring device (Fig. 4). A good agreement of the seepage rates per m^2 measured with the rhombic and open devices was obtained for discharge zones extending less than 6 m

above the open device. Discharge rates were calculated by dividing the collected pore water volume per time by the respective seepage area (Fig. 4) of the open or rhombic device.

Chamber flux measurements

During the July 2003 campaign, in situ measurements with cylindrical chambers (19 cm inner diameter) were carried out to measure advective fluxes of oxygen, DIC and nutrients across the sediment water interface. At the lower sand flat site, the chambers were additionally used to assess seepage of solutes from the sediment. The chamber measurements were conducted on two consecutive days at the upper and lower sand flat site with 6 chambers (3 transparent and 3 opaque) at each site. At the lower sand flat site, chamber incubations were longer (8 h) and water depth reached 2.3 m, compared to the upper flat measurements with 4 h incubations and 1.5 m water depth. Within the incubation time, water temperature varied in a range within 1°C and concentrations of nutrients, DIC and oxygen in the ambient seawater remained relatively constant. During low tide, the chambers were gently inserted to a sediment depth of 19 cm, and neoprene collars (20 cm diameter) were placed around them to prevent erosion. Upon inundation, the chambers were sealed with acrylic lids each enclosing a water volume of 3.4 L and a sediment area of 0.028 m². Inside the chambers a rotating disc (15 cm diameter, 20 rpm) producing a radial pressure gradient of 0.1 Pa cm^{-1} caused flushing of the upper sediment layer thus mimicking the natural advective pore water exchange (Huettel & Gust 1992, Huettel & Rusch 2000). Advective tracer and solute fluxes caused by this very low pressure gradient (corresponding to a gradient created by flow of 10 cm s^{-1} at 10 cm above the bed interacting with a sediment ripple of 0.5 cm height) should be considered conservative. Each lid had a sampling port and a small opening with a 1 m Tygon™ tubing coil attached to it to allow pressure equilibration between chamber and surrounding water and inflow of discharged pore water into the chambers. Oxygen concentrations inside each chamber were monitored every 2 minutes for 20 seconds with fibre optic optodes inserted through the chamber lid. After closing the chambers, 20 ml of a 3 mol L^{-1} NaBr inert tracer solution was injected into one dark and one light chamber for the assessment of the advective fluid exchange between sediment and overlying water (Forster et al. 1999). After the bromide tracer was allowed to mix with the chamber water for 15 minutes, all chambers were sampled in hourly intervals as water level and currents permitted. At each sampling,

samples of ambient seawater were taken and a total of 80 ml of water was drawn with a syringe from each chamber, of which the first 20 ml of sample were discarded to account for the sampling tube volume (15 ml). At the end of the incubations, with the water level still above the chambers, sediment cores from the chambers treated with bromide tracer were retrieved with cut off 60 ml syringes. The sediment cores were sliced in 0.5 cm intervals within 30 minutes after retrieval and kept frozen until analysis. Benthic chamber measurements could not be carried out during March due to adverse weather conditions.

Sampling and analyses

For sedimentary chlorophyll *a* determination, samples of the upper 5 cm of the sand were sectioned in 0.5 cm intervals for analyzed according to Lorenzen (1967). For the characterization of ambient seawater, samples collected at high tide and samples from gullies (ebb tide) were collected in plastic centrifuge tubes (glass vials for DIC and DOC), filtered through 0.2 µm nylon syringe filters. Aliquots were either kept frozen (for nutrients, DOC) or preserved with mercury chloride (for DIC analysis). For POC and PN contents, samples were filtered onto pre-combusted Whatman® GFF filters and kept frozen. For pore water nutrient and DIC determinations, sediment cores were collected with 36 mm core liners shortly after exposure of the study sites and sectioned within an argon-flushed glove box to a depth of 20 cm in 1 cm intervals. Equivalent slices from 4 sediment cores were pooled and transferred to a small pressure container with an inert gas inlet and a pore water outlet. By flushing the container ca. 20 seconds with argon gas, the pore water was separated from the sediment matrix. After filtration through 0.2 µm nylon syringe filters, aliquots were frozen for nutrients analysis or preserved with saturated mercury chloride solution for subsequent DIC analysis. Bromide in the pore water was analyzed by ion chromatography with a Waters® anion-exchange column, using NaBr as a standard for calibration. Filters for POC and PN analysis were treated with a few drops of 1 mol L^{-1} HCl to remove inorganic carbon prior to analysis on a Heraeus® CHNO-rapid elemental analyzer with sulfanilamid as calibration standard.. Nutrient analyses of silicate, phosphate, ammonium, nitrate, and nitrite were performed spectrophotometrically with a Skalar Continuous-Flow-Analyzer according to Grasshoff et al. (1999). DIC was determined by flow injection analysis (Hall & Aller 1992) or coulometric titration on a UIC CM5012 (for chamber water). Seawater DOC analysis was performed by high temperature catalytic oxidation on a

Shimadzu™ TOC-5050A analyzer and obtained by subtracting the measured DIC concentration from the measured total DC. Oxygen concentrations of chamber water were determined by Winkler titration and used for calibration of the chambers' oxygen optodes (for details see Klimant et al. 1995, Holst et al. 1997). Dilution of the chamber waters due to the sampling was corrected by adding the difference of the solute inventory between the sampled and replaced volume to the chamber volume solute inventory. Solute fluxes were evaluated by linear regression on concentration changes over time, or from start and end concentrations when linear regression was not applicable.

RESULTS

Pore water level

The water level in the sediment changed when the Janssand became exposed at ebb tide (Fig. 5).

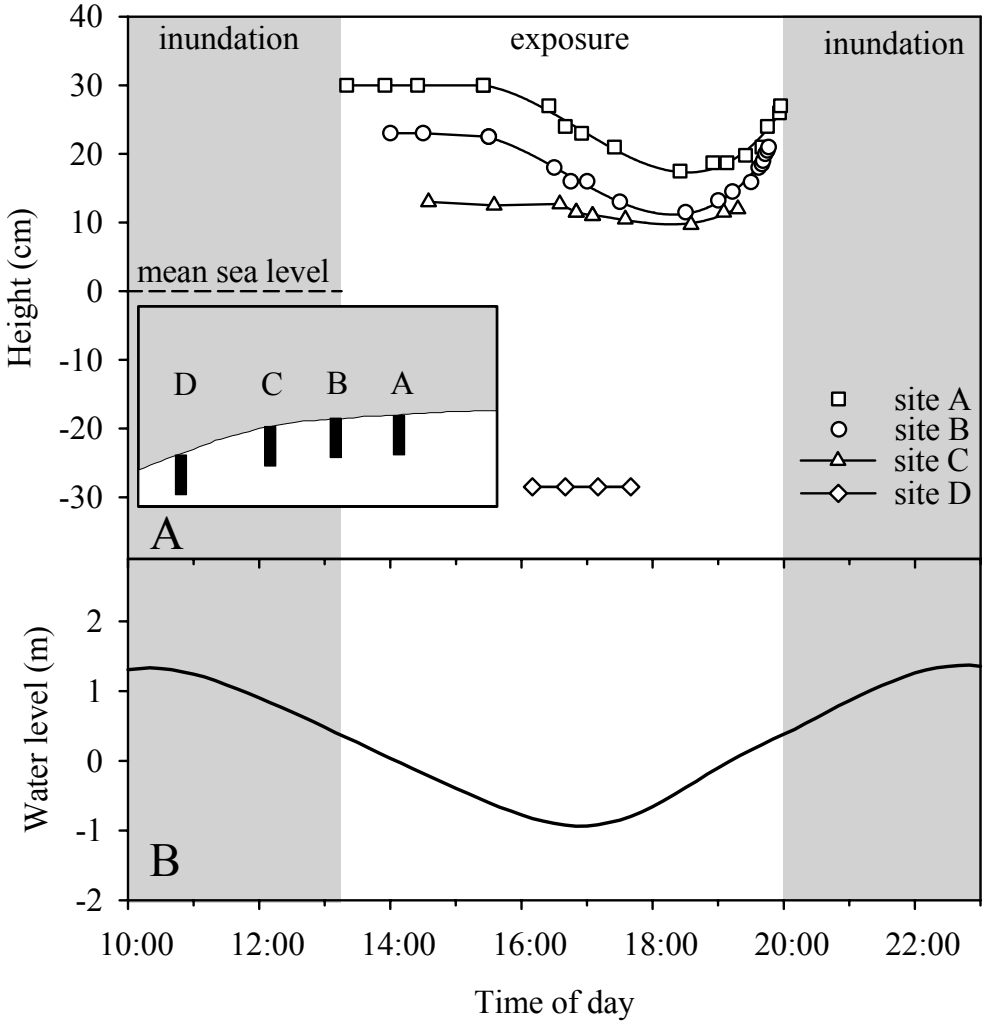

Figure 5: (A) Response of the pore water level relative to mean sea level to the fluctuation of the tidal water level at sites A-D within an accuracy of ± 1 mm during an average tidal range (pore water levels may differ for other tidal ranges). Trend lines were manually drawn through the data sets. The small inserted panel schematically shows the locations of the respective measurement sites on the tidal flat (refer also to Fig. 2). Grey shaded areas mark the inundation period of the upper sand flat site A. (B) Tidal water level based on mean sea level.

At the sites A and B on the upper sand flat, the pore water level remained at the sediment surface during the first 2 hours of exposure and dropped gradually thereafter, reaching its lowest point approximately 1.5 hours after low tide. The pore water level then increased again with rising tide, but never reached the sediment surface until re-

inundation. At site C, the pore water level dropped less deep and did not drop at all at the lower sand flat position D. At D, a pore water level at times above sediment elevation cannot be ruled out, as the open end of the standpipe was level with the sand surface. The maximum measured difference in pore water level between the upper (site A) and lower sand flat (site D) was 46 cm over a horizontal distance of 4300 cm.

Pore water flow

The fiberoptical measurements revealed pore water flows directed towards the low water line over the measured sediment depth of 50 cm during exposure (Table 2).

Table 2: Pore water flow velocities at different sediment depths for the upper sand flat site during the July and March campaigns. Flow velocities at respective depths are given as the average of measurements between consecutive sensors ± standard deviation (n = 3 to 5).

	July 2003	March 2004
Sediment depth (cm)	Flow velocity (cm h^{-1})	
2	0.87 ± 0.32	0.68 ± 0.27
5	0.74 ± 0.23	0.61 ± 0.11
10	0.98 ± 0.13	
20		0.58 ± 0.25
30		0.62 ± 0.39
40		0.45 ± 0.17
50		0.32 ± 0.06
Average:	0.86	0.54

During July 2003, an average pore water flow velocity of 0.87 cm h^{-1} (SD ± 0.32 cm h^{-1}) was calculated for the measurement at 2 cm sediment depth with similar velocities at 5 and 10 cm sediment depths (Fig. 6, Table 2). This pore water flow started after the exposure of the tidal flat and continued for 6.5 h until the measuring position became inundated again. After submergence of the measuring position, a fluorescence signal remained at the seaward sensor during the entire inundation period (Fig. 6) and decreased rapidly once the tidal flat became exposed again showing that the pore water flow ceased during submergence and resumed again after exposure. Other pore water flow measurements confirmed this finding (data not shown).

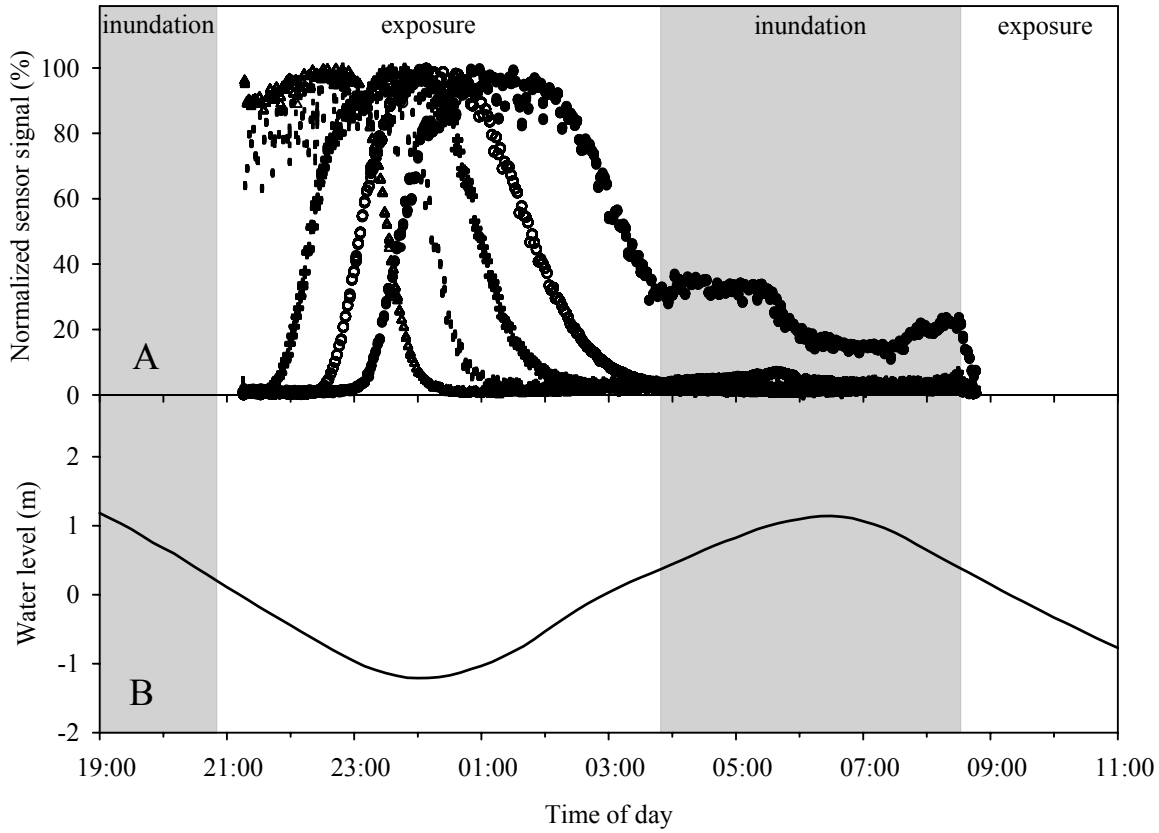

Figure 6: (A) Tracer signal curves from pore water flow velocity measurements in 2 cm sediment depth at the upper sand flat site in July 2003. Normalized signals (% of maximum signal) of 5 consecutive sensors are shown during exposure (white) and inundation (grey shading) of the measuring position. Sensor 6 is not shown because of excessive data noise. (B) Tidal water level based on mean sea level.

During the March campaign, wind conditions resulted in up to 9 hour long periods of exposure as compared to 7.5 hours in July. Nevertheless, measured flow velocities in the upper 10 cm of the sediment (0.54 cm h^{-1}) were less than during the July campaign. In March, pore water flow velocities were similar down to a sediment depth of 30 cm but decreased below (Table 2). During both measuring campaigns, pore water flow velocities remained relatively constant for the duration of the exposure period. Thirty meters upslope the upper sand flat site (6 cm vertical gain), puddles of water persisted on the almost level sediment surface during most of the exposure period and no pore water flow could be detected during the first 6.5 hours of exposure in March 2004. Pore water flow at 5 cm depth started within the last 2.5 hours of exposure and coincided with a “drying” of the sediment surface due to a gradual drop of the pore water table. In contrast, pore water flow was detected during the entire period of exposure at the steeper sloping upper sand flat site.

Pore water seepage

Pore water was released from the sediment at the lower sand flat site during ebb tide, which could be quantified during the March 2004 campaign. At low tide, seepage was restricted to an area extending from the low water line to about 20 to 30 meters upwards the slope, as indicated by its "glassy" sediment surface. Discharge continued throughout the period of exposure. In four measurements with the open seepage meters, initial rates of seepage ranged between 0.7 and 3.0 L m^{-2} h^{-1}, decreasing to 0.1 to 0.4 L m^{-2} h^{-1} shortly before re-inundation (Fig. 7A). Measurements with the rhombic seepage meters resulted in comparable discharge. Nutrient concentrations of the discharged pore water increased with time for silicate, phosphate and ammonium, and decreased or remained constant for NOx (Fig. 7B). At similar rates of pore water seepage, the discharge of nutrients varied between measurements (Table 3).

Table 3: Average discharge rates for nutrients (µmol m^{-2} h^{-1}) and pore water (L m^{-2} h^{-1}) of four measurements during the March 2004 campaign. Values are means with range in parentheses.

Nutrient discharge (µmol m^{-2} h^{-1})			Seepage rate (L m^{-2} h^{-1})
Silicate	Phosphate	Ammonium	
0.94 (0.34 - 1.57)	0.13 (0.04 - 0.20)	3.59 (1.19 - 3.70)	0.38 (0.11 - 0.67)
100.76 (66.97 - 117.69)	196.15 (90.14 - 262.15)	724.45 (449.31 - 924.50)	1.98 (1.58 - 2.99)
10.23 (9.25 - 11.25)	19.97 (12.64 - 24.84)	205.55 (163.86 - 230.76)	0.60 (0.34 - 1.38)
29.06 (16.11 - 34.46)	63.59 (33.08 - 81.68)	140.61 (109.95 - 172.66)	0.54 (0.30 - 0.96)

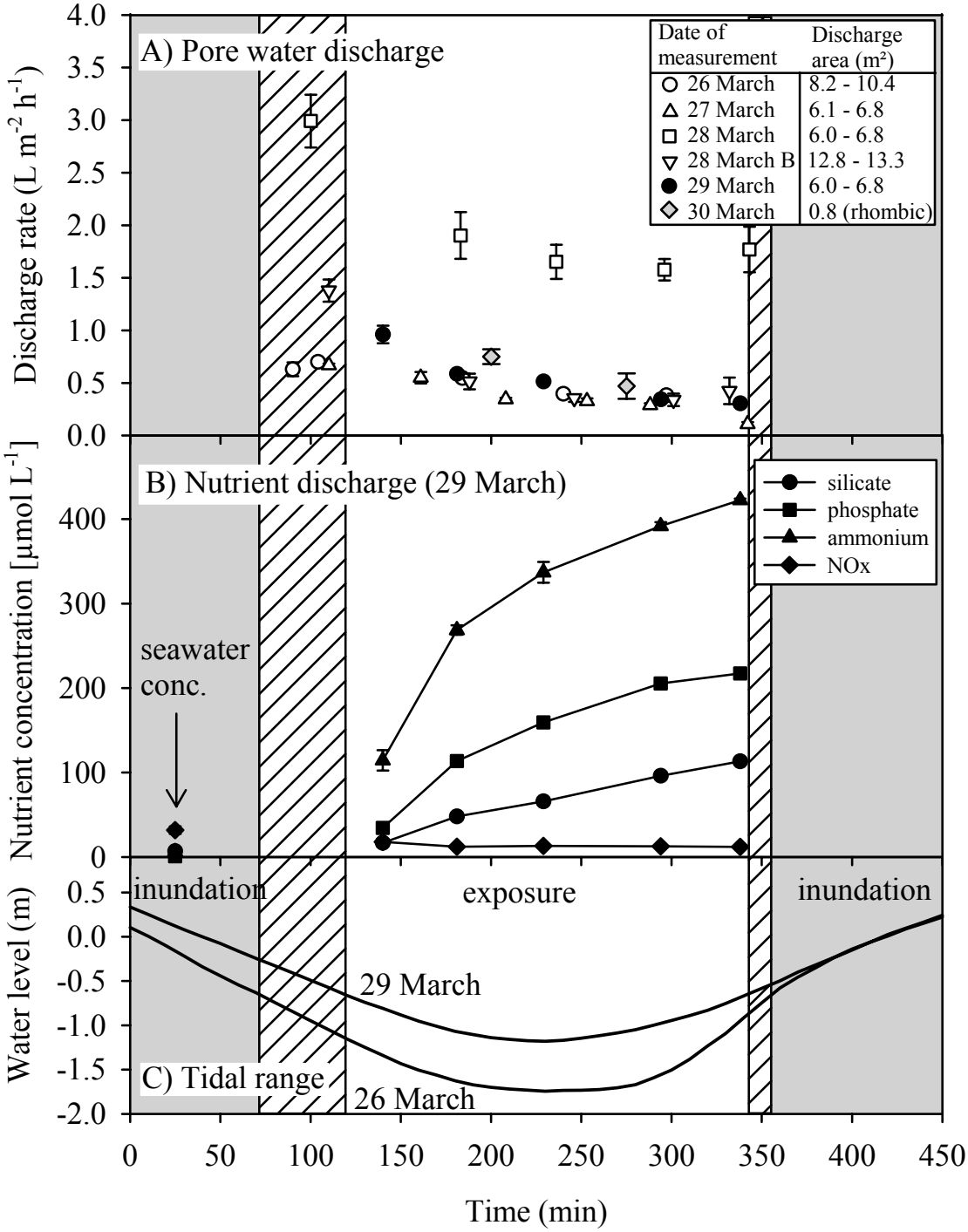

Figure 7: (A) Low tide pore water seepage rates during five consecutive days at the lower sand flat (n = 10) and associated sampling discharge areas (inset table). (B) Nutrient concentrations of the discharged pore water corresponding to the measurement of 29 March (filled symbols in (A); n = 3). All measurements were conducted within 20 m distance and reported values are means with standard deviation as error bars. (C) Lines mark minimum and maximum range of water level between 26 March and 30 March measurements based on mean sea level. Grey shading: inundation period of tidal flat. Hatched area: period of inundation or exposure depending on tidal range.

Pore water solute and seawater concentrations

In July and March, we measured significant differences in the pore water nutrient and DIC concentrations between the upper and the lower Janssand sites (two-tailed U-test after Wilcoxon, Mann and Whitney $\alpha < 0.002$). At the lower sand flat site, where water drained from the Janssand sediment, pore water silicate, phosphate and ammonium concentrations exceeded the respective concentrations at the upper flat by about one order of magnitude during both measuring campaigns (Fig. 8).

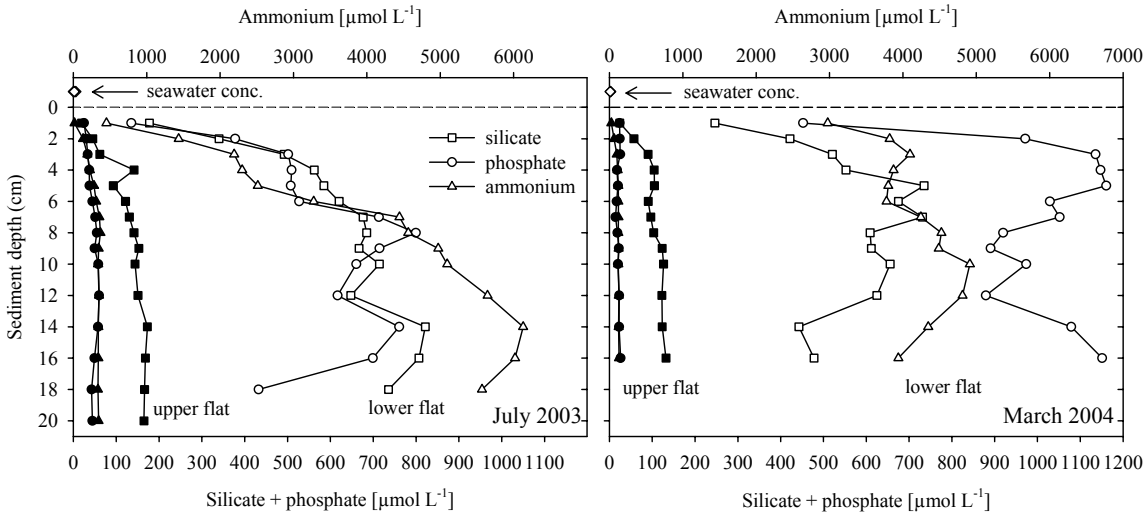

Figure 8: Pore water concentrations [µmol L^{-1}] of silicate, phosphate, and ammonium at the upper (filled symbols) and lower (open symbols) sand flat sites during July 2003 and March 2004. The concentrations of the overlying seawater are shown above the dashed line.

Likewise, pore water DIC concentrations at the lower site were 2 to 5-fold higher than at the upper site in July, and 5 to 6-fold higher in March (Fig. 9), reaching up to 20 mmol L^{-1} in concentration during both campaigns. Pore water solute concentrations exceeded those of the ambient water by far (Table 4). Water column C:N ratios of POM were on average between 6 and 7, indicating fresh organic matter. During July 2003, chlorophyll *a* inventory in the upper 5 cm of the sediment was similar for both sites (range: 8-14 µg g^{-1} Chl *a*).

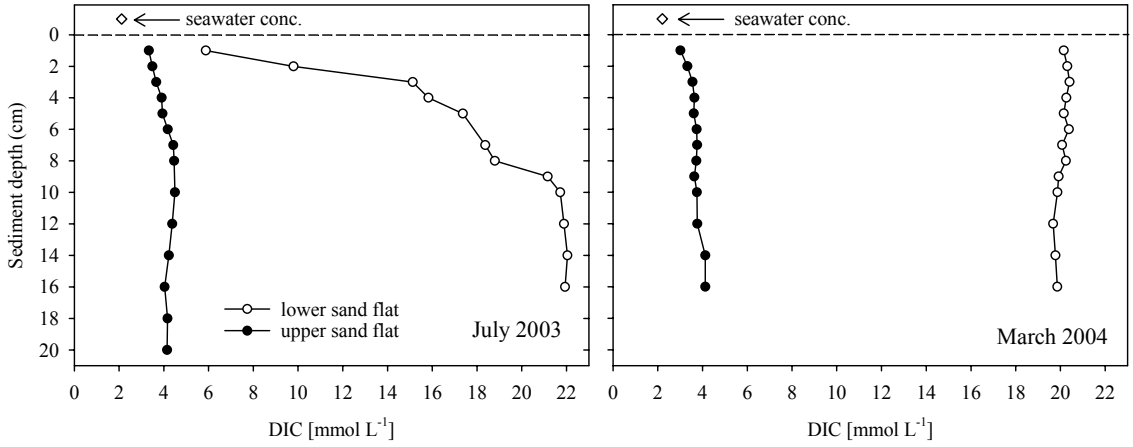

Figure 9: Pore water DIC concentration [mmol L^{-1}] at the upper (filled symbols) and lower sand flat (open symbols) sites. DIC concentration of the overlying seawater is shown above the dashed line.

Table 4: Seawater characteristics at the study site during the March and July campaigns.

	July 2003	March 2004
Temperature (°C)	20.5 - 23.1	5.6 - 8.4
Salinity	31 - 32	29 - 31
Silicate [µmol L^{-1}]	5.91 ± 0.51 (n=4)	6.86 ± 2.63 (n=4)
Phosphate [µmol L^{-1}]	1.80 ± 0.27 (n=4)	0.91 ± 0.76 (n=4)
Ammonium [µmol L^{-1}]	0.21 ± 0.07 (n=4)	6.03 ± 4.11 (n=4)
Nitrate+Nitrite [µmol L^{-1}]	0.30 ± 0.02 (n=4)	31.75 ± 4.45 (n=4)
DIC [µmol L^{-1}]	2082.82 ± 21.61 (n=4)	2200.02 (n=1)
DOC [mg L^{-1}]	4.79 ± 1.98 (n=5)	2.59 ± 1.48 (n=6)
POC [mg L^{-1}]	1.56 ± 0.13 (n=2)	2.47 ± 0.06 (n=3)
PN [mg L^{-1}]	0.23 ± 0.01 (n=2)	0.31 ± 0.03 (n=3)

Chamber flux measurements

The bromide tracer was transported down to a sediment depth of 2 to 3 cm revealing advective flushing of the incubated permeable sediment (Table 5). At the upper sand flat, phosphate was released from the sediment, while silicate was consumed (Fig. 10). Concentrations of ammonium, nitrate and nitrite stayed below the detection limits. Fluxes of DIC and oxygen reflected photosynthetic activity. Oxygen was produced in the transparent (1500-2000 µmol m^{-2} h^{-1}) and consumed (1300-1600 µmol m^{-2} h^{-1}) in the opaque chambers, corresponding to an average gross photosynthetic production of 3300 µmol C m^{-2} h^{-1}.

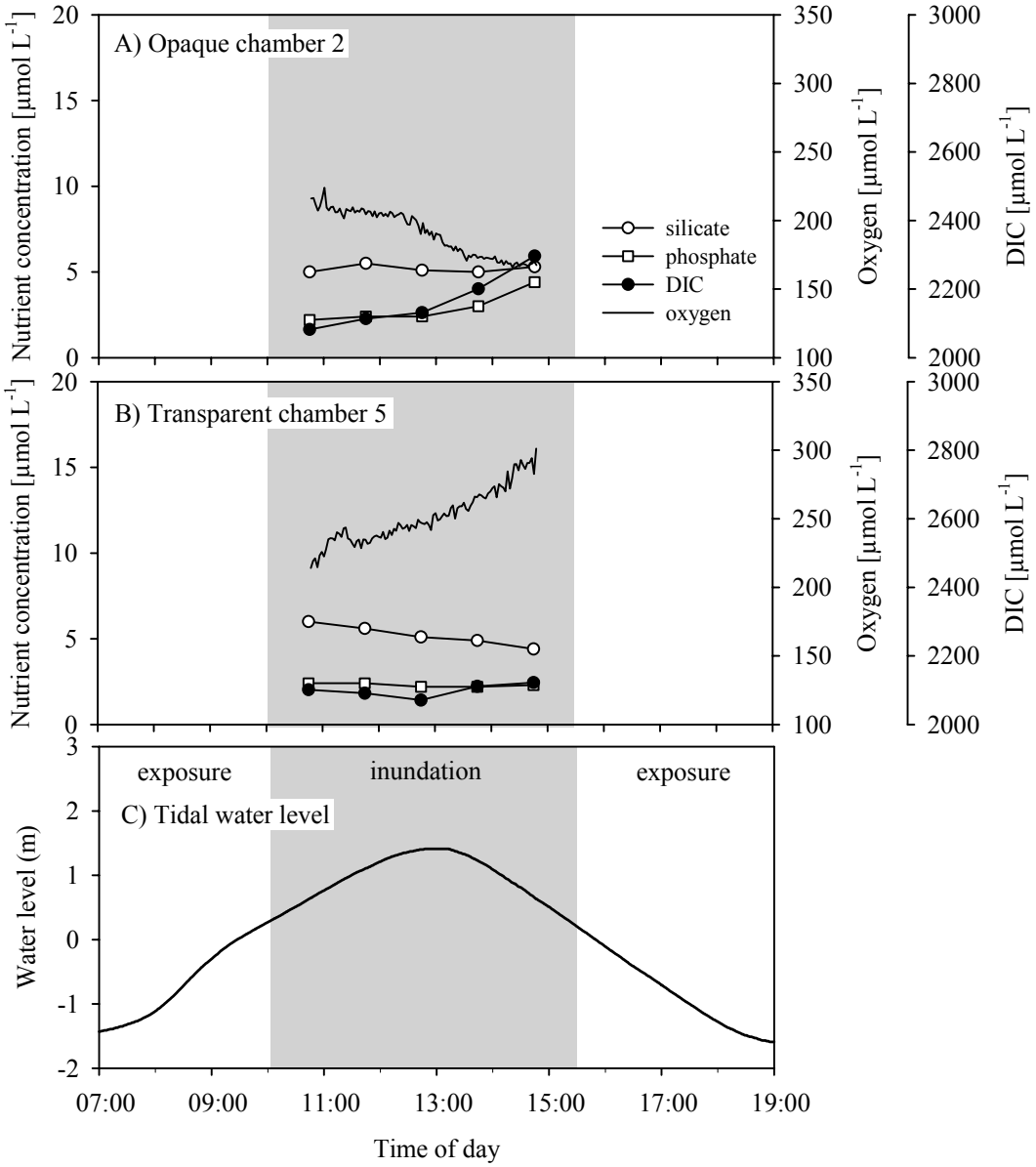

Figure 10: (A) Solute concentration changes at the upper sand flat site in the overlying water of one opaque and (B) one transparent benthic chamber in July 2003. Inundation period of the upper flat site is highlighted with gray shading. (C) Tidal water level based on mean sea level.

Table 5: Effluxes (positive values) and influxes (negative values) in µmol m^{-2} h^{-1} of nutrients, DIC and oxygen of chamber experiments conducted at the upper and lower sand flat in July 2003. For fluxes calculated by linear regression, the r^2 is given in parentheses. All other fluxes were calculated from start-end concentrations. Advective and drainage fluxes are given as the average of 6 chambers, except for the average upper sand flat DIC flux, calculated from dark incubations only.

		Silicate		Phosphate		Ammonium		DIC		Oxygen	
Upper sand flat		0 - 4 h		0 - 4 h		0 - 4 h		0 - 4 h		0 - 4 h	
	1	-47 (0.70)		10 (0.30)		0		4354 (0.89)		-1290 (0.95)	
Opaque	2	2 (0.01)		60 (0.76)		0		6824 (0.90)		-1642 (0.93)	
	3	-60 (0.51)		28 (0.28)		0		2513 (0.86)		-1469 (0.91)	
	4	-56 (0.91)		0 (0.00)		0		1223		2050 (0.95)	
Transparent	5	-46 (0.98)		-5 (0.56)		0		747		1930 (0.90)	
	6	-34 (0.74)		83 (0.72)		0		4055		1493 (0.90)	
Advective flux			-40		29				4564		
Lower sand flat		0 - 6.5 h	6.5 - 8 h	0 - 6.5 h	6.5 - 8 h	0 - 6.5 h	6.5 - 8 h	0 - 6.5 h	6.5 - 8 h	0 - 6.5 h	6.5 - 8 h
	1	50 (0.45)	-166	12 (0.22)	178	92 (0.68)	576	1202 (0.98)	13792	-697 (0.95)	-1276 (0.87)
Opaque	2	285 (0.99)	2419	309 (0.97)	3070	1144 (0.98)	9449	12911 (0.85)	86993	-862 (0.92)	-5042 (0.98)
	3	-42 (1.00)	275	-1 (0.05)	58	-18 (0.31)	300	2623 (1.00)	17740	-1241 (0.95)	-3174 (0.86)
	4	35 (0.47)	836	55 (0.65)	794	391 (0.73)	3306	3199 (0.89)	28714	-646 (0.89)	-660 (0.54)
Transparent	5	158 (0.90)	767	155 (0.85)	1265	734 (0.96)	3455	6949 (0.96)	36594	-789 (0.88)	-1449 (0.62)
	6	108 (0.76)	-111	78 (0.91)	247	497 (0.96)	986	7540 (0.98)	36447	-695 (0.82)	-397 (0.19)
Advective flux			99		101		473		5737		
Drainage flux			571		834		2539		30976		

At the lower sand flat site, pore water started seeping from the sediment after the upper Janssand became exposed during ebb tide. In order to assess the contribution of seepage to the total solute release, fluxes measured during inundation of the lower flat (0-6.5 h) were subtracted from the total fluxes recorded during the period of 1.5 h when the upper flat was exposed and seepage occurred at the lower site (6.5-8 h) (Table 5). During the first 6.5 hours of the lower sand flat incubation, effluxes of silicate, phosphate and ammonium were observed in all but one chamber (Fig. 11). Fluxes of silicate and phosphate were slightly higher and ammonium fluxes were largely increased compared to the upper sand flat chamber measurements (Table 5). Concentrations for nitrate and nitrite always stayed below the detection limit. In contrast to the upper flat site, there was no visible influence of photosynthesis on DIC- and oxygen fluxes. Efflux of DIC was higher than on the upper flat, and oxygen was consumed to the same extent in dark and light chambers (Table 5). During the last 1.5 hours (6.5-8 h) of the lower sand flat incubations, an increased efflux of reduced solutes could be observed in all chambers (Table 5) suggesting that pore water was released from the submerged margin of the Janssand when the upper section of the flat became exposed. The venting port of the chambers permitted release of seepage water into the chambers. Irrespective of dark or light incubations, silicate, phosphate and ammonium concentrations in the chamber waters increased at a higher rate during this period (Fig. 11). The efflux of DIC increased up to 87000 μmol m^{-2} h^{-1} relative to the initial 6.5 h and an increased consumption of oxygen in the opaque chambers was observed. The fluxes of nutrients and DIC during the last 1.5 h exceeded the fluxes recorded prior to this period on average 5 to 8-fold. Advection of pore water into the chambers due to the interaction of the chambers with waves and currents (Shinn et al. 2002) could be ruled out as cause for this increase because no increased pore water discharge into the chambers was measured shortly after submergence of the tidal flat, when strong tidal currents were present.

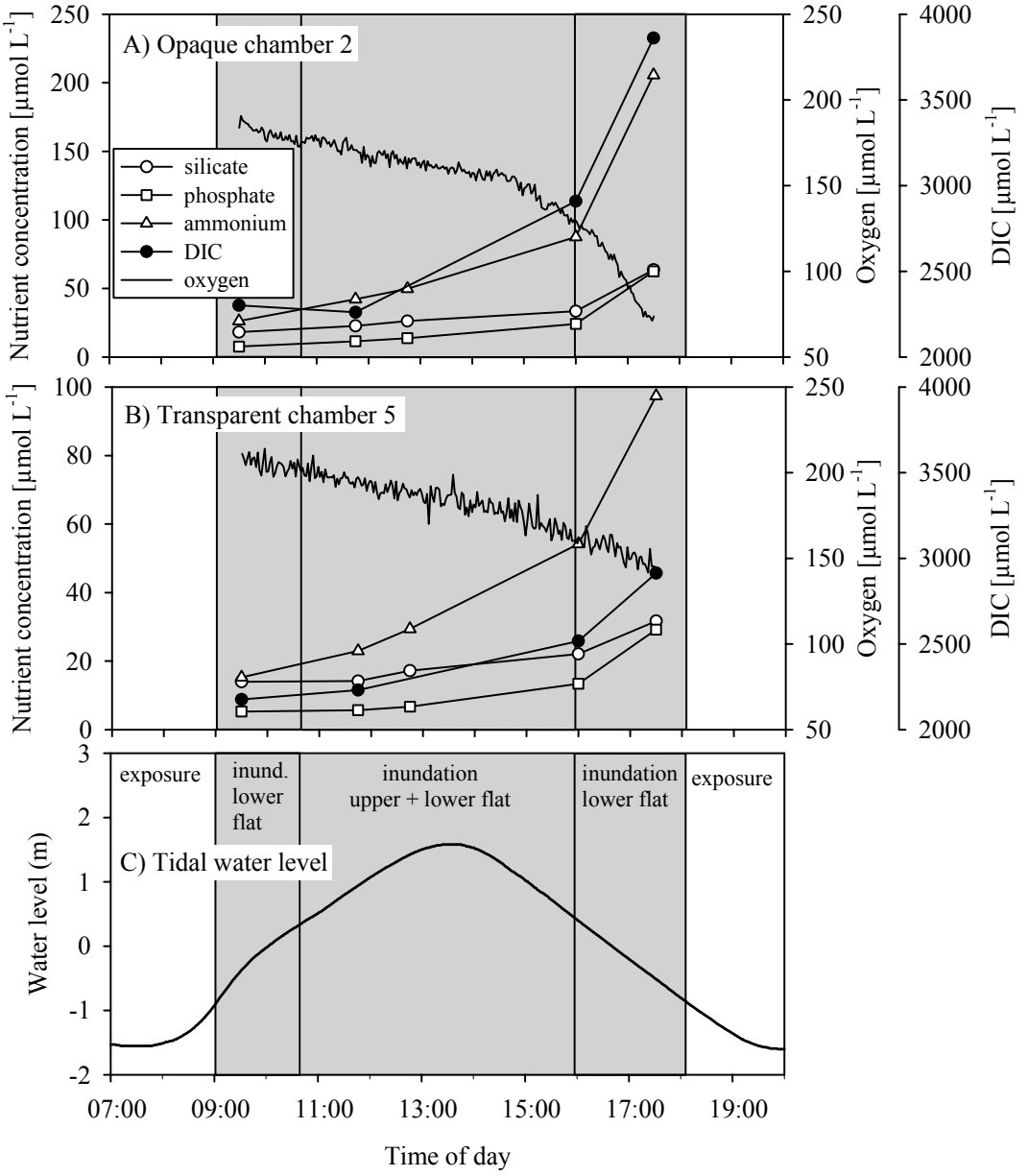

Figure 11: Solute concentration changes at the lower sand flat site measured in the overlying water of (A) one opaque and (B) one transparent benthic chamber in July 2003. Grey shading marks the period of inundation for the upper and lower flat or lower flat only (delimited by vertical lines). (C) Tidal water level change based on mean sea level. Note the different scaling for nutrient concentrations.

DISCUSSION

Our study highlights a process unique to intertidal sediments: the periodic release of concentrated nutrients through pore water seepage. This release is caused by the exposure of the sediments during ebb tide, which sets up a hydraulic pressure gradient between the pore water level and sea water level (Nielsen 1990). The pressure gradient causes water flow through permeable sediment layers towards the seepage zone at the margin of the tidal flat, where pore water is released into tidal gullies. Re-inundation of the flat during flooding removes the pressure gradient, thereby stopping the seepage. In the following, we contrast sediment-water exchange in subtidal and intertidal sand beds and discuss the characteristics of the drainage release and its potential implications.

Sediment-water exchange in intertidal versus subtidal zones

Through this draining mechanism, sediment-water exchange of matter in intertidal flats distinctly differs from that in constantly submerged marine deposits during segments of the tidal cycle. While submerged, diffusion, pore water advection and bioturbation govern sediment-water exchange in both, subtidal and intertidal beds. With the onset of exposure of the intertidal sediment during ebb tide, however, the exchange mechanisms in these sediments change abruptly. With little or no water being present above most of the sediment, diffusive and advective release of sedimentary materials and the activities of bioirrigating macrofauna are reduced to a minimum. The continuing drop of the water level initiates a decline in the water level in the sediment: A slow but directed pore water flow sets in, carrying solutes and small particles along the increasing hydraulic gradient towards the lower rim of the flat and the drainage gullies. Here, pore water release zones develop, similar to those in sandy beaches when a quickly falling tide decouples from the slower falling pore water table (Nielsen 1990, Horn 2002). Material release (except gases) from the exposed intertidal flats, thus, becomes mainly restricted to the seepage zones, and here the observed fluxes were significantly higher than interfacial fluxes recorded during inundation.

The chamber experiments indicate that pore water was already discharged in submerged parts of the tidal flat as soon as a sufficient hydraulic gradient was present. The pronounced increase of nutrient and DIC concentrations in all submerged chambers deployed on the lower flat site after the elevated upper flat became exposed revealed

increased discharge of nutrient-rich seepage water into the chambers (the venting port of the chambers permitted slow fluid exchange) (Fig. 11 and Table 5). We can exclude that an enhanced metabolic activity at the lower site was the cause for these observed increases, because oxygen consumption rates measured during the first 6.5 hours of chamber incubations (Table 5) and sulfate reduction rates (Billerbeck et al. submitted) were similar at both study sites. A similar discharge of pore water into benthic chambers caused by tidal water level fluctuations was reported by Jahnke et al. (2003) for an intertidal salt marsh.

Different qualities of fluxes in submerged and exposed sediment

While in the subtidal and submerged intertidal sediment-water fluxes may reflect seasonal changes in organic matter loading, biological activity and hydrodynamical forcings (Kristensen et al. 1997, D'Andrea et al. 2002, de Beer et al. 2005), the compositional changes of the seepage fluxes during exposure are governed by the length and biogeochemical characteristics of the pathways the pore water follows through the sediment. Although the measured drainage fluid velocity (July 0.86 cm h^{-1}, March 0.54 cm h^{-1}) exceeds transport by molecular diffusion by orders of magnitude, about 16 to 29 tidal cycles are needed for the pore water to travel 1 m through the sediment. Organic materials progressively degrade during the passage through the sediment with the degradation of buried organic matter (e.g., macroalgae) contributing to the solute inventory of the pore water flow. This may explain why the DIC and nutrient concentrations in the seepage water exceeded those recorded in the pore water in the upper 20 cm of the upper flat by factors 10 to 15. Furthermore, the pore water nutrient and DIC concentrations at the lower flat did not show any seasonality in contrast to the upper flat due to the long residence time, dispersion and mixing of the pore water in deeper layers of the tidal flat (Billerbeck et al. submitted).

When integrated over areas exceeding several ripple wavelengths, the quality and quantity of solute fluxes from submerged sand beds is relatively homogeneous (Huettel 1990, Marinelli et al. 1998). In contrast, we observed large changes in the seepage solute concentrations draining from the exposed sand flat (Table 3). Draining of different sections and layers of the intertidal sand, while the water level falls and rises produces variability of seepage water composition. Likewise, we found flux differences between the chambers simultaneously deployed at the lower flat site suggesting seepage heterogeneity on a relatively small spatial scale (Table 5). As a result of sediment

heterogeneities (i.e. zones of different permeabilities), water flowed on preferential paths through the sand (Beven & Germann 1982, Harvey et al. 1995, DiCarlo et al. 1999), which led to spatial variability of seepage in the release zone. This variability was also reflected by black spots (diam. <50 cm) in the seepage zone, produced by local release of sulfidic pore water. However, discharge rates for most measurements in the seepage zone were similar (Fig. 7), when seepage was integrated over larger sediment areas as done by our seepage collectors (6 to 13 m^2 collection area).

Origin of the seepage water

On average, 2.4 to 4.2 L m^{-2} d^{-1} of pore water was discharged on the lower sand flat site during spring and summer, respectively. The subsurface flows drain fluid from the sediment surface, water puddles that had remained on the surface gradually disappeared, and sections of the upper flat became visually "dry". The infiltration of surface water into the sediment carried oxygenated water (possibly O_2-oversaturated due to strong benthic photosynthesis (Revsbech et al. 1980, Revsbech & Jorgensen 1986)), solutes and small particles into the sand (Huettel et al. 1998, Rusch et al. 2001, Ehrenhauss et al. 2004). Despite a continuous drop of the pore water level in the standpipes, the "drying" of the sediment surface ceased with the development of a water saturated capillary fringe (Gillham 1984, Turner & Nielsen 1997), extending upwards the pore water table to the sediment surface (Drabsch et al. 1999, Atherton et al. 2001).

Persistent sediment surface water saturation, while pore water flows and seepage continued, suggested fueling of the pore flows either through other sources (e.g. groundwater (Simmons 1992, Moore 1996)), or a gradual decrease in total tidal flat pore water volume through the drainage. Terrestrial groundwater input is unlikely because pore water chloride concentration remained nearly constant at sea water concentration down to 4 m depth (Koelsch pers. comm.) and salinity of the seepage water did not change. The gradual decrease in total tidal flat pore water volume without entrainment of air (which was never observed at the Janssand) would require shrinkage of the tidal flat during exposure and subsequent swelling during inundation. Such oscillating changes in sediment elevation within a range of 1-3 mm due to tidal water level changes have been detected in intertidal salt marshes (Paquette et al. 2004). We suggest that the seepage in Janssand also resulted in such pore volume changes but the resulting elevation changes would be smaller and difficult to detect. From each meter of the on average 20 m wide release zone, about 24 to 42 L of pore water were discharged per

tidal cycle during March and July, respectively. These volumes would correspond to a sediment elevation change of 0.5 mm for March and 0.8 mm for July, assuming this volume was drained from the approximately 50 m wide zone adjacent to the release zone where we observed water infiltration into the sediment. During re-inundation, the partial release of the capillary tension may initiate expansion of the pore space with simultaneous uptake of water.

Tidal filtration

Uptake and release of water during a tidal cycle represents a filtration process that characterizes the Janssand as a large biocatalytical sand filter (Fig.12). From pore water release rates and seepage nutrient concentrations, we can roughly estimate the total filtration and potentially associated mineralization for the investigated section of tidal flat. As measured during March, about 1.2 L m^{-2} pore water was discharged each tidal cycle from the release zone of the sand flat, when assuming an average exposure time of 2 hours for that zone. On a length of 3.5 km on the northern and northeastern boundary of the Janssand tidal flat (see Fig. 1), the topography and sediment is similar to our study site. With an average width of the release zone of 20 m, a total of 84,000 L pore water was discharged each tidal cycle from this area. In July, the drainage rates calculated based on the benthic chamber incubations were higher, producing on average 2.1 L m^{-2} $tide^{-1}$ or a total discharge of 147,000 L $tide^{-1}$ for the 3.5 km long Janssand section. Assuming degradation of organic matter with a composition close to Redfield ratio, the nutrient discharge associated with seepage would correspond to a mineralization of about 200 mg m^{-2} organic carbon per tide during March (178 to 499 mg OC m^{-2} based on P, 43 to 115 mg OC m^{-2} based on N) and 1700 mg OC m^{-2} $tide^{-1}$ during July (1592 to 5268 mg OC m^{-2} $tide^{-1}$ based on P, 303 to 990 mg OC m^{-2} $tide^{-1}$ based on N, 558 and 1333 mg OC m^{-2} $tide^{-1}$ based on DIC). The observed low N:P ratios (3-4) may have resulted from a loss of NH_4^+ through coupled nitrification/denitrification or release of PO_4 from previously immobilized ironhydoxide-complexes ensuing the release of anoxic pore waters. It has to be kept in mind, however, that the large body of the tidal flat is acting as a seasonally independent nutrient source to the ecosystem through the drainage (Billerbeck et al. submitted). Therefore, the nutrients released from the lower flat may reflect mineralization processes occurring over long time spans and flow paths within the tidal flat. Nevertheless, the estimated mineralization rates are in the range of rates determined in

both seasons for full tidal cycles on this tidal flat (484 and 1201 mg OC m^{-2} $tide^{-1}$ for March and July, respectively, (Billerbeck et al. submitted).

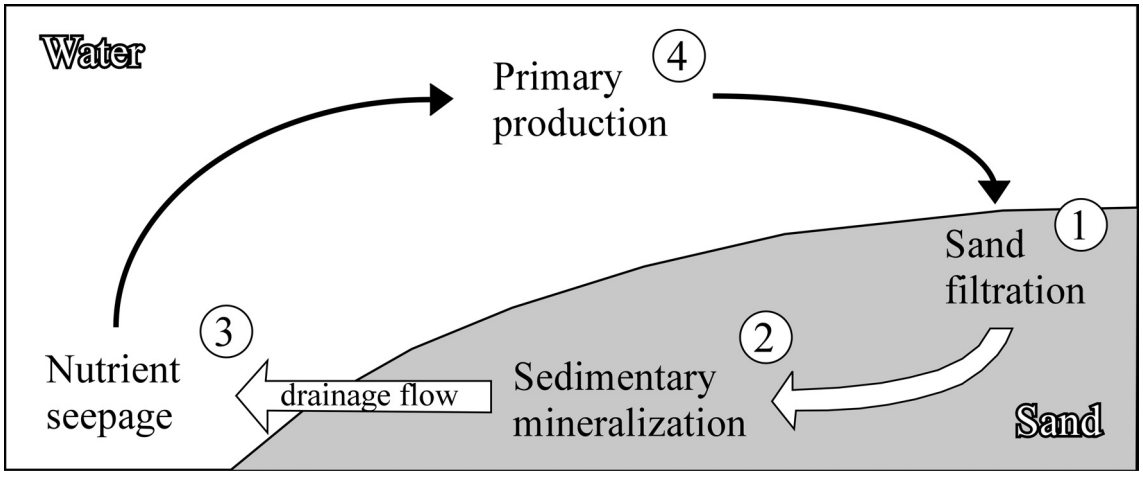

Figure 12: Conceptual model of the Janssand filtration cycle. During low tide, the sedimentary water table in the sediment drops slower than the retreating seawater, producing a hydraulic pressure gradient. As a result, water, suspended and dissolved matter infiltrates the sediment (1) and pore water flows through the permeable sediment along the hydraulic gradient towards the tidal gully. The drainage flows transport substrates to the sedimentary microbial community fueling mineralization (2) and carry metabolic products toward the seepage zone, where nutrient enriched pore water is discharged (3). The seepage nutrients enhance primary production in the water column and on the sediments in the Wadden Sea (4). Replacement of the discharged water volume with seawater during high tide filters organic matter into the permeable sand (1) and the cycle starts anew.

Extrapolated to the 3.5 km long region of the Janssand tidal flat, the pore water discharge would amount to a total required organic carbon mineralization of 6 to 25 kg d^{-1} during March and 42 to 223 kg d^{-1} during July, when based on ammonium and phosphate discharge, respectively (78.1 kg d^{-1} based on DIC fluxes in July). Assuming that 100 % of the DOC and 50 % of POC in the overlying seawater (Table 4) can percolate into the sediment, a total of 0.6 kg (March) or 1.6 kg (July) was filtered each day into the Janssand section as a consequence of drainage. These amounts can only account for a fraction of the mineralization required to produce the observed nutrient release. Buried peat layers may be another source of carbon mineralization (Volkman et al. 2000). Additionally, fresh organic matter may be introduced to the sediment by advective infiltration during inundation (Huettel & Rusch 2000) and by filtering, bioirrigating and bioturbating fauna (Graf & Rosenberg 1997, Aller 2001). Probably the most important organic carbon source on this tidal flat is, however, benthic primary production. Extrapolated to the total area of 245,000 m² of tidal flat that is influenced by infiltration and discharge, and assuming 10 h of light period during July, the average

gross photosynthetic production of 3300 µmol C m^{-2} h^{-1} from the upper sand flat chamber incubations corresponds to a total organic carbon production of 97 kg d^{-1}. This rough estimate can explain about half of the carbon mineralization required to match the observed nutrient export during summer, but benthic primary production should be even higher during exposure of the tidal flat.

Regardless of the origin of the organic matter, our estimate indicates that the Janssand intertidal flat does not accumulate organic matter but releases mineralization products that can account for all if not more than the organic matter that is potentially filtered through the permeable beds with each tidal cycle by the drainage and possibly also for benthic primary production. This observation suggests that these sands mineralize all organic matter that is introduced to the sediment, emphasizing their role as biocatalytical filter systems.

Potential significance of the seepage

The pore water release locally affects the benthos and on a larger spatial scale the nutrient concentrations in intertidal zone. In the vicinity of the seepage zone, the increased nutrient concentrations in the seepage water can support the benthic primary production however, in July 2003, chlorophyll *a* inventory in the upper 5 cm of the sediment was similar for the upper and lower flat sites (8-14 µg g^{-1} Chl *a* at both study sites). Adverse effects of the seepage water may have masked the positive influence of nutrient enrichment. During summer, when seepage sulfide reached up to 1 mmol L^{-1}, the otherwise omnipresent diatoms were replaced by green flagellates and sulfide oxidizers (Burke, deBeer pers. comm.) and *Arenicola marina* fecal mounds in the release zone decreased from 3.6 m^{-2} at the upper flat to 0.6 m^{-2} at the lower flat (6-fold).

Most of the nutrients released through seepage are transported through the tidal gullies towards the North Sea (Niesel & Günther 1999), where they can fuel primary production seawards the barrier islands. Tidal currents transport the organic matter produced within these highly net autotrophic coastal waters back to the Wadden Sea where it is mineralized (Postma 1954, van Beusekom et al. 1999). Because the seepage becomes most active only near maximum low tide and the average width of the sand flat belt along the southern coast of the North Sea is 13 km (van Beusekom & de Jonge 2002), a large fraction of the nutrients will also remain within the Wadden Sea, where they can enhance primary production of phytoplankton and microphytobenthos.

Microalgal production, tidal flat filtration of this organic matter, mineralization within the intertidal sands and subsequent release of nutrients, thus, close a recycling loop, in which the seepage plays an important role (Fig. 12). In the Janssand, nutrient fluxes associated with the seepage exceeded 5 to 8-fold those fluxes caused by the combined effects of diffusion, advection and bioirrigation during inundation. The ecological importance of ground- or pore water discharge and the associated export of metabolic products to the water column has been emphasized in studies covering submarine groundwater discharge, wave dominated beaches and salt marshes (Table 6). However, only few data are available on drainage for intertidal flats. Nutrient export from the Janssand through seepage surpassed the release rates reported from most other studies (Table 6), emphasizing the ecological importance of seepage process in intertidal sands and the need for further, more detailed studies.

Table 6: Comparison of discharge volumes and nutrient release rates from this study to rates reported from other coastal systems.

	Study	Location	Discharge rate $L\ m^{-2}\ d^{-1}$	N-discharge $\mu mol\ m^{-2}\ d^{-1}$	P-discharge $\mu mol\ m^{-2}\ d^{-1}$	Si-discharge $\mu mol\ m^{-2}\ d^{-1}$	Method
Beaches	Mc Lachlan and Illenberger (1986)	Alexandria dune field, South Africa	1000 *	151857 *	2065 *		Darcy´s law, nutrients
	Mc Lachlan (1989)	Threemile Beach, OR	3000 - 4500 *				Darcy´s law
	Campbell and Bate (1998)	Alexandria dune field, South Africa	157 - 328 *	185714 - 400000 *			Darcy´s law, nutrients
	Uchiyama (2000)	Kashima coast, Japan	283.5 - 405 *	77676 *	5132 *	452626 *	Darcy´s law, nutrients
	Ullman et al. (2003)	Cape Henlopen, DEL	600 - 3200 *	300000 - 1600000 *	30000 - 160000 *	140000 - 800000 *	Darcy´s law, nutrients
Submarine groundwater discharge	Bokuniewicz and Pavlik (1990)	Long Island, NY	10.0 - 70.0				seepage meter
	Giblin and Gaines (1990)	Cape Cod, MA	24.0 - 72.0	300 mmol N $m^{-3}\ yr^{-1}$			seepage meter
	Simmons (1992)	Florida Keys	5.4 - 8.9	1.3 - 2.7 mol s^{-1}	0.5 - 1.0 mol s^{-1}		seepage meter
		Wilmington, NC	6.0 - 20.0				seepage meter
	Reay et al (1992)	Cherrystone Inlet, VA	0.48 - 88.6	3926.4			seepage meter
	Moore (1996)	South Atlantic Bight	5.0				226 Ra-activity
	Piekarek-Jankowska (1996)	Puck Bay, Baltic Sea	0.4				nutrients, isotopes
	Cable et al. (1997)	Northeast Gulf of Mexico, FL	15.8 - 33.1				seepage meter
	Corbett et al. (1999)	Florida Bay	10.4 - 30.5	301.4	0.6		seepage meter
	Charette et al. (2003)	Great Sippewissett, MA	9.8				226 Ra-activity
	Schlueter et al. (2004)	Eckernfoerde Bay, Baltic Sea	0.5				pore water modeling
	Taniguchi (2004)	Osaka Bay, Japan	10.3 - 81.9				seepage meter
Salt marshes	Hemond and Fifield (1982)	Great Sippewissett, MA	12.0				Darcy´s law
	Agosta (1985)	North Inlet, SC	15.2 - 168.0				water balance
	Jordan and Correll (1985)	Rhode River, MD	60 *	45.7 - 62.1 *	7.8 - 15.5 *		Darcy´s law, nutrients
	Yelverton and Hackney (1986)	Pender County, NC	0.1 - 0.9				seepage meter
	Whiting and Childers (1989)	North Inlet, SC	7.8 - 28.0	344.4 - 615.6	6.5 - 15.8		seepage meter
	Harvey and Odum (1990)	Eagle Bottom, Carter Creek, VA	0.2 - 1				Darcy´s law
	Howes and Goehringer (1994)	Great Sippewissett, MA	30.4	332.9			seepage meter
	Morris (1995)	North Inlet, SC	9.4 - 16.6				salt balance
	Harvey and Nuttle (1995)	Phillips Creek, VA	0.4				water balance
	Osgood (2000)	Pritchards Island, SC	114.8	476.7	30.1		seepage meter
		Hog Island, VA	120.2	531.5	189		seepage meter
	Tobias et al. (2001)	Ringfield Marsh, VA	0.6 - 22.6	802.5			salt balance
	Jahnke et al. (2003)	Satilla River Estuary, GA	0.4-0.6 †	500000			benthic chambers
Tidal flats	Le Hir et al. (2000)	Le Havre, Marennes-Oleron, France Humber Estuary, United Kingdom	20.0				runnel-runoff velocity
	This study	Island of Spiekeroog, Germany	2.4	1074.2	279.8	141.0	V-shaped laths (March)
			4.2	5077.5	1668.4	1141.9	benthic chambers (July)

* discharge per m shoreline † localized discharge in L $cm^{-2}\ d^{-1}$

ACKNOWLEDGEMENTS

We thank Martina Alisch for the assistance in field and laboratory work and also acknowledge the hospitality and help of the Plattboden-ship crews during the cruises. We also thank Gaby Schüßler, Susanne Menger, Daniela Franzke, and Sindy Pabel for their help with laboratory work and Cäcilia Wiegand for the preparation of the oxygen optodes. This study would not have been possible without the technical assistance of Jens Langreder, Axel Nordhausen, Georg Herz, Alfred Kutsche, Paul Färber, Volker Meyer, and Harald Osmers. Thomas Badewien of the ICBM in Oldenburg and Waldemar Anton of the WSA Emden kindly provided tide gauge data. We appreciate the valuable comments of Antje Boetius, Perran Cook, Stefan Jansen, and Christian Wild on the manuscript. This study was supported by the Deutsche Forschungsgemeinschaft (DFG) within the research group "Biogeochemistry of the Wadden Sea" (FG 432-5), coordinated by Jürgen Rullkötter. We are grateful to Bo Barker Jørgensen and Michael Böttcher for their support of this work and coordination of the sub-project "Biogeochemical processes at the sediment-water interface of intertidal sediments".

LITERATURE CITED

Agosta K. (1985) The effect of tidally induced changes in the creekbank water table on pore water chemistry. Estuar. Coast. Shelf Sci. 21:389-400

Aller R. C. (2001) Transport and reactions in the bioirrigated zone. In: Boudreau B. P., Jorgensen B. B. (eds) The Benthic Boundary Layer. Oxford University Press, Oxford, p 269-301

Atherton R. J., Baird A. J., Wiggs G. F. S. (2001) Inter-tidal dynamics of surface moisture content on a meso-tidal beach. J. Coast. Res. 17:482-489

Beven K., Germann P. (1982) Macropores and water flow in soils. Water Resour. Res. 18:1311-1325

Billerbeck M., Werner U., Polerecky L., Walpersdorf E., de Beer D., Huettel M. (submitted) Surficial and deep pore water circulation governs spatial and temporal scales of nutrient recycling in intertidal sand flat sediment. Mar. Ecol. Prog. Ser.

Bokuniewicz H., Pavlik B. (1990) Groundwater seepage along a barrier-island. Biogeochemistry 10:257-276

Cable J. E., Burnett W. C., Chanton J. P., Corbett D. R., Cable P. H. (1997) Field evaluation of seepage meters in the coastal marine environment. Estuar. Coast. Shelf Sci. 45:367-375

Campbell E. E., Bate G. C. (1998) Tide-induced pulsing of nutrient discharge from an unconfined aquifer into an *Anaulus australis*-dominated surf-zone. Water SA 24:365-370

Charette M. A., Splivallo R., Herbold C., Bollinger M. S., Moore W. S. (2003) Salt marsh submarine groundwater discharge as traced by radium isotopes. Mar. Chem. 84:113-121

Corbett D. R., Chanton J., Burnett W., Dillon K., Rutkowski C., Fourqurean J. W. (1999) Patterns of groundwater discharge into Florida Bay. Limnol. Oceanogr. 44:1045-1055

D'Andrea A. F., Aller R. C., Lopez G. R. (2002) Organic matter flux and reactivity on a South Carolina sandflat: The impacts of porewater advection and macrobiological structures. Limnol. Oceanogr. 47:1056-1070

de Beer D., Wenzhoefer F., Ferdelman T. G., Boehme S. E., Huettel M., van Beusekom J. E. E., Boettcher M. E., Musat N., Dubillier N. (2005) Transport and mineralization rates in North Sea sandy intertidal sediments, Sylt-Rømø Basin, Wadden Sea. Limnol. Oceanogr. 50:113-127

DiCarlo D. A., Bauters T. W. J., Darnault C. J. G., Steenhuis T. S., Parlange J. Y. (1999) Lateral expansion of preferential flow paths in sands. Water Resour. Res. 35:427-434

Drabsch J. M., Parnell K. E., Hume T. M., Dolphin T. J. (1999) The capillary fringe and the water table in an intertidal estuarine sand flat. Estuar. Coast. Shelf Sci 48:215-222

Ehrenhauss S., Witte U., Buhring S. L., Huettel M. (2004) Effect of advective pore water transport on distribution and degradation of diatoms in permeable North Sea sediments. Mar. Ecol. Prog. Ser. 271:99-111

Flemming B. W., Ziegler K. (1995) High-resolution grain size distribution patterns and textural trends in the backbarrier environment of Spiekeroog Island (southern North Sea). Senckenb. Marit. 26:1-24

Forster S., Glud R. N., Gundersen J. K., Huettel M. (1999) In situ study of bromide tracer and oxygen flux in coastal sediments. Estuar. Coast. Shelf Sci. 49:813-827

Giblin A. E., Gaines A. G. (1990) Nitrogen inputs to a marine embayment - the importance of groundwater. Biogeochemistry 10:309-328

Gillham R. W. (1984) The capillary-fringe and its effect on water-table response. J. Hydrol. 67:307-324

Graf G., Rosenberg R. (1997) Bioresuspension and biodeposition: A review. J. Mar. Syst. 11:269-278

Grasshoff K., Kremling K., Ehrhardt M. (1999) Methods of seawater analysis, Wiley-VCH Verlag

Hall P. O. J., Aller R. C. (1992) Rapid, small-volume, flow injection analysis for ΣCO_2 and NH_4^+ in marine and freshwaters. Limnol. Oceanogr. 37:1113-1119

Harvey J. W., Chambers R. M., Hoelscher J. R. (1995) Preferential Flow and Segregation of Porewater Solutes in Wetland Sediment. Estuaries 18:568-578

Harvey J. W., Nuttle W. K. (1995) Fluxes of water and solute in a coastal wetland sediment. 2. Effect of macropores on solute exchange with surface water. J. Hydrol. 164:109-125

Harvey J. W., Odum W. E. (1990) The influence of tidal marshes on upland groundwater discharge to estuaries. Biogeochemistry 10:217-236

Hemond H. F., Fifield J. L. (1982) Subsurface flow in salt-marsh peat - a model and field-study. Limnol. Oceanogr. 27:126-136

Hertweck G. (1995) Distribution patterns of characteristic sediment bodies and benthos populations in the Spiekeroog backbarrier tidal flat area, southern North Sea. 1. Results of a survey of tidal flat structure 1988-1992. Senckenb. Marit. 26:81-94

Holst G., Glud R. N., Kuhl M., Klimant I. (1997) A microoptode array for fine-scale measurement of oxygen distribution. Sens. Actuator. B-Chem. 38:122-129

Horn D. P. (2002) Beach groundwater dynamics. Geomorphology 48:121-146

Howes B. L., Goehringer D. D. (1994) Porewater drainage and dissolved organic carbon and nutrient losses through the intertidal creekbanks of a New England salt marsh. Mar. Ecol. Prog. Ser. 114:289-301

Huettel M. (1990) Influence of the lugworm *Arenicola marina* on porewater nutrient profiles of sand flat sediments. Mar. Ecol. Prog. Ser. 62:241-248

Huettel M., Gust G. (1992) Solute release mechanism from confined sediment cores in stirred benthic chambers and flume flows. Mar. Ecol. Prog. Ser. 82:187-197

Huettel M., Roy H., Precht E., Ehrenhauss S. (2003) Hydrodynamical impact on biogeochemical processes in aquatic sediments. Hydrobiologia 494:231-236

Huettel M., Rusch A. (2000) Transport and degradation of phytoplankton in permeable sediment. Limnol. Oceanogr. 45:534-549

Huettel M., Ziebis W., Forster S. (1996) Flow-induced uptake of particulate matter in permeable sediments. Limnol. Oceanogr. 41:309-322

Huettel M., Ziebis W., Forster S., Luther G. W. (1998) Advective transport affecting metal and nutrient distributions and interfacial fluxes in permeable sediments. Geochim. Cosmochim. Acta 62:613-631

Jahnke R. A., Alexander C. R., Kostka J. E. (2003) Advective pore water input of nutrients to the Satilla River Estuary, Georgia, USA. Estuar. Coast. Shelf Sci. 56:641-653

Jordan T. E., Correll D. L. (1985) Nutrient chemistry and hydrology of interstitial water in brackish tidal marshes of Chesapeake Bay. Estuar. Coast. Shelf Sci. 21:45-55

Klimant I., Meyer V., Kuhl M. (1995) Fiberoptic oxygen microsensors, a new tool in aquatic biology. Limnol. Oceanogr. 40:1159-1165

Kristensen E., Jensen M. H., Jensen K. M. (1997) Temporal variations in microbenthic metabolism and inorganic nitrogen fluxes in sandy and muddy sediments of a tidally dominated bay in the northern Wadden Sea. Helgol. Mar. Res. 51:295-320

Kuwae T., Hosokawa Y., Eguchi N. (1998) Dissolved inorganic nitrogen cycling in Banzu intertidal sand-flat, Japan. Mangroves Salt Marshes 2:167-175

Le Hir P., Roberts W., Cazaillet O., Christie M., Bassoullet P., Bacher C. (2000) Characterization of intertidal flat hydrodynamics. Cont. Shelf Res. 20:1433-1459

Lorenzen C. J. (1967) Determination of chlorophyll and pheo-pigments: Spectrophotometric equations. Limnol. Oceanogr. 12:343-346

Marinelli R. L., Jahnke R. A., Craven D. B., Nelson J. R., Eckman J. E. (1998) Sediment nutrient dynamics on the South Atlantic Bight continental shelf. Limnol. Oceanogr. 43:1305-1320

McLachlan A. (1989) Water filtration by dissipative beaches. Limnol. Oceanogr. 34:774-780

McLachlan A., Illenberger W. (1986) Significance of groundwater nitrogen input to a beach surf zone ecosystem. Stygologia 2:291-296

Moore W. S. (1996) Large groundwater inputs to coastal waters revealed by Ra-226 enrichments. Nature 380:612-614

Morris J. T. (1995) The mass-balance of salt and water in intertidal sediments - Results from North-Inlet, South-Carolina. Estuaries 18:556-567

Nielsen P. (1990) Tidal dynamics of the water table in beaches. Water Resour. Res. 26:2127-2134

Niesel V., Günther C. P. (1999) Distribution of nutrients, algae and zooplankton in the Spiekeroog backbarrier system. In: Dittmann S. (ed) The Wadden Sea Ecosystem - Stability Properties and Mechanisms. Springer-Verlag, Berlin Heidelberg New York, p 77-94

Osgood D. T. (2000) Subsurface hydrology and nutrient export from barrier island marshes at different tidal ranges. Wetlands Ecol. Manage. 8:133-146

Paquette C. H., Sundberg K. L., Boumans R. M. J., Chmura G. L. (2004) Changes in saltmarsh surface elevation due to variability in evapotranspiration and tidal flooding. Estuaries 27:82-89

Piekarek-Jankowska H. (1996) Hydrochemical effects of submarine groundwater discharge to the Puck Bay (Southern Baltic Sea, Poland). Geographia Polonica 67:103-119

Pilditch C. A., Emerson C. W., Grant J. (1997) Effect of scallop shells and sediment grain size on phytoplankton flux to the bed. Cont. Shelf Res. 17:1869-1885

Postma H. (1954) Hydrography of the Dutch Wadden Sea. Arch. néerl. Zool. 10:405-511

Precht E., Huettel M. (2004) Rapid wave-driven advective pore water exchange in a permeable coastal sediment. J. Sea Res. 51:93-107

Reay W. G., Gallagher D. L., Simmons G. M. (1992) Groundwater discharge and its impact on surface-water quality in a Chesapeake Bay inlet. Water Resour. Bull. 28:1121-1134

Revsbech N. P., Jorgensen B. B. (1986) Microelectrodes: Their use in microbial ecology. In: Marshall K. C. (ed) Advances in microbial ecology, Vol 9. Plenum Press, New York and London, p 293-352

Revsbech N. P., Sorensen J., Blackburn T. H., Lomholt J. P. (1980) Distribution of oxygen in marine sediments measured with microelectrodes. Limnol. Oceanogr. 25:403-411

Rusch A., Forster S., Huettel M. (2001) Bacteria, diatoms and detritus in an intertidal sandflat subject to advective transport across the water-sediment interface. Biogeochemistry 55:1-27

Schlueter M., Sauter E. J., Andersen C. E., Dahlgaard H., Dando P. R. (2004) Spatial distribution and budget for submarine groundwater discharge in Eckernfoerde Bay (Western Baltic Sea). Limnol. Oceanogr. 49:157-167

Shinn E. A., Reich C. D., Hickey T. D. (2002) Seepage meters and Bernoulli's revenge. Estuaries 25:126-132

Simmons G. M., Jr. (1992) Importance of submarine groundwater discharge (SGWD) and seawater cycling to material flux across sediment/water interfaces in marine environments. Mar. Ecol. Prog. Ser. 84:173-184

Taniguchi M., Iwakawa H. (2004) Submarine groundwater discharge in Osaka Bay, Japan. Limnology 5:25-32

Tobias C. R., Harvey J. W., Anderson I. C. (2001) Quantifying groundwater discharge through fringing wetlands to estuaries: Seasonal variability, methods comparison, and implications for wetland-estuary exchange. Limnol. Oceanogr. 46:604-615

Turner I. L., Nielsen P. (1997) Rapid water table fluctuations within the beach face - implications for swash zone sediment mobility. Coast. Eng. 32:45-59

Uchiyama Y., Nadaoka K., Rolke P., Adachi K., Yagi H. (2000) Submarine groundwater discharge into the sea and associated nutrient transport in a sandy beach. Water Resour. Res. 36:1467-1479

Ullman W. J., Chang B., Miller D. C., Madsen J. A. (2003) Groundwater mixing, nutrient diagenesis, and discharges across a sandy beachface, Cape Henlopen, Delaware (USA). Estuar. Coast. Shelf Sci. 57:539-552

Usui T., Koike I., Ogura N. (1998) Tidal effect on dynamics of pore water nitrate in intertidal sediment of a eutrophic estuary. J. Oceanogr. 54:205-216

van Beusekom J. E. E., Brockmann U. H., Hesse K. J., Hickel W., Poremba K., Tillmann U. (1999) The importance of sediments in the transformation and turnover of nutrients and organic matter in the Wadden Sea and German Bight. German Journal of Hydrography 51:245-266

van Beusekom J. E. E., de Jonge V. N. (2002) Long-term changes in Wadden Sea nutrient cycles: importance of organic matter import from the North Sea. Hydrobiologia 475:185-194

Volkman J. K., Rohjans D., Rullkoetter J., Scholz-Boettcher B. M., Liebezeit G. (2000) Sources and diagenesis of organic matter in tidal flat sediments from the German Wadden Sea. Cont. Shelf Res. 20:1139-1158

Whiting G. J., Childers D. L. (1989) Subtidal advective water flux as a potentially important nutrient input to southeastern U.S.A. saltmarsh estuaries. Estuar. Coast. Shelf Sci. 28:417-431

Yelverton G. F., Hackney C. T. (1986) Flux of dissolved organic carbon and pore water through the substrate of a *Spartina alterniflora* marsh in North Carolina. Estuar. Coast. Shelf Sci. 22:255-267

Ziebis W., Huettel M., Forster S. (1996) Impact of biogenic sediment topography on oxygen fluxes in permeable sediments. Mar. Ecol. Prog. Ser. 140:227-237

Surficial and deep pore water circulation governs spatial and temporal scales of nutrient recycling in intertidal sand flat sediment

Markus Billerbeck, Ursula Werner, Lubos Polerecky, Eva Walpersdorf, Dirk de Beer and Markus Huettel

submitted to Marine Ecology Progress Series

ABSTRACT

We studied aerobic and anaerobic mineralization in permeable sediment of a sloping intertidal sand flat near the island of Spiekeroog, southern North Sea. One site near the water line and one site on the upper flat were studied on a tidal and seasonal basis to assess the temporal and spatial scales of mineralization. Hydrodynamic forcing during inundation of the tidal flat caused deeper oxygen penetration through flushing of the uppermost sediment layer. This flushing resulted in higher areal oxygen consumption and lower depth integrated sulfate reduction rates in the submerged flat than during exposure. Mineralization rates in the top 15 cm of the sediment were similar between both study sites and ranged from 38 (winter) to 280 mmol C m^{-2} d^{-1} (summer), with sulfate reduction contributing 3 to 25 % to total mineralization, depending on the season. At the upper flat, the seasonal differences were reflected in the pore water concentrations of nutrients, DIC and DOC. Near the low water line, however, pore water nutrient and DIC concentrations were independent of the season and up to 15-times higher compared to the upper flat. The differences in concentrations of metabolic products between the two sites resulted from a low tide drainage extending deep below the uppermost flushed layer and causing seepage of pore water near the low water line. Mineralization and nutrient release in these permeable intertidal sediments is affected by two circulation processes that work on distinctly different temporal and spatial scales: 1) rapid “skin circulation” through the uppermost sediment layer during inundation that is characterized by short flow paths, low pore water residence time and immediate feedback to the ecosystem; 2) slow “body circulation” through deeper sediment layers during low tide that is characterized by long flow paths and pore water residence times, and is acting as a buffered nutrient source to the ecosystem.

INTRODUCTION

Sandy sediments prevail in the intertidal regions of the German Wadden Sea (Flemming & Ziegler 1995). Despite rather small bacterial numbers and low organic matter content of sandy sediments (Bergamaschi et al. 1997, Llobet-Brossa et al. 1998, Rusch et al. 2003), their high mineralization capacity has been recognized in recent studies (Cammen 1991, D'Andrea et al. 2002, Huettel et al. 2003). The permeability of the sand facilitates advective pore water transport through the upper sediment layers in contrast to muddy sediments, where diffusional processes are dominating (Huettel & Gust 1992, Huettel & Webster 2001). The advective pore water transport can exceed diffusion by orders of magnitude (Lohse et al. 1996, Boudreau et al. 2001).

During inundation of intertidal sand flats, the percolation of water through the sediment is driven by pressure gradients generated by the interaction of bottom currents with the sediment topography (Thibodeaux & Boyle 1987, Glud et al. 1996) and by waves passing over the permeable bed (Van der Loeff 1981, Precht & Huettel 2003). This hydrodynamic forcing provides oxygen to the upper sediment layers and enhances aerobic mineralization of organic matter during inundation (Forster et al. 1996, Dauwe et al. 2001, Werner et al. submitted). The high aerobic mineralization capacity in the upper sediment layers and anaerobic degradation processes deeper in the sediment are fueled by the filtration of suspended particles and dissolved organic matter from the water column into the permeable bed (Huettel et al. 1996, Rusch et al. 2001). Furthermore, bioturbation and bioirrigation by benthic macrofauna adds to the supply of electron acceptors and organic matter to the sediment (Graf & Rosenberg 1997, Aller 2001). Inorganic nutrients, the products of mineralization, are removed from the sand by the advective flushing (Huettel et al. 1998) and can support primary production in the water column. The depth of the advective flushing is dependent on the permeability of the sediment and usually is restricted to the top few mm to cm of the sand bed (Brotas et al. 1990, de Beer et al. 2005). Within this surface layer of the tidal flat, organic matter can be recycled quickly and immediate feedback may be provided to the ecosystem in a matter of hours to days by the removal of the metabolic products from the sediment.

The lack of advective flushing during low tide exposure of the intertidal flat leads to accumulation of metabolic products in the sediment (Rocha 1998, Kuwae et al. 2003). Transport, however, is not restricted to diffusion during exposure. Some benthic bioturbators are still active during exposure (Orvain & Sauriau 2002). Also, pore water may be drained through the permeable sand driven by the buildup of a hydraulic

gradient between the sea water level and the slower dropping pore water level (Nielsen 1990). The drainage mechanism transports pore water mainly laterally through the sediment towards the low water line, where pore water discharge can be observed also at the exposed sediment surface constituting an important nutrient input to coastal waters (Howes & Goehringer 1994, Osgood 2000, Jahnke et al. 2003). Sediment layers extending deep below the regularly flushed upper layer can be affected by the drainage over horizontal distances between tens and hundreds of meters (Whiting & Childers 1989, Jahnke et al. 2003). Due to the long residence time and pathways of the pore water within these deeper layers of the intertidal flat, the feedback of mineralization products to the ecosystem is delayed. This large body of the sand flat, thus, may act as a source of nutrients that can support primary production in the system during times of low nutrient concentrations in the sea water.

We hypothesize that in an intertidal sand flat the recycling of sedimentary mineralization products is governed by two main pore water circulation patterns operating on distinctly different temporal and spatial scales: 1) a rapid “skin circulation” within the top sediment layer, characterized by short flow paths and residence times of the pore water with an immediate feedback to the system; 2) a slower “body circulation” through the surface and deeper layers of the sediment with long flow paths and pore water residence times. Due to the relatively long time interval between organic matter input and mineralization product release, this “body circulation” may act as a large buffer system for nutrients. In order to test this hypothesis, measurements of oxygen consumption and sulfate reduction were conducted on a sloping intertidal sand flat in the German Wadden Sea and combined with measurements of oxygen penetration depth and pore water concentrations of metabolic products. In order to assess the temporal scales of the mineralization processes, one study site near the low water line and one site at the upper flat were studied on a tidal and seasonal basis.

METHODS

Site description

Sampling and in situ measurements were carried out at the north eastern margin of the 11 km² large Janssand tidal flat (53°44`07`` N, 007°41`57`` E), an intertidal sand flat located in the backbarrier area of the island of Spiekeroog, North Sea, Germany (Fig. 1A). The marginal area of this tidal flat is sloping on average 1.6 cm m^{-1} towards the low water line, and the tidal flat is covered by 1.5-2 m of water during high tide (Fig. 1B).

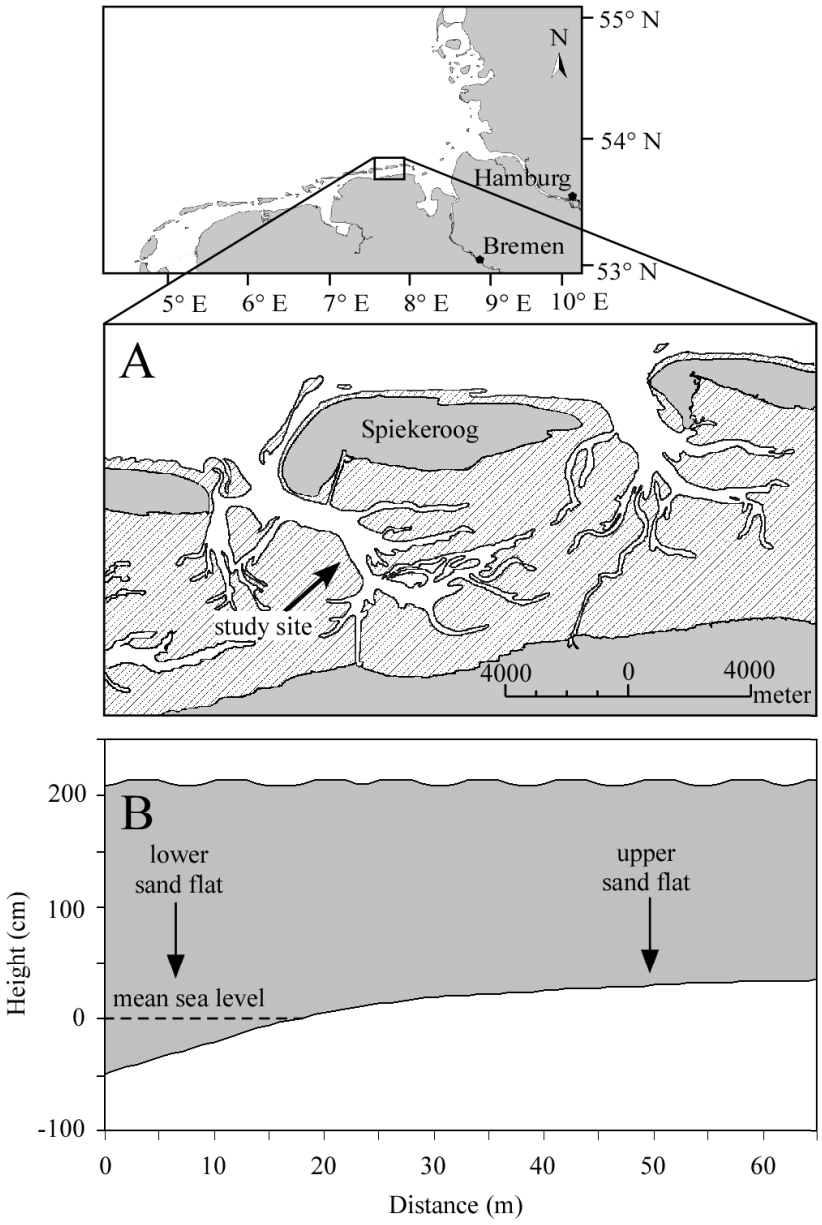

Figure 1: (A) Study site near the island of Spiekeroog, Wadden Sea, Germany. (B) Tidal flat topography as surveyed during July 2003 relative to mean sea level.

During low tide, the sand flat becomes exposed for approximately 6 to 8 hours, depending on tidal range. A "lower sand flat" site close to the low water line and an "upper sand flat" site approximately 45 m upslope the tidal flat (Fig. 1B) were chosen as the main study areas and investigated on a seasonal basis between December 2001 and March 2004 (Table 1). The lower flat site is inundated approximately 3-4 h d^{-1} longer than at the upper flat due to the tidal flat topography (Fig. 1B).

Sediment characteristics

Grain size was analyzed by dry-sieving the top 10 cm of the sediment and classified according to Wentworth (1922). The porosity of the top 15 cm of the sediment was determined in 1 cm intervals from the weight loss of a known volume of sediment after drying at 60° C until weight constancy. In July 2003, porosity of the top10 cm of the sediment was measured every 2 hours during exposure at the upper tidal flat. The permeability of the top 15 cm of the sediment was measured using the constant head method described in Klute & Dirksen (1986).

Pore water solutes

For pore water analysis (nutrients, DIC, DOC and sulfate), four to six sediment cores were collected with a 36 mm core liner during low tide from the upper and lower sand flat site. Additional sediment cores were collected over a tidal cycle from the upper sand flat site (20 minutes after inundation, high tide peak and low tide) between March and December 2002. The sediment cores were processed immediately after collection inside a glove box that was flushed with inert argon gas. The cores were sectioned to a depth of 10 to 20 cm (1 cm intervals to 10 cm depth, 2 cm intervals below), and sediment slices of the same depth were pooled to obtain a sufficient volume of pore water. The pooled sediment was transferred to a plastic Buechner-funnel with a nylon mesh preventing loss of sediment through the funnel. The funnel with sediment was inserted into a pressure container such that the outflow end of the funnel protruded from lower end of the container. An inlet on the opposite side of the funnel permitted gas flow into the container. The pore water was separated from the sediment matrix by flushing the pressure container for ca. 20 seconds with argon gas.

Table 1: Measurements conducted during the field campaigns between December 2001 and March 2004 with measured temperature range. Numbers in brackets denote replicate measurements.

		Sediment characteristics			Porewater solutes			In situ measurements and rates		
Campaign	°C	Porosity	Permeability	Grain size	Nutrients	DIC	DOC	Oxygen penetration	Oxygen consumption	Sulfate reduction
December 2001	4-5				upper (12)		upper (1)	upper (1) *		upper (3)
03 - 14.12.01					lower (6)		lower (1)	lower (1)		lower (3)
March 2002	6-8	upper (1)			upper (4)	upper (3)	upper (4)	upper (1)		upper (3)
11 - 20.03.02										
June 2002	16-25	upper (2)	upper (5)		upper (4)	upper (2)	upper (4)	upper (1)	upper (2) microsensor	upper (3)
04 - 15.06.02		lower (1)	lower (4)		lower (1)	lower (1)	lower (1)	lower (1)	lower (2) microsensor	lower (3)
September 2002	11-22	upper (1)			upper (4)	upper (3)	upper (3)	upper (1)	upper (2) optode	upper (3)
25 - 29.09.02		lower (1)			lower (1)	lower (1)	lower (1)	lower (1)	lower (2) optode	lower (2)
December 2002	-2-6	upper (2)			upper (4)	upper (2)			upper (2) optode	
03 - 09.12.02		lower (1)			lower (1)	lower (1)				
July 2003	15-28	upper (2) †	upper (6)	upper (1)	upper (2)	upper (2)	upper (2)	upper (1)	upper (3) optode	
22 - 31.07.03		lower (1)	lower (6)		lower (1)	lower (1)	lower (1)	lower (1)		
March 2004	3-14				upper (1)	upper (1)	upper (1)	upper (1)	upper (2) microsensor	
25 - 31.03.04					lower (1)	lower (1)	lower (1)	lower (1)		

* combined with Acoustic Doppler Velocimeter measurement † 4 additional porosity measurements over exposure period

In December 2001, pore water was sampled down to 15 cm sediment depth in 2.5 cm intervals with a pore water sipper as described in Huettel (1990). Pore water profiles were replicated 12 times at the upper flat and 6 times at the lower flat with the sipper. All pore water samples were passed through 0.2 µm nylon syringe filters. Aliquots for DIC analysis were then preserved with 20 µl of a saturated mercury chloride solution in 2 ml Zinnser™ vials without headspace and kept refrigerated until further processing. Volumes of 3 to 5 ml of pore water were transferred to pre-combusted glass vials for DOC analysis or into plastic vials for nutrient and sulfate measurements and kept frozen.

Pore water nutrients were measured spectrophotometrically with a Skalar Continuous-Flow-Analyzer according to Grasshoff et al. (1999). Pore water DIC was determined by flow injection analysis (Hall & Aller 1992) with freshly prepared $NaHCO_3$ calibration standards. For the analysis of DOC, total dissolved carbon and DIC were measured by high temperature catalytic oxidation on a Shimadzu TOC-5050A analyzer connected to a Shimadzu ASI 5000A autosampler using bicarbonate and phthalate as calibration standards. DOC concentration was obtained by subtraction of DIC from total dissolved carbon. Pore water sulfate concentration was determined with a Dionex® ion chromatograph using IonPac® AS9-HC analytical and IonPac® AG9-HC guard columns.

In situ sensor measurements

In situ measurements of oxygen penetration depth were performed by microsensors mounted on an autonomous profiler as described in Glud et al. (1999) and Wenzhöfer et al. (2000). Oxygen concentration was measured with Clark type oxygen microelectrodes (Revsbech 1989) with 300 µm tip diameter, an actual sensing surface of 5 µm and less than 5 seconds response time (t_{90}). The profiler was set up during low tide on the sediment with the microsensors initially positioned 1-2 cm above the sediment surface. Downward oxygen profiles were measured over at least one tidal cycle to a sediment depth of 6 cm in 1 mm intervals. Repeated profiles were measured every 20 to 60 minutes. The oxygen sensors sometimes produced persisting holes in the sediment during low tide and such profiles were discarded from the data set.

Measurement of oxygen consumption rates (pOCR and aOCR)

Volumetric oxygen consumption rates were measured at in situ temperatures on freshly collected sediment cores in the laboratory. The sediment cores were percolated with aerated ambient sea water until oxygen was present in high concentrations at the desired measurement depth. After stopping the percolation, the decrease in oxygen concentration was monitored either with a Clark type oxygen microelectrode or a planar optode (de Beer et al. 2005, Polerecky et al. 2005) (Table 1). Consistency of both methods was demonstrated by Polerecky et al. (2005). The initial decrease in oxygen concentration was considered as the potential volumetric oxygen consumption rate (pOCR). Assessment of pOCR with the microsensor was carried out by positioning the sensor in the sediment core at defined depths in 2 mm to 5 mm intervals and repetitively percolating water through the same core. The planar optode technique permitted the calculation of respiration rates with a resolution of ≈ 300 µm over the optode area (ca. 25 x 150 mm; resulting oxygen image size 80x 480 pixels). All measurements were performed on two replicate cores down to 8 cm sediment depth and in the dark to prevent photosynthesis.

Areal oxygen consumption rates (aOCR) were obtained by integrating the measured pOCR over the oxygen penetration depths measured in situ by the autonomous profiler. As pOCR data were only available from June 2002, pOCR determined during December 2002 and March 2004 were combined with oxygen penetration depths measured in December 2001 and March 2002, respectively, to estimate areal OCR for the latter months. Areal oxygen consumption was estimated to be equal to total mineralization, assuming that reduced substances from anaerobic decay (e.g. sulfide from sulfate reduction) contributed to the measured oxygen consumption rates (Jørgensen 1982).

Potential (pSRR) and maximum/minimum sulfate reduction rates (SRRmax and SRRmin)

Sulfate reduction rates were measured in two to three replicate sediment cores with the tracer whole core incubation method (Jørgensen 1978) modified for permeable sediments (de Beer et al. 2005) (Table 1). Radiolabeled $^{35}SO_4^{2-}$ (Amersham™) was added to 70 ml of ambient seawater in the laboratory to obtain a specific activity of 340 MBq per mol SO_4^{2-}. The seawater-tracer solution was allowed to percolate into the sediment from the top of the core leading to a homogenous distribution of tracer within

the permeable sand. After incubating the sediment at average in situ temperatures for 4 to 6 hours, the core was sliced into 1 cm sections and the incubation stopped by placing the slices into 20% ZnAc. The samples were processed with the cold chromium distillation procedure (Kallmeyer et al. 2004) that is based on the single step chromium reduction method (Fossing & Jørgensen 1989). Radioactivity of $^{35}SO_4^{2-}$ and Total Reduced Inorganic Sulfure (TRIS) was measured with a liquid scintillation counter (Packard™ 2500 TR) using the Lumasafe Plus® scintillation cocktail. The calculation of sulfate reduction rates accounted for the measured porosities and pore water sulfate concentrations. Sediment horizons that are regularly supplied with oxygen by in situ advective transport can become anoxic during the stagnant incubation conditions and the measured sulfate reduction rates may, therefore, represent an overestimation of actual in situ rates. On the other hand, pore water flow conditions cannot be applied during the incubation due to the resulting relocation of the radiolabeled sulfides from their place of production. Hence, in situ sulfate reduction rates were estimated in a maximum/minimum scenario, with the maximum (SRRmax) estimated by integrating pSRR over the entire measurement depth. The minimum (SRRmin) was obtained by integrating pSRR only over the varying anoxic sediment depths down to 15 cm, as inferred from the in situ oxygen penetration depths.

Measurement of near bottom flow velocities

Near bottom water flow was measured using a Nortek™ Acoustic Doppler Velocimeter (ADV) combined with the in situ determination of oxygen penetration depths in December 2001. The ADV measured 3 component (x, y, z) flow velocities at a sampling frequency of 25 Hz within a cylindrical sampling volume (ca. 6mm Ø x 6mm) located 100 mm below the probe. The ADV was mounted on a tripod with a profiling unit and flow velocities were measured stepwise for 30 seconds in 1 cm intervals from 1 to 25 cm above the sea floor over the inundation period. The average water current velocities were calculated for each height as the scalar of the 3 velocity vectors averaged over the 30 second measurement intervals.

Data analysis

Statistical analysis of differences between sampling sites and seasons were performed at a 95 % confidence level ($p<0.05$). Pore water data as well as rates of oxygen consumption and sulfate reduction were analyzed with the nonparametric Mann-Whitney U-Test for pairwise comparisons and the Kruskal Wallis H-Test for between-group analysis. After detection of significance in the group analysis, the χ^2 approach was used as a post hoc test to identify the significance between the populations.

RESULTS

Sediment characteristics

The Janssand tidal flat is characterized by well sorted (σ<0.38 phi) fine quartz sands with a mean grain size of 176 µm (2.5 phi). With permeabilities ranging between 7.2 – 9.5 x 10^{-12} m² at the upper flat and 0.5 – 3.1 x 10^{-12} m² at the lower flat, the sediment at both study sites permitted advective pore water flows. The porosity of the top 15 cm of the sediment was 34.7 and 39.5 % at the upper and lower flat, respectively. The porosity measurements taken at 2 hour intervals in July 2003 showed that the porosity of the top 10 cm of the sediment remained almost constant during the entire exposure period (range between 36.4 and 38.6 %). A glassy sediment surface and visual observation of water runoff at the lower flat site during exposure indicated a discharge of drained pore water. This was not observed at the upper sand flat site, where the sediment surface had a "dry" appearance during low tide.

Potential volumetric rates of oxygen consumption (pOCR) and sulfate reduction (pSRR)

Interestingly, pOCR at the lower sand flat was similar to that measured at the upper flat during June and September 2002 (Fig. 2), except in a zone of higher pOCR activity that was detected between 0.8 and 1.6 cm sediment depth in June 2002 ($p<0.001$). During September 2002, mean pOCR were slightly lower at the lower sand flat site ($p<0.01$) but very variable between cores in the top cm of sediment (Fig. 2). After a repeated flushing of the sediment core from the lower flat that exhibited highest pOCR, the rates decreased considerably, suggesting that oxidation of reduced solutes or particle bound material largely contributed to the higher rates during the first measurement in September 2002. No reduction in pOCR in the regularly oxygenated sediment layer was observed during repeated measurements of sediment cores from the upper sand flat (see also Polerecky et al. 2005).

In the regularly oxygenated sediment layer down to the maximum oxygen penetration depth, the volumetric rates of oxygen consumption (pOCR) showed a clear seasonal trend at the upper sand flat (Fig. 3) with lower rates during the winter months (December, March) than during summer (June, September, July) ($p<0.001$). While pOCR did not differ between June and September 2002, highest pOCR were measured during the extraordinarily warm July in 2003. Below the maximum oxygen penetration depth, pOCR increased at both study sites during most months, but remained constant or

decreased during September 2002 at the upper and lower flat, respectively (data not shown).

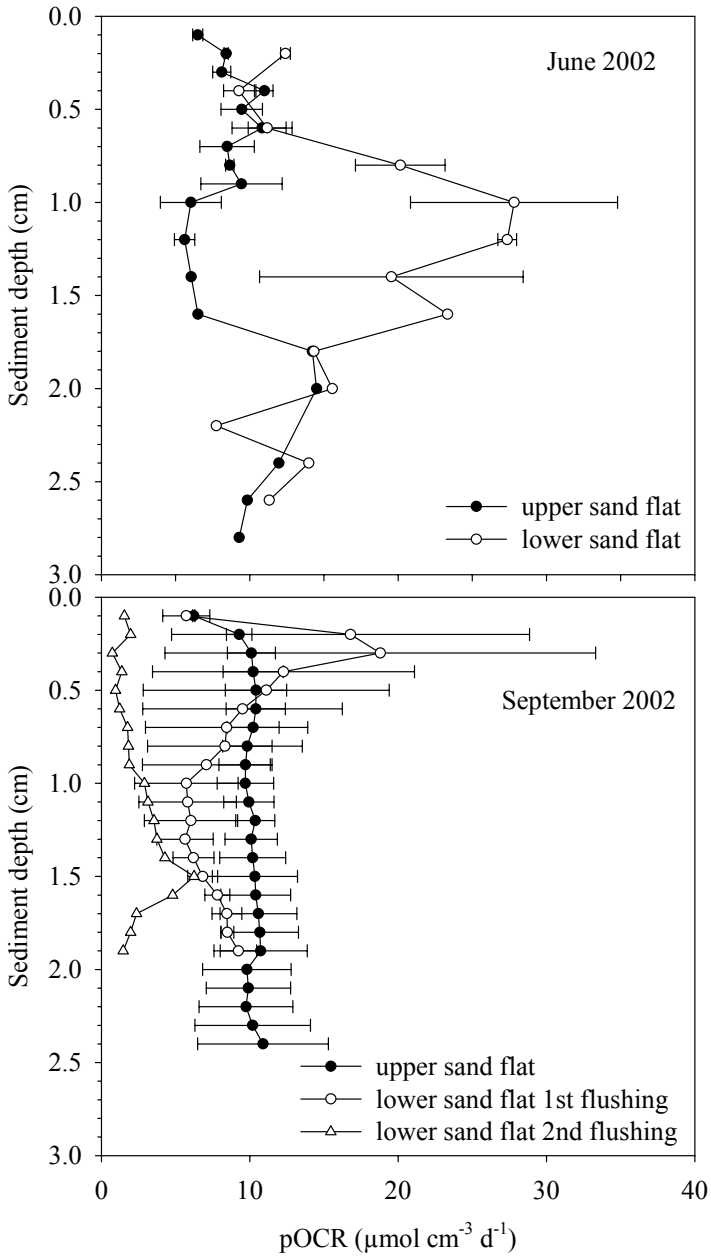

Figure 2: Potential volumetric oxygen consumption rates (pOCR) at the upper and lower sand flat during June and September 2002. Rates are plotted as the mean of 2 cores with the range as error bars down to the maximum penetration depth of oxygen for the respective months. For clarity, only every third data point (every 1mm) is shown from the planar optode measurements in September.

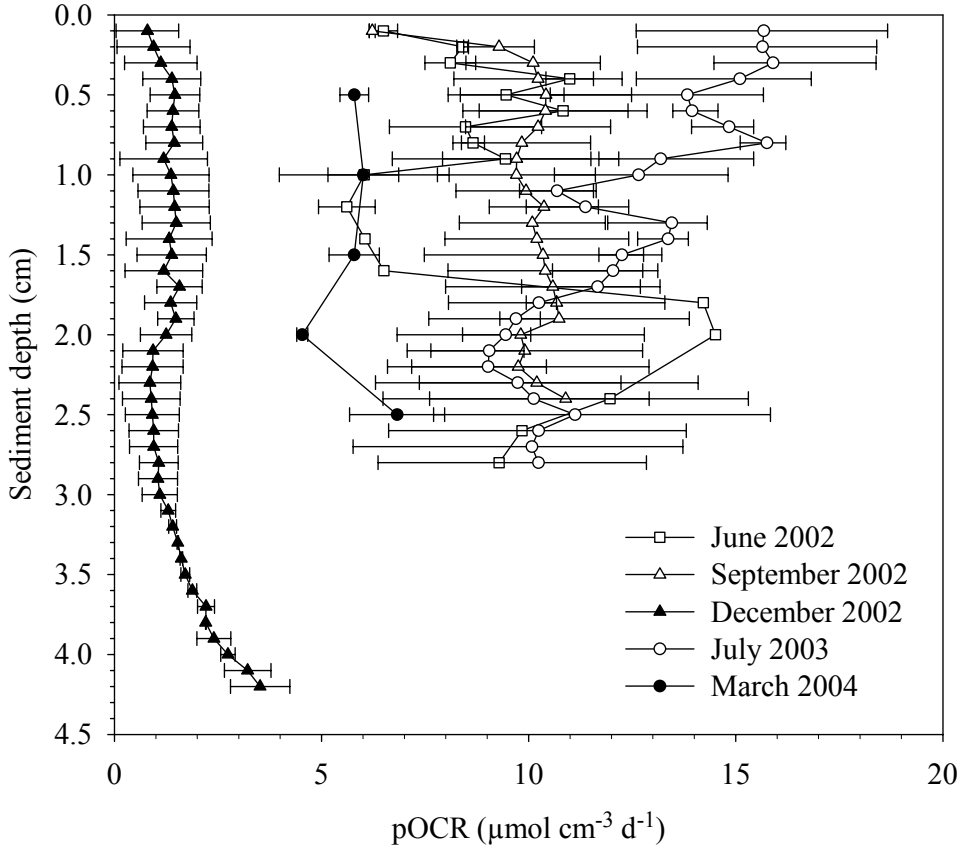

Figure 3: Potential volumetric oxygen consumption rates (pOCR) at the upper sand flat between June 2002 and March 2004. All rates are plotted as the mean of 2 cores (3 cores in July 2003) with the range as error bars down to the maximum oxygen penetration depth for the respective months. For clarity, only every third datapoint (every 1mm) is shown from the planar optode measurements in September, December and July.

Similar to the pOCR measurements, site differences in pSRR were small between the upper and lower flat (Fig. 4). The pSRR rates were only marginally higher at the lower sand flat site ($p<0.05$) during December 2001 and June 2002 and did not differ between the upper and lower flat during September 2002.

As compared to pOCR, the seasonal trend was less pronounced for pSRR (Fig. 4). Highest SRR were measured in September 2002 in 2 to 3 cm sediment depth at both study sites. Except this zone of higher activity, no difference in pSRR was detected between September 2002, June 2002, and December 2001 for the upper and lower sand flat sites. Significantly lower potential of sulfate reduction was, however, measured at the upper sand flat during March 2002 ($p<0.001$). The highest potential of sulfate reduction was usually measured in sediment layers located near the maximum depth of oxygen penetration (Fig. 4). Below this zone of higher activity, pSRR decreased with sediment depth in most profiles.

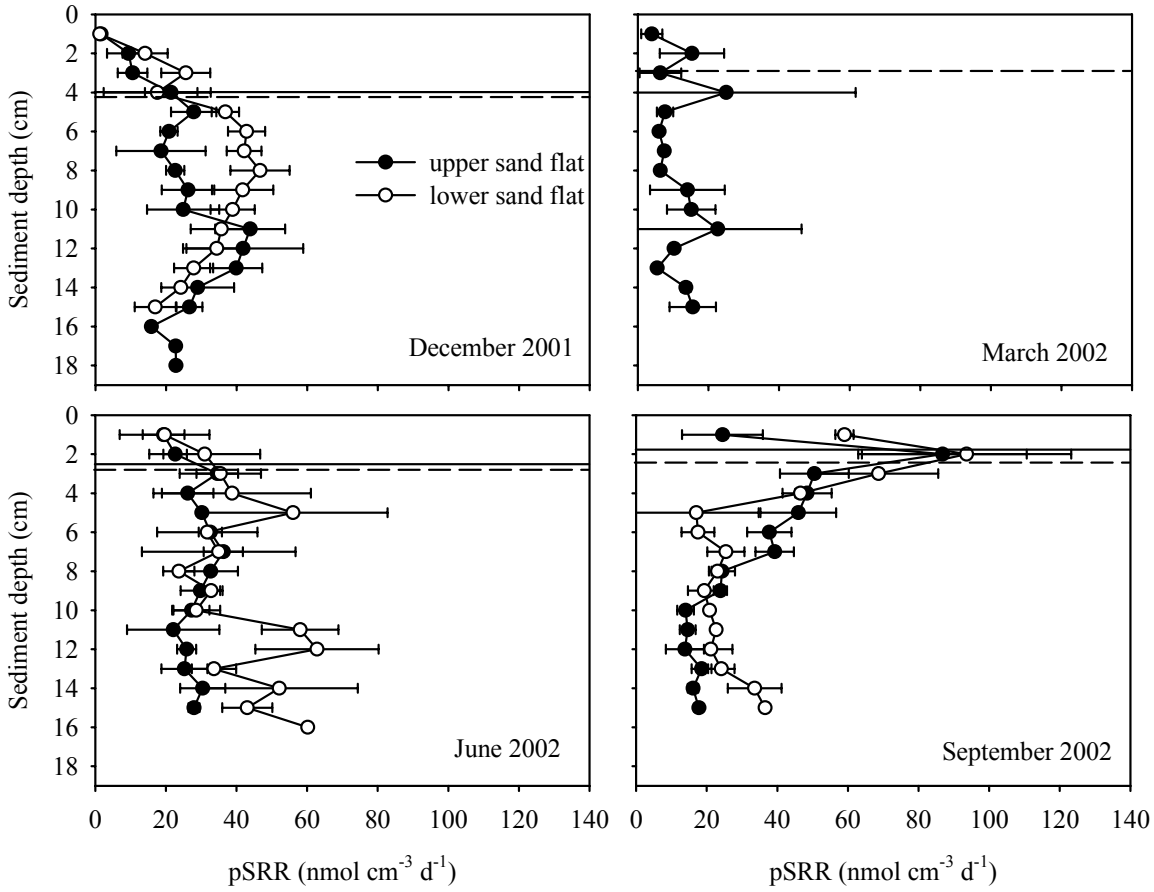

Figure 4: Volumetric sulfate reduction rates (pSRR) at the upper and lower sand flat sites between December 2001 and September 2002 (March 2002 only upper flat). Mean and standard deviation (error bars) were calculated from 3 replicate cores. The maximum oxygen penetration depth is marked with dashed (upper flat) and solid (lower flat) lines.

Areal rates of oxygen consumption (aOCR) and depth integrated sulfate reduction (SRRmax; SRRmin)

In situ areal rates of oxygen consumption (aOCR) and sulfate reduction (SRRmin) were calculated from the measured potential rates (pOCR, pSRR) and in situ oxygen penetration depths, since oxygen can inhibit the activity of sulfate reducers (Marschall et al. 1993). The maximum value for depth integrated sulfate reduction (SRRmax) is not corrected for oxygen penetration depth, as sulfate reduction activity has also been measured within the regularly oxygenated sediment layer (Jørgensen 1977, Jørgensen & Bak 1991).

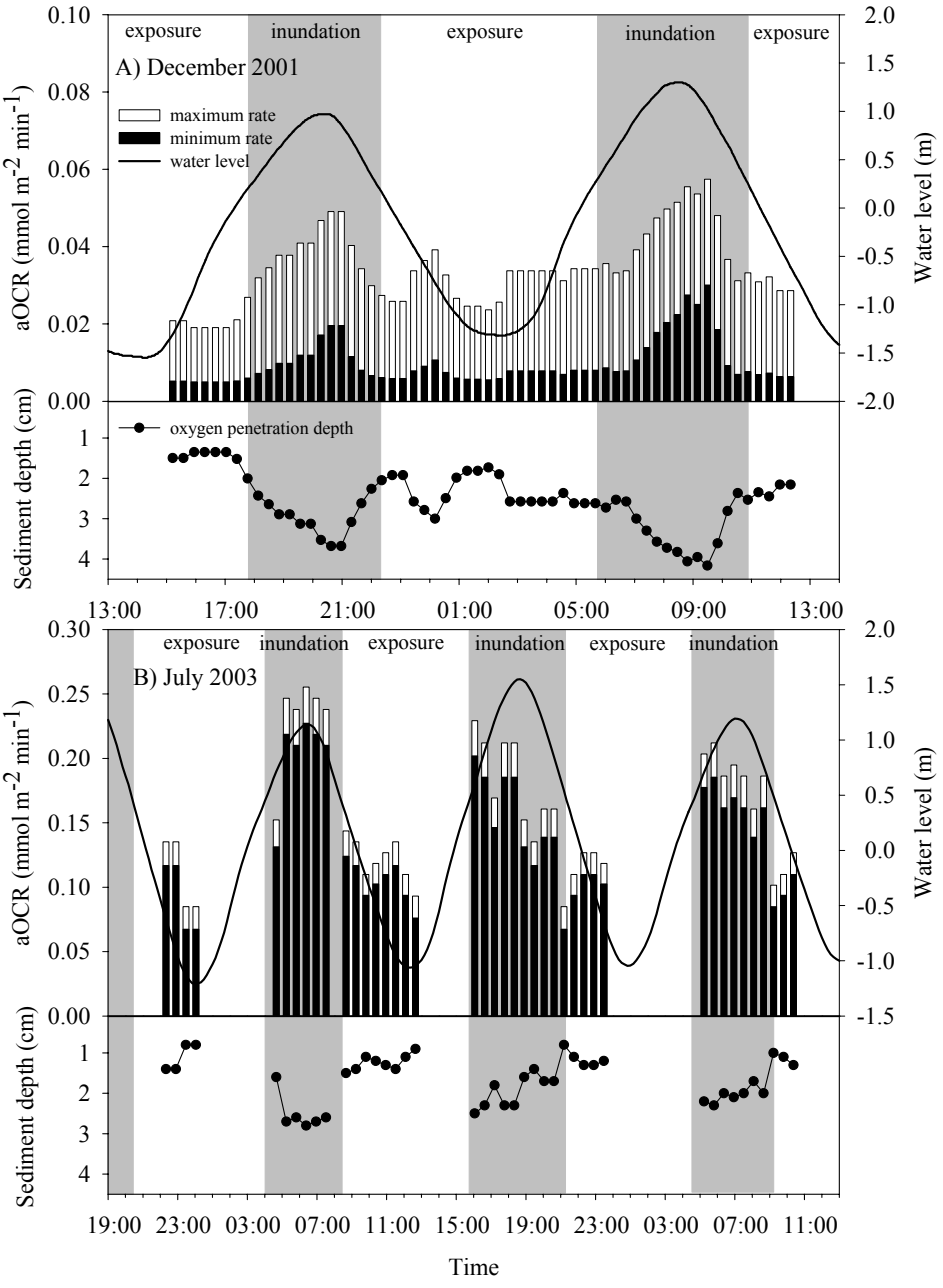

Figure 5: Areal oxygen consumption rates (aOCR), sea water level and oxygen penetration depth over several tidal cycles during (A) December 2001 and (B) July 2003 (Note different scalings for aOCR). Rates are given as minimum and maximum of two replicate pOCR measurements (3 replicates in July 2003). December rates were calculated from oxygen penetration measured in December 2001 and pOCR measured in December 2002.

Oxygen generally penetrated deeper into the sediment during inundation than during exposure of the tidal flat (Fig. 5). At the upper sand flat, the maximum penetration depth of oxygen into the sediment was 4.2 cm in December and varied between 2.4 – 2.8 cm for all other investigated months. Due to the deeper oxygen penetration, aOCR (Fig. 5 and 6A) was significantly higher during inundation as compared to exposure (at least $p<0.05$).

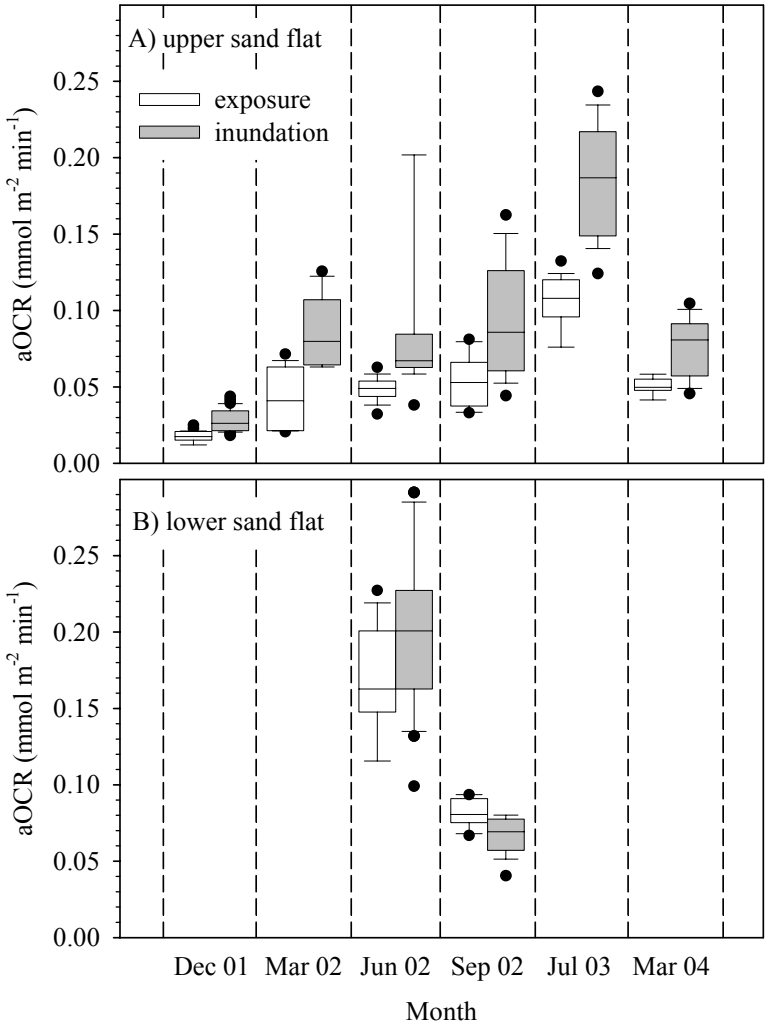

Figure 6: Areal oxygen consumption rates during exposure (white boxes) and inundation (grey boxes) at the (A) upper and (B) lower sand flat between December 2001 and March 2004. The boxes comprise the 25th and 75th percentiles and the line within the boxes represents the median. The 10th and 90th percentiles are represented by whiskers and outliers by filled circles.

Areal OCR followed a seasonal trend at the upper flat with lowest rates during December 2001, intermediate during March, June, September 2002 and March 2004 and highest rates during the very warm July 2003 (Fig. 6). Also at the lower sand flat, the maximum oxygen penetration depth was 2.4 – 2.8 cm. The aOCR at the lower flat was higher during June 2002 and similar to the upper flat during September 2002 (Fig. 6B).

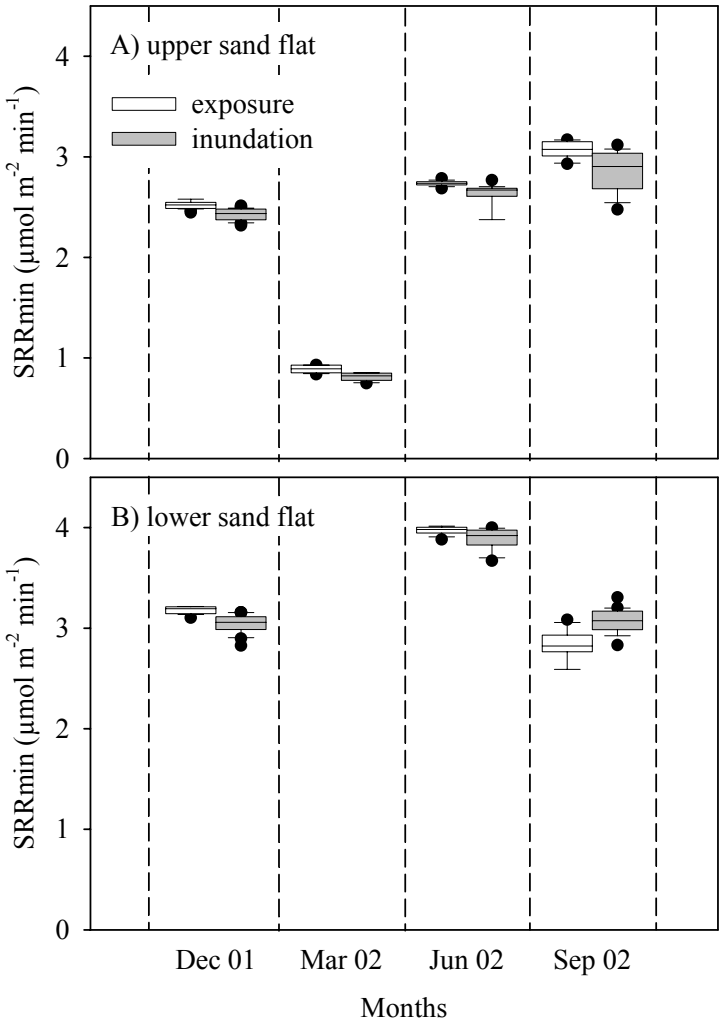

Figure 7: Sulfate reduction rates integrated over the anoxic sediment up to 15 cm depth (SRRmin) during exposure (white boxes) and inundation (grey boxes) at the (A) upper and (B) lower sand flat. The boxes comprise the 25th and 75th percentiles and the line within the boxes represents the median. The 10th and 90th percentiles are represented by whiskers and outliers by filled circles.

The conservative minimum value for depth integrated sulfate reduction (SRRmin) was obtained by integrating pSRR over the anoxic sediment depth down to 15 cm. Thus, SRRmin rates were inversely related to OCR with slightly lower rates during inundation than during exposure (Fig. 7). SRRmin were low during March 2002 and rather constant during all other months. The depth integrated sulfate reduction rates at the upper and lower flat were similar. Daily rates of areal oxygen consumption and depth integrated sulfate reduction for all investigated months are presented for a full day and for exposure and inundation periods in Table 2.

Table 2: Daily rates of areal oxygen consumption and sulfate reduction between December 2001 and March 2004 at the upper and lower sand flat site with respective inundation and exposure times. All rates represent mineralization in mmol C m^{-2} d^{-1} with the range in parentheses.

Upper sand flat	December 01/02	March 02	June 02	September 02	July 03	March 04
Exposure (hrs:min)	14:55	14:20	13:50	11:50	13:50	19:20
Inundation (hrs:min)	09:05	09:40	10:10	12:10	10:10	04:40
Exposure /Inundation	1.6	1.5	1.4	1.0	1.4	4.1
aOCR (total mineral.) daily	30.5 (13.5 - 47.6) *	84.8 (81.6 - 87.9) †	93.9 (87.7 - 100.1)	106.0 (88.9 - 123.1)	200.1 (186.5 - 215.9)	80.6 (78.9 - 82.2)
aOCR (total mineral.) exposure	15.8 (6.0 - 25.6) *	40.5 (39.2 - 41.9) †	43.1 (39.9 - 46.3)	37.9 (32.9 - 43.0)	90.1 (84.0 - 98.9)	57.5 (56.7 - 58.4)
aOCR (total mineral.) inundation	14.7 (7.4 - 22.0) *	44.2 (42.4 - 46.1) †	50.7 (47.7 - 53.8)	68.1 (56.0 - 80.2)	110.1 (102.6 - 117.0)	23.1 (22.3 - 23.9)
SRRmax daily	7.6 (6.6 - 8.8)	2.8 (1.8 - 4.2)	8.2 (7.4 - 9.0)	9.5 (9.0 - 10.2)		
SRRmax exposure	4.8 (4.2 - 5.6)	1.8 (1.1 - 2.7)	5.0 (4.5 - 5.5)	4.7 (4.4 - 5.0)		
SRRmax inundation	2.8 (2.4 - 3.2)	1.0 (0.6 - 1.5)	3.2 (2.9 - 3.5)	4.9 (4.6 - 5.2)		
SRRmin daily	7.2 (6.0 - 8.2)	2.5 (1.6 - 3.8)	7.7 (6.9 - 8.5)	8.5 (8.2 - 8.9)		
SRRmin exposure	4.6 (3.9 - 5.3)	1.6 (1.0 - 2.5)	4.8 (4.3 - 5.3)	4.3 (4.2 - 4.6)		
SRRmin inundation	2.6 (2.1 - 2.9)	0.8 (0.5 - 1.3)	2.9 (2.6 - 3.2)	4.2 (4.1 - 4.4)		
% SRRmin;max of aOCR daily	23.4 - 24.9	2.9 - 3.3	8.3 - 8.8	8.0 - 9.0		
% SRRmin;max of aOCR exposure	29.2 - 30.5	4.1 - 4.4	11.1 - 11.7	11.4 - 12.3		
% SRRmin;max of aOCR inundation	17.3 - 18.8	1.9 - 2.2	5.8 - 6.3	6.2 - 7.2		
Lower sand flat						
Exposure (hrs:min)	11:20		10:40	09:40		
Inundation (hrs:min)	12:40		13:20	14:20		
Exposure /Inundation	0.9		0.8	0.7		
aOCR (total mineral.) daily			268.8 (257.5 - 280.1)	105.6 (35.9 - 175.4)		
aOCR (total mineral.) exposure			105.8 (99.6 - 112.0)	48.6 (18.0 - 79.2)		
aOCR (total mineral.) inundation			163.0 (157.9 - 168.1)	57.1 (18.0 - 96.2)		
SRRmax daily	9.4 (8.6 - 10.4)		11.7 (9.9 - 13.6)	10.3 (9.2 - 11.5)		
SRRmax exposure	4.4 (4.0 - 4.9)		5.3 (4.5 - 6.2)	4.1 (3.7 - 4.6)		
SRRmax inundation	5.0 (4.5 - 5.5)		6.4 (5.4 - 7.4)	6.2 (5.5 - 6.9)		
SRRmin daily	8.9 (7.9 - 9.9)		11.3 (9.7 - 12.8)	8.6 (7.7 - 9.6)		
SRRmin exposure	4.3 (3.9 - 4.8)		5.2 (4.4 - 5.9)	3.3 (2.9 - 3.7)		
SRRmin inundation	4.6 (4.1 - 5.1)		6.1 (5.2 - 6.9)	5.3 (4.7 - 5.9)		
% SRRmin;max of aOCR daily			4.2 - 4.4	8.2 - 9.8		
% SRRmin;max of aOCR exposure			4.9 - 5.0	6.8 - 8.5		
% SRRmin;max of aOCR inundation			3.7 - 3.9	9.3 - 10.9		

* pOCR measured in December 2002, OPD measured in December 2001

† pOCR measured in March 2004, OPD measured in March 2002

Daily oxygen consumption rates at the lower sand flat were 2.8 times higher during June 2002 as compared to the upper flat as a result of the higher volumetric OCR rates, but did not differ between the two sites during September 2002 (Table 2, Fig. 2). During average tidal cycles with about 14 hours of exposure per day, daily rates of oxygen consumption were approximately the same during exposure and inundation (Table 2), but this ratio shifted corresponding to longer inundation (September 2002) or exposure periods (March 2004).Daily sulfate reduction rates were only slightly higher at the lower sand flat site. Assuming that sulfate reduction was the dominant anaerobic mineralization process, sulfate reduction contributed between 3 and 25 % to total mineralization (aOCR), depending on the season (Table 2).

Pore water solute concentrations

The pore water nutrient and DIC concentrations were one order of magnitude higher at the lower sand flat than at the upper flat during most months (Fig. 8). This difference was most distinct during December 2001 and from December 2002 until March 2004 ($p<0.001$) but less pronounced during June and September 2002 ($p<0.001$, $p<0.01$ for silicate). Pore water DOC concentrations were, on the other hand, never different between both study sites.

At the upper sand flat, the solute concentrations (nutrients, DIC, DOC) showed a seasonal trend with higher concentrations during the warmer months (June, July, September) and lower concentrations during the colder months (March, December) ($p<0.001$). Surprisingly, no seasonality was apparent for the lower sand flat, as nutrient and DIC concentrations were lower in Summer 2002 than in Winter 2002 and a further increase in concentrations was observed in summer 2003 and spring 2004.

The pore water solute concentrations varied only slightly between the tidal cycle samplings at the upper sand flat and no particular pattern could be observed. All upper sand flat profiles were regarded as replicates, as they did not differ significantly ($p>0.05$).

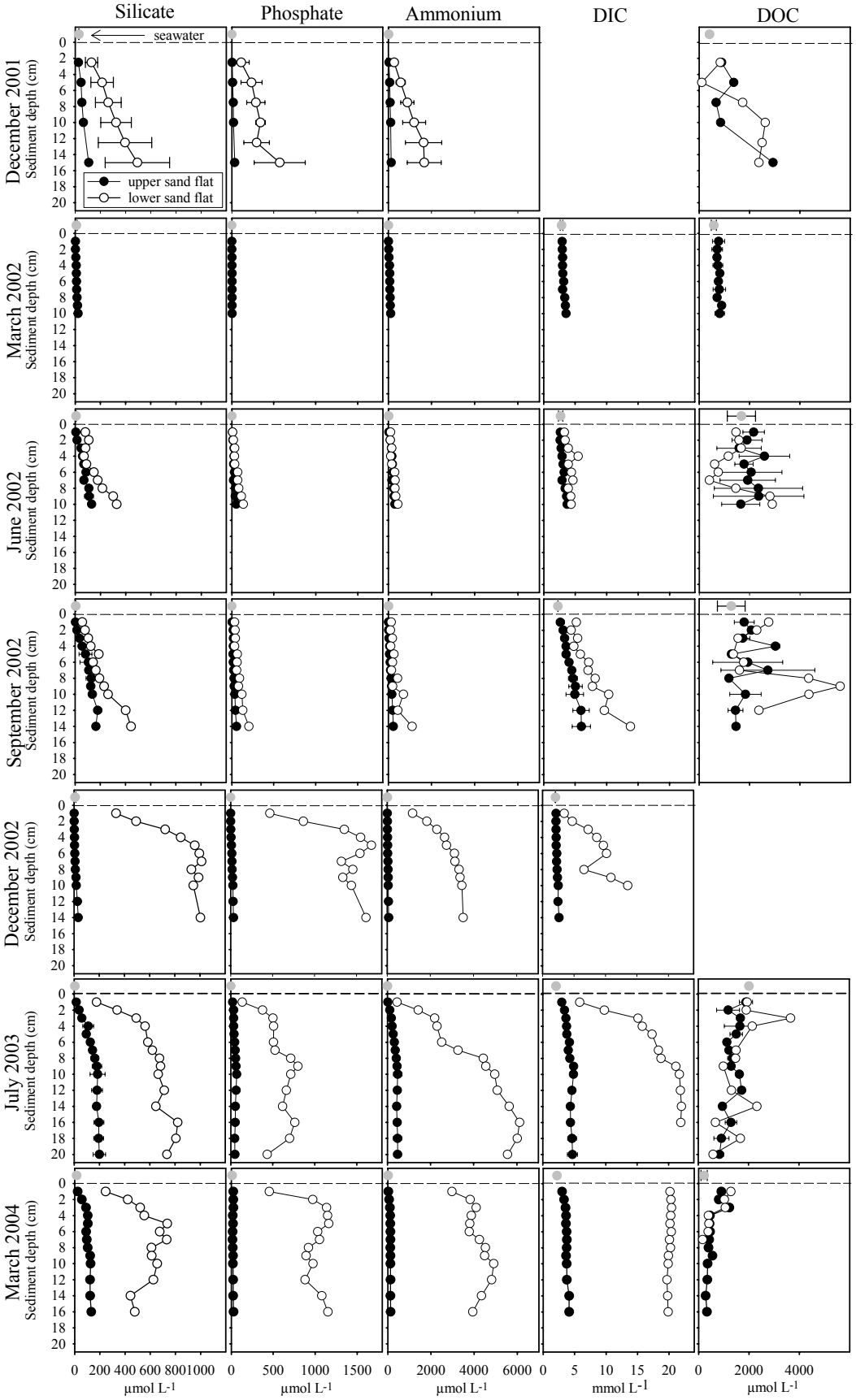

Figure 8: Average pore water nutrient, DIC and DOC concentrations at the upper and lower sand flat sites with error bars denoting standard deviation.

DISCUSSION

Variability of areal OCR and depth integrated SRR over the tidal cycle

Oxygen generally penetrated deeper into the sediment during inundation of the Janssand tidal flat. The deeper oxygen penetration resulted in higher areal oxygen consumption and lower sulfate reduction rates (minimum assessment) during submergence of the tidal flat.

In laboratory measurements, however, Brotas et al. (1990) attributed a deeper oxygen penetration into exposed sandy sediment to intrusion of air and this was also postulated by Usui et al. (1998) for an intertidal flat based on the observation that upper sediment layers became undersaturated in water content. Porosity measurements during July 2003 at the Janssand tidal flat, however, did not reveal a significant decrease in water content during low tide. In fine sands such as the Janssand tidal flat, the sediment stays completely water saturated during exposure due to capillary forces (Drabsch et al. 1999, Atherton et al. 2001) preventing intrusion of air. Nevertheless, in situ oxygen penetration was much deeper (down to 15 mm in July 2003 and March 2004) than in retrieved laboratory cores (2 to 3.5 mm for July and March, respectively).

Although benthic photosynthesis can generate high oxygen concentrations in the surface layer of the sediment (Revsbech et al. 1980, Berninger & Huettel 1997), we never observed consistently deeper oxygen penetration and, hence, higher OCR during daylight exposure than during nighttime exposure (Fig. 5). Macrofauna can strongly enhance interfacial exchange processes (Rhoads 1974, Huettel 1990, Graf & Rosenberg 1997), but faunal activity is heterogeneous and unlikely to completely stop during the laboratory measurements. Thus, other mechanisms were responsible for the deeper in situ penetration of oxygen during low tide than in the laboratory. We observed that during exposure the Janssand sand flat continuously drains pore water that flows through the sediment towards the low water line. This drainage permits intrusion of the oxygen-rich water that remained as puddles on the sediment surface into the sand and also penetration of oxygen contained in surface layer pore water deeper into the bed. Dispersion of the pore water flow within the porous sediment matrix may further enhance oxygen penetration depth. These mechanisms are not active in the retrieved cores, explaining the lesser oxygen penetration in the laboratory.

During inundation of the tidal flat, the interaction of unidirectional or oscillating water currents with sediment topography induces advective flow of pore water through the permeable bed (Webb & Theodor 1968, Thibodeaux & Boyle 1987, Huettel & Gust

1992). Pressure oscillations caused by waves passing over the permeable sediment also contribute to the pore water flow (Riedl et al. 1972, Van der Loeff 1981). Bottom currents and waves lead to a continuous change of sediment topography, e.g. by ripple migration. Oscillating flow interacting with sediment ripples generates an intrusion of oxygenated water into the ripple faces and outflow of anoxic pore water near the ripple crests (Precht & Huettel 2003). This leads to varying oxygen penetration depths at small spatial scales corresponding to the ripple length. Along with ripple migration during inundation, as observed in several oxygen profiles from the study site, the intrusion/outflow-zones move along the sediment surface (Precht et al. 2004, Franke et al. submitted). Additionally, the bioirrigation activity of benthic macrofauna during submergence can lead to a deeper transport of oxygen into the sediment (Aller 2001, Wenzhöfer & Glud 2004). Benthic photosynthesis, on the other hand, may decrease with increasing water depth due to diminishing light penetration in the turbid Wadden Sea waters (Colijn & Cadee 2003).

Combined measurements of near bottom water flow and oxygen profiles at the Janssand tidal flat revealed a deeper oxygen penetration with increasing average flow velocities (Fig. 9). The observation of the same co-variance in a recent study of another permeable, intertidal sand flat (Werner et al. submitted) suggests that hydrodynamic forcing is the determining factor for the variability of oxygen penetration. The hydrodynamically induced advective transport of oxygenated water into the sediment, therefore, is responsible for the higher areal OCR and lower depth integrated SRR during inundation of the Janssand tidal flat.

The importance of advective pore water exchange and resultant oxygen supply to the sediment for the mineralization of organic matter is reflected by the potential oxygen consumption rates that were at least one order of magnitude higher than the potential sulfate reduction rates (compare Fig. 2 and Fig. 4). Consequently, the share of depth integrated sulfate reduction to total mineralization was relatively low in the investigated top 15 cm of the Janssand sediment (3 to 10 % during most months). The microbial community can access the high energy yield of aerobic mineralization as soon as oxygen is supplied to the respective sediment layers. Despite the enhancement of potential mineralization rates by the advective oxygen supply during submergence and the lower potential rates during exposure, total mineralization during low tide can be as high as during submergence due to the relatively long exposure of the Janssand during an average tidal cycle. This may also partially explain why no tidal differences in pore

water nutrient and DIC concentrations were measured. Tidal differences in pore water nutrients and DIC were not evident even during extraordinarily long (September 2002) and short (March 2004) inundation periods. Possible pore water concentration differences were probably too small within this short timeframe and may have been masked by spatial heterogeneity.

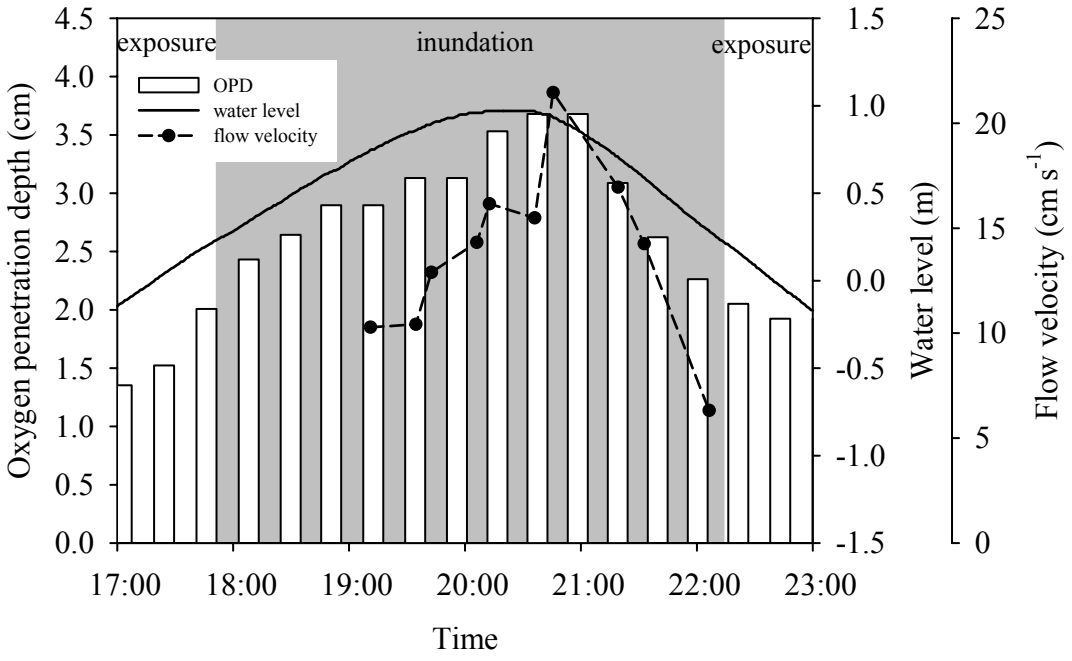

Figure 9: Relationship between the average water flow velocity 5 cm above the sea floor and oxygen penetration depth (OPD) during December 2001. The solid line denotes the change of the sea water level relative to mean sea level.

Seasonal variability of OCR and SRR

The oxygen consumption rates were consistent with the temperature dependence of aerobic mineralization (Thamdrup et al. 1998). A higher availability and degradability of organic matter during the summer months may have contributed to the observed seasonality of oxygen consumption. For sulfate reduction, seasonality was only partially evident in the low March values, but December rates were close to the summer measurements. This is surprising, as the temperature dependence for sulfate reduction is even stronger than that of aerobic mineralization (Thamdrup et al. 1998). In September 2002, high rates of sulfate reduction in the uppermost sediment layers of both study sites suggest a recent input of fresh organic matter, possibly by an autumn algal bloom. In December 2001, the sulfate reducers possibly profited from the

mineralization of such an algal bloom as reflected in only slightly lower pore water DOC concentrations in winter as compared to June and September 2002 (see Fig. 8).

Differences between the upper and lower sand flat sites

Higher mineralization rates should lead to more degradation products such as DIC and nutrients. Indeed, the seasonal trend of oxygen consumption rates was reflected in the solute concentrations at the upper sand flat site. Interestingly, this was not the case for the lower sand flat, where nutrient and DIC concentrations were not linked to season. Depth integrated sulfate reduction and areal OCR were comparable between both study sites and thus cannot explain the observed 5-15 times higher concentrations of degradation products at the lower flat. Benthic chamber incubations confirmed the similar oxygen consumption rates for both study sites (Billerbeck et al. submitted) and comparable sulfate reduction rates between both sites were also measured in another study at this tidal flat (Bosselmann in prep.). The higher oxygen consumption at the lower flat in June 2002 was restricted to a 1 cm thick sediment layer (see Fig. 2) suggesting the presence of buried organic material such as macroalgae and may reflect spatial variability. In order to produce the large difference in solute concentrations between the two sites in July 2003 and March 2004, mineralization rates (as estimated from aOCR) need to be about 10 times higher at the lower flat. As this clearly was not the case, the high concentration of metabolic products and seasonal independence of these concentrations at the lower sand flat points to a non-local source for the nutrients and DIC at this site.

As the Janssand sediment has a permeability permitting pore water flow, the exposure of the tidal flat during low tide and ensuing hydraulic gradient between the pore water table and sea water level lead to drainage transport of pore water through the sediment from the upper flat directed towards the low water line (Nielsen 1990). Tracer injections revealed that this drainage affects at least the sediment layers down to 50 cm depth with drainage transport velocities of 0.07 to 0.12 m d^{-1} (Billerbeck et al. submitted) Sedimentary decomposition processes and drainage transport result in a concentration increase of metabolic products towards the low water line (Billerbeck et al.submitted). With the rather slow drainage transport, about 1 to 2 years are needed for the pore water to travel the distance of 50 m from the upper flat to the lower flat. Due to mixing and dispersion within the sediment during this passage, seasonal fluctuations in concentrations of metabolic products are evened out and, thus, are absent at the point of

emergence. Slow pore water flows likely exist also below 50 cm sediment depth with degradation products originating from the large inner area of the tidal flat. Such deep flows may additionally contribute to the high pore water solute concentrations at the lower flat sampling site.

In contrast to nutrients and DIC, DOC concentrations followed a seasonal trend at the lower flat, similar to the situation at the upper flat. We explain this observation with the different transport characteristics of dissolved and particulate material in the sand (Huettel et al. 1996) and the tight link between particulate and dissolved organic matter concentrations observed in marine sediments (Ehrenhauss et al. 2004). Degradable organic particles, e.g. phytoplankton cells, are retained in the uppermost sediment layer in permeable sediment when water is filtered through the bed due to drainage or bottom current driven sediment percolation (Pilditch et al. 1997, Huettel & Rusch 2000). The degradation of this material may cause only a non-significant change in the nutrient concentration at the lower flat site due to the relatively high background concentrations, however, it may have caused the noticeable seasonal changes in the DOC concentration at that site and also at the upper flat site.

At the lower sand flat, drained pore water is discharged via the sediment surface from a seepage face that extends from the low water line about 30 meters upslope the tidal flat. As a consequence of this discharge, reduced substances are highly concentrated also in the upper sediment layer that is regularly flushed with sea water during inundation (Billerbeck et al. submitted). The contribution of chemical oxidation to measurements of total oxygen consumption in the regularly oxygenated sediment layer of the lower flat needs to carefully be accounted for, especially during periods with high concentration of reduced substances at this site. This was evident in the September 2002 measurement of pOCR at the lower flat, where the repeated flushing of the sediment resulted in a distinct decrease in oxygen consumption. Probably, the rates measured after flushing the large pool of reduced substances out of the sediment may best represent the actual aerobic mineralization. At the upper sand flat, the contribution of chemical oxidation to total oxygen consumption is likely small in the regularly oxygenated sediment layer (Polerecky et al. 2005).

Our results indicate that the nutrient recycling by the filtration system sand flat works on two distinctly different temporal and spatial scales (Fig. 10):

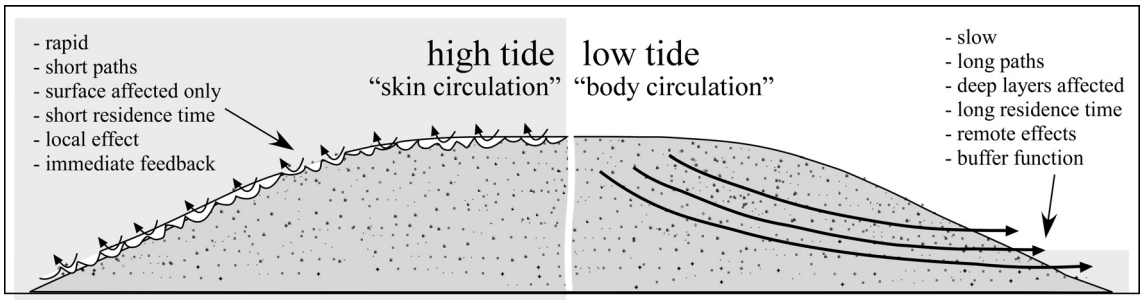

Figure 10: "Skin" and "Body" circulation in an intertidal sand flat. During high tide, boundary flow-topography interaction causes flushing of the surface sediment layer. Organic particles are filtered from the water, degraded and nutrients are returned promptly. During low tide, drainage removes nutrient-rich pore water from the entire sand flat, providing a season-independent nutrient source acting as a buffer.

(1) Filtration of water through the surface layer of the sediment, due to bottom flow-topography interaction, flushes the upper few centimeters of the sand bed resulting in retention of degradable organic particles in the surface layer and flushing of metabolic products (inorganic nutrients, DIC) from this layer. The spatial scale of these "skin circulation cells" is in the order of centimeters and the time scale is in the order of hours to days. Based on the measured oxygen penetration depths and pore water solute profiles, we suggest that approximately the top 5 cm of the sediment is affected by the skin filtration during periods of average hydrodynamics. The process is active only during inundation. Solute concentrations in these small and rapid circulation cells reflect tidal, daily and seasonal patterns. The recycling of nutrients of the small cells, thus, provides immediate feedback to the ecosystem during inundation.

(2) Filtration of water through the sand flat due to a tidal drainage process that is active only during exposure. This "body circulation cell" filters a large water volume (total discharge in Janssand about 80,000 to 130,000 L on each tidal cycle, Billerbeck et al. submitted) through the entire body of the sand flat at a relatively small pore flow velocity. Since the spatial scales of this large flow cell are in the order of tens to hundreds of meters, the residence time is rather long with time scales in the order of years to tens of years. This recycling, thus, is independent of seasonal oscillations and can act as a nutrient reservoir and nutrient source during times of low nutrient concentrations in the water column.

With the combination of a fast and a slow nutrient recycling system, the tidal sand filter rapidly responds to organic matter input by instantaneous nutrient regeneration and release, while at the same time the sand flat acts as a buffer for

nutrients that is independent of short-term and seasonal fluctuations. The rapid "skin circulation" feeds back nutrients only during inundation and thus supports benthic and pelagic primary production within the intertidal area. The slow "body circulation" returns nutrients only during exposure of the tidal flat and contributes to the increase in nutrient concentration of the Wadden Sea water during low tide (Niesel & Günther 1999). The export of this nutrient rich water by tidal currents and a decreased turbidity in the open North Sea can lead to high primary production in a belt of coastal waters seaward of the barrier islands (Colijn et al. 1987, Colijn & Cadee 2003). The ecological consequence of such a recycling system operating on two different alternating time scales is a dampening of short term and seasonal fluctuations in primary productivity through immediate feed back as well as continuous nutrient return to the system. Because the slow "body circulation" releases pore water only during low tide, this process may act also as an efficient pump that removes metabolic products from the intertidal zone to the North Sea with the tidal currents. This removal may be essential for maintaining the biocatalytical filtration capacity of the intertidal sands.

ACKNOWLEDGEMENTS

We thank M. Alisch for the assistance in field and laboratory work and acknowledge the hospitality and help of the Plattboden-ship crews during the cruises. We thank G. Schüßler, S. Menger, D. Franzke and S. Pabel for their help with laboratory work. We acknowledge G. Eickert, I. Schröder, K. Hohman, I. Dohrmann and C. Wiegand for making the sensors and thank J. Langreder, A. Nordhausen, G. Herz, A. Kutsche, P. Färber, V. Meyer and H. Osmers for technical assistance. W. Anton of the WSA Emden kindly provided tide gauge data. This study was supported by the Deutsche Forschungsgemeinschaft (DFG) within the research group "Biogeochemistry of the Wadden Sea" (FG 432-5), coordinated by Prof. J. Rullkötter. We are grateful to Prof. B. B. Jørgensen and Dr. M. E. Böttcher for their support of this work and coordination of the sub-project "Biogeochemical processes at the sediment-water interface of intertidal sediments".

LITERATURE CITED

Aller R. C. (2001) Transport and reactions in the bioirrigated zone. In: Boudreau BP, Jørgensen BB (eds) The Benthic Boundary Layer. Oxford University Press, Oxford, p 269-301

Atherton R. J., Baird A. J., Wiggs G. F. S. (2001) Inter-tidal dynamics of surface moisture content on a meso-tidal beach. J. Coast. Res. 17:482-489

Bergamaschi B. A. , Tsamakis E., Keil R. G., Eglinton T. I., Montlucon D. B., Hedges J. I. (1997) The effect of grain size and surface area on organic matter, lignin and carbohydrate concentration, and molecular compositions in Peru Margin sediments. Geochim. Cosmochim. Acta. 61:1247-1260

Berninger U. G., Huettel M. (1997) Impact of flow on oxygen dynamics in photosynthetically active sediments. Aquat. Microb. Ecol. 12:291-302

Billerbeck M., Werner U., Bosselmann K., Walpersdorf E., Huettel M. (submitted) Nutrient release from an exposed intertidal sand flat. Mar. Ecol. Prog. Ser.

Boudreau B., Huettel M., Forster R., Jahnke A., McLachlan J., Middelburg J., Nielsen P., Sansone F., Taghon G., Van Raaphorst W., Webster I., Weslawski J., Wiberg P., Sundby B. (2001) Permeable Marine Sediments: Overturning an Old Paradigm. EOS Trans. Am. Geophys. Union 82:133-136

Brotas V., Amorim-Ferreira A., Vale C., Catarino F. (1990) Oxygen profiles in intertidal sediments of Ria Formosa (S. Portugal). Hydrobiologia 207:123-129

Cammen L. M. (1991) Annual Bacterial Production in Relation to Benthic Microalgal Production and Sediment Oxygen-Uptake in an Intertidal Sandflat and an Intertidal Mudflat. Mar. Ecol. Prog. Ser. 71:13-25

Colijn F., Admiraal W., Baretta J. W., Ruardij P. (1987) Primary production in a turbid estuary, the Ems-Dollard: field and model studies. Cont. Shelf Res. 7:1405-1409

Colijn F., Cadee G. C. (2003) Is phytoplankton growth in the Wadden Sea light or nitrogen limited? J. Sea Res. 49:83-93

D'Andrea A. F., Aller R. C., Lopez G. R. (2002) Organic matter flux and reactivity on a South Carolina sandflat: The impacts of porewater advection and macrobiological structures. Limnol. Oceanogr. 47:1056-1070

Dauwe B., Middelburg J. J., Herman P. M. J. (2001) Effect of oxygen on the degradability of organic matter in subtidal and intertidal sediments of the North Sea area. Mar. Ecol. Prog. Ser. 215:13-22

de Beer D., Wenzhoefer F., Ferdelman T. G., Boehme S. E., Huettel M., van Beusekom J. E. E., Boettcher M. E., Musat N., Dubillier N. (2005) Transport and mineralization rates in North Sea sandy intertidal sediments, Sylt-Rømø Basin, Wadden Sea. Limnol. Oceanogr. 50:113-127

Drabsch JM, Parnell KE, Hume TM, Dolphin TJ (1999) The capillary fringe and the water table in an intertidal estuarine sand flat. Estuar Coast Shelf Sci 48:215-222

Ehrenhauss S., Witte U., Buhring S. L., Huettel M. (2004) Effect of advective pore water transport on distribution and degradation of diatoms in permeable North Sea sediments. Mar. Ecol. Prog. Ser. 271:99-111

Flemming B. W., Ziegler K. (1995) High-resolution grain size distribution patterns and textural trends in the backbarrier environment of Spiekeroog Island (southern North Sea). Senckenb. Marit. 26:1-24

Forster S., Huettel M., Ziebis W. (1996) Impact of boundary layer flow velocity on oxygen utilisation in coastal sediments. Mar. Ecol. Prog. Ser. 143:173-185

Fossing H., Jørgensen B. B. (1989) Measurement of Bacterial Sulfate Reduction in Sediments - Evaluation of a Single-Step Chromium Reduction Method. Biogeochemistry 8:205-222

Franke U., Polerecky L., Precht E., Huettel M. (submitted) Wave tank study of particulate organic matter degradation in permeable sediments. submitted to Limnol. Oceanogr.

Glud R. N., Forster S., Huettel M. (1996) Influence of radial pressure gradients on solute exchange in stirred benthic chambers. Mar. Ecol. Prog. Ser. 141:303-311

Glud R. N., Klimant I., Holst G., Kohls O., Meyer V., Kuhl M., Gundersen J. K. (1999) Adaptation, test and in situ measurements with O-2 microopt(r)odes on benthic landers. Deep-Sea Res. Part I-Oceanogr. Res. Pap. 46:171-183

Graf G., Rosenberg R. (1997) Bioresuspension and biodeposition: A review. J. Mar. Syst. 11:269-278

Grasshoff K., Kremling K., Ehrhardt M. (1999) Methods of seawater analysis, Vol. Wiley-VCH Verlag

Hall P. O. J., Aller R. C. (1992) Rapid, small-volume, flow injection analysis for ΣCO_2 and NH_4^+ in marine and freshwaters. Limnol. Oceanogr. 37:1113-1119

Howes B. L., Goehringer D. D. (1994) Porewater drainage and dissolved organic carbon and nutrient losses through the intertidal creekbanks of a New England salt marsh. Mar. Ecol. Prog. Ser. 114:289-301

Huettel M. (1990) Influence of the lugworm Arenicola marina on porewater nutrient profiles of sand flat sediments. Mar. Ecol. Prog. Ser. 62:241-248

Huettel M., Gust G. (1992) Impact of bioroughness on interfacial solute exchange in permeable sediments. Mar. Ecol. Prog. Ser. 89:253-267

Huettel M., Roy H., Precht E., Ehrenhauss S. (2003) Hydrodynamical impact on biogeochemical processes in aquatic sediments. Hydrobiologia 494:231-236

Huettel M., Rusch A. (2000) Transport and degradation of phytoplankton in permeable sediment. Limnol. Oceanogr. 45:534-549

Huettel M., Webster I. T. (2001) Porewater flow in permeable sediments. In: Boudreau BP, Jørgensen BB (eds) The Benthic Boundary Layer. Oxford University Press, Oxford, p 144-179

Huettel M., Ziebis W., Forster S. (1996) Flow-induced uptake of particulate matter in permeable sediments. Limnol. Oceanogr. 41:309-322

Huettel M., Ziebis W., Forster S., Luther G. W. (1998) Advective transport affecting metal and nutrient distributions and interfacial fluxes in permeable sediments. Geochim. Cosmochim. Acta 62:613-631

Jahnke R. A., Alexander C. R., Kostka J. E. (2003) Advective pore water input of nutrients to the Satilla River Estuary, Georgia, USA. Estuar. Coast. Shelf Sci. 56:641-653

Jørgensen B. B. (1977) Bacterial Sulfate Reduction Within Reduced Microniches of Oxidized Marine-Sediments. Mar. Biol. 41:7-17

Jørgensen B. B. (1978) Comparison of Methods For the Quantification of Bacterial Sulfate Reduction in Coastal Marine-Sediments .1. Measurement With Radiotracer Techniques. Geomicrobiol. J 1:11-27

Jørgensen B. B. (1982) Mineralization of Organic-Matter in the Sea Bed - the Role of Sulfate Reduction. Nature 296:643-645

Jørgensen B. B., Bak F. (1991) Pathways and Microbiology of Thiosulfate Transformations and Sulfate Reduction in a Marine Sediment (Kattegat, Denmark). Appl. Environ. Microbiol. 57:847-856

Kallmeyer J., Ferdelman T.G., Weber A., Fossing H., Jørgensen B. B. (2004) A cold chromium distillation procedure for radiolabeled sulfide applied to sulfate reduction measurements. Limnol. Oceanogr.: Methods 2:171-180

Klute A, Dirksen C (1986) Hydraulic conductivity and diffusivity: laboratory methods. In: Klute A (ed) Methods of soil analysis - part 1 - Physical and mineralogical methods. American Society of Agronomy, p 687-700

Kuwae T., Kibe E., Nakamura Y. (2003) Effect of emersion and immersion on the porewater nutrient dynamics of an intertidal sandflat in Tokyo Bay. Estuar. Coast. Shelf Sci. 57:929-940

Llobet-Brossa E., Rossello-Mora R., Amann R. (1998) Microbial community composition of wadden sea sediments as revealed by flourescence in situ hybridization. Appl. Environ. Microbiol. 64:2691-2696

Lohse L., Epping E. H. G., Helder W., vanRaaphorst W. (1996) Oxygen pore water profiles in continental shelf sediments of the North Sea: Turbulent versus molecular diffusion. Mar. Ecol. Prog. Ser. 145:63-75

Marschall C., Frenzel P., Cypionka H. (1993) Influence of oxygen on sulfate reduction and growth of sulfate-reducing bacteria. Arch. Microbiol. 159:168-173

Nielsen P. (1990) Tidal dynamics of the water table in beaches. Water Resour. Res. 26:2127-2134

Niesel V., Günther C. P. (1999) Distribution of nutrients, algae and zooplankton in the Spiekeroog backbarrier system. In: Dittmann S. (ed) The Wadden Sea Ecosystem - Stability Properties and Mechanisms. Springer-Verlag, Berlin Heidelberg New York, p 77-94

Orvain F., Sauriau P. G. (2002) Environmental and behavioural factors affecting activity in the intertidal gastropod *Hydrobia ulvae*. J. Exp. Mar. Biol. Ecol. 272:191-216

Osgood D. T. (2000) Subsurface hydrology and nutrient export from barrier island marshes at different tidal ranges. Wetlands Ecol. Manage. 8:133-146

Pilditch C. A., Emerson C. W., Grant J. (1997) Effect of scallop shells and sediment grain size on phytoplankton flux to the bed. Cont. Shelf Res. 17:1869-1885

Polerecky L., Franke U., Werner U., Grunwald B., de Beer D. (2005) High spatial resolution measurement of oxygen consumption rates in permeable sediments. Limnol. Oceanogr.: Methods 3:75-85

Precht E., Franke U., Polerecky L., Huettel M. (2004) Oxygen dynamics in permeable sediments with wave-driven pore water exchange. Limnol. Oceanogr. 49:693-705

Precht E., Huettel M. (2003) Advective pore-water exchange driven by surface gravity waves and its ecological implications. Limnol. Oceanogr. 48:1674-1684

Revsbech N. P. (1989) An Oxygen Microsensor With a Guard Cathode. Limnol. Oceanogr. 34:474-478

Revsbech N. P., Sorensen J., Blackburn T. H., Lomholt J. P. (1980) Distribution of Oxygen in Marine-Sediments Measured with Microelectrodes. Limnol. Oceanogr. 25:403-411

Rhoads D. C. (1974) Organism-sediment relations on the muddy sea floor. Oceanogr. Mar. Biol., Annu. Rev. 12:263-300

Riedl R. J., Huang N., Machan R. (1972) The subtidal pump: Mechanism of interstitial water exchange by wave action. Mar. Biol. 13:210-221

Rocha C. (1998) Rhythmic ammonium regeneration and flushing in intertidal sediments of the Sado estuary. Limnol. Oceanogr. 43:823-831

Rusch A., Forster S., Huettel M. (2001) Bacteria, diatoms and detritus in an intertidal sandflat subject to advective transport across the water-sediment interface. Biogeochemistry 55:1-27

Rusch A., Huettel M., Reimers C. E., Taghon G. L., Fuller C. M. (2003) Activity and distribution of bacterial populations in Middle Atlantic Bight shelf sands. FEMS Microbiol. Ecol. 44(1): 89-100

Thamdrup B., Hansen J. W., Jørgensen B. B. (1998) Temperature dependence of aerobic respiration in a coastal sediment. FEMS Microbiol. Ecol. 25:189-200

Thibodeaux L. J., Boyle J. D. (1987) Bedform-generated convective transport in bottom sediment. Nature 325:341-343

Usui T., Koike I., Ogura N. (1998) Tidal effect on dynamics of pore water nitrate in intertidal sediment of a eutrophic estuary. J. Oceanogr. 54:205-216

Van der Loeff M. M. R. (1981) Wave effects on sediment water exchange in a submerged sand bed. Neth. J. Sea Res. 15:100-112

Webb J. E., Theodor J. (1968) Irrigation of Submerged Marine Sands through Wave Action. Nature 220:682-683

Wentworth C. K. (1922) A scale of grade and class terms for clastic sediments. J. Geol. 30:377-392

Wenzhöfer F., Glud R. N. (2004) Small-scale spatial and temporal variability in coastal benthic O-2 dynamics: Effects of fauna activity. Limnol. Oceanogr. 49:1471-1481

Wenzhöfer F., Holby O., Glud R. N., Nielsen H. K., Gundersen J. K. (2000) In situ microsensor studies of a shallow water hydrothermal vent at Milos, Greece. Mar. Chem. 69:43-54

Werner U., Billerbeck M., Polerecky L., Franke U., Huettel M., van Beusekom J. E. E., de Beer D. (submitted) Spatial and temporal pattern of mineralization rates and oxygen distribution in a permeable intertidal sandflat (Sylt, Germany). submitted to Limnol. Oceanogr.

Whiting G. J., Childers D. L. (1989) Subtidal advective water flux as a potentially important nutrient input to southeastern U.S.A. saltmarsh estuaries. Estuar. Coast. Shelf Sci. 28:417-431

Page left blank intentionally

Spatial and temporal patterns of mineralization rates and oxygen distribution in a permeable intertidal sand flat (Sylt, Germany)

Ursula Werner, Markus Billerbeck, Lubos Polerecky, Ulrich Franke, Markus Huettel, Justus van Beusekom and Dirk de Beer

submitted to Limnology and Oceanography

ABSTRACT

Oxygen distribution and benthic mineralization rates were investigated in a permeable (3.9 x 10^{-11} m^2) intertidal sand flat (Hausstrand, Sylt, German Wadden Sea) in a transect from the low- towards the high-waterline. At all stations, oxygen penetration was deep and dynamic during inundation due to pore water advection. During exposure oxygen penetration was reduced. Oxygen consumption rates (OCR) and sulfate reduction rates (SRR) were linked to the inundation time of the stations: Oxygen consumption rates were elevated at the lower flat in summer (lower flat 131 -187; middle- and upper flat 64 -108 mmol C m^{-2} d^{-1}). Sulfate reduction rates decreased sharply from the low- to the high-waterline during all seasons (e.g., in summer: lower flat 18 - 40; middle flat 8.8 - 9.4, upper flat 0.5 - 4 mmol C m^{-2} d^{-1}). The advective supply of oxygen was a major determinant for the magnitude and pattern found in OCR. Driven by the oxygen availability, 71 - 90% of oxygen consumption took place during inundation. Due to the deep oxygen penetration, aerobic mineralization was the dominant degradation process at all stations. A simple estimate of the organic matter supplied to the sediments by pore water advection only explained a fraction of the mineralization rates. Advective exchange between water column and sediments may thus contribute to high mineralization rates with the supply of oxygen being the chief factor and the supply of organic carbon being subordinate. Mineralization rates were higher in summer than in winter. Only in summer sulfate reduction became a significant process.

INTRODUCTION

Permeable sandy sediments act as biocatalytic filter systems for organic matter from the water column (Webb & Theodor 1968, Huettel & Gust 1992, Shum & Sundby 1996). Benthic mineralization rates can be high and, consistent with a deep oxygen penetration, aerobic mineralization was found to be dominant (D'Andrea et al. 2002, De Beer et al. 2005). In shallow water sediments, benthic photosynthesis supplies organic material and oxygen to the sediments (Cammen 1991, Berninger & Huettel 1997). However, the magnitude and depth distribution of benthic mineralization processes depend to a large extent on the transport of electron acceptors and electron donors from the water column to the sediment and from the sediment surface to deeper sediment layers. While in cohesive sediments the main transport mechanisms are diffusion and fauna-mediated (bioturbation/bioirrigation), in permeable sediments pore water advection additionally contributes to interfacial exchange (Huettel & Gust 1992, Shum 1992, Shum & Sundby 1996). Pore water advection can exceed diffusive transport rates by orders of magnitude (Huettel & Gust 1992, Boudreau et al. 2001). Pore water advection is considered the major reason for high mineralization rates in the organic poor sands (Webb & Theodor 1968, Shum & Sundby 1996, Huettel & Rusch 2000) as it provides solutes such as oxygen (Forster et al. 1996, Ziebis et al. 1996) and particulate organic carbon (Rusch & Huettel 2000, Ehrenhauss & Huettel 2004) to the sediments while removing potentially inhibitory end-products of mineralization processes.

At an inundated intertidal sand flat advection is driven by pressure gradients caused by the interaction of tidal and wind driven currents and waves with sediment topography, (Riedl et al. 1972, Huettel & Gust 1992, Precht & Huettel 2003), or by density changes (Webster et al. 1996, Rocha 1998). At an exposed intertidal sand flat advection may occur as pore water drainage, driven by a hydraulic gradient developing between the sea water level and the slower dropping pore water level (Nielsen 1990). Thus, at intertidal sand flats, the advective exchange rates may vary over the tidal cycle. During inundation, pressure gradients are generated by hydrodynamics that are reduced or absent during exposure. The advective supply of oxygen and organic matter from the water column should therefore depend on the inundation time of the sediment and, thus, on the distance to the low water line. This may lead to a spatial heterogeneity in mineralization rates, with mineralization rates increasing towards the low water line.

Field studies on transport and mineralization rates in permeable intertidal sediments (Rusch & Huettel 2000, D'Andrea et al. 2002, De Beer et al. 2005) are rare, as the dynamic nature of permeable sediments complicates in situ measurements (Reimers et al. 2004). A deep oxygen penetration was found during the inundation period of an intertidal flat due to pore water advection (De Beer et al. 2005), however, at another intertidal flat, a deeper oxygen penetration was found during the exposure period due to air intrusion (Brotas et al. 1990). An in situ study found that the advective supplied organic carbon was in balance with the organic carbon required for benthic mineralization (Rusch & Huettel 2000). However, as the activity of permeable sands may be closely linked to pore water advection, the choice of the methods for mineralization rates measurements is critical. Stirred benthic chambers generate pressure gradients and pore water circulation patterns, resembling those generated by currents interacting with topography (Huettel & Rusch 2000), but, in order to mimic natural pore water advection rates, intensive studies on local hydrodynamics and sediment topography are necessary. For the measurement of oxygen consumption rates (OCR) that include the effects of pore water advection, we chose a recently introduced method that combines in situ time series of oxygen depth measurements with laboratory measurements of potential volumetric sedimentary OCR (De Beer et al. 2005, Polerecky et al. 2005).

Our aim was to investigate in situ the influence of pore water advection on mineralization rates and on sediment oxygenation. We investigated whether inundation time of the sediments leads to spatial patterns of oxygen distribution and dynamics and mineralization rates across an intertidal sandflat. We, therefore, measured oxygen dynamics, sedimentary oxygen consumption rates and sulfate reduction rates at three stations along a transect stretching from the low water line towards the high water line during different seasons. We discuss the role of transport processes that are connected to inundation time, such as pore advection and drainage, for the determination of magnitude and patterns of mineralization rates.

METHODS

The study site

The study was conducted on the intertidal sand flat "Hausstrand" in the Sylt/Rømø Basin in the North Frisian Wadden Sea, Germany (Fig. 1). The basin is a semi-enclosed lagoon, connected to the North Sea through a channel (Lister Tief) in the north. The influence of freshwater in the basin via atmospheric input or fresh water runoff is small, being less than one thousandth of the tidal water exchange with the North Sea. The investigated intertidal flat is situated south of List Harbour and stretches over approx. 500 m in north south direction. From the low water line the tidal flat stretches over a 100 m wide, rather level zone, followed by a 30 m wide, steeper sloping beach face. The tidal flat is protected from the prevailing westerly winds by the island and from currents by a short dam. Current velocities reach 0.5 m s^{-1}.The tidal amplitude is ca. 1-2 m. The origin of the sand is mainly eolic.

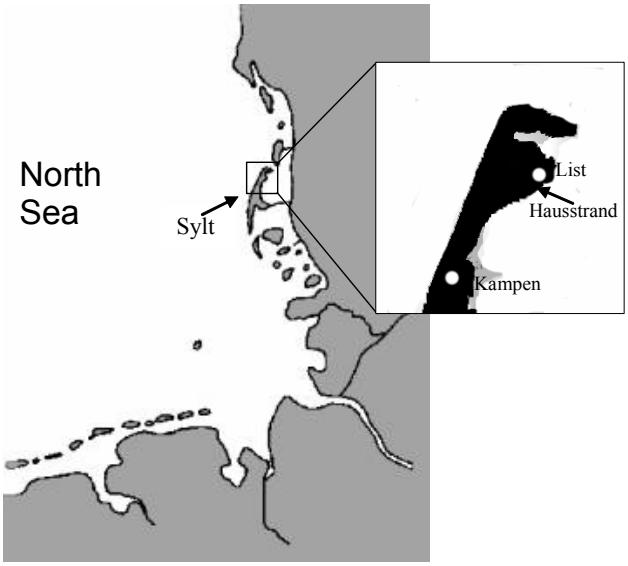

Figure 1: Location of the island Sylt in the North Sea and close up on the northern part with the investigated intertidal flat Hausstrand.

The investigation campaigns covered three seasons, and were conducted in April and August 2002 and February and June 2003. Investigations were conducted on the level part of the tidal flat, where sediments remain water saturated during exposure due to capillary forces. Three stations were chosen, with a distance of ca. 40 m between stations. The lower flat station was situated close to the mean low water line

(N 55°00'52.8; E 008°26'16.9), the middle flat station was situated in the middle of the transect and was in February and June 2003 influenced by a shallow (ca.0.5-2 cm deep) but broad (up to 5 m wide) tidal gully. The upper flat station was located at the upper end of the dissipative zone (ca. 10 m in front of the mean high water line). The mean water level above the sediment during inundation was 1.9 m at the lower station, 1.50 m at the middle station and 1.30 m at the upper station. The abundance of macrofauna at the Hausstrand is rather low (7 individuals per 10 cm^2), whereas meiofauna is abundant (6000 individuals per 10 cm^2) (Armonies & Hellwig-Armonies 1987).

Sampling

If not stated differently below, sediment samples for laboratory analysis or experiments were taken with plastic core liners with an inner diameter of 3.6 cm. Sampling depth was 10 to 15 cm. All samples at one station were randomly taken within 2 m^2. The investigated parameters, number of replicates and incubation temperature used for rate assessment are summarized in Table 1.

Sediment characteristics

Grain sizes were determined by sieving sediments through a calibrated sieve stack. Sediments were pooled over 0-3, 4-10 and 11-15 cm depth intervals. Porosity was calculated from the weight loss of a known volume of wet sediment after drying at 60°C until weight constancy (1 cm depth resolution). Permeability was measured using the constant head method (Klute & Dirksen 1986) on cores of ca. 15 cm length. Four different pressure heads were applied per replicate core.

In situ sensor studies

For in situ profiles, microsensors were mounted on a deep-sea profiler as described previously (Glud et al. 1999, Wenzhöfer et al. 2000). Oxygen was measured using Clark type oxygen microelectrodes (Revsbech 1989) with a tip diameter of 300 µm to prevent damage by the coarse grains, an actual sensing surface of 5 µm and a response time (t_{90}) of less than 5 seconds. Temperature was measured with a Pt100 electrode (tip diameter: 3 mm; Umweltsensortechnik, Germany). For the monitoring of the sediment surface, a resistivity sensor was employed. The profiling device was positioned on the sediment with the microsensors initially 1-2 cm above the sediment surface. Downward profiles were continuously measured over several tidal cycles

(up to 56 h) to a sediment depth of 6 to 7 cm, (step size of 1 mm). One profile was recorded within 25-35 min, with a minimum pause of 5 min between the profiles to reduce effects of holes formed by the intruding microsensors.

Table 1: Overview of investigated parameters per station for the four investigation campaigns. Numbers in parentheses identify the number of replicate sediment cores or seawater samples taken for analysis. Number in brackets for water column current velocities and pore water flow velocities identify the number of inundation or exposure periods where measurements were conducted. For additional details see text.

Parameter	April 2002	August 2002	February 2003	June 2003
in situ O_2	all	all	all	all
OCR	MF (3)	LF, MF (1); UF (2)	all (3-4)	all (3)SRR all (3)
	all (3)	all (3)	all (2)	all (3)
Add. OCR			LF, UF (1)	all (1)
Add. SRR			all (2)	all (2-3)
Incub. T (°C)	10	20	2	18
Porosity	all (2)	all (3)	all (2)	
Grain sizes	all (2)	all (2)	all (2)	
Permeability	LF, MF (2[a])	MF (3[a])		
TOC (sed.)	all (2)	all (2-3)	all (2)	all (2)
PW solutes	LF, MF(3[b])	LF, MF(3[b]);UF (2)	LF,MF(3[b]);UF (2)	all (1)
SW sol./OC	(3)	(4)	(4)	(3)
Water column current velocity			LF, MF [2]	MF [2]
Pore water flow velocity at sediment depth:				
2 cm				MF, LF [2-3]
5 cm				MF [3]
10 cm				MF [1]

Abbreviations:
all = all stations; LF= lower flat station; MF= middle flat station; UF= upper flat station; Add. = addition experiment OCR and SRR; Incub. T= incubation temperature for OCR and SRR, PWsolutes= pore water solutes (DOC, nutrients, sulfate, salinity); SW sol./OC =sea water column solutes and particulate organic matter
[a] 4 different pressure heads were applied per replicate core
[b] 5-6 cores pooled per replicate; replicates taken at three time points over the tidal cycle

Oxygen consumption rates

Measurements of potential volumetric oxygen consumption rates (pOCR) were performed in the laboratory on freshly collected intact sediment cores as described previously (De Beer et al. 2005; Polerecky et al. 2005). Experiments were conducted in the dark at the average in situ temperature of the respective month (Table 1). Air-saturated ambient sea water was percolated through the sediment cores until oxygen was present in high concentrations at the depth of measurement. After the percolation was stopped, the decrease of oxygen in time was monitored by an oxygen microsensor (April 2002) or a planar oxygen optode (all other campaigns). The initial oxygen concentration decrease at the measuring depths was taken as the potential OCR. For the

assessment of pOCR with planar optodes, we used rectangular stainless steal cores (inner diameter 36 mm, height 200 mm) that had at one side a polycarbonate window to which a semi-transparent oxygen optode was glued. The planar optode technique allowed the calculation of pOCR with a resolution of ≈ 300 µm over the entire optode area (ca.25 x 150 mm; resulting oxygen image size 80x 480 pixels). For the assessment of pOCR with oxygen microsensors, the microsensor was positioned at a defined depth within the sediment cores and the cores were repetitively percolated to obtain a profile of pOCR with depth intervals of 2 mm (0-3 cm depth) to 5 mm (below 3 cm).

The obtained volumetric data represent the potential oxygen consumption, whenever oxygen is present at the specific sediment depth. To obtain the areal OCR of the sediments, the rates were integrated over the various depths of oxygen penetration as obtained in situ from the automatic profiler as described previously (De Beer et al. 2005). We assumed pOCR to follow zero order kinetics with respect to oxygen (Thamdrup et al. 1998). For the assessment of daily areal OCR, all oxygen penetration depths measured over full tidal cycles were used, so that daily areal OCR reflect the oxygen availability of the distinctive inundation and exposure periods of the three stations.

Sulfate reduction rates

Potential sulfate reduction rates (pSRR) were measured with the whole core $^{35}SO_4^{2-}$ radiotracer incubation method (Jørgensen 1978) modified for permeable sediments (De Beer et al. 2005). Radiolabeled $^{35}SO_4^{2-}$ (Amersham) was added to 70 mL of ambient seawater to a specific activity of 340MBq/mol SO_4^{2-}. The seawater-tracer solution was placed on top of the sediment and allowed to percolate into the core. The permeability of the sediment allowed an even distribution of tracer in the pore water. After an incubation of 4 to 6 h at the average in situ temperature (Table 1), sediments were sliced in 1 cm sections and incubation was terminated by transferring the sediments into 20% ZnAc. Samples were processed using the cold chromium distillation procedure (Kallmeyer et al. 2004). Radioactivity of $^{35}SO_4^{2-}$ and Total Reduced Inorganic Sulfur (TRIS) was determined with a liquid scintillation counter (Packard 2500 TR), using Lumasafe Plus® (Lumac BV, Holland) scintillation cocktail.

Sulfate reduction rates were assessed in the laboratory under stagnant flow conditions, the supply of oxygen was thus restricted to molecular diffusion. In the field oxygen penetrates much deeper into the sediments and may lower sulfate reduction

rates. The anoxic conditions during incubation may lead to an overestimation of sulfate reduction rates, although sulfate reduction has been measured in oxidised and oxic sediments (Jørgensen 1977, Jørgensen & Bak 1991). Because of the uncertainty about the inhibitory effects of oxygen, we made maximum and minimum estimations. The maximum depth integrated sulfate reduction rates (SRR_{max}) were not corrected for possible oxygen inhibition. To obtain a minimum assessment of depth integrated SRR (SRR_{min}), i.e., assuming that oxygen completely inhibits sulfate reduction, pSRR were integrated over the anoxic sediment depths only, as deduced from the in situ oxygen measurements.

Estimation of aerobic mineralization rates

Aerobic mineralization cannot be directly measured and was, therefore, calculated from areal OCR and SRR_{max}. Oxygen consumption rates represent the sum of aerobic mineralization and oxidation of reduced substances from anaerobic decay (e.g., Fe^{2+} and H_2S). The sulfides produced by sulfate reduction are oxidized back to sulfate within the sediments, using oxygen as the ultimate electron acceptor. Therefore the aerobic mineralization rates were calculated by subtracting the sulfate reduction rates (expressed in equivalents of oxygen used for the oxidation of sulfides to sulfate) from the measured oxygen consumption rates. We considered sulfate reduction to be the most important anaerobic respiration process (Jørgensen 1982), the others were not considered.

Organic matter addition experiments

The percolation methods for the measurement of pOCR and pSRR allow the addition of water soluble substances together with the seawater solution to the whole sediment cores. We added glucose (2 mmol L^{-1}) to determine a stimulation of pOCR by organic substances, whereas acetate (2 mmol L^{-1}) was added to determine a stimulation of pSRR. The assessment of pOCR before and after addition were performed in the same core, for pSRR separate cores were taken.

Estimated bottom water filtration rates

The estimation of bottom water filtration rates (L m^{-2} d^{-1}) during inundation was based on the simplified assumption that the oxygen penetration depth is controlled by the balance between a vertical downward transport of oxygen and the sedimentary

pOCR. By combining the oxygen penetration depth and pOCR data the rate of oxygen supply to the sediment was calculated. From the supply rate of oxygen, one can calculate how much water is pumped through the sediments (bottom water filtration rates) by using the oxygen concentration in the overlying water (Polerecky et al. 2005):

$$v_f = \int_0^{z_p} OCR(z)dz \times c_o^{-1}$$

with v_f being the flow rate in L m^{-2} h^{-1}, $\int_0^{z_p} OCR(z)dz$ being the oxygen consumption rates integrated over the oxygen penetration depth (z_p) in mol m^{-2} h^{-1} and c_0 being the oxygen concentration in the overlying water in mol L^{-1}. By using the bottom water filtration rate and the POC content or the chlorophyll *a* concentrations of the water column, one estimate the amount of organic carbon that is transferred to the sediments by pore water advection.

Water column current velocities

Water currents 5 cm above the sea floor were measured using a Nortek™ Acoustic Doppler Velocimeter (ADV) that measures 3 components (*x*, *y*, *z*) of the flow velocities within a cylindrical sampling volume (ca. 6 mm in diameter and 6 mm in height) located 100 mm below the probe. Flow velocities were recorded with a sampling frequency of 0.5 Hz during February 2003 and with 25 Hz during June 2003. The water current velocity was calculated for each sampling using the scalar of the 3 velocity components and averaged over 1 minute intervals.

Pore water flow velocity

Pore water flow velocity was measured on the middle station and at the lower flat station in June 2003 using a slight modification of the method described by (Precht & Huettel 2004). The passage of a fluorescent dye tracer (Fluorescein, 100 mg L^{-1}) through the sediments was followed by 6 optical glass fibre sensors (tip diameter 140µm, Radiall®) fixed to a plane wire mesh. As the in situ dye signal intensity is influenced by the pore space in front of the sensor, values are given as normalized sensor signals. Prior to measurements of the drainage flow during exposure, dye was injected directly into the sand and dug out later, to visually determine the main flow direction. Then, a small incision was cut into the sediment to the desired depth (see Table 1) and the set-up was carefully inserted horizontally several cm into the undisturbed part of the sediment. After rebuilding the sediment surface, 1 mL of dye

solution was injected through a syringe needle that was fixed to the upstream end of the mesh. The average pore water flow velocity was calculated for all measurements from the time interval between the geometric centroids of the signal curves at consecutive sensors. Dye was injected during exposure at falling tide, at low tide and rising tide and on the transition to inundation. Experiments during inundation were tested with the set-up being inserted into the sediments with various angles with respect to the sediment surface.

Sedimentary organic carbon and pore water solutes

Sediment samples for TOC analysis were sectioned into 1 cm slices and stored at -20°C. Before analysis, samples were freeze dried, ground, and acidified with 1 N HCL to remove the inorganic carbon. The samples were transferred into tin cups and [TOC] was measured using a Heraeus CHNO-rapid elemental analyzer with sulfanilamid as a calibration standard.

Pore water was extracted from all stations (1 cm depth intervals, 5 to 6 cores pooled) for the analysis of DOC, pore water nutrients (ammonium, nitrate, nitrite, phosphate, and silicate), sulfate and salinity. The sediment samples were placed into a Buechner-funnel on top of a nylon mesh. The funnel was inserted into a pressure chamber with the outflow of the funnel protruding from the chamber. Inert gas was then blown into the chamber and the pore water was collected at the outflow of the funnel. The pore water was filtered through a nylon syringe filter with 0.2 µm pore size (Millex GN, Millipore) and transferred into pre-combusted glass vials (DOC) or plastic vials (nutrients, sulfate, salinity). The whole procedure was conducted under anoxic conditions in a glove box. Pore water samples were stored at -20°C until analysis. For the calculation of DOC, total dissolved carbon (TDC) and dissolved inorganic carbon (DIC) concentration was measured by high temperature catalytic oxidation using a Shimadzu^{TM} TOC-5050A analyzer connected to a Shimadzu ASI 5000A autosampler. Bicarbonate and phthalate were used as calibration standards. DOC was obtained by subtracting DIC from TDC. Pore water nutrients were analysed spectrophotometrically with a Skalar Continuous-Flow-Analyzer according to (Grasshoff et al. 1999). For the upper flat station, pore water had to be stored in glass vials in some cases, therefore, silicate measurements for the first campaigns were not considered. Pore water sulfate concentrations were determined by non-suppressed ion-chromatography and conductivity detection with a Waters 510 HPLC pump, Waters WISP 712 autosampler,

Waters IC-Pak anion exchange column (50 x 4.6 mm) and a Waters 430 Conductivity detector. The eluant was 1 mM isophthalate buffer in 10% methanol, adjusted to pH 4.5. Salinity was measured using a refractometer. To test whether advective exchange of pore and overlying water is reflected in altering DOC and nutrients concentrations, pore water was extracted on different times during the tidal cycle on the lower and the middle flat. The first sampling was 20 min after incoming tide, the second sampling at high tide and the third sampling at low tide.

Water column parameters

Water samples for the analysis of particulate organic carbon (POC) and suspended matter (SM) were filtered on weighted and pre-combusted (600°C, 6h), Whatman GF/F filters (0.7µm pore size), rinsed with Milli Q to remove the sea salt and stored frozen until analysis. Before analysis of POC, samples were pre-treated with 1N HCL to remove the inorganic carbon, dried and transferred into tin cups. POC was analyzed using a Heraeus CHNO-rapid elemental analyzer with sulfanilamid as a calibration standard. SM was determined by the weight differences of the empty and loaded dry filter. The filtrate was further filtrated through a nylon syringe filters (see above) and analyzed for DOC and nutrients as described above.

Water samples for the analysis of chlorophyll a content were filtered on Whatman GF/C filters (0.7µm pore size). Acetone was used as extraction solvent (extraction time 18h at 4°C) and the chlorophyll a content was determined photometrically. Samples were taken every 3-5 days within an annual sampling campaign of water column parameters at Sylt.

RESULTS

General site description

The average daily inundation time was 7.5 h longer at the lower flat station than at the upper flat station (Table 2). In June, inundation times were longest at all stations. The inundation times were calculated over a 4 weeks period, including the three weeks of the investigation campaigns (tide gauge List, with permission of Wasser- und Schifffahrtsamt Tönning, Germany). The sediment properties did not vary between stations nor between seasons. The sediments consisted of silicate grains with a median grain size of 380 µm and were very well sorted medium sands (Wentworth 1922). Porosity was on average (± S.D.) 41 (± 3) % in the upper 2 cm of the sediment and 35 (± 3) % below. The sediments were highly permeable, on average 3.9 x 10^{-11} (± 0.3) m^2.

Table 2: Averaged inundation times, bottom water filtration and organic carbon infiltration during inundation at the three transect stations. For the calculation of daily bottom water filtration rates (L m^{-2} d^{-1}) for each station, the average bottom water filtration rate from all stations recorded in April, June and August (19 L m^{-2} d^{-1}) and the averaged inundation times of the respective stations were used. The amount of infiltrated organic carbon per station was calculated from the daily bottom water filtration rate and an averaged water column POC content of 0.06 mol L^{-1}.

Inundation time (h d^{-1})	upper flat	middle flat	lower flat
April	12.9	15.2	20.2
June	15	17.8	22.4
August	14.1	16.6	22.4
February	13	15.7	20.4
Bottom water filtration rate (L m^{-2} h^{-1})			
April		12 ± 2	
August	25 ± 5	16 ± 6	34 ± 13
June	13 ± 5	15 ± 6	21 ± 7
February	1.8 ± 0.5	3.3 ± 0.6	1.4 ± 0.4
Daily bottom water filtration rate (L m^{-2} d^{-1})			
	260	310	405
Organic carbon infiltration (mmol C m^{-2} d^{-1})			
	15	18	24

The average water temperatures during the measurement campaigns are presented in Table 3. Highest temperatures were measured in August 2002.

Table 3: Water column temperature, water column and pore water salinity, water column and pore water sulfate concentrations, water column POC, suspended matter (SM) and water column chlorophyll *a* content. Numbers after ± indicate standard deviation.

	Temp. (°C)	Salinity	SO_4^{2-} (mmol L^{-1})	POC (µmol L^{-1})	SM (mg L^{-1})	Chl a (µg L^{-1})
February	- 0.1 ± 0.4	28	22.2 ± 0.6	108 ± 20	84 ± 12	2.6 ± 0.4
April	8.5 ± 1.2	26-27	21.0 ± 0.6	60 ± 21	26 ± 4	16.6 ± 7.8
June	16.5 ± 1.0	31	24.1 ± 0.4	51 ± 4	74 ± 4	2.6 ± 1.9
August	21.0 ± 0.7	29-30	23.2 ± 0.5	56 ± 6	34 ± 25	3.6 ± 0.8

Oxygen penetration depth and dynamics

Oxygen penetrated deep and varied dynamically in time at all stations. The oxygen penetration depths were significantly different (non parametric U-test, $p < 0.01$, all stations, except at lower flat in February) between inundation and exposure periods of the flat, with the oxygen penetration being deeper and more variable during inundation. Exemplary time series of oxygen profiles are shown in Figure 2a-c and a summary of all oxygen penetration depths during exposure and inundation is given in Figure 3.

The simultaneous employment of the ADV and the automatic profiler clearly showed a covariance of the oxygen penetration depth and current velocity of the overlying water during inundation (Fig. 4). Oxygen penetration and dynamics during inundation were also enhanced during strong winds and waves (Fig. 5). The oxygen profiles that were measured during inundation often had a sigmoidal shape (Fig. 6 a). During the exposure of the flat, some oxygen profiles had a nearly parabolic shape (Fig. 6 b). During exposure benthic photosynthesis could increase oxygen penetration depth (Fig. 6 b).

The oxygen penetration depths and dynamics were comparable between the three transect stations during the inundation period within a campaign (Fig. 3). Also the oxygen penetration depths were similar between the three transect stations during exposure periods of a campaign (Fig. 3). Only in April, oxygen penetrated deeper at the lower flat during both inundation and exposure.

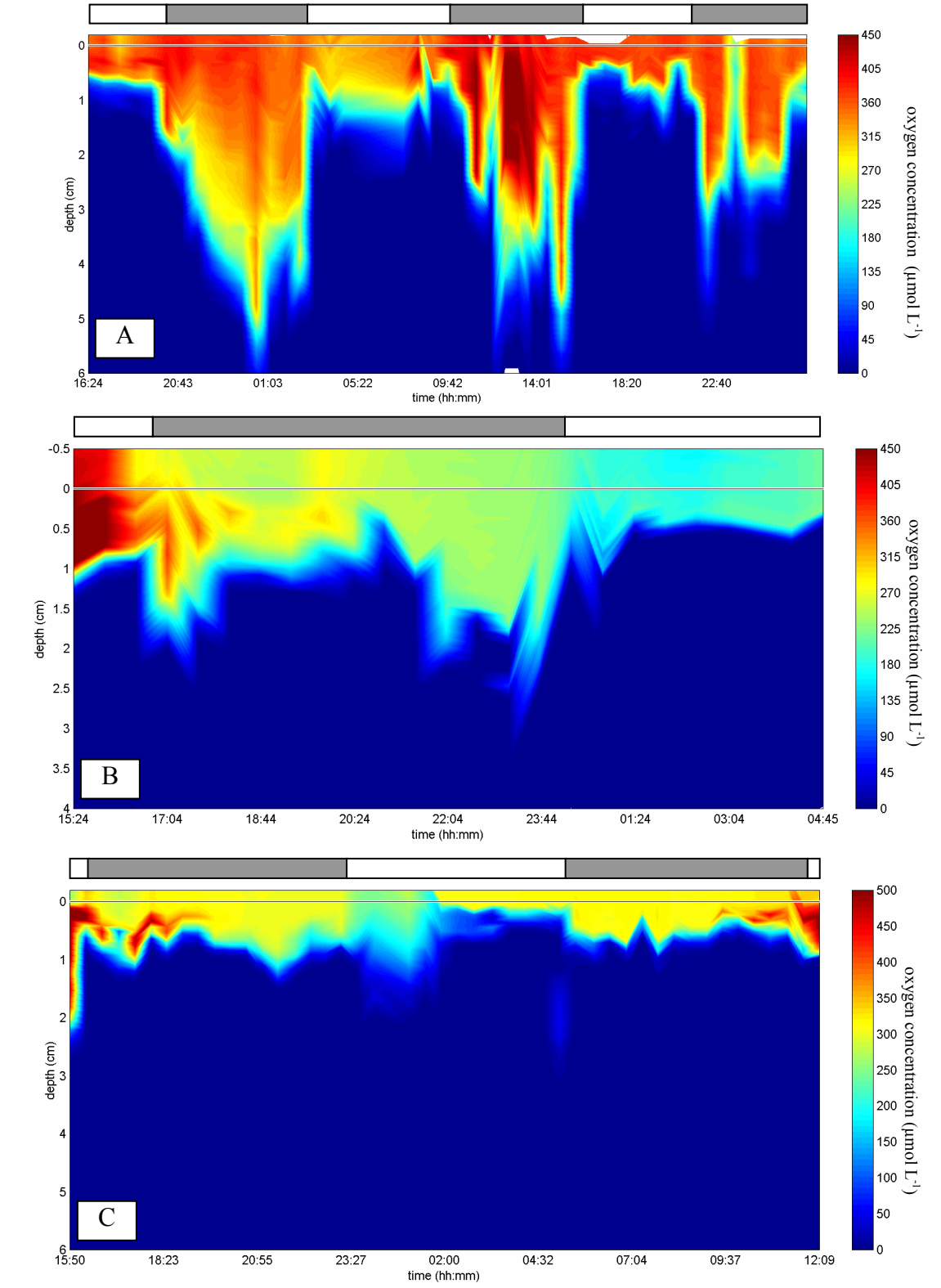

Figure 2 a-c: Time series of oxygen concentration profiles in the upper flat station in a) February, b) April and c) June. White and grey bars indicate exposure and inundation periods at the stations, respectively. Note that the total duration of the time series differs in all graphs.

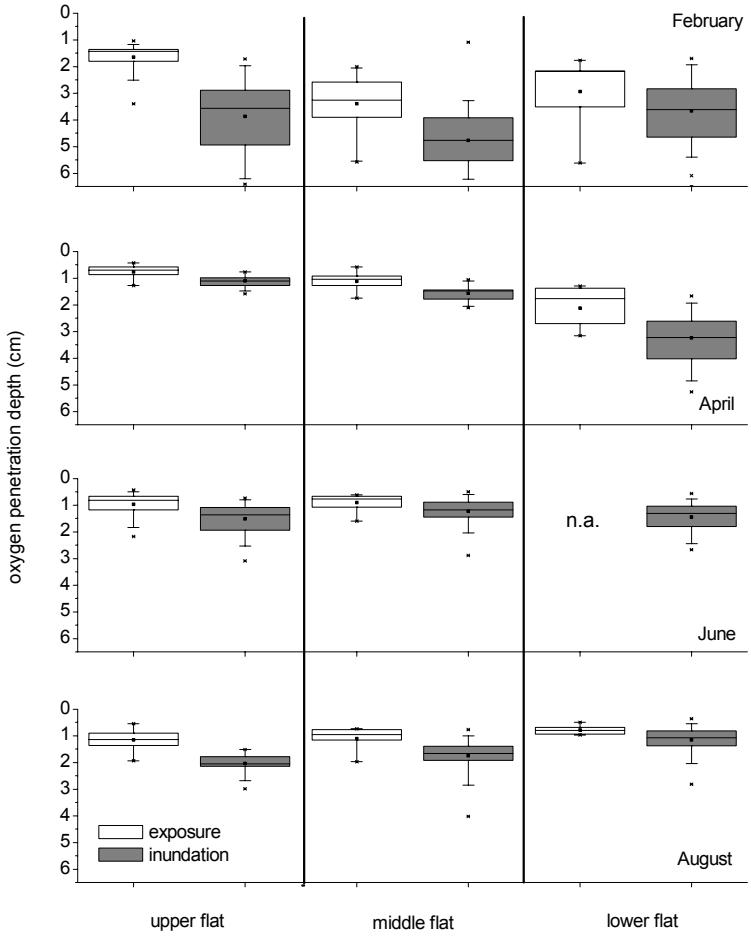

Figure 3: Oxygen penetration depths measured at the three transect stations during exposure and inundation of the flat. The horizontal lines of the box denote the 25th, 50th, and 75th percentiles, the square dot side the box represents the mean. The error bars denote the 5th and 95th percentiles, the symbols above and below the whiskers represent the extremes. The lower station was not exposed in June to the high water level in the Sylt Rømø Basin.

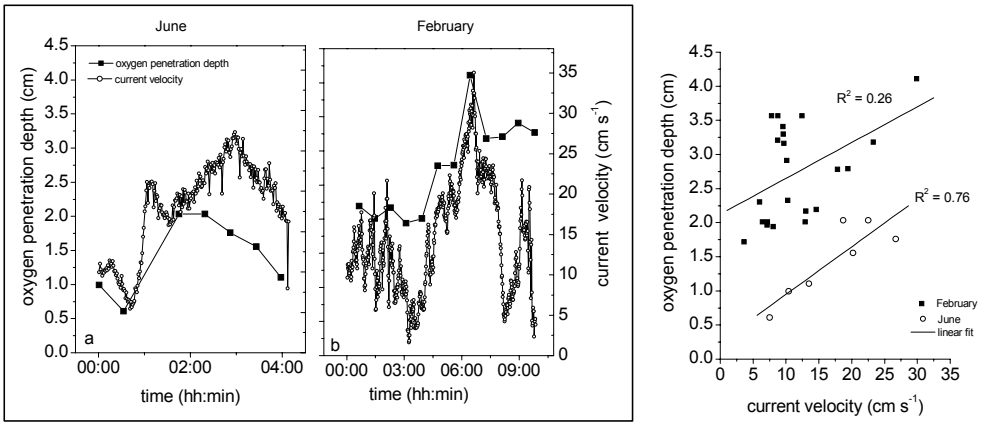

Figure 4: Current velocity measured at 5 cm above the sediment in relation to oxygen penetration depth for June (a) and an exemplary data set from February (b). Linear regression plots of oxygen penetration depth against current velocity for all June and February data.

There was a strong dependency of oxygen penetration depth with season (e.g., Fig. 3). With similar current velocities of the overlying water oxygen penetrated deeper in winter than in summer (Fig. 4).

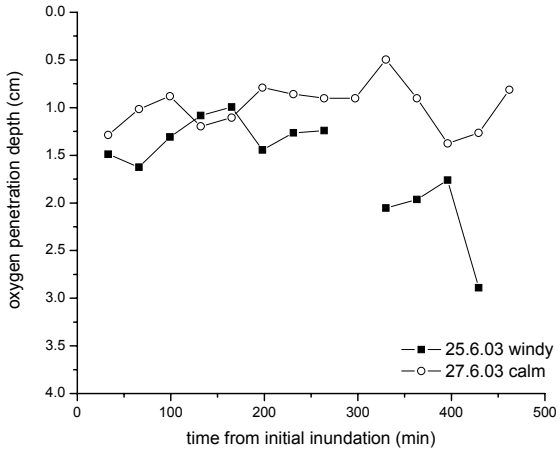

Figure 5: Dependence of oxygen penetration depth on the weather conditions, measured during inundation at the middle flat station in June.

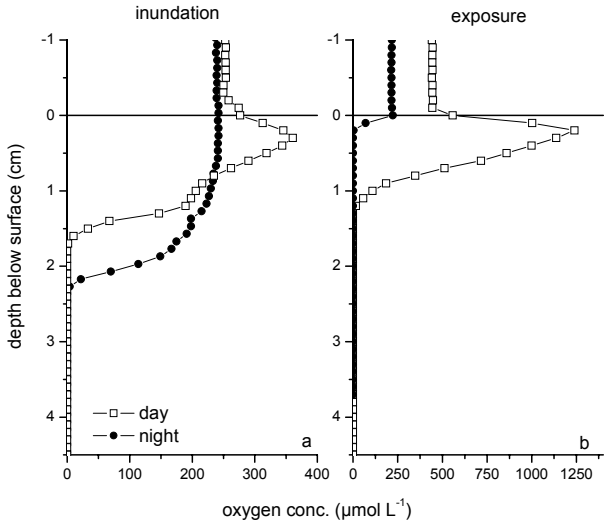

Figure 6: Exemplary day (open symbols) and night (filled symbols) oxygen profiles during inundation (a) and exposure (b) measured at the upper station (June). The subsurface oxygen peak of the day profiles indicates oxygen production by benthic photosynthesis. The night profile during inundation shows the oxygen supply to deep sediment layers by advection, whereas the oxygen distribution measured during exposure at night is dominated by diffusion.

Oxygen consumption rates

The potential OCR in the oxygenated sediment layers are presented in Figure 7. Most of the potential OCR profiles had a small peak in the top centimeter of the sediment, and were otherwise rather constant with depth. In the summer months June and August, the highest potential OCR were found near the low water line. The potential OCR rates were strongly influenced by season, being approx. 10 to 20 times higher in the summer months than during winter. Areal OCR were higher during inundation than during exposure because oxygen penetrated deeper when water was present over the sediment (Fig. 8). At all stations, 71 to 90% of the daily areal OCR took place during inundation (Fig. 9). In August and June, highest areal OCR were found at the lower flat station, in February, the intermediate station showed the highest rates (Fig. 9 and Table 4). The differences between the remaining stations were not pronounced. Areal OCR showed a pronounced seasonal variability, with lowest rates found in winter. In spring and summer areal OCR were comparably high.

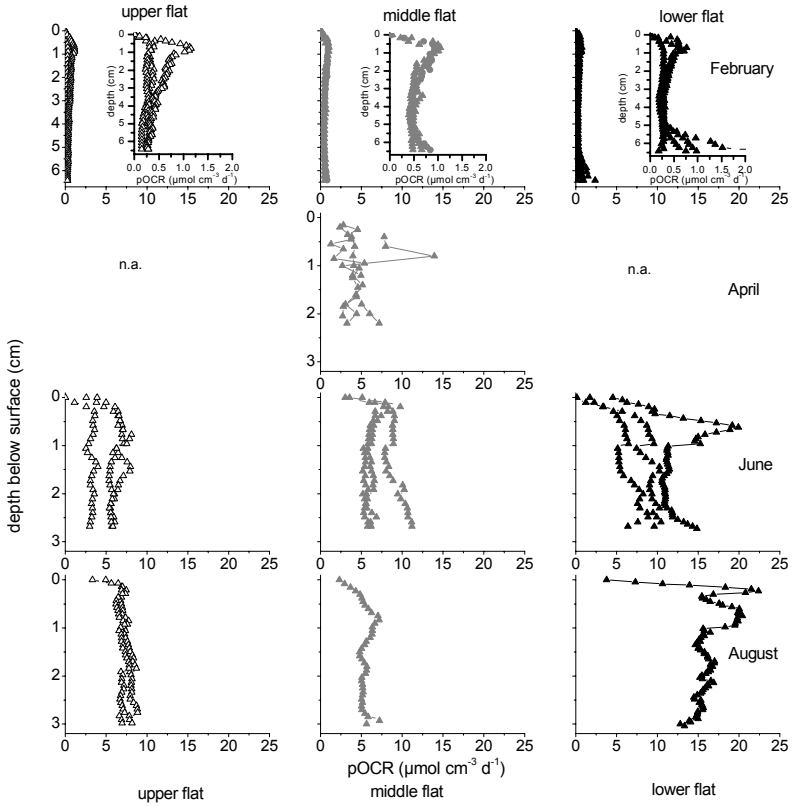

Figure 7: Depth profiles of volumetric potential OCR (pOCR) in the oxygenated sediment layer at the three transect stations during the four measurement campaigns. The different lines per layer represent replicate cores. The inserted graphs for February show the pOCR values in different scale.

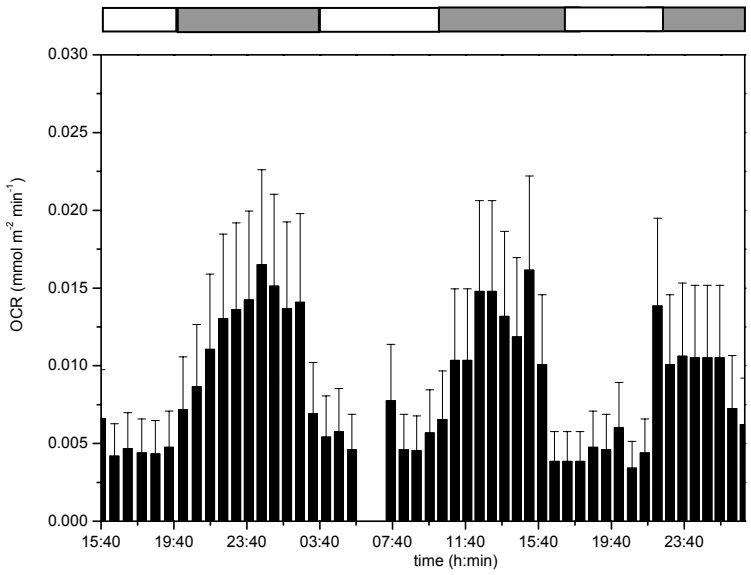

Figure 8: Effect of inundation on areal OCR shown for three tidal cycles at the upper flat in February. White and grey bars above the figure indicate exposure and inundation period of the station, respectively.

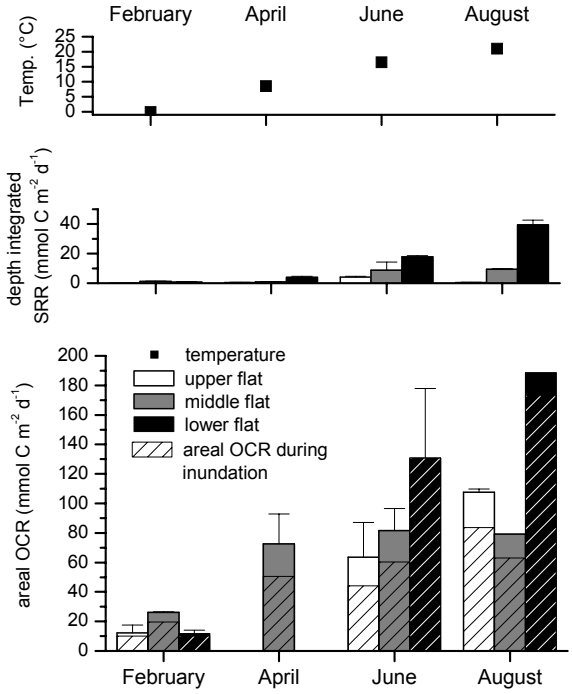

Figure 9: Areal OCR and depth integrated SRR calculated for the actual daily inundation and exposure times at the three stations, and average water column temperature. The hatched parts of the column show the part of the daily areal OCR that takes place during inundation. Note that in June the lower flat station remained inundated.

Sulfate reduction rates

Potential sulfate reduction rates decreased from the lower flat station towards the upper flat during all seasons (Fig. 10). The differences between stations were most pronounced in August. Potential SRR had a peak or increased below 1-2 cm depth in spring and summer, with the peak width increasing towards the lower flat. In winter, pSRR increased below 4-5 cm depth. The pSRR were the highest in summer. In contrast to the pOCR, pSRR were low in spring. The extent of seasonal variability depended on the station (Fig. 10, Table 4), with highest seasonal variability found at the lower flat and smallest seasonal differences at the upper flat. Pore water sulfate concentrations at all depths were equal to sea water concentrations at all stations (Table 4) and were, thus, not limiting pSRR. Differences between the depth integrated maximum and minimum SRR (SRR_{max} and SRR_{min}) were small (Table 4).

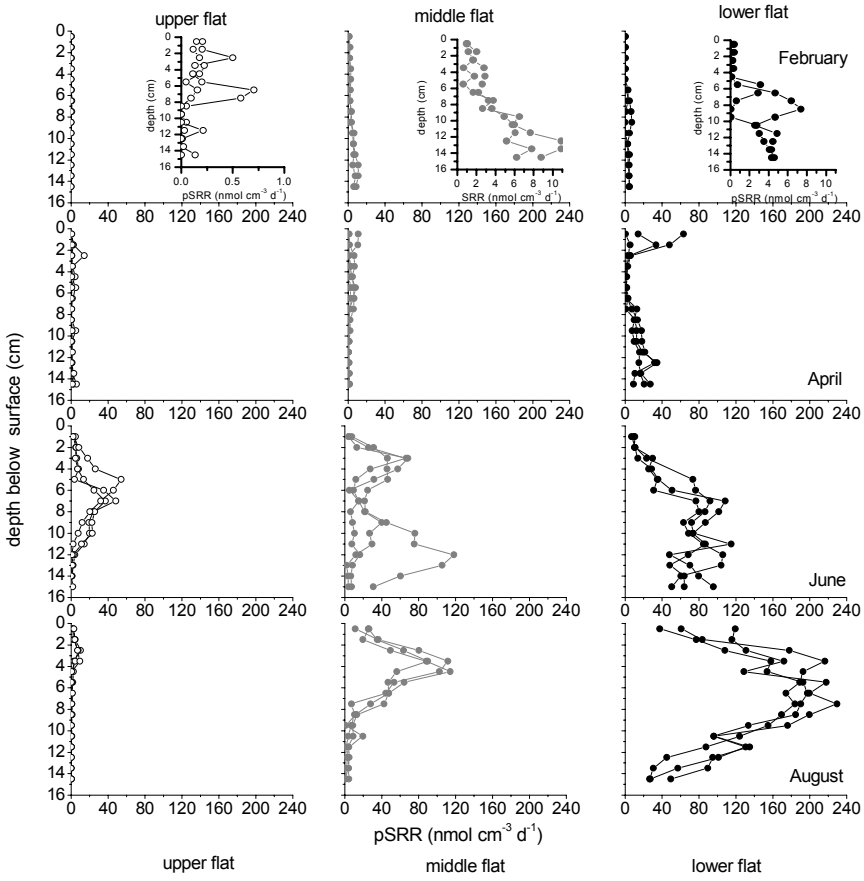

Figure 10: Potential SRR at the three transect stations during the four measurement campaigns. The different line graphs represent replicate cores. The inserted graphs in February show the pSRR in different scale.

The contribution of sulfate reduction to total mineralization increased towards the low water line (Table 4). A maximum contribution of 21% was found in August at the lower flat station. At the upper flat station sulfate reduction contributed less than 1% to total mineralization in August and February, but 6% in June. These estimates assume that other anaerobic processes had only negligible influence on mineralization.

Aerobic mineralization

The calculated areal aerobic mineralization rates (areal OCR corrected for the oxygen uptake by the H_2S produced by sulfate reduction) were high and deviated less than 10% from areal OCR (Table 4), as SRR were comparably low.

Table 4: Average areal OCR, estimated aerobic mineralization rates and depth integrated SRR (mmol C m^{-2} d^{-1}), and contribution of SRR to total mineralization (in %). SRR_{max} are SRR integrated over the top 15 cm of sediments, whereas SRR_{min} are SRR integrated only over the anoxic layers of the sediment. The contribution of SRR to total mineralization is based on SRR_{max}. Numbers after ± indicate standard deviation.

Min. rates (mmol C m^{-2} d^{-1})	upper flat	middle flat	lower flat
February			
OCR	12.2 ± 5.3	26.2 ± 0.3	11.9 ± 2.3
aerobic min.	12	25	11
SRR_{max}	0.04[a] ± 0.02	1.24[a] ± 0.24	0.71[a] ± 0.28
SRR_{min}	0.03 ± 0.02	1.11 ± 0.22	0.69 ± 0.28
contribution SRR (%)	0.3	4.7	6.0
April			
OCR		72.5 ± 20.3	
aerobic min.		71	
SRR_{max}	0.47 ± 0.18	0.78 ± 0.18	3.8 ± 0.9
SRR_{min}	0.44 ± 0.19	0.37 ± 0.28	2.7 ± 0.2
contribution SRR (%)		1.1	
June			
OCR	63.6 ± 23.5	81.5 ± 15.0	130.7 ± 47.2
aerobic min.	59	73	113
SRR_{max}	4.1 ± 0.5	8.8 ± 5.5	17.7 ± 0.9
SRR_{min}	3.9 ± 0.4	8.6 ± 5.5	17.4 ± 0.9
contribution SRR (%)	6.4	10.8	13.6
August			
OCR	107.6 ± 2.1[a]	79.2[b]	188.6[b]
aerobic min.	107	70	149
SRR_{max}	0.51 ± 0.07	9.4 ± 0.4	39.4 ± 3.2
SRR_{min}	0.40 ± 0.05	8.6 ± 0.5	37.6 ± 2.2
contribution SRR (%)	0.5	11.9	20.9

[a] n=2, [b] n=1

Stimulation of OCR and SRR by organic matter addition

Addition of dissolved organic carbon usually stimulated OCR and SRR (Table 5), except for February, where no stimulation of OCR was measurable. Glucose addition in June enhanced OCR 1.3 to 1.5-fold. The stimulation of SRR was most pronounced at the lower flat, where in February an almost 7-fold increases of SRR was recorded after acetate addition. The increase of pSRR varied with sediment depth, with rates being particularly enhanced in the sediment layers where pSRR already had been high prior to the addition of dissolved organic carbon.

Table 5: Organic matter addition experiment. Areal OCR control and areal OCR after the addition of 2 mmol L^{-1} glucose and depth integrated SRR control and depth integrated SRR after the addition of 2 mmol L^{-1} acetate. Numbers after ± indicate standard deviation.

Rates (mmol C m^{-2} d^{-1})		upper flat	middle flat	lower flat
OCR (Feb. 2003)	control	18		11
	addition	16		8
OCR (June 2003)	control	45	82	110
	addition	68	104	147
SRR (Feb. 2003)	control	0.04 ± 0.02		0.7 ± 0.3
	addition	0.08 ± 0.01		4.7 ± 2.9
SRR (June 2003)	control	4.1 ± 0.3	8.8 ± 5.5	17.7 ± 0.9
	addition	5.2 ± 2.1	16.5 ± 4.8	36.1 ± 2.6

Bottom water filtration rates

The advective filtration rates of bottom water through the sediments were calculated from oxygen penetration depths and sedimentary pOCR and ranged from 1.4 to 34 L m^{-2} h^{-1}. Differences in calculated bottom water filtration rates per hour inundation time (Table 2) were small between the three transect stations in April, June and August. However, the total daily volume of water pumped through the sediments decreased from 405 to 260 L m^{-2} d^{-1} towards the upper station due to decreasing inundation periods. In winter, the bottom water filtration rates showed unrealistically low results and were not included in further calculations. In winter the oxygen penetration depths were mainly influenced by the pressure field across the sediment surface and not by the low sedimentary OCR, thus the basic concept of the estimation could not be applied. Therefore, the winter data were not included in the calculations of advective organic matter supply to the sediments.

The total amount of advective carbon received by the sediments from the water column by advective filtration increased towards the lower flat station (Table 2). This calculation is based on the simplifying assumption that all POC in the infiltrated water volume is captured by the sediments (based on an averaged water POC content of 0.06 mol L^{-1}). If the infiltration rates are based on the water column chlorophyll a content, the amount of easily degradable organic carbon supplied to the sediments would in most months be even lower: During the plankton bloom in April, 18, 21 and 28 mmol C m^{-2} d^{-1}, in the other month 3, 4 and 5 mmol C m^{-2} d^{-1} were filtered at the high, middle and lower station, respectively (assuming 1 µg chlorophyll a represents algae cells of 50 µg organic carbon).

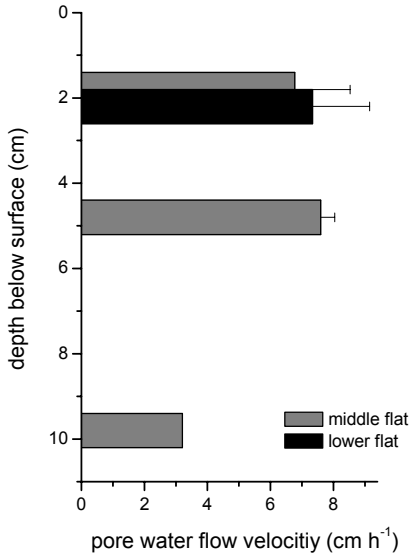

Figure 11: Pore water flow velocities during exposure at 2, 5 and 10 cm sediment depth at the middle and in 2 cm sediment depth at the lower flat station in June.

Surface pore water flow velocities

As concluded from the dye experiments, pore water drained towards the low water line during exposure of the flat (Fig. 11). At 10 cm sediment depth the pore water flow velocity (3-4 cm h^{-1}) was only half of that in the layers above 5 cm (6-8 cm h^{-1}) (Fig.11). The pore water flow velocities were the same at falling and low tide at 2 and 5 cm depth, only at 2 cm depth the flow velocities decreased shortly before re-inundation of the station (data not shown). The flow direction reversed not before the incoming tide was nearly above the measuring set up. During inundation the tracer dye quickly dispersed and was no longer detected by the planar sensor set-up.

Sediment and water column parameters

The average TOC content of the sediments was below 0.1% at all stations. The lowest TOC content was always found at the upper station (0.04 ± 0.02% for all investigations). At the middle and lower flat stations the average TOC content varied between 0.05 and 0.09%. The TOC content was highest in the upper 2 cm of the sediments and usually decreased with depth. There was no clear seasonal trend.

Water column POC concentrations were similar in all investigated months except for high values in February (Table 3). There, the high POC content coincided

with a high load of suspended matter that may be related to a storm event. The chlorophyll *a* content in the water column was highest in April and comparable between the other investigation months.

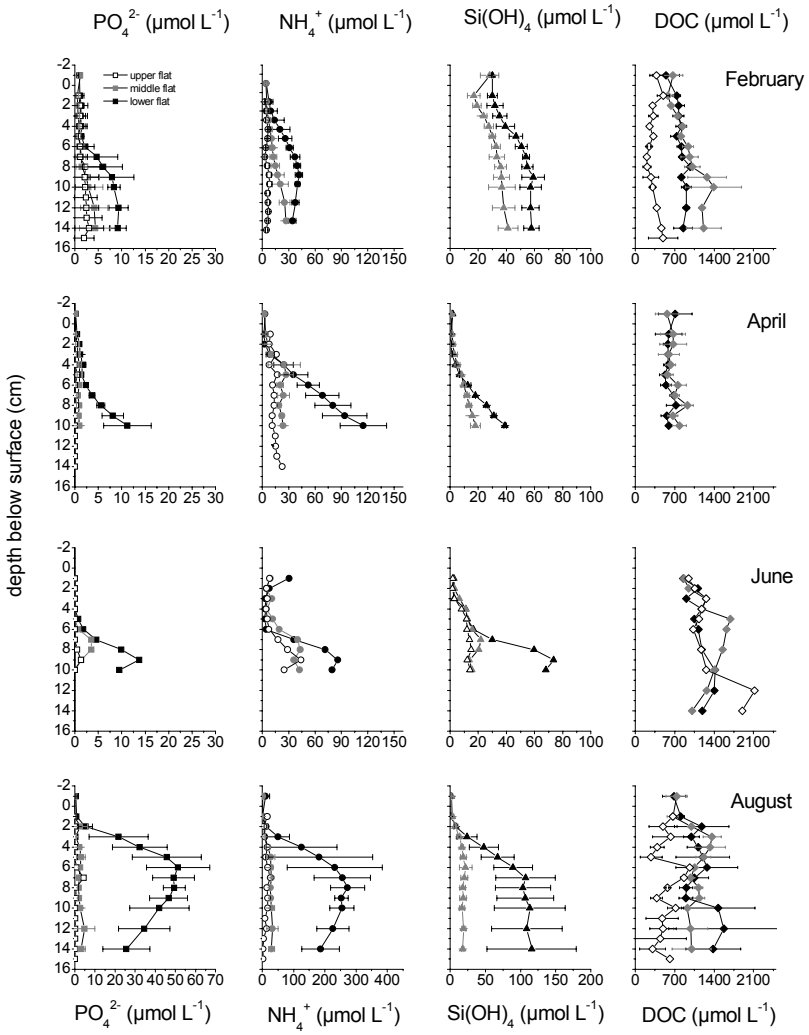

Figure 12: Nutrient and DOC concentrations in pore- and overlying water of the three investigation sites during the four sampling campaigns.

The pore water concentrations of DOC, phosphate, ammonium, and silicate (Fig. 12), did not vary over the tidal cycle, thus measurements were taken as replicates. Pore water DOC in the top centimeter of sediment was close to the DOC content of the water column, below, pore water DOC increased slightly with depth in most measurements. In August and in February, the lower and middle flat station had similar

DOC contents, while the upper station had lower DOC concentrations. In June, DOC content was similar at all stations. DOC was lower in winter than in summer.

Phosphate, ammonium and silicate concentrations in the pore water were highest at the lower flat station and showed a distinct increase below 2-4 cm depth. At the other two stations, this increase was less pronounced or absent. A seasonal effect in pore water nutrient concentrations was only detectable at the lower flat where higher concentrations were found in the summer months. The determination of nitrate and nitrite gave peculiar results. The concentrations were high over the entire sediment depths (in 10 cm depth ca. 35 µmol L^{-1} nitrate or up to 1 µmol L^{-1} nitrite, data not shown). Although these solutes may be transported to deeper sediment layers by pore water advection, ground water inflow or faunal transport, these data may as well be artefacts from the pore water extraction or analysis. The nitrate and nitrite concentrations were thus not included in the data set.

DISCUSSION

The significance of pore water advection for the oxygen distribution in the sediments

The sediments at the investigation site are highly permeable and facilitate pore water advection (e.g. (Riedl & Machan 1972, Thibodeaux & Boyle 1987, Huettel & Gust 1992). The sandy deposits were homogeneous along the transect as concluded from our data on grain size distribution, permeability and porosity. The flow rate of fluids in highly permeable sediments is proportional to the pressure gradient driving the flow and sediment permeability (Darcy 1856). Given similar hydrodynamical conditions over the length of the transect, pore water advection at the three stations should be comparable in magnitude. Indeed, during inundation, the oxygen penetrations depths and the estimated bottom water filtration rates were similar between the three stations for most measurements. Thus, differences in hydrodynamics that may exist between the stations due to different water depths or due to a decrease of the flow velocity towards the shore, had no detectable influence on the oxygen penetration depths between stations.

The oxygen distribution and dynamics were strongly linked to the presence or absence of pore water advection. During inundation, oxygen penetrated deeper and varied more dynamically than during the exposure of the flat. The co-variance of oxygen penetration depth with the current velocity of the overlying water (Fig. 4) indicates that the dynamics and deep penetration of oxygen were linked to pore water advection. Constraints in the correlation between oxygen penetration depths and water current velocity are due to the influence of sediment topography on pore water advection and the influence of location on our one dimensional oxygen penetration depths measurements: While highest oxygen penetration occurs below zones of high pressure (i.e. ripple troughs), where the oxygen rich bottom water is forced into the sediment, low penetration depths are found below zones of low pressure (i.e., ripple crests), where anoxic pore water is drawn to the sediment surface (Huettel & Gust 1992, Shum & Sundby 1996, Precht et al. 2004). Nevertheless, the average oxygen penetration depth increases due to advective pore water exchange because in a sediment surface with wave or current ripples, as found at our study site, the area of bottom water intrusion is approximately 6-times larger than the area of pore water emergence (Precht et al. 2004). In winter, the low correlation of oxygen penetration and water current

velocity may partly be a result of the low OCR, as the sediments remained oxygenated for some time, even if current velocities decreased (Fig. 4). Pore water advection can also be inferred from the sigmoid shape of the oxygen profiles during inundation (Revsbech et al. 1980).The quick response of the oxygen penetration depth to wind-enhanced currents and waves emphasizes the strong coupling of these permeable sediments and the overlying water by physical (or hydraulic) forcing.

During the exposure of the flat, oxygen penetration remained dynamic but was less than during inundation time, even when the upper sediment layers were directly exposed to air. In some measurements the oxygen profiles exhibited the nearly parabolic shape of diffusion dominated profiles (Fig. 6 b) as also found in retrieved cores, where diffusion was the only transport mechanism (oxygen penetration depth ca. 2 mm in summer; data not shown). A major cause of a deeper oxygen penetration during exposure of the flat was the oxygen production by benthic photosynthesis. However, other factors may contribute to the oxygen dynamics during exposure, such as an inflow of oxygen rich water below superficial water runoff or pore water drainage.

During inundation and exposure of the flat, oxygen is transported into the sediments by bioirrigating benthic fauna (Aller 2001, Wenzhöfer & Glud 2004). Evidence for bioirrigation are oxygen profiles that showed irregularities within the oxygenated layer or ephemeral oxygen peaks below the oxygen penetration depth. These deep oxygen peaks were not included in the determination of oxygen penetration depth, as a quantification of bioirrigation from one dimensional oxygen measurements is not possible. This may lead to an underestimation of areal OCR.

Our findings on the variability of oxygen dynamics over the tidal cycle differ from previous findings (Brotas et al. 1990), that showed deepest oxygen penetration during exposure of an intertidal sand flat due to air intrusion. The oxygen penetration depth measurements in that study were, however, conducted in sediment cores, and thus without an impact of in situ hydrodynamics.

Significance of pore water advection for benthic mineralization rates: oxygen

The advective supply of oxygen and organic matter from the water column to the benthic system is considered a major reason for high mineralization rates in permeable sediments (Webb & Theodor 1968, Huettel & Gust 1992, Shum & Sundby 1996). The advective supply of oxygen was a major factor for the magnitude and patterns found in benthic mineralization rates in our measurements. Mineralization rates were high and

due to the deep oxygen penetration aerobic mineralization rates dominated organic matter degradation processes at all stations (Table 4), as previously concluded from a more limited data set from the same site (De Beer et al. 2005). The high aerobic mineralization rates are in contrast to findings in finer grained coastal sediments, where the aerobic mineralization is restricted to a few millimetres and sulfate reduction can account for up to 50% of total mineralization (Jørgensen 1982). That the deep oxygen supply promoted aerobic organisms in the oxygenated sediment layer may also be seen in the potential OCR, which were at each measuring depth at least an order of magnitude higher as the potential SRR. Although in the oxygenated layer reduced substances should not contribute significantly to the pOCR, a quantification of aerobic mineralization remains difficult. In permeable sediments, the contribution of reduced substances may be even more complicated, as pore water advection may transport reduced substances to the upper sediment layer (Huettel et al. 1998, Precht et al. 2004) or to sediment regions remote of their origin. Also, the magnitude of iron and manganese reduction is not known.

The oxygen penetration depth determined how much of the potential aerobic mineralization could actually take place. The varying oxygen supply over the tidal cycle resulted in a pronounced temporal variability of areal OCR (Fig. 8). Due to the deeper oxygen penetration during inundation, between 71 to 90% of the total mineralization took place during inundation of the flat. The advective supply of oxygen may be a major factor for the pattern found in mineralization rates: due to the longer inundation time, the amount of oxygen flushed through the sediments was highest at the lower flat station and this should contribute to the high potential and areal OCR, which exceeded those recorded in the other stations (beneficial conditions for aerobes over longer time periods). The variability of areal OCR over the tidal cycle as presented in Figure 8 reflects the influence of the variable oxygen availability on total mineralization. Other factors leading to a variability of aerobic mineralization over the day such as dial rhythm of faunal activity (e.g. (Wenzhöfer & Glud 2004) were beyond the scope of this study.

Significance of pore water advection for benthic mineralization rates: filtration of organic carbon

The second reason why inundation time influences benthic mineralization rates is the supply of organic matter from the water column to the sediments. Due to the longer inundation time in the lower station, more organic matter from the water column can reach the sediments at the lower flat station. The inundation-coupled filtration and sedimentation time along the transect may explain the low sedimentary TOC and DOC content in the upper station. Further, OCR and SRR increased upon the addition of dissolved organic carbon. Thus, the decreasing supply of organic matter due to decreasing inundation times along the transect may significantly contribute to the pattern found in the benthic mineralization rates. The differences in mineralization rates between stations were most pronounced for SRR. Sulfate was not limiting and similar between stations, thus our data indicate an increasing limitation of SRR by suitable organic substances towards the upper flat. The low SRR and the low absolute increase of SRR after acetate addition at the upper flat point to a low abundance of sulfate reducing bacteria (SRB). The environmental conditions for SRB must, therefore, be unfavourable over long time periods, preventing the development of SRB. For OCR, differences between sites were less pronounced as for SRR, which may be explained by a variety of factors. The organic material at the upper station may be more refractory and thus aerobic mineralization may be faster as anaerobic mineralization (Hulthe et al. 1998, Kristensen & Holmer 2001). There may be an increasing contribution of meio- and macrofauna to the utilization of oxygen towards the upper flat stations, as highest abundances of meio- and macrofauna were found at the middle and upper intertidal flat at the Hausstrand (Armonies & Hellwig-Armonies 1987).

The increase of mineralization rates in parallel with inundation time (i.e., time of pore water advection) point towards the importance of pore water advection for benthic mineralization. However, our estimation on bottom water filtration rates indicates that the organic matter supply through bottom water filtration cannot solely explain the magnitude of benthic mineralization rates (Table 2 and 4). As the stoichiometry of organic carbon oxidation is roughly 1 mol C-org: 1 mol O_2, the results suggest that in the summer months areal OCR at the respective sites are more than 4 to 8 times higher (up to 38 times higher, when calculated from chlorophyll *a*) than the amount of infiltrated organic matter. One reason for the relatively small estimated contribution of pore water advection to the required organic carbon is that the simple model used to

calculate bottom water filtration rates underestimates the actual amount of filtrated water. The concept behind the estimation is that the oxygen penetration depth is controlled by the balance between a vertical downward transport of oxygen and the sedimentary oxygen consumption rates. For permeable sediments this is a strong simplification as the flow of filtered water through the sediments follows a more curved path between in- and outflow areas and these horizontal flow components are neglected in the chosen approach. The more U-shaped flow path means that in the upper sediment layers the oxygen entering the sediments will leave it before it is used, and this infiltrated water volume is not comprised in the estimation. Particulates, however, transported by the same water bodies, will efficiently be trapped and subsequently be transported deeper in the sediment, e.g. by bioturbation (Krantzberg 1985) or wave-driven sediment reworking. Thus, the bottom water filtration rates calculated from oxygen supply are underestimated because the solute oxygen behaves differently than the particulate organic carbon. However, a suitable modelling of pore water advection rates is still missing (Boudreau et al. 2001). An indication that our bottom water filtration rates are a reasonable approximation, is that the rates are in line with other studies (Precht & Huettel 2003, Precht & Huettel 2004).

The misfit of respired to filtered organic carbon may also indicate that other processes than pore water advection are significant sources for organic carbon at the intertidal flat. These may be gravitational sedimentation, benthic photosynthesis and transport of organic matter from the water column by filter feeding macrofauna. Benthic photosynthesis may be of major importance for the supply of organic matter in permeable sediments. At the middle flat, benthic photosynthesis supplied organic material in the order of 35 to 50 mmol C m^{-2} d^{-1} (net rates) in the summer and autumn (De Beer et al. 2005, Billerbeck, unpublished data). Thus, ca. 50% of the organic carbon used in benthic mineralization could be provided by benthic photosynthesis. On a nearby sublittoral station, the sands were found to be net-autotrophic and photosynthesis rates even increased with increasing pore water advection rates (P. Cook, unpublished data). However, more measurements are needed that compare patterns of benthic photosynthesis with patterns of benthic mineralization rates. Generally low abundances of macrofauna and the decrease of macrofaunal abundance towards the low water line (Armonies & Hellwig-Armonies 1987) may suggest that faunal transport of organic matter from overlying water to the sediments is not the dominant source of organic carbon at the investigation site. Other sources for organic material such as terrestrial-,

groundwater- or eolic fluxes may be of minor importance for the pattern and magnitude found in benthic mineralization rates in surface sediments, e.g. a groundwater inflow was not detected in the surface sediments.

The input of organic material form the water column or from the top sediment layer by photosynthesis is reflected in the depth distribution of the potential OCR and SRR. In some measurements peaking pOCR were found above the pSRR peaks (Fig. 7 and 10). Highest pSRR where often measured at the interface of oxygenated and anoxic sediment layers, i.e., in an almost anoxic zone where the supply of organic carbon from above was maximal. Most sedimentary bacteria are attached to sand grains, thus a horizontal stratification of microbial populations in the top sediment layers was not expected due to the regular reworking of sediments by migrating ripples and bioturbation. Our results indicate, nevertheless, that a zonation of pOCR and pSRR can establish.

Significance of pore water advection for the distribution of pore water nutrients

The low concentrations of ammonium, phosphate and silicate in the upper sediment layers nutrients indicate an uptake by organisms, the removal by pore water advection and oxidation processes. Over the tidal cycle, no differences in pore water nutrient concentrations were found. This is in contrast to previous findings (Rocha 1998), where increasing pore water ammonium concentrations during exposure were observed. At our study site the missing contrast in pore water solute concentrations between inundation and exposure time may be caused by the reduced mineralization rates during exposure and ensuing slow nutrient concentration build-up. Also, diatoms and other autotrophic organisms are able to accumulate and store nutrients as soon as they become available. Below 3 to 5 cm sediment depth the pore water nutrient concentrations increased. The higher nutrient concentration found below 3 to 5 cm at the lower flat station may be supported by the pore water drainage flow during exposure, that was directed towards the low water line. During this transport organic matter may become further mineralised and end products can accumulate in the pore water below the regularly flushed sediment layer, as found for another intertidal flat (Billerbeck, unpublished). The elevated nutrient concentrations may stimulate mineralization rates and photosynthesis at the lower station, thus additionally supporting higher mineralization rates at the lower flat station.

The measurements of the electron acceptor nitrate showed unreliable results. Anaerobic processes like nitrate reduction can be of major important in sediments (Canfield et al. 1993a, Canfield et al. 1993b) and may be of special importance in permeable sediments due to the dynamic oxygen distribution. We could not clarify whether the measurements are artefacts caused by the pore water extraction procedure (e.g., due to ammonium oxidation), a result from the interfering substances during analysis or whether they represent the real situation (caused, e.g., by pore water advection and faunal activity). High nitrate concentrations have been measured in other permeable sediments down to 15 cm depth (e.g. (Ehrenhauss et al. 2004), however, in situ measurements with nitrate biosensors are necessary to clarify the results.

Seasonal pattern of mineralization rates and oxygen distribution

As reported by numerous studies, benthic mineralization rates vary in the sediments of the Wadden Sea over the year due to a direct stimulation of chemical and biological processes by temperature and due to a variation of the organic matter load in the water column (Kristensen et al. 1997). Our results support these observations, as OCR, aerobic mineralization and SRR were highest in the warmer months. From the two summer months, June had lower mineralization rates, which can be explained by the lower ambient temperatures and the low carbon content in the overlying water column. At the upper flat, however, SRR did not vary over season, stressing the limitation of SRR by organic matter at this station. In April measurements were preceded by the spring bloom (van Beusekom, unpublished data). The high load of easily degradable organic carbon promoted OCR in April, which were comparable to OCR measured in summer, although temperatures were still lower. The response of SRR seems to be more delayed, as SRR in April showed only a small peak in the upper sediment layer but was generally still low.

Although hydrodynamics were comparable between summer and winter (Fig. 4), oxygen penetrated deeper in winter than in summer, due to increased oxygen solubility and reduced sedimentary pOCR. The low areal OCR during winter show that the deeper penetration of oxygen could not compensate the lower volumetric pOCR.

Lower temperatures and lower pOCR may explain the in comparison to the other stations deeper oxygen penetration depths at the lower flat station in April. The oxygen distribution measurements at the lower flat were conducted first within the

campaign, at the outset of the spring bloom and 3 to 4°C lower ambient temperatures as compared to the remaining time of the campaign.

Conclusions

Our results stress the overall importance of pore water advection for benthic mineralization rates. We found highest areal and volumetric OCR and SRR at the lower flat station, were the inundation time and thus the exposure time of the sediments to pore water advection were longest. The advective supply of oxygen shifted total benthic mineralization towards aerobic processes. It is likely that this advective effect is not restricted to the intertidal but extends to the shallow shelf where permeable beds permit flushing of the upper sediment layer (Marinelli et al. 1998, Jahnke et al. 2000, Reimers et al. 2004). The importance of oxygen supply by pore water advection for total benthic mineralization was reflected in the elevated OCR during inundation as compared to exposure time of the sand flat. However, the contribution of organic matter supply by pore water advection for total benthic mineralization remains to be investigated. The high benthic mineralization rates emphasize the importance of sands for the coastal marine carbon cycle.

ACKNOWLEDGEMENTS

We thank Martina Alisch, Christiane Hüerkamp and Kyriakos Vamvakopoulos for the support at the cruises. Gabriele Eikert, Ines Schröder, Karin Hohman, Ingrid Dohrmann, and Cäcilia Wiegand are thanked for making the sensors and their help. Volker Meyer, Paul Färber, Harald Osmers, Alfred Kutsche and Georg Herz are acknowledged for the technical help. A big thank goes to the staff of the Wadden Sea Station on Sylt (Alfred Wegener Institute), for their support and great hospitality. Thomas Krieger of Wasser- und Schifffahrtsamt Tönning - Gewässerkunde- for the friendly permission of Sylt tide gauge data. This study was financed by the Max Planck Society (MPG), Germany.

LITERATURE CITED

Aller R. C. (2001) Transport and reactions in the bioirrgated zone. In: Boudreau B. P., Jørgensen B. B. (eds) The benthic boundary layer. Oxford University Press, p 269-301

Armonies W., Hellwigarmonies M. (1987) Synoptic patterns of meiofaunal and macrofaunal abundances and specific composition in littoral sediments. Helgol. Meeresunters. 41:83-111

Berninger U. G., Huettel M. (1997) Impact of flow on oxygen dynamics in photosynthetically active sediments. Aquat. Microb. Ecol. 12:291-302

Boudreau B., Huettel M., Forster R., Jahnke A., McLachlan J., Middelburg J., Nielsen P., Sansone F., Taghon G., Van Raaphorst W., Webster I., Weslawski J., Wiberg P., Sundby B. (2001) Permeable marine sediments: Overturning an old paradigm. EOS,Trans. AGU 82:133-136

Brotas V., Amorimferreira A., Vale C., Catarino F. (1990) Oxygen profiles in intertidal sediments of ria formosa (s portugal). Hydrobiologia 207:123-129

Cammen L. M. (1991) Annual bacterial production in relation to benthic microalgal production and sediment oxygen-uptake in an intertidal sandflat and an intertidal mudflat. Mar. Ecol.-Prog. Ser. 71:13-25

Canfield D. E., Jørgensen B. B., Fossing H., Glud R., Gundersen J., Ramsing N. B., Thamdrup B., Hansen J. W., Nielsen L. P., Hall P. O. J. (1993a) Pathways of organic-carbon oxidation in three continental-margin sediments. Mar. Geol. 113:27-40

Canfield D. E., Thamdrup B., Hansen J. W. (1993b) The anaerobic degradation of organic-matter in danish coastal sediments - iron reduction, manganese reduction, and sulfate reduction. Geochim. Cosmochim. Acta 57:3867-3883

D'Andrea A. F., Aller R. C., Lopez G. R. (2002) Organic matter flux and reactivity on a south carolina sandflat: The impacts of porewater advection and macrobiological structures. Limnol. Oceanogr. 47:1056-1070

Darcy H. (1856) Les fontaines publiques de la ville de dijon. Dalmont, Paris

de Beer D., Wenzhoefer F., Ferdelman T. G., Boehme S. E., Huettel M., van Beusekom J. E. E., Boettcher M. E., Musat N., Dubillier N. (2005) Transport and mineralization rates in north sea sandy intertidal sediments, sylt-rømø basin, wadden sea. Limnol. Oceanogr. 50:113-127

Ehrenhauss S., Huettel M. (2004) Advective transport and decomposition of chain-forming planktonic diatoms in permeable sediments. J. Sea Res. 52:179-197

Ehrenhauss S., Witte U., Janssen F., Huettel M. (2004) Decomposition of diatoms and nutrient dynamics in permeable north sea sediments. Cont. Shelf Res. 24:721-737

Forster S., Huettel M., Ziebis W. (1996) Impact of boundary layer flow velocity on oxygen utilisation in coastal sediments. Mar. Ecol.-Prog. Ser. 143:173-185

Glud R. N., Klimant I., Holst G., Kohls O., Meyer V., Kuhl M., Gundersen J. K. (1999) Adaptation, test and in situ measurements with o-2 microopt(r)odes on benthic landers. Deep-Sea Res. Part I-Oceanogr. Res. Pap. 46:171-183

Grasshoff K., Kremling K., Ehrhardt M. (1999) Methods of seawater analysis. Wiley-VCH Verlag

Huettel M., Gust G. (1992) Impact of bioroughness on interfacial solute exchange in permeable sediments. Mar. Ecol.-Prog. Ser. 89:253-267

Huettel M., Rusch A. (2000) Transport and degradation of phytoplankton in permeable sediment. Limnol. Oceanogr. 45:534-549

Huettel M., Ziebis W., Forster S., Luther G. W. (1998) Advective transport affecting metal and nutrient distributions and interfacial fluxes in permeable sediments. Geochim. Cosmochim. Acta 62:613-631

Hulthe G., Hulth S., Hall P. O. J. (1998) Effect of oxygen on degradation rate of refractory and labile organic matter in continental margin sediments. Geochim. Cosmochim. Acta 62:1319-1328

Jahnke R. A., Nelson J. R., Marinelli R. L., Eckman J. E. (2000) Benthic flux of biogenic elements on the southeastern us continental shelf: Influence of pore water advective transport and benthic microalgae. Cont. Shelf Res. 20:109-127

Jørgensen B. B. (1977) Bacterial sulfate reduction within reduced microniches of oxidized marine-sediments. Mar. Biol. 41:7-17

Jørgensen B. B. (1978) Comparison of methods for the quantification of bacterial sulfate reduction in coastal marine-sediments .1. Measurement with radiotracer techniques. Geomicrobiology Journal 1:11-27

Jørgensen B. B. (1982) Mineralization of organic-matter in the sea bed - the role of sulfate reduction. Nature 296:643-645

Jørgensen B. B., Bak F. (1991) Pathways and microbiology of thiosulfate transformations and sulfate reduction in a marine sediment (kattegat, denmark). Appl. Environ. Microbiol. 57:847-856

Kallmeyer J., Ferdelman T. G., Weber A., Fossing H., Jørgensen B. B. (2004) A cold chromium distillation procedure for radiolabeled sulfide applied to sulfate reduction measurements. Limnol. Oceanogr.: Methods. 2:171-180

Klute A., Dirksen C. (1986) Hydraulic conductivity and diffusivity: Laboratory methods. In: Klute A. (ed) Method of soil analysis - part 1 - physical and mineralogical methods., 2 nd edn. American Society of Agronomy, p 687 ff

Krantzberg G. (1985) The influence of bioturbation on physical, chemical and biological parameters in aquatic environments - a review. Environmental Pollution Series a-Ecological and Biological 39:99-122

Kristensen E., Holmer M. (2001) Decomposition of plant materials in marine sediment exposed to different electron accepters (o-2, no3-, and so42-), with emphasis on substrate origin, degradation kinetics, and the role of bioturbation. Geochim. Cosmochim. Acta 65:419-433

Kristensen E., Jensen M. H., Jensen K. M. (1997) Temporal variations in microbenthic metabolism and inorganic nitrogen fluxes in sandy and muddy sediments of a tidally dominated bay in the northern wadden sea. Helgol. Meeresunters. 51:295-320

Marinelli R. L., Jahnke R. A., Craven D. B., Nelson J. R., Eckman J. E. (1998) Sediment nutrient dynamics on the south atlantic bight continental shelf. Limnol. Oceanogr. 43:1305-1320

Nielsen P. (1990) Tidal dynamics of the water-table in beaches. Water Resour. Res. 26:2127-2134

Polerecky L., Franke U., Werner U., Grunwald B., de Beer D. (2005) High spatial resolution measurement of oxygen consumption rates in permeable sediments. Limnol. Oceanogr.: Methods 3:75-85

Precht E., Franke U., Polerecky L., Huettel M. (2004) Oxygen dynamics in permeable sediments with wave-driven pore water exchange. Limnol. Oceanogr. 49:693-705

Precht E., Huettel M. (2003) Advective pore-water exchange driven by surface gravity waves and its ecological implications. Limnol. Oceanogr. 48:1674-1684

Precht E., Huettel M. (2004) Rapid wave-driven advective pore water exchange in a permeable coastal sediment. J. Sea Res. 51:93-107

Reimers C. E., Stecher H. A., Taghon G. L., Fuller C. M., Huettel M., Rusch A., Ryckelynck N., Wild C. (2004) In situ measurements of advective solute transport in permeable shelf sands. Cont. Shelf Res. 24:183-201

Revsbech N. P. (1989) An oxygen microsensor with a guard cathode. Limnol. Oceanogr. 34:474-478

Revsbech N. P., Jørgensen B. B., Blackburn T. H. (1980) Oxygen in the sea bottom measured with a microelectrode. Science 207:1355-1356

Riedl R. J., Machan R. (1972) Hydrodynamic patterns in lotic intertidal sands and their biolimatological implications. Mar. Biol. 13:179-&

Riedl R. J., Machan R., Huang N. (1972) Subtidal pump - mechanism of interstitial water exchange by wave action. Mar. Biol. 13:210-&

Rocha C. (1998) Rhythmic ammonium regeneration and flushing in intertidal sediments of the sado estuary. Limnol. Oceanogr. 43:823-831

Rusch A., Huettel M. (2000) Advective particle transport into permeable sediments - evidence from experiments in an intertidal sandflat. Limnol. Oceanogr. 45:525-533

Shum K. T. (1992) Wave-induced advective transport below a rippled water-sediment interface. J. Geophys. Res.-Oceans 97:789-808

Shum K. T., Sundby B. (1996) Organic matter processing in continental shelf sediments - the subtidal pump revisited. Mar. Chem. 53:81-87

Thamdrup B., Hansen J. W., Jørgensen B. B. (1998) Temperature dependence of aerobic respiration in a coastal sediment. FEMS Microbiol. Ecol. 25:189-200

Thibodeaux L. J., Boyle J. D. (1987) Bedform-generated convective-transport in bottom sediment. Nature 325:341-343

Webb J. E., Theodor J. (1968) Irrigation of submerged marine sands through wave action. Nature 220:682-683

Webster I. T., Norquay S. J., Ross F. C., Wooding R. A. (1996) Solute exchange by convection within estuarine sediments. Est. Coast. Shelf Sci. 42:171-183

Wentworth C. K. (1922) A scale of grade and class terms for clastic sediments. J. Geol. 30:377-392

Wenzhofer F., Glud R. N. (2004) Small-scale spatial and temporal variability in coastal benthic o-2 dynamics: Effects of fauna activity. Limnol. Oceanogr. 49:1471-1481

Wenzhofer F., Holby O., Glud R. N., Nielsen H. K., Gundersen J. K. (2000) In situ microsensor studies of a shallow water hydrothermal vent at milos, greece. Mar. Chem. 69:43-54

Ziebis W., Huettel M., Forster S. (1996) Impact of biogenic sediment topography on oxygen fluxes in permeable seabeds. Mar. Ecol.-Prog. Ser. 140:227-237

Benthic photosynthesis in submerged Wadden Sea intertidal flats

Markus Billerbeck, Hans Røy, Katja Bosselmann and Markus Huettel

in preparation

ABSTRACT

We studied benthic photosynthesis during inundation in a coarse sand, fine sand, and mixed sand/mud intertidal flat in the German Wadden Sea. In situ determination of oxygen-, DIC- and nutrient fluxes in stirred benthic chamber incubations were combined with measurements of sedimentary chlorophyll, incident light intensity at the sea surface and scalar irradiance within the sediment. Oxygen, DIC and nutrient fluxes reflected benthic photosynthesis at all study sites. In the net autotrophic fine sand and coarse sand flats, gross photosynthesis was on average 4 and 11 times higher than in the net heterotrophic mud flat, despite higher total chlorophyll concentration in mud. Benthic photosynthesis may be enhanced in intertidal sands due to: 1) a more active microphytobenthos community due to a higher turnover of microalgal biomass in the sands. This was indicated by low phaeophytin concentrations in the sands, whereas the mud flat accumulated chlorophyll degradation products and organic matter. 2) a higher light availability within the sandy sediments as depth integrated scalar irradiance was 2 to 3 times higher in the sands than in the mud. A quick response of gross photosynthesis to changing incident light at the sea floor indicated light limitation of the microphytobenthos at all study sites, which was less severe at the sandy sites than at the mud site. 3) more efficient transport of photosynthesis-limiting solutes to the microalgae as indicated by an enhanced flushing of the permeable, sandy sediment. The advective flushing may have counteracted a possible CO_2 limitation of the microalgae in the sandy sediment.

INTRODUCTION

In the intertidal regions of the German Wadden Sea, sandy sediments are predominant, while muddy sediments are restricted to relatively narrow low energy zones close to the coastline (Flemming & Ziegler 1995). Within the intertidal ecosystem, the microphytobenthos contributes significantly to total primary production (MacIntyre et al. 1996, Underwood & Kromkamp 1999). Benthic microalgae influence oxygen and nutrient fluxes across the sediment water interface (Bartoli et al. 2003, Tyler et al. 2003), constitute an important carbon source for benthic heterotrophs (Middelburg et al. 2000, Herman et al. 2001) and can stabilize the sediment surface through the production of extracellular polymeric substances (Smith & Underwood 1998, Widdows et al. 2000, Yallop et al. 2000). Biomass, light- and CO_2 availability have been identified to determine microphytobenthic production (Admiraal et al. 1982, MacIntyre et al. 1996, Barranguet et al. 1998). Nutrients are often not a limiting factor in intertidal sediment (Barranguet et al. 1998, Serôdio & Catarino 2000, Migne et al. 2004) as the microphytobenthos can assimilate nutrients from both the overlying water and the sediment pore water (MacIntyre et al. 1996, Cahoon 1999).

Muddy sediments exhibit high rates of benthic primary production (Pomeroy 1959, Leach 1970) and tend to have a higher microphytobenthic biomass than sandy sediments (Colijn & Dijkema 1981, de Jong & de Jonge 1995). Nevertheless, primary production in intertidal sand flats can be equally high as in mud flats during low tide exposure (Barranguet et al. 1998). In the dynamic intertidal habitat, high microphytobenthic productivity can be sustained by regular resuspension events that keep the algal standing stock below the maximum carrying capacity of the system (Blanchard et al. 2001). Resuspension of benthic algae is more likely in higher energy environments like sand flats. More frequent resuspension events and higher degradation rates in sand than in mud caused a higher turnover of algal biomass in intertidal sandy sediment of the Dutch Wadden Sea (Middelburg et al. 2000). Therefore, high benthic productivity can possibly be more effectively sustained in sandy sediments than in muds.

As a result of the frequently highly turbid water near the coast, light is the principal limiting factor for primary production in the water column of the Wadden Sea (Veldhuis et al. 1988, Tillmann et al. 2000, Colijn & Cadee 2003) and may also limit benthic photosynthesis. Therefore, microphytobenthos production in intertidal sediments has been assumed to be restricted to the exposure period in several studies

(e.g. Serôdio & Catarino 2000, Guarini et al. 2002, Migne et al. 2004). Nevertheless, photosynthetic production of benthic microalgae can be sustained at low light intensities of about 5-10 µmol photons m^{-2} s^{-1} (Cahoon 1999 and references therein). Furthermore, the early studies of Cadee & Hegeman (1974) and Cadee & Hegeman (1977) suggested that benthic primary production takes place also during inundation. Asmus (1982) showed that the microphytobenthos contributed 68 % to total primary production during inundation of a sand flat in Sylt, Germany. The water is relatively clear in this area (Asmus et al. 1998) and light limitation during flooding is possibly more severe over mud flats than sand flats, as fine sediments are more easily resuspended by waves and currents. Motile benthic microalgae migrate into the sediment surface layer during inundation to prevent erosion (Janssen et al. 1999, Mitbavkar & Anil 2004) and consequentially depend on the light availability within the sediment. Light is typically more effectively absorbed in muddy sediment than in sand (Haardt & Nielsen 1980, Kühl et al. 1994). Thus, benthic microalgae in sand flats may profit from a higher light availability within the sediment as compared to the microphytobenthos in mudflats.

The production of benthic microalgae can be limited by CO_2 availability (Admiraal et al. 1982, Rasmussen et al. 1983). Intense CO_2 assimilation of microphytobenthos can result in pH values above 9 within the photic zone of the sediment (Revsbech & Jørgensen 1986) and reduced free CO_2 concentrations limiting primary production (Rasmussen et al. 1983, Cook & Røy in press). Recent laboratory and field studies suggest that this CO_2 limitation can be relieved by increased advective flushing of the photic zone (Wenzhöfer et al. in preparation, Cook & Røy in press).

We hypothesize that during inundation, benthic photosynthesis may be enhanced in intertidal sand flats as compared to mud flats due to a more active metabolic state of the microalgal community, higher light availability and more efficient relieve of CO_2 limitation in sandy sediment. We tested this hypothesis by conducting light and dark incubations with stirred benthic chambers in coarse, fine, and mixed sand/mud intertidal sediments of the German Wadden Sea. Interpretations of the flux recordings were supported by concurrent measurements of sedimentary chlorophyll, in situ incident light intensity and scalar irradiance within the sediment.

METHODS

Study sites

In situ measurements and sampling were carried out at two intertidal sand flats and one mixed sand/mud flat in the German Wadden Sea (Fig. 1). The coarse sand site is located on the sand flat "Hausstrand" (55° 00` 53`` N, 008° 26` 17`` E) at List on the island of Sylt. The fine sand site is located on the intertidal flat "Janssand" (53° 44`07`` N, 007° 41` 57`` E) and the mixed flat (53° 42` 09`` N, 007° 42` 33`` E) is situated near the harbour of Neuharlingersiel in the backbarrier area of the island of Spiekeroog.

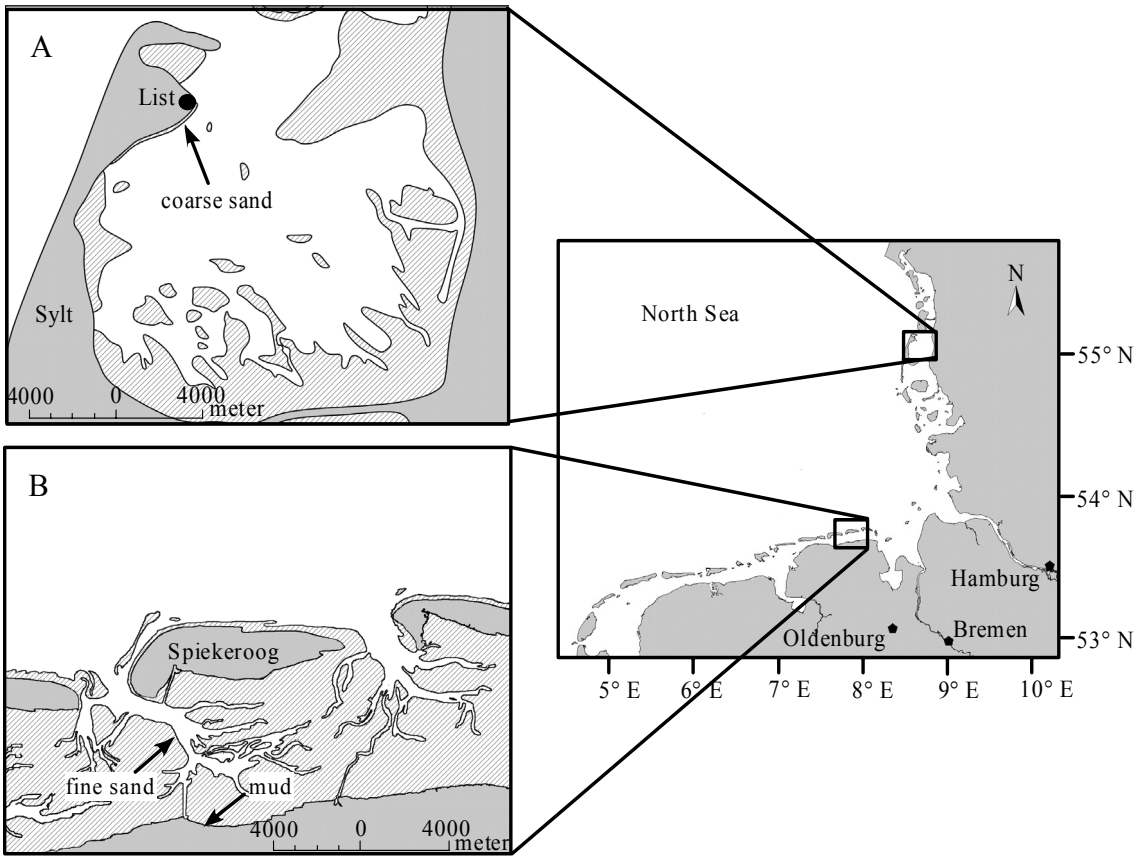

Figure 1: (A) The coarse sand, (B) fine sand and mixed sand /mud intertidal study sites in the German Wadden Sea

Henceforth, the Sylt, Janssand and Neuharlingersiel sites are denoted as coarse sand, fine sand and mud, respectively. During high tide, the coarse sand and fine sand sites are covered by 1.5-2 m of water, the mud site by 1-1.5 m of water. The study sites were investigated during Spring, Summer and Autumn 2002, and Summer 2003 (Table 1). In situ measurements with benthic chambers were not possible during Winter due to frozen sediments and adverse weather conditions.

Table 1: Sampling and in situ benthic chamber incubations during the measurement campaigns at the 3 study sites. Numbers denote replicate measurements (dark/light incubations for benthic chambers).

Campaigns	Sediment parameters			Benthic chambers				
Coarse sand	Permeability	TOC	Chlorophyll	Oxygen	DIC	Nutrients	Br^- tracer	Incident light
Spring 2002	12	13	4	5/4	2/2	4/4		1
16./17.04.02				Optodes				only 17.4.
Summer 2002	15	13	4	4/2		4/2	5	1
18./22.08.02				Winkler				
Fine sand								
Spring 2002		10		3/2	2/2	2/2		
13.03.02				Optodes				
Summer 2002	9	10	4	2/2		2/2	5	1
07.06.2002				Winkler				
Autumn 2002		10	2	5/4	3/2	4/2	5	1
25./26.09.02				Optodes				
Summer 2003	6	8	2	3/3	3/3	3/3	2	1
29.07.2003				Optodes				
Mud								
Spring 2002	3	10	4	2/2		2/1	2	
04.04.2002			top 0-5 cm	Winkler				
Summer 2002		8	4	2/2		2/2	4	1
19.06.2002				Winkler				
Autumn 2002		8	2	3/2		2/1		1
30.09.2002				Optodes				
Summer 2003		8	2	3/2	2/2	2/2		1
02.08.2003				Optodes				

Sediment characteristics

Grain size was analyzed by dry-sieving the top 10 cm of the sediment and classified according to Wentworth (1922). Permeability was determined with the constant head method (Klute & Dirksen 1986) for the top 15 cm of the sediment at the two sandy sites and for the top 4 cm at the mud site. Sediment samples for total carbon (TC) and total inorganic carbon (TIC) measurements were sectioned into 1 cm intervals and stored frozen.

Chlorophyll analysis

For the measurement of chlorophyll, the top 10 cm of the sediment at the two sandy sites were sectioned in 0.5 cm intervals down to 5 cm depth and in 1 cm intervals below. At the mud site, the top 5 cm of the sediment were sectioned in 0.2 - 0.5 cm intervals down to 2 cm depth and in 0.5 cm intervals below. During Spring 2002, the upper 5 cm of the sediment at the mud site were pooled. All sediment samples for chlorophyll analysis were kept frozen and dark until analysis.

Light measurements in the sediment

A microsensor for scalar irradiance measurement was prepared by placing a 70 µm spherical diffuser on the tapered tip of a 100 µm optical glass fibre (Kühl & Jørgensen 1992). The same sensor was used for all profiles and connected to a photo-multiplier tube with custom support electronic. Light profiles within the sediment were measured in the laboratory in sediment cores (36 mm diameter) from all study sites. The sediment surface was uniformly illuminated with two white light sources placed opposite from each other at 20-degree zenith angle. The light intensity within the sediment is given normalized to the incident irradiance.

Benthic chamber incubations

In situ incubations with cylindrical benthic chambers (19 cm inner diameter) were conducted to measure fluxes of oxygen, DIC and nutrients across the sediment water interface. Two transparent and two opaque chambers were used in one or two deployments (Table 1) at each study site. During Summer 2003, 3 transparent and 3 opaque chambers were used. The stirring of the chamber water by a rotating disc (15 cm diameter) at 20 rpm induces advective flow through the surface layer of permeable sediment (Huettel & Gust 1992a). During low tide, the chambers were placed onto the respective sediment, with the walls of the chambers penetrating down to a sediment depth of 19 cm. After inundation, the chambers were sealed with transparent or opaque lids, each enclosing a water volume of 3.4 L and a sediment area of 0.028 m². Twenty ml of a 3 mol L^{-1} NaBr inert tracer solution was then injected into each chamber for the assessment of the advective fluid exchange between enclosed sediment and overlying water (Forster et al. 1999). During most incubations (see Table 1), the oxygen concentration inside each chamber was monitored every 2 minutes for 20 seconds with fibre optic optodes inserted through the chamber lid. For oxygen, nutrient and DIC analysis, a total of 80 – 140 ml volume of chamber water was sampled in 0.5 - 1 h intervals via a flexible tube (15 ml volume) that was fastened above the maximum water level and attached to a sampling port on the chamber lid. The first 20 ml of each sample was discarded to account for the sampling tube volume. The sampled water was replaced with ambient sea water via a second port in the chamber lid. Additionally, samples of ambient sea water were taken at each sampling interval. Samples for nutrient analysis were filtered through 0.2 µm nylon syringe filters into plastic vials and kept frozen until analysis. DIC samples were stored without headspace in glass vials and

preserved with a saturated mercury chloride solution (end concentration 0.01 %) in a refrigerator until analyzed in the laboratory. At the end of the chamber incubations, with the water level still above the chambers, sediment cores were retrieved with cut off 60 ml syringes for bromide tracer analysis. The sediment cores were sliced in 0.5 cm intervals (0.2 cm intervals at the mud site) within 30 minutes after retrieval and kept frozen. Incident light at the sediment surface during the chamber incubations was measured with an Onset® photometric light logger that was sealed watertight into a transparent acrylic tube and positioned close to the sea floor (Table 1). The data, logged in lumen m^{-2}, were transformed into µmol Quanta m^{-2} s^{-1} by calibrating the light logger within the acrylic tube against a Licor® LI-250A quantum light meter in the laboratory.

Analytical procedures

The sediment samples for TC and TIC analysis were freeze-dried and ground in the laboratory. Sample aliquots were then transferred into tin-cups for TC measurements and analysed with a Heraeus CHNO-rapid elemental analyzer using sulfanilamide as a calibration standard. TIC sample aliquots were measured by coulometric titration on a UIC CM5012 and TOC was calculated by subtracting TIC from TC. Pigments were extracted in the laboratory by sonification of sediment subsamples in 10 ml 90% acetone and subsequent measurement of the supernatant on a Shimadzu® UV-160 A spectrophotometer before and after acidification. Phaeogigment concentrations were then calculated according to Lorenzen (1967). Because concentrations of chlorophyll degradation products were very low at the two sandy sites and in some cases produced erroneous results when used for the calculation of chlorophyll *a*, pigment concentrations were given as total chlorophyll (absorption at 665 nm without acidification) for all study sites. For the analysis of bromide, the pore water of the sediment samples was extracted by centrifugation and 100 µl of the pore water then analyzed by ion chromatography with a Waters anion-exchange column, using NaBr as a standard for calibration. Nutrient analysis of silicate, phosphate, ammonium, nitrate, and nitrite were performed spectrophotometrically with a Skalar® Continuous-Flow-Analyzer according to Grasshoff et al. (1999). In the following, NOx fluxes denote the sum of nitrate and nitrite fluxes. Chamber water DIC was determined in the laboratory by flow injection analysis using freshly prepared $NaHCO_3$ calibration standards (Hall & Aller 1992). In Summer 2003, DIC was measured by coulometric titration on a UIC® CM5012. Oxygen concentrations of the chamber water were

determined by Winkler titration and used for calibration of the chamber oxygen optodes (Klimant et al. 1995, Holst et al. 1997). The dilution of the chamber waters due to the sampling was corrected by adding the difference of the solute inventory between the sampled and replaced volume to the chamber volume solute inventory. As linear regression of the concentration changes over time was sometimes not satisfactory, all solute fluxes are given as calculated from start and end concentrations (lowest end concentration for oxygen was 46 μmol L^{-1} in mud incubations).

RESULTS

Sediment characteristics

Sedimentary parameters are presented in Table 2. At the coarse and fine sand sites, the mud fraction (< 63 µm) was below 0.2 %, while reaching 12.5 % at the mixed sand/mud site. As a consequence, the sediment was highly permeable at the coarse sand, permeable at the fine sand and almost impermeable at the mud site (Table 2). The sandy sites were organic poor with TOC contents of 0.1 % or less in the upper 10 cm of the sediment, whereas the TOC content ranged between 0.5 and 0.7% at the mud flat (Table 2).

Table 2: Sediment parameters, permeability (top 15 cm at sandy sites, top 4 cm at mud site) and percentage of TOC per sediment weight (top 10 cm) at the 3 study sites. The standard deviation (n = 3-15 for permeability, n = 8-11 for TOC) is given in parentheses.

	coarse sand	fine sand	mud
Median grain size (µm)	380	176	139
Sorting	very well	well	moderately
Permeability (m²)			
Spring 2002	4.0×10^{-11} (0.3)		6.0×10^{-14} (0.2)
Summer 2002	3.9×10^{-11} (0.3)	9.0×10^{-12} (0.8)	
Autumn 2002			
Summer 2003		7.2×10^{-12} (0.6)	
TOC (%)			
Spring 2002	0.06 (0.02)	0.05 (0.02)	0.71 (0.28)
Summer 2002	0.08 (0.04)	0.06 (0.01)	0.51 (0.08)
Autumn 2002		0.06 (0.02)	0.52 (0.12)
Summer 2003		0.08 (0.03)	0.56 (0.10)

Tracer transport

The stirring of the benthic chambers generated an advective flushing of the upper sediment layer. Reflecting the different permeabilities at the 3 study sites, the tracer was transported down to a sediment depth of 7.0 cm (SD ± 1.6, n = 5) in the coarse sand, 2.3 cm (SD ± 0.5, n = 12) in the fine sand and 1.3 cm (SD ± 0.4, n = 6) at the mud site.

Light availability in the sediment

Light distributions within the sediment of the 3 study sites are shown in Fig. 2. The increase above the sediment surface of the coarse and fine sand is due to reflection by the quartz sand. The irradiance peak below the surface is due to multiple scattering within the sediment. These features are less pronounced at the mud site due to less reflection and higher light absorption of the mud. The depth integrated scalar irradiance is factor 3.45 higher in the coarse sand and factor 2.04 higher in the fine sand than in the mud.

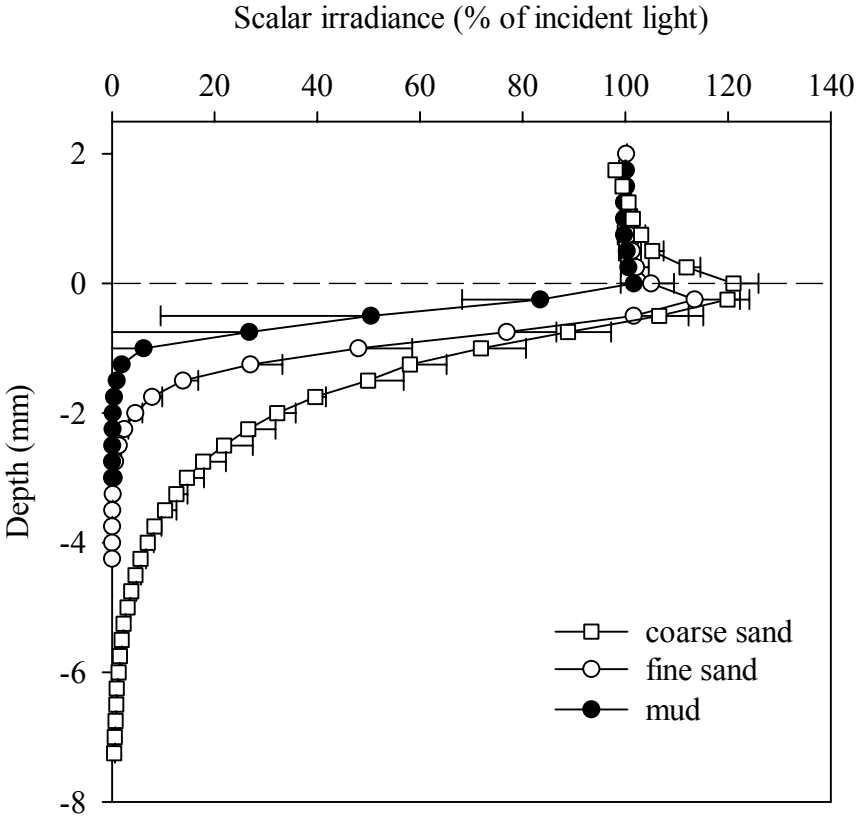

Figure 2: Depth profiles of scalar irradiance normalized to incident light at the coarse sand, fine sand and mud site. Error bars indicate standard deviation of 3 to 6 measurements.

Sediment total chlorophyll

Total chlorophyll concentrations decreased with sediment depth at the 3 study sites and were generally higher at the muddy site than at the two sandy sites (Fig. 3). Total chlorophyll in the uppermost cm of the sediment was on average 185 mg m^{-2} (range 176-194 mg m^{-2}) in the coarse sand, 150 mg m^{-2} (range 134-172 mg m^{-2}) in the fine sand and 291 mg m^{-2} (194-356 mg m^{-2}) in the mud during the study seasons. At the two sandy sites, phaeophytin was never detectable in the top 3 cm and did not exceed

10 % of the total chlorophyll below. At the mud site, phaeophytin was present at all sediment depths reaching up to 18 % of total chlorophyll in the uppermost cm of the sediment and up to 38 % below.

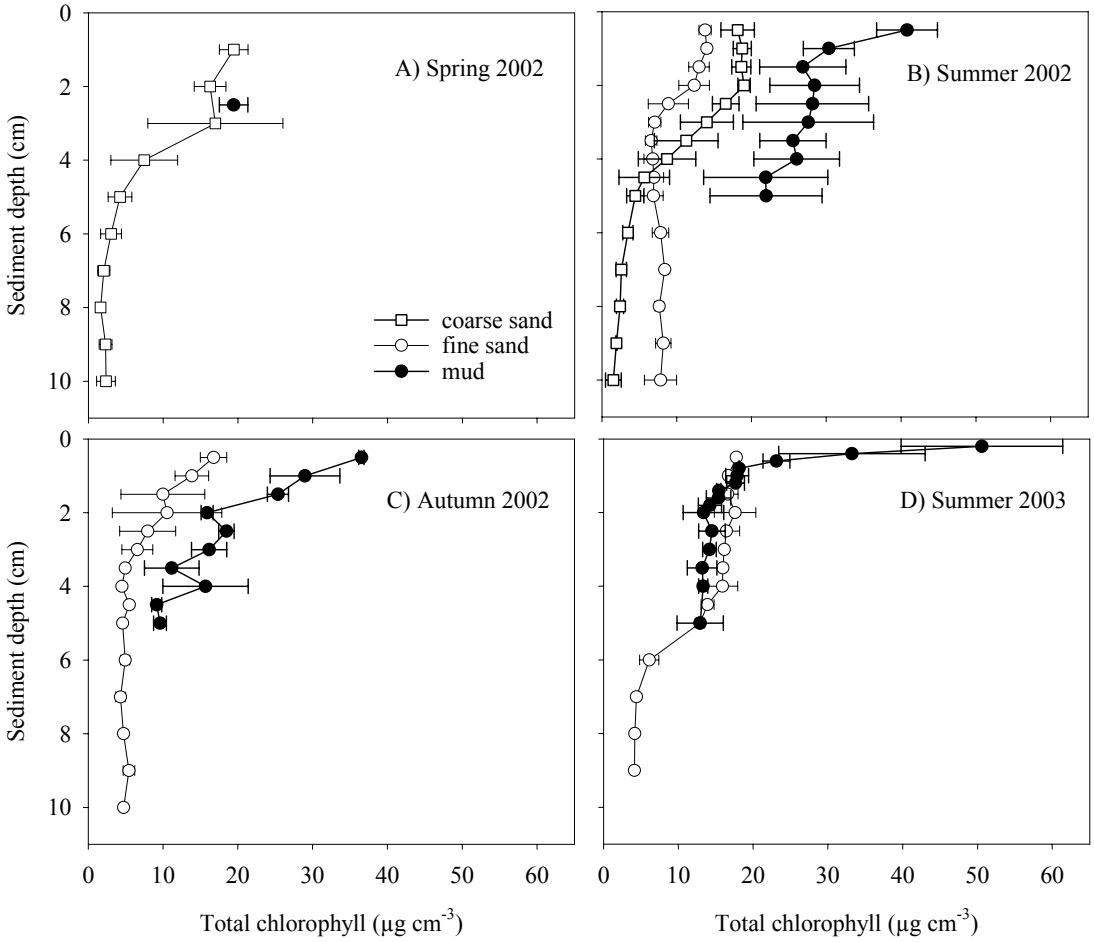

Figure 3: Total chlorophyll concentration of the sediment at the study sites (µg cm^{-3}) with the standard deviation (n = 2-4) as error bars.

Oxygen and DIC fluxes

Benthic photosynthesis during inundation was measured at all stations during all seasons as reflected in the oxygen and DIC fluxes (Fig 4). Despite the higher total chlorophyll concentrations in the upper sediment layer of the mud site, areal gross photosynthesis was about 4-fold higher in the fine sand and 10-fold higher in the coarse sand than at the mud site (Table 3). Figure 5 shows the direct response of areal gross photosynthesis rates to the changing incident light regime at all study sites. During Summer 2002, areal gross photosynthesis rates in the coarse sand were much higher than those in the fine sand and mud, despite similar or even lower in situ photon flux at the coarse sand site compared to the two other sites (Fig. 5).

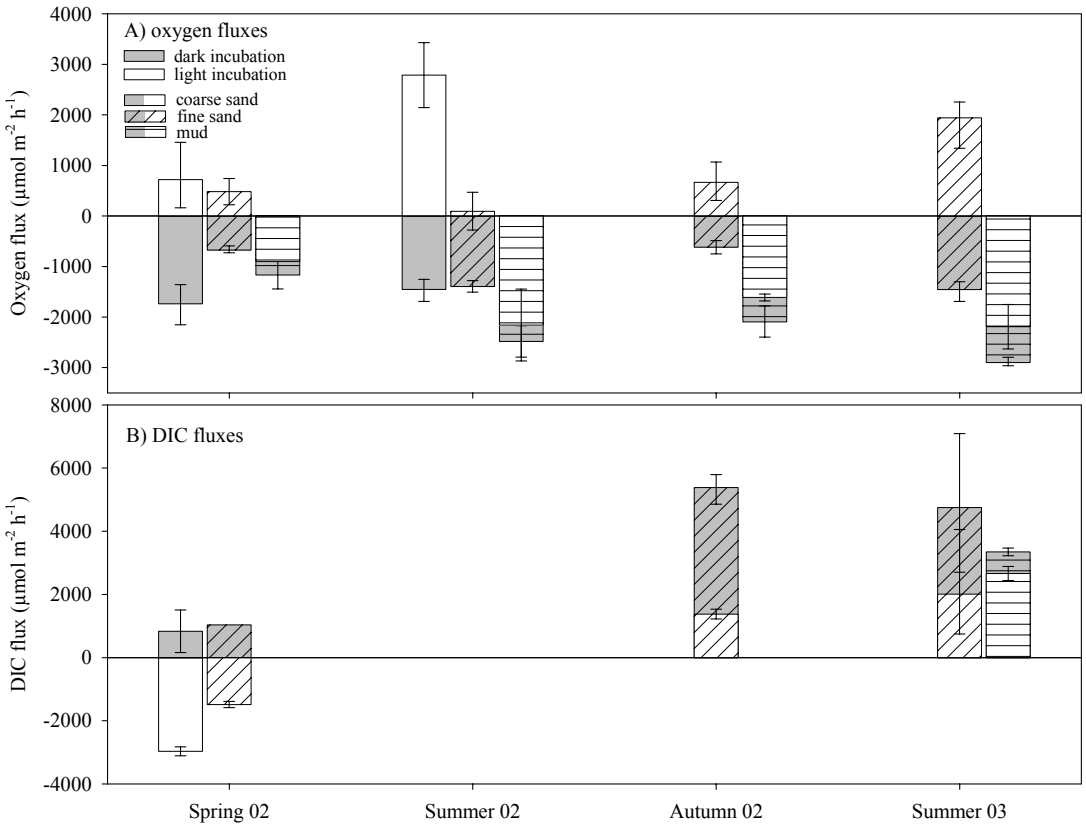

Figure 4: Average benthic chamber fluxes of (A) oxygen and (B) DIC at the 3 study sites with range as error bars. Negative and positive values denote influx and efflux via the sediment surface, respectively.

The high photosynthetic activity at the two sandy study sites led to an efflux of oxygen during daytime inundation, whereas the oxygen produced at the mud site was completely consumed within the sediment (Fig. 4A). Production in the water column measured with in situ bottle incubations during July 2003 at the fine sand and mud sites was less than 3 % of the benthic production.

Table 3: Net oxygen and DIC fluxes in µmol m^{-2} h^{-1} in dark and light incubations at the 3 study sites and calculated gross photosynthetic production of oxygen and consumption of DIC (GP). Negative and positive values denote influx and efflux via the sediment surface, respectively.

	coarse sand			fine sand			mud		
Oxygen	dark	light	GP	dark	light	GP	dark	light	GP
Spring 2002	-1737	718	2455	-676	482	1158	-1169	-903	266
Summer 2002	-1453	2788	4241	-1394	94	1488	-2483	-2159	325
Autumn 2002				-617	668	1284	-2098	-1613	485
Summer 2003				-1456	1942	3398	-2901	-2191	710
DIC									
Spring 2002	834	-2968	-3803	1035	-1486	-2521			
Summer 2002									
Autumn 2002				5499	1534	-3965			
Summer 2003				4751	2008	-2743	3350	2665	-684

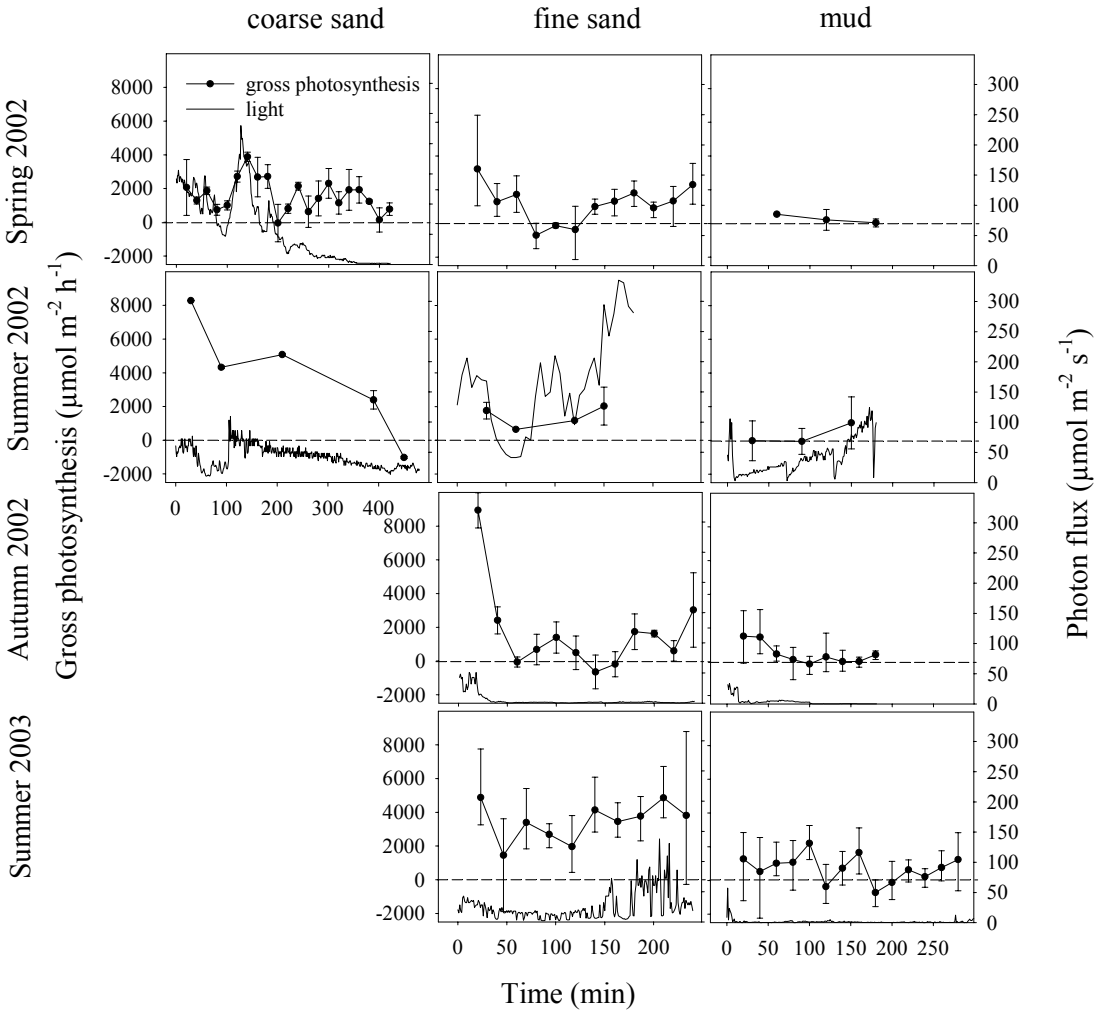

Figure 5: Average gross photosynthesis (µmol m^{-2} h^{-1}) calculated from dark and light chamber incubations and in situ photon flux (µmol m^{-2} s^{-1}) at the 3 study sites. Error bars denote minimum and maximum estimates of gross photosynthesis. Dashed lines denote zero gross photosynthesis.

Nutrient fluxes

Benthic photosynthesis affected the chamber nutrient fluxes (Fig. 6). While phosphate and ammonium were generally released from the sediment in the dark incubations, the light chamber fluxes indicated an uptake of inorganic nutrients by the microphytobenthos. Silicate was released in the dark incubations at all sites and the light fluxes indicated photosynthetic assimilation of silicate in the fine sand (data not shown). Nitrate + nitrite (NOx) was usually taken up by the sediment in both dark and light incubations during all months at the two sandy sites (Fig. 6C). An efflux of NOx was recorded in the dark incubations during Spring and Autumn at the mud site. There was no apparent causal connection between benthic photosynthesis and chamber NOx fluxes (Fig. 6C).

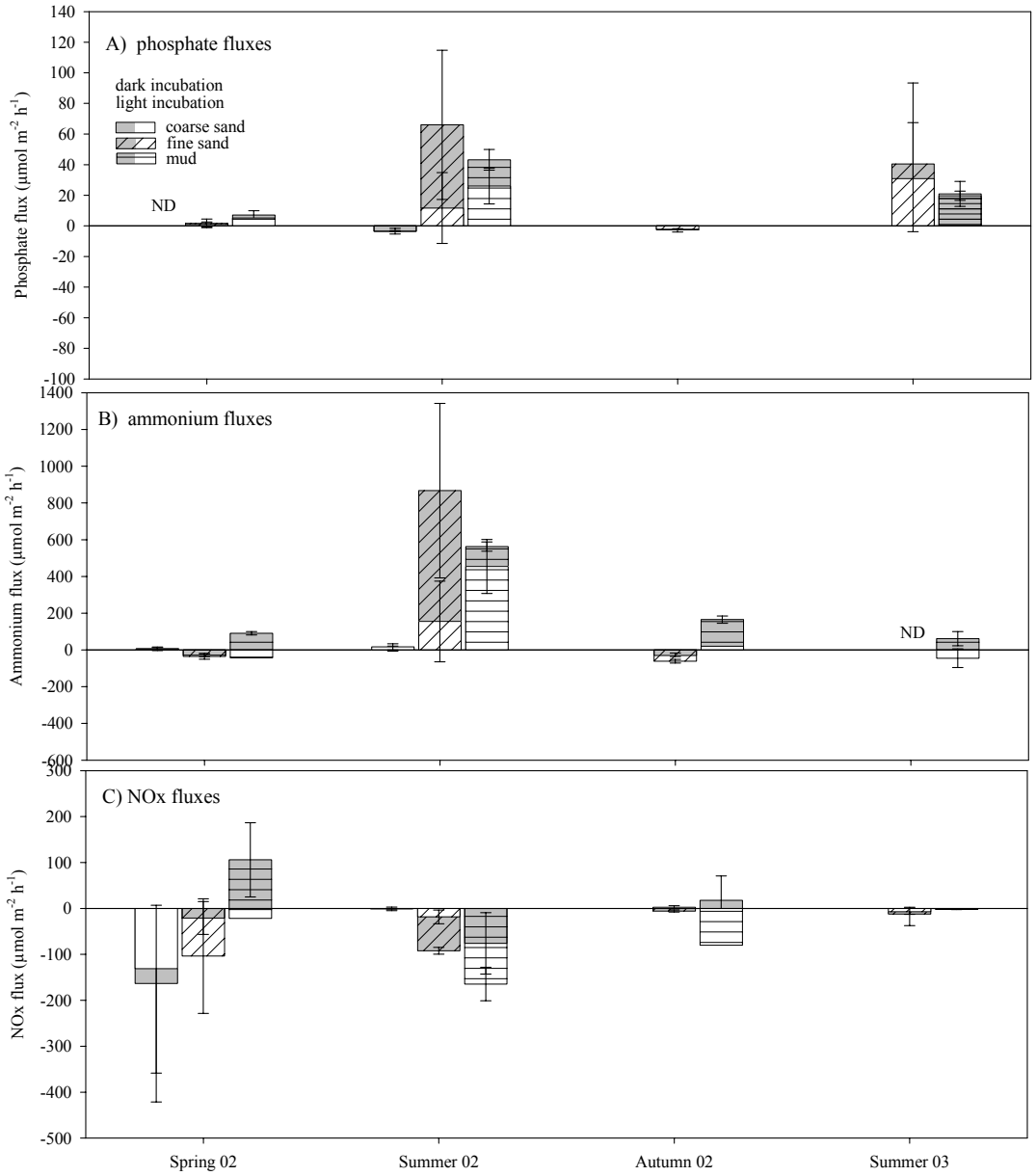

Figure 6: Average benthic chamber fluxes of A) phosphate, B) ammonium and C) nitrate+nitrite (NOx) at the 3 study sites with range as error bars. Negative and positive values denote influx and efflux via the sediment surface, respectively. ND denotes not detectable fluxes.

At the coarse sand site, very low nutrient fluxes resulted from the low organic content in this sediment (Table 2) and an effective nutrient cycling within the sediment by a very active microphytobenthic community, as reflected in the high rates of gross photosynthesis at this site (Table 3). Relatively high release rates of phosphate and ammonium from the fine sand and mud during Summer reflected higher mineralization and ensuing remobilization of bound phosphate due to a lowering of the oxygen penetration depths. The nutrient concentrations of the ambient seawater were generally

highest at the mud site, intermediate at the fine sand and lowest at the coarse sand site (Table 4).

Table 4: Average nutrient concentrations of the ambient seawater at the 3 study sites during the chamber incubations.

Campaign	coarse sand				fine sand				mud			
	Si	PO_4^{3-}	NH_4^+	NOx	Si	PO_4^{3-}	NH_4^+	NOx	Si	PO_4^{3-}	NH_4^+	NOx
Spring 2002	0.2	0.0	0.5	23.3	26.1	0.6	2.7	53.8	23.1	1.2	14.9	29.5
Summer 2002	2.5	0.4	2.7	0.8	8.5	0.6	5.9	2.6	15.1	1.5	10.6	2.6
Autumn 2002					8.2	1.1	5.9	1.9	31.5		7.0	3.7
Summer 2003					5.9	1.8	0.2	0.3	14.9	2.6	2.9	0.4

DISCUSSION

Our study demonstrates that during inundation rates of benthic photosynthesis in sandy intertidal zones can be similar to those in mud flats, despite higher total chlorophyll content in the top cm of the mud sediment. Relatively high gross photosynthesis rates in the investigated tidal flats were associated with coarse grain size and high permeability of the sediment and resulted in a net-autotrophy for the two sandy study sites (Fig. 3). The mud site had lower photosynthesis rates and higher mineralization rates, which led to a net heterotrophy of the benthic community. The higher gross photosynthesis at the two sandy sites is surprising, as the total chlorophyll content of the top cm of the sediment was highest at the mud site. Thus, the chlorophyll specific photosynthesis was much higher in the sand than in the mud. Possible mechanisms causing the more active chlorophyll in the sandy sediments that will be discussed here are 1) differences in metabolic state of the microphytobenthos. 2) differences in light availability to the microphytobenthos 3) site specific inorganic carbon limitation.

Metabolic state of the microphytobenthos

The higher gross photosynthesis at the sandy study sites may have been produced by a more active microphytobenthic community. The measurement of phaeophytin content at the 3 study sites indicated an accumulation of chlorophyll degradation products in the muddy sediment, whereas no chlorophyll degradation products were measured in the top 3 cm of the sediment at the sandy sites. This is in agreement to other studies of intertidal flats (Cadee & Hegeman 1977, Barranguet et al. 1997, Lucas & Holligan 1999, Middelburg et al. 2000). Sandy sediments are sites of high organic matter turnover (Forster et al. 1996, Huettel & Rusch 2000, D'Andrea et al. 2002) and algal cells can be rapidly degraded within these sediments (Ehrenhauss et al. 2004). Additionally, dead algal cells can be removed by advective flushing and resuspension of the permeable sand during inundation (de Jonge & van Beusekom 1995, Lucas et al. 2000, Rusch et al. 2001). This is in contrast to fine grained sediments that accumulate organic matter (Table 2). This possibly involves settling of phytoplankton cells (Lucas & Holligan 1999) that may not meet favourable conditions upon sedimentation on the mud flat and, hence, are inactive.

More frequent resuspension and mixing in sandy sediment may also relocate the phototrophic community into deeper, dark layers, while cells from the aphotic sediment

zone may end up in the photic surface layer. Relative constant chlorophyll concentrations (Fig. 3) indicate that this mixing affects the upper 3 to 6 cm of the sands and only the uppermost 1 to 2 cm in the mud (see also MacIntyre et al. 1996, Lucas & Holligan 1999). Because many diatoms can survive over long time periods in the dark (Steele & Baird 1968, French & Hargraves 1980) and benefit from the higher nutrient concentrations at depth (Saburova & Polikarpov 2003), frequent mixing of the sediment can keep a phototrophic community alive and active down to the mixing depth. The mixing may also reduce the potentially benthic-photosynthesis-diminishing effect of grazing (Hargrave 1970, Connor et al. 1982), which is most intense at the sediment surface. In sands, the mixing of the sediment may quickly compensate for the grazing effect, while the recovery may take longer in muds, where phototrophs have to move or grow into the grazed surface areas.

Light availability

The turbidity of the sea water increases from the relatively clear open North Sea towards the near-shore areas (Postma 1961). Light therefore limits primary production in the water column of the Wadden Sea (Colijn & Cadee 2003) and possibly also benthic primary production during inundation. Integral primary productivity of intact sediment has been previously shown to be saturated at a wide range of light intensities between 100 to 1260 µmol photons m^{-2} s^{-1} (MacIntyre et al. 1996 and references therein). Incident light intensities at the sea floor were generally below this level in our study, which caused a quick response of gross photosynthesis to incident light. Incident light intensities during inundation were generally lower at the mud site than at the fine sand site during all investigated study seasons (Fig. 5), which can partly explain the lower gross photosynthesis at the mud site as compared to the only 4 km distant fine sand site. The effect of the more severe light limitation in the mud is a higher chlorophyll specific production at the sandy site during submersion.

In addition to differences in incident light, also the light distribution within the sediment varies between the muddy site and the sands. Due to less adsorption in the sand, two to three times more light was available to the microphytobenthos at identical incident light (Fig. 2). The higher light absorption in the mud sediment can not be explained by the higher total chlorophyll content, as chlorophyll was maximal 42 µg g^{-1} dry sediment in the mud. Note that the light availability in the mud is less than half of that in the sand, but that the chlorophyll content is doubled. Potentially, these effects

cancel each other out with respect to total production, but again cause a higher chlorophyll specific production in the sand. The different optical properties of the sediments helps explain why at the coarse sand site gross photosynthesis was 3 and 13 times higher during Summer 2002 than at the fine sand and mud site, respectively, despite relatively low incident light intensity at the sea floor (Fig. 5).

Inorganic carbon limitation

Cook & Røy (in press) showed that advective flushing enhanced benthic primary production in a photosynthetically active permeable sand layer, because this flushing reduced CO_2 limitation of the microphytobenthos. The effect explains in-situ observation of enhanced photosynthesis with increased sediment flushing (Wenzhöfer et al. in preparation). The flushing rates in our benthic chambers induced by the radial stirring (Huettel & Gust 1992b, Janssen et al. 2005) corresponded to the different permeabilities of the three sediment types. The bromide tracer measurements documented the higher flushing rates in the coarse sand compared to the fine sand and mud sites. Enhanced transport of solutes with the advective pore water flows in the sands, thus, may have contributed to higher photosynthesis rates in these sands during inundation. However, inorganic carbon limitation was possibly only a factor at the highest observed photosynthesis rates (Cook & Røy in press). Due to the relatively low stirring rates employed in our experiments, advective flushing and benthic photosynthesis may be even higher at in situ flow conditions than measured in the benthic chambers.

Our study demonstrated that during inundation benthic photosynthesis may be enhanced in intertidal sands due to a more active microphytobenthos, increased light availability and relief of inorganic carbon limitation through increased flushing of the permeable sediment. Sand flats, thus, can act as islands of net autotrophy in the heterogenous Wadden Sea system that is generally considered net-heterotrophic (Gattuso et al. 1998, van Beusekom et al. 1999). The high primary production in the sands is associated with relatively low chlorophyll contents, which complicates extrapolations of photosynthesis rates from chlorophyll data acquired by remote sensing.

ACKNOWLEDGEMENTS

We thank M. Alisch, U. Werner, C. Hüerkamp and K. Vamvakopoulos for assistance during the cruises. We thank M. Alisch, G. Schüßler, S. Menger, D. Franzke and S. Pabel for their help with laboratory work and Cäcilia Wiegand for the preparation of the oxygen optodes. The technical assistance by J. Langreder, A. Nordhausen, G. Herz, A. Kutsche, P. Färber, V. Meyer and H. Osmers is gratefully acknowledged. Big thanks go to the crews of the Plattboden-ships and the Staff of the Wadden Sea station on Sylt (Alfred Wegener Institute) for their support and hospitality. This study was supported by the Deutsche Forschungsgemeinschaft (DFG) within the research group "Biogeochemistry of the Wadden Sea" (FG 432-5), coordinated by Prof. J. Rullkötter. We are grateful to Prof. B. B. Jørgensen and Dr. M. E. Böttcher for their support of this work and coordination of the sub-project "Biogeochemical processes at the sediment-water interface of intertidal sediments".

LITERATURE CITED

Admiraal W., Peletier H., Zomer H. (1982) Observations and experiments on the population dynamics of epipelic diatoms from an estuarine mudflat. Est. Coast. Shelf Sci. 14:471-487

Asmus R. (1982) Field measurements on seasonal variation of the activity of primary producers on a sandy tidal flat in the northern Wadden Sea. Neth. J. Sea Res. 16:389-402

Asmus R., Jensen M. H., Murphy D., Doerffer R. (1998) Primary production of microphytobenthos, phytoplankton and the annual yield of macrophytic biomass in the Sylt-Rømø Wadden Sea. In: Gätje C., Reise K. (eds) The Wadden Sea ecosystem - Exchange, transport and transformation processes. Springer, Berlin, Heidelberg, New York, p 367-391

Barranguet C., Herman P. M. J., Sinke J. J. (1997) Microphytobenthos biomass and community composition studied by pigment biomarkers: importance and fate in the carbon cycle of a tidal flat. J. Sea Res. 38:59-70

Barranguet C., Kromkamp J., Peene J. (1998) Factors controlling primary production and photosynthetic characteristics of intertidal microphytobenthos. Mar. Ecol. Prog. Ser. 173:117-126

Bartoli M., Nizzoli D., Viaroli P. (2003) Microphytobenthos activity and fluxes at the sediment-water interface: interactions and spatial variability. Aquat. Ecol. 37:341-349

Blanchard G. F., Guarini J. M., Orvain F., Sauriau P. G. (2001) Dynamic behaviour of benthic microalgal biomass in intertidal mudflats. J. Exp. Mar. Biol. Ecol. 264:85-100

Cadee G. C., Hegeman J. (1974) Primary production of the benthic microflora living on tidal flats in the Dutch Wadden Sea. Neth. J. Sea Res. 8:260-291

Cadee G. C., Hegeman J. (1977) Distribution of primary production of the benthic microflora and accumulation of organic matter on a tidal flat area, Balgzand, Dutch Wadden Sea. Neth. J. Sea Res. 11:24-41

Cahoon L. B. (1999) The role of benthic microalgae in neritic ecosystems. Oceanogr. Mar. Biol., Annu. Rev. 37:47-86

Colijn F., Cadee G. C. (2003) Is phytoplankton growth in the Wadden Sea light or nitrogen limited? J. Sea Res. 49:83-93

Colijn F., Dijkema K. S. (1981) Species composition of benthic diatoms and distribution of Chl *a* on an intertidal flat in the Dutch Wadden Sea. Mar. Ecol. Prog. Ser. 4:9-21

Connor M. S., Teal J. M., Valiela I. (1982) The effect of feeding by mud snails, *Ilyanass obsoleta* (Say), on the structure and metabolism of a laboratory benthic algal community. J. Exp. Mar. Biol. Ecol. 65:29-45

Cook P. L. M., Røy H. (in press) Advective relief of inorganic carbon limitation in microphytobenthos in highly productive sandy sediments. Limnol. Oceanogr.

D'Andrea A. F., Aller R. C., Lopez G. R. (2002) Organic matter flux and reactivity on a South Carolina sandflat: The impacts of porewater advection and macrobiological structures. Limnol. Oceanogr. 47:1056-1070

de Jong D. J., de Jonge V. N. (1995) Dynamics and distribution of microphytobenthic chlorophyll-*a* in the Western Scheldt estuary (SW Netherlands). Hydrobiologia 311:21-30

de Jonge V. N., van Beusekom J. E. E. (1995) Wind- and tide-induced resuspension of sediment and microphytobenthos from tidal flats in the Ems estuary. Limnol. Oceanogr. 40:766-778

Ehrenhauss S., Witte U., Buhring S. L., Huettel M. (2004) Effect of advective pore water transport on distribution and degradation of diatoms in permeable North Sea sediments. Mar. Ecol. Prog. Ser. 271:99-111

Flemming B. W., Ziegler K. (1995) High-resolution grain size distribution patterns and textural trends in the backbarrier environment of Spiekeroog Island (southern North Sea). Senckenb. Marit. 26:1-24

Forster S., Glud R. N., Gundersen J. K., Huettel M. (1999) In situ study of bromide tracer and oxygen flux in coastal sediments. Estuar. Coast. Shelf Sci. 49:813-827

Forster S., Huettel M., Ziebis W. (1996) Impact of boundary layer flow velocity on oxygen utilisation in coastal sediments. Mar. Ecol.-Prog. Ser. 143:173-185

French F. W., Hargraves P. E. (1980) Physiological characteristics of plankton diatom resting spores. Mar. Biol. Lett. 1:185-195

Gattuso J.-P., Frankignoulle M., Wollast R. (1998) Carbon and carbonate metabolism in coastal aquatic ecosystems. Annu. Rev. Ecol. Syst. 29:405-434

Grasshoff K., Kremling K., Ehrhardt M. (1999) Methods of seawater analysis, Vol. Wiley-VCH Verlag

Guarini J. M., Cloern J. E., Edmunds J., Gros P. (2002) Microphytobenthic potential productivity estimated in three tidal embayments of the San Francisco Bay: a comparative study. Estuaries 25:409-417

Haardt H., Nielsen G. A. E. (1980) Attenuation measurements of monochromatic light in marine sediments. Oceanol. Acta 3:333-338

Hall P. O. J., Aller R. C. (1992) Rapid, small-volume, flow injection analysis for ΣCO_2 and NH_4^+ in marine and freshwaters. Limnol. Oceanogr. 37:1113-1119

Hargrave B. T. (1970) The effect of deposit-feeding amphipod on the metabolism of benthic microflora. Limnol. Oceanogr. 15:21-30

Herman P. M. J., Middelburg J. J., Heip C. H. R. (2001) Benthic community structure and sediment processes on an intertidal flat: results from the ECOFLAT project. Cont. Shelf Res. 21:2055-2071

Holst G., Glud R. N., Kuhl M., Klimant I. (1997) A microoptode array for fine-scale measurement of oxygen distribution. Sens. Actuator. B-Chem. 38:122-129

Huettel M., Gust G. (1992a) Impact of bioroughness on interfacial solute exchange in permeable sediments. Mar. Ecol. Prog. Ser. 89:253-267

Huettel M., Gust G. (1992b) Solute release mechanisms from confined sediment cores in stirred benthic chambers and flume flows. Mar. Ecol. Prog. Ser. 82:187-197

Huettel M., Rusch A. (2000) Transport and degradation of phytoplankton in permeable sediment. Limnol. Oceanogr. 45:534-549

Janssen F., Faerber P., Huettel M., Meyer V., Witte U. (2005) Pore-water advection and solute fluxes in permeable marine sediments (I): Calibration and performance of the novel benthic chamber system *Sandy*. Limnol. Oceanogr. 50:768-778

Janssen M., Hust M., Rhiel E., Krumbein W. E. (1999) Vertical migration behaviour of diatom assemblages of Wadden Sea sediments (Dangast, Germany): a study using cryo-scanning electron microscopy. Internatl. Microbiol. 2:103-110

Klimant I., Meyer V., Kuhl M. (1995) Fiberoptic oxygen microsensors, a new tool in aquatic biology. Limnol. Oceanogr. 40:1159-1165

Klute A., Dirksen C. (1986) Hydraulic conductivity and diffusivity: laboratory methods. In: Klute A. (ed) Methods of soil analysis - part 1 - Physical and mineralogical methods. American Society of Agronomy, p 687-700

Kühl M., Jørgensen B. B. (1992) Spectral light measurements in microbenthic phototrophic communities with a fiber-optic microprobe coupled to a sensitive diode array detector. Limnol. Oceanogr. 37:1813-1823

Kühl M., Lassen C., Jørgensen B. B. (1994) Light penetration and light intensity in sandy sediments measured with irradiance and scalar irradiance fiber-optic microprobes. Mar. Ecol. Prog. Ser. 105:139-148

Leach J. H. (1970) Epibenthic algal production in an intertidal mudflat. Limnol. Oceanogr. 15:514-521

Lorenzen C. J. (1967) Determination of chlorophyll and pheo-pigments: Spectrophotometric equations. Limnol. Oceanogr. 12:343-346

Lucas C. H., Holligan P. M. (1999) Nature and ecological implications of algal pigment diversity on the Molenplaat tidal flat (Westerschelde estuary, SW Netherlands). Mar. Ecol. Prog. Ser. 180:51-64

Lucas C. H., Widdows J., Brinsley M. D., Salked P. N., Herman P. M. J. (2000) Benthic-pelagic exchange of microalgae at a tidal flat: 1. Pigment analysis. Mar. Ecol. Prog. Ser. 196:59-73

MacIntyre H. L., Geider R. J., Miller D. C. (1996) Microphytobenthos: The ecological role of the 'Secret Garden' of unvegetated, shallow-water marine habitats. I. Distribution, abundance and primary production. Estuaries 19:186-201

Middelburg J. J., Barranguet C., Boschker H. T. S., Herman P. M. J. (2000) The fate of intertidal microphytobenthos carbon: An in situ ^{13}C-labeling study. Limnol. Oceanogr. 45:1224-1234

Migne A., Spilmont N., Davoult D. (2004) In situ measurements of benthic primary production during emersion: seasonal variations andannual production in the Bay of Somme (eastern English Channel, France). Cont. Shelf Res. 24:1437-1449

Mitbavkar S., Anil A. C. (2004) Vertical migratory rhythms of benthic diatoms in a tropical intertidal sand flat: influence of irradiance and tides. Mar. Biol. 145:9-20

Pomeroy L. R. (1959) Algal productivity in salt marshes of Georgia. Limnol. Oceanogr. 4:386-397

Postma H. (1961) Transport and accumulation of suspended matter in the Dutch Wadden Sea. Netherl. J. Sea Res. 1:148-190

Rasmussen M. B., Henriksen K., Jensen A. (1983) Possible causes of temporal fluctuations in primary production of the microphytobenthos in the Danish Wadden Sea. Mar. Biol. 73:109-114

Revsbech N. P., Jørgensen B. B. (1986) Microelectrodes: Their use in microbial ecology. In: Marshall K. C. (ed) Advances in microbial ecology, Vol 9. Plenum Press, New York and London, p 293-352

Rusch A., Forster S., Huettel M. (2001) Bacteria, diatoms and detritus in an intertidal sandflat subject to advective transport across the water-sediment interface. Biogeochemistry 55:1-27

Saburova M. A., Polikarpov I. G. (2003) Diatom activity within soft sediments: behavioural and physiological processes. Mar. Ecol. Prog. Ser. 251:115-126

Serôdio J., Catarino F. (2000) Modelling the primary production of intertidal microphytobenthos: time scales of variability and effects of migratory rhythms. Mar. Ecol. Prog. Ser. 192:13-30

Smith D. J., Underwood G. J. C. (1998) Exopolymer production by intertidal epipelic diatoms. Limnol. Oceanogr. 43:1578-1591

Steele J. H., Baird I. E. (1968) Production ecology of a sandy beach. Limnol. Oceanogr. 13:14-25

Tillmann U., Hesse K. J., Colijn F. (2000) Planktonic primary production in the German Wadden Sea. J. Plankton Res. 22:1253-1276

Tyler A. C., McGlathery K. J., Anderson I. C. (2003) Benthic algae control sediment-water column fluxes of organic and inorganic nitrogen compounds in a temperate lagoon. Limnol. Oceanogr. 48:2125-2137

Underwood G. J. C., Kromkamp J. (1999) Primary production by phytoplankton and microphytobenthos in estuaries. In: Nedwell D. B., Raffaelli D. G. (eds) Advances in Ecological Research - Estuaries, Vol 29. Academic Press, p 93-153

van Beusekom J. E. E., Brockmann U. H., Hesse K. J., Hickel W., Poremba K., Tillmann U. (1999) The importance of sediments in the transformation and turnover of nutrients and organic matter in the Wadden Sea and German Bight. 51:245-266

Veldhuis M. J. W., Colijn F., Venekamp L. A. H., Villerius L. (1988) Phytoplankton primary production and biomass in the western Wadden Sea (The Netherlands); a comparison with an ecosystem model. Neth. J. Sea Res. 22:37-49

Wentworth C. K. (1922) A scale of grade and class terms for clastic sediments. J. Geol. 30:377-392

Wenzhöfer F., Glud R. N., Cook P. L. M., Huettel M. (in preparation) Benthic primary production of two sandy subtidal sediments.

Widdows J., Brinsley M. D., Salked P. N., Lucas C. H. (2000) Influence of biota on spatial and temporal variation in sediment erodability and material flux on a tidal flat (Westerschelde, The Netherlands). Mar. Ecol. Prog. Ser. 194:23-37

Yallop M. L., Paterson D. M., Wellsbury P. (2000) Interrelationships between rates of microbial production, exopolymer production, microbial biomass, and sediment stability in biofilms of intertidal sediments. Microb. Ecol. 39:116-127

CHAPTER 6: CONCLUSIONS AND OUTLOOK

The important role of marine sands in the biogeochemical cycling of organic matter has been fully appreciated only recently. In this context, advective pore water transport through the permeable sands is of particular relevance. However, most studies on permeable, sandy sediments were confined to laboratory measurements. Field measurements, which account for the often highly variable hydrodynamic conditions encountered in the near-shore habitats, are still rather scarce. The role of *in situ* pore water transport processes for organic matter mineralization and interfacial solute fluxes in intertidal, sandy sediments of the Wadden Sea formed the core part of this thesis.

Mineralization rates were generally high in the intertidal sands, ranging between 30 (winter) and 270 mmol C m^{-2} d^{-1} (summer). These rates are in the upper range of the 2 to 170 mmol C m^{-2} d^{-1} determined previously in other intertidal sands (Cammen 1991, Kristensen et al. 1997, Rusch et al. 2001, D'Andrea et al. 2002). The supply of oxygen to the sediment by pore water advection was a key factor for high aerobic mineralization rates, while sulfate reduction rates contributed only 0.3 to 25 % to total mineralization. The deeper oxygen penetration during inundation could be clearly related to hydrodynamic forcing at the sediment-water interface. Therefore, the combination of the percolation method (Polerecky et al. 2005) with the in situ determination of oxygen penetration depths (de Beer et al. 2005) proved to be a useful tool for the determination of areal oxygen consumption rates in permeable sediment. In dynamic, coastal environments such as the Wadden Sea, the influence of natural hydrodynamic conditions on interfacial oxygen fluxes should be accounted for by these minimal-invasive microsensor measurements or with the non-invasive eddy-correlation technique. This technique employs the simultaneous determination of fluctuations of flow velocity and solute concentration at the same point in the water above the sediment to assess net interfacial solute fluxes (Berg et al. 2003).

The influence of advective pore water flow on mineralization was particularly evident at the Sylt Hausstrand study site, where 70 to 90 % of total mineralization occurred during inundation. The rates of oxygen consumption and sulfate reduction increased with inundation time from the upper flat towards the low water line at the Sylt study site, indicating the importance of advective pore water flow for this site. Nevertheless, the simple model used to calculate the bottom filtration rates probably underestimated the organic matter supply to the sediment, which only explained a fraction of the measured mineralization rates. At the Janssand near Spiekeroog, about 50 % of total mineralization took place during both, inundation and exposure. However, this site was inundated less than 50 % of the day time. Mineralization rates were independent of inundation time and similar between the upper and lower flat at this site.

During the relatively short inundation periods, the influence of advective flushing was probably smaller in the less permeable sediment at Spiekeroog as compared to Sylt. Future studies in intertidal areas should account for the possible differences in mineralization rates along an inundation gradient. Additionally, *in situ* determination of bottom water filtration rates and associated supply of organic matter to the sediment needs further investigation.

During low tide exposure, drainage through the permeable sediment became the dominant advective transport process in the intertidal sands, driving nutrient release from the sediment. While the drainage flow velocity was relatively slow (0.5 to 0.9 cm h^{-1}) at Spiekeroog, pore water flow velocities were up to 10 times faster at Sylt corresponding to the higher permeability at this site. The optode technique developed by (Precht & Huettel 2004) to assess wave driven pore water flow, worked reliably for the determination of drainage flow velocities. However, the 6 sensors restricted measurements to a one-dimensional plane and the setup had to be aligned with the prevailing flow direction. Future improvements of this method could use more sensors in two- or three-dimensional setups to allow determination of more complex pore water flow paths, especially during submersion. This is currently part of an ongoing project (Janssen, pers. communication).

The drainage associated release of pore water from the sediment amounted to an estimated 84,000 to 147,000 L from the sandy northeast margin of the tidal flat near Spiekeroog (3.5 km length). Nutrient release surpassed 5 to 8-fold those fluxes caused by combined effects of diffusion, advection and bioirrigation (as measured in benthic chambers) and exceeded the release rates reported from most other studies conducted in coastal ecosystems. The measured drainage transport at Sylt implies a similar mechanism and may have contributed to the elevated pore water nutrient concentrations near the low water line at this site. Since seepage via the sediment/air interface was not observed at Sylt, a substantial release of nutrient rich pore water may occur in the subtidal area, where high rates of benthic primary production were recently observed (Cook, pers. communication). Since the nutrients in the discharged water reflect a combined signal of local and distant mineralization processes, pore water nutrient concentrations were independent of the season in the seepage zone at the Spiekeroog site. Therefore, two major pore water circulation patterns are active on intertidal sand flats: 1) a rapid “skin circulation” during inundation within the surface sediment layer, characterized by short flow paths and residence times of the pore water with an immediate feedback to the system; 2) a slower “body circulation” through the surface and deeper layers of the sediment during exposure with long flow paths and pore water residence times that is acting as a buffered nutrient source to the ecosystem.

The ecological importance of the drainage has received only limited attention for intertidal flats and needs further, more detailed studies. Slower pore water flow velocities during spring than summer may have resulted from a higher pore water viscosity during spring. This suggests a seasonal pattern of drainage flow and discharge rates that has to be elucidated. Furthermore, a detailed hydrological survey of tidal flats with piezometers could provide more insights to the flow paths within the sediment and origin of the discharged pore water.

The studies suggested benthic primary production to be the most important source of fresh organic matter on the investigated tidal flats, as the filtration of organic matter from the water column could only explain a fraction of the high mineralization rates. During inundation, higher gross benthic photosynthesis could be sustained in sandy sediment than in mud, despite higher chlorophyll content at the silty site. Pore water advection was possibly a key factor for the higher chlorophyll specific photosynthesis in the sands. Mixing and advective flushing removes inactive cells and chlorophyll degradation products from the sands suggesting a more active microphytobenthic community in sandy sediment, whereas mud flats accumulate organic matter and fine particles. High organic matter content and fine particles led to an increased light attenuation in the mud, whereas more light was available to the microalgae in the sands. Furthermore, more light could penetrate through the water column over the sands, whereas light limitation was more severe at the mud site, possibly due to re-suspension of fine particles by waves and currents. In addition, the advective flushing of the permeable sediments may have counteracted a possible CO_2 limitation of the microalgae in the sands.

The stirred benthic chambers are a useful tool for the *in situ* assessment of benthic photosynthesis in undisturbed sediment under advective flow. By adjusting the stirring speed of the chamber water, the influence of different flushing rates on benthic photosynthesis can be elucidated (Wenzhöfer et al. in prep.). In order to establish budgets over the full tidal cycle, however, measurements should be extended to the exposure period. With the recently developed closed-chamber CO_2-flux method (Migne et al. 2002), *in situ* benthic primary production and respiration during exposure can be assessed by measuring CO_2 exchange of undisturbed sediment using an infrared gas analyser.

LITERATURE CITED

Berg P., Roy H., Janssen F., Meyer V., Jørgensen B. B., Huettel M., de Beer D. (2003) Oxygen uptake by aquatic sediments measured with a novel non-invasive eddy-correlation technique. Mar. Ecol. Prog. Ser. 261:75-83

Cammen L. M. (1991) Annual Bacterial Production in Relation to Benthic Microalgal Production and Sediment Oxygen-Uptake in an Intertidal Sandflat and an Intertidal Mudflat. Mar. Ecol. Prog. Ser. 71:13-25

D'Andrea A. F., Aller R. C., Lopez G. R. (2002) Organic matter flux and reactivity on a South Carolina sandflat: The impacts of porewater advection and macrobiological structures. Limnol. Oceanogr. 47:1056-1070

de Beer D., Wenzhoefer F., Ferdelman T. G., Boehme S. E., Huettel M., van Beusekom J. E. E., Boettcher M. E., Musat N., Dubillier N. (2005) Transport and mineralization rates in North Sea sandy intertidal sediments, Sylt-Rømø Basin, Wadden Sea. Limnol. Oceanogr. 50:113-127

Kristensen E., Jensen M. H., Jensen K. M. (1997) Temporal variations in microbenthic metabolism and inorganic nitrogen fluxes in sandy and muddy sediments of a tidally dominated bay in the northern Wadden Sea. Helgol. Mar. Res. 51:295-320

Migne A., Davoult D., Spilmont N., Menu D., Boucher G., Gattuso J.-P., Rybarczyk H. (2002) A closed-chamber CO2-flux method for estimating intertidal primary production and respiration under emersed conditions. Mar. Biol. 140:865-869

Polerecky L., Franke U., Werner U., Grunwald B., de Beer D. (2005) High spatial resolution measurement of oxygen consumption rates in permeable sediments. Limnol. Oceanogr.: Methods 3:75-85

Precht E., Huettel M. (2004) Rapid wave-driven advective pore water exchange in a permeable coastal sediment. J. Sea Res. 51:93-107

Rusch A., Forster S., Huettel M. (2001) Bacteria, diatoms and detritus in an intertidal sandflat subject to advective transport across the water-sediment interface. Biogeochemistry 55:1-27

Erklärung gemäß §6 Abs. 5 der Promotionsordnung der Universität Bremen für die mathematischen, natur- und ingenieurwissenschaftlichen Fachbereiche

Hiermit versichere ich, dass ich die Doktorarbeit mit dem Titel

Pore water transport and microbial activity in intertidal Wadden Sea sediments

selbständig verfasst und keine als die angegebenen Quellen und Hilfsmittel benutzt, sowie Zitate gekennzeichnet habe.

Bremen, den 8. November 2005